INTERLAMINAR STRESSES AT STRAIGHT FREE EDGES

OF COMPOSITE LAMINATES

by

CHRISTOS KASSAPOGLOU

B.S., Massachusetts Institute of Technology
(1982)

SUBMITTED IN PARTIAL FULFILLMENT
OF THE REQUIREMENTS OF THE
DEGREES OF

MASTER OF SCIENCE IN
AERONAUTICS AND ASTRONAUTICS

and

MASTER OF SCIENCE IN
MECHANICAL ENGINEERING

at the

MASSACHUSETTS INSTITUTE OF TECHNOLOGY

October 1984

© MASSACHUSETTS INSTITUTE OF TECHNOLOGY 1984

Signature of Author _____ Signature redacted _____
Department of Aeronautics and Astronautics
October 31, 1984

Certified by _____ Signature redacted _____
Professor Paul A. Lagace
Thesis Supervisor

Certified by _____ Signature redacted _____
Professor James H. Williams Jr.
Thesis Reader

Accepted by _____ Signature redacted _____
Professor Harold Y. Wachman
Chairman, Departmental Graduate Committee

Accepted by _____ Signature redacted _____
Professor Warren M. Rohsenow, Chairman
Departmental Committee on Graduate Studies
Department of Mechanical Engineering
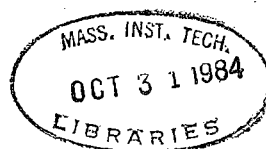
INTERLAMINAR STRESSES AT STRAIGHT FREE EDGES

OF COMPOSITE LAMINATES

by

CHRISTOS KASSAPOGLOU

Submitted to the Department of Aeronautics and Astronautics
and the Department of Mechanical Engineering
on October 31, 1984 in partial fulfillment of the
requirements for the Degree of Master of Science
in Aeronautics and Astronautics and the Degree of Master
of Science in Mechanical Engineering

ABSTRACT

A simple approximate method to predict interlaminar
stresses at straight free edges of symmetric composite
laminates under uniaxial loads has been developed based
on overall force and moment equilibrium and on the principle
of minimum complementary potential energy. Results using
the present method compare well with other analytical methods.
The present method is considerably more efficient, especially
in its ability to easily analyze thick laminates, and could
be implemented on a personal computer. The solution for
the special cases of angle-plied and cross-plied laminates
is also obtained (in closed form) and is simpler than for
general laminates. This solution for certain cross-plied
laminates coincides with a previous solution derived from
a special version of plate theory. Using the analysis,
the sensitivity of the solution to various parameters such
as different elastic constants and different ways of determin-
ing the longitudinal in-plane normal stress is examined.
In addition, the solution shows that the thin resin layer
which exists between plies does not affect the interlaminar
stresses calculated from the orthotropic and homogeneous
assumption for individual plies. The boundary layer where
the interlaminar stresses are significant is defined and
discussed and the concept of the "effective ply thickness"
introduced. Finally, an experimental technique to measure
in-plane displacement at the top surface of the laminate
inside the boundary layer was developed. The experimental
results are in good agreement with the predictions from
theory.

Thesis Supervisor: Paul A. Lagace

Title: Draper Assistant Professor of Aeronautics
and Astronautics

ACKNOWLEDGEMENTS

Dass ich nicht mehr mit saurem Schweiss

Rede von dem, was ich nicht weiss.

Dass ich erkenne, was die Welt

Im Innersten zusammenhält,

Schau alle Würkungskraft und Samen

Und tu nicht mehr in Worten kramen.

Johann Wolfgang von Goethe Faust

6

TABLE OF CONTENTS

TABLE OF CONTENTS (Continued)

TABLE OF CONTENTS (Continued)

LIST OF FIGURES

LIST OF FIGURES (Continued)

LIST OF FIGURES (Continued)

LIST OF FIGURES (Continued)

LIST OF FIGURES (Continued)

LIST OF FIGURES (Continued)

LIST OF TABLES

NOMENCLATURE

a	Half laminate length.
$A_i \ (i=1,2,\ldots 6)$	Coefficients in the x dependencies of the stresses.
A_σ	Area over which displacements of the laminate are prescribed.
b	Half laminate width.
B	1% of $f_{23}(x)$ when $x=x_o$ Intermediate term used in the determination of the boundary layer width.
$B_i \ (i=1,2,3,4)$	Coefficients in the z dependencies of the stresses.
$\tilde{B}_i \ (i=2,4,5)$	B_i multiplied by $\sigma^L_{22_{[\theta i]}}$.
$\tilde{B}_i^{(j)} \ (i=2,4,5; \ (j=1,\ldots n)$	$\tilde{B}_i$ for the jth ply.
C	ε_{11}
CLPT	Classical Laminated-Plate Theory.
C_1	ε_{11}
d_i	Coefficients in the expressions for f_i.
$E_{ij} \ (i=1,\ldots 6; \ j=1,\ldots 6)$	Stiffnesses.
f_i	Coefficients in the energy expression
$f_{ij}(x) \ (i=1,2,3; \ j=1,2,3)$	Functions describing the x dependence of the stresses.
$F(x_2,z)$	Unknown function in the expression for the u displacement.
FD	Finite differences.
FE	Finite elements.
$g_{ij}(z) \ (i=1,2,3; \ j=1,2,3)$	Functions describing the z dependence of the stresses
$G(x_1,z)$	Unknown function in the expression for the v displacement.
h	Laminate thickness.

NOMENCLATURE (Continued)

$H(x_1, x_2)$	Unknown function in the expression for the w displacement.
$k_1^{(i)}$	Longitudinal strain normalized by compliance S_{11} for the ith ply.
M	Center point at the ends (1^+, 1^- face) of the laminate.
$M_1^{(i)}(z)$	σ_{22} for the ith ply for angle-plied laminates
n	Number of plies in the laminate.
$N_1^{(i)}(x_2)$	σ_{zz} for the ith ply for angle-plied laminates.
$N_2^{(i)}(x_2)$	σ_{1z} for the ith ply for cross-plied laminates.
p	Strength of the stress singularity at the free edge.
$Q(x_2)$	Unknown function equal to ε_{11}.
r	Distance from the free edge.
$R(z)$	Unknown function equal to ε_{11}.
$\underset{\sim}{S}$	Compliance matrix.
S_{ij} ($i=1,\ldots6$; $j=1,\ldots6$)	Compliances.
$S_{ij}^{(k)}$ ($k=1,\ldots6$; $j=1,\ldots6$; $k=1,n$)	Compliances for the kth ply.
t	Ply thickness.
$t^{(i)}$	Thickness of the ith ply.
$\tilde{t}$	Thickness of the section of the laminate between the z^+ and the z^- face.
$\underset{\sim}{T}$	Traction vector corresponding to the prescribed displacements of the laminate.

NOMENCLATURE (Continued)

u	Longitudinal displacement.
u_m	Displacement of center point M at the two ends of the laminate.
$\bar{u}$	Vector of prescribed displacements.
$U(x_2, z)$	Function describing the dependence of the u displacement on x_2 and z.
v	Transverse displacement.
V	Volume of the laminate.
$V(x_2, z)$	Function describing the dependence of the w displacement on x_2 and z.
w	Out of plane displacement.
$W(x_2, z)$	Function describing the dependence of the w displacement on x_2 and z.
x	Transverse direction with the origin at the laminate free edge.
x_o	Value of x at which σ_{zz} is zero
x_1	Longitudinal direction.
x_2	Transverse direction with the origin at the center of the laminate.
x_{BL}	Boundary layer width.
z	Out of plane direction
z^+, z^-	Faces created by cuts made perpendicular to the out of plane direction.
ϵ_{ij} (i=1,2,z; j=1,2,z)	Strains in any ply in laminate axes.
θ	Lamination angle.
θ_i	Lamination angle for the ith ply.
λ	Exponent used in the eigenfunctions describing the stresses.
$\nu_{12}, \nu_{13}, \nu_{23}$	Poisson's ratios.

NOMENCLATURE (Continued)

π_c	Complementary energy for the laminate.
$\pi_c^{(i)}$	Complementary energy for the ith ply.
σ_{ij} (i=1,2,z; j=1,2,z)	Stresses in any ply in laminate axes.
$\sigma_{ij}^L{}_{[\theta_k]}$ (h,j=1,2; k=1,n)	CLPT stresses in laminate axes for the kth ply.
σ_{11}	Average applied longitudinal stress.
ΣF_i (i=1,2,3)	Summation of forces in the ith direction.
ΣM_i (i=1,2,3)	Summation of moments about the x_i axis.
ϕ	Exponent used in the eigenfunctions describing the stresses.
ϕ_{init}	Initial value for ϕ used to start the iterations.
1^+, 1^-	End faces of the laminate, perpendicular to the longitudinal direction.
2^+	Free edge face.
2^-	Face parallel to the free edge, inside the laminate.

CHAPTER ONE

INTRODUCTION

The failure of composite laminates can be classified into two basic modes: (1) In-plane fracture and (2) Out of plane delamination. Both types of fracture have been the object of extensive research [1-3,4-27] in recent years. However, even though significant progress has been made in the case of in-plane fracture, little is still known about the mechanisms that govern delamination and the interaction between these two failure types. Delamination is a very important type of failure because it may occur at loads appreciably lower than the loads at which in-plane fracture would occur.

At the free edges of composite laminates, interlaminar stresses σ_{zz}, σ_{2z}, and σ_{1z} develop due to mismatch in elastic properties between adjacent plies. However, between adjacent plies, there exists only a thin resin layer where no fibers are present [3]. This is a relatively weak layer and, depending on the stacking sequence and the applied loading, the interlaminar stresses present in that layer may cause delamination.

The Classical Laminated-Plate Theory, (CLPT), which is commonly used to analyze composite laminates [4], predicts that interlaminar stresses are zero everywhere in a laminate.

Therefore, near the free edges of a laminate, where the interlaminar stresses are most important, CLPT must be modified to account for the existence of the interlaminar stresses.

Many methods have been proposed for the determination of these stresses but most of these analyses are complicated and have severe computational limitations. The present investigation proposes a simple approximate scheme to compute these stresses for symmetric laminates under tensile loads. Laminates of any number of plies including hybrid laminates can be analyzed. In addition, an experimental method is used to measure in-plane displacements at the top surface of a laminate near the free edge in order to compare with theoretical predictions.

In the second chapter, a summary of the previous analyses of the problem is presented along with a brief discussion. The governing equations and boundary conditions are presented in the third chapter. In the fourth chapter, the force-balance method is presented in detail. This method resorts to force and moment equilibrium in a laminate in order to obtain the basic behavior of the stress field. The solution details are given in chapter five. The final equations are solved iteratively with the use of a computer. The solution for two important special cases, angle-plied laminates and cross-plied laminates, is given and discussed in chapter six. Results and

comparisons with other analyses are given in chapter seven. The experimental method used to measure the displacements at the top of a laminate is described in chapter eight. Experimental results are compared with the theoretical predictions in chapter nine. Finally, chapter ten contains the conclusions and some suggestions for further work.

Appendix 5 contains the listing of the computer program that was used to solve the resulting equations.

CHAPTER TWO

Previous Work

2.1 Laminate geometry and basic characteristics

A symmetric laminate loaded in tension is illustrated in Figure 2.1. The origin of the axis system is at the center of the laminate. Throughout this investigation, stresses, strains, displacements, and elastic constants correspond to an individual ply and not to the entire laminate unless so noted. Interlaminar stresses will have z as one of the subscripts to emphasize that they are out of plane quantities. All stresses and strains are in laminate axes. The strip region near the free edge, where interlaminar stresses are important, is commonly referred to as the boundary layer.

2.2 Analytical methods

The underlying assumptions common to almost all of the works to be presented are: 1. Each ply can be treated as macroscopically homogeneous and orthotropic; and 2. Stresses do not vary in the longitudinal (x_1) direction.

One of the first solutions to the interlaminar stress problem was developed by Pipes and Pagano [5]. Their analysis

$\overline{\sigma}_{11}$

z

TOP SURFACE

h

x_2

2a

FREE EDGE

2b

x_1

$\overline{\sigma}_{11}$
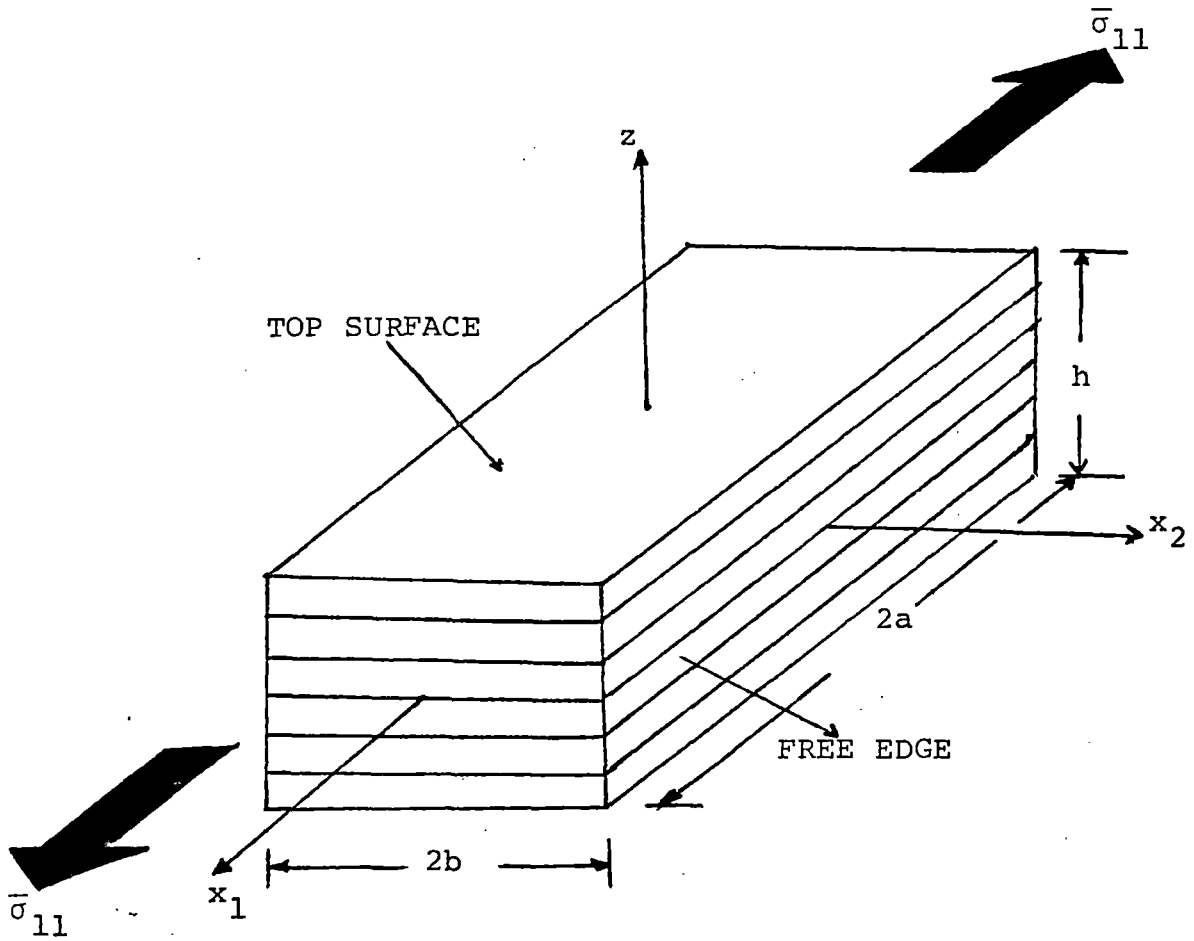
(NOTE: NOT TO SCALE)

Figure 2.1. Composite laminate under uniaxial tension

led to three coupled partial differential equations in the three displacements u, v, and w. The equations were solved using a finite difference (FD) scheme. They applied their solution to a [±45]s laminate and observed that, as the FD grid was made finer, the maximum value of the interlaminar shear stress σ_{1z} at the +45/-45 interface increased, apparently without bound. This led them to suggest that σ_{1z} may be singular at the free edge. They also found that the interlaminar stresses σ_{zz}, σ_{2z}, and σ_{1z} were only appreciable in a small region close to the free edge (the boundary layer). Its size was found to be on the order of one laminate thickness.

It should be noted that the solution by Pipes and Pagano involves a 1200 x 1200 system of linear algebraic equations for a four-ply laminate. Also, the stress values at the ply interfaces were found by extrapolation.

At about the same time, Puppo and Evensen [6], proposed another method of analysis to calculate the shear stresses σ_{2z} and σ_{1z}. They modelled the laminate as a set of anisotropic layers separated by isotropic adhesive layers. A set of ordinary differential equations was obtained by considering the equilibrium of an infinitesimal element consisting of two anisotropic layers separated by an isotropic layer. The interlaminar normal stress σ_{zz} was neglected and the shear stress σ_{1z} was found to be finite at the free edge.

Several other solutions followed. Rybicki [7] used a three dimensional finite element (FE) analysis based on the complementary energy formulation. Stanton et al [8] used a tri-cubic isoparametric solid element. Another FE method was used by Wang and Crossman [9]. Due to the very large number of elements required, they used the sky-line storage technique for the stiffness matrix. Even then, the working vector in the computer program had 27000 elements for a four ply laminate. To further improve their method, the same investigators [10], introduced a substructuring scheme so that laminates with a larger number of plies could be analyzed. They pointed out that the guidelines used to determine which part of the laminate should be treated as a substructure and which should be analyzed in detail, were unclear and subject to discussion.

A three-dimensional FD scheme was proposed by Altus et al [11]. Pagano [12], based on a theory developed by Whitney and Sun [13], determined a closed-form solution for σ_{zz} at the midplane of a [0/90]s laminate. The method was a modified plate theory that included shear deformations and through the thickness stretching.

Tang [14], and Tang and Levy [15], treated the problem as a combination of plane strain and torsion. They solved separately for the boundary layer region and for the interior of the laminate. Their solution at the interior region coincided with the CLPT. The solution in the boundary layer region was

in good agreement with the solution of Pipes and Pagano [5], but the stress-free condition ($\sigma_{2z}=0$) was not satisfied at the free edge.

A perturbation method was suggested by Hsu and Herakovich [16]. One major problem with this method is the fact that the solution is in terms of an unknown parameter, the value of which can only be estimated in an indirect way by making sure that, for the particular value assumed for that parameter, stresses do not exceed "elastic limits".

Another method was suggested by Pagano [17,18] based on Reissner's variational principle. A solution can be obtained by solving a system of 13N ordinary differential equations, where N is the number of sublayers (not necessarily coinciding with the plies) into which the laminate is divided. However, N is limited to 6-10 because any higher N values result in intermediate numerical results that are much higher than the highest number most computers can store.

Fracture mechanics principles were applied by Wang and Crossman [19] in order to determine the onset of delamination. Bar-Yoseph and Pian [20] proposed a perturbation and assumed-stress approach for the determination of the interlaminar stresses.

In most of the analyses presented so far, the results suggested that σ_{1z} and, possibly, σ_{zz} may be singular at the free edge of a laminate [5,7,9,17]. The approximate nature of

these methods however, does not permit a reliable determination of such a singularity.

Complete elasticity solutions for infinite wedges [21,22] showed indeed that such a singularity existed for isotropic materials. The corresponding elasticity solution for anisotropic materials was presented by Wang and Choi [23,24]. Based on Lekhnitskii's stress potentials [25], two coupled partial differential equations were obtained, which were solved by an eigenfunction expansion method using complex variables. It was found that the stress field was indeed singular at the free edge. However, the strength of the singularity was not completely determined because, as it was shown by Zwiers et al [26], and Dempsey and Sinclair [27], apart from the singularity predicted by Wang and Choi, other singularities of different strength may be present.

The existence of a singularity may be considered to imply that an approximate method used to compute the interlaminar stresses should somehow reflect this fact. This would mean that FE schemes should include singular elements because, as it was shown by Tong and Pian [28], the convergence of the FE solution in problems with a singularity is not improved by using a finer mesh or higher order elements, if the FE formulation does not include the singularity.

Wang and Yuan [29] presented a FE method based on a hybrid functional, derived from the Hellinger-Reissner princi-

ple, that included a singular element to model the singular region in the laminate. They obtained excellent agreement with the results of Wang and Choi in [24].

One problem associated with FE analyses that incorporate the stress singularity in the formulation, is that the strength of the singularity must be known beforehand so that the singular element stiffness matrix can be assembled. This is a serious drawback because the strength of the singularity is obtained analytically after a complicated and lengthy process [23,26], and is different for different interfaces of a laminate.

A way to overcome that was suggested by Swedlow [30]. In this analysis, the strength of the singularity is included in the formulation as an unknown. The displacement interpolation should therefore include terms of the form r^p where r is the distance from the free edge and p is the unknown strength of the singularity. Differentiation of the functional with respect to p gives an additional equation from which p can be determined.

Another recent solution to the interlaminar stress problem, without taking into account the existence of the singularity, was presented by Pagano and Soni [31]. They divide the laminate in a global and a local region. The global region is that part of the laminate that is far from the ply interface of interest and is treated as a substructure with

equivalent loads. The local region is around the ply interface of interest and the solution there is more detailed and complicated. It is based on assumed functions for the stresses in that region. This method can be used to analyze thick laminates but is sensitive to the size of the local region and the transition from the local region to the global region. There are no specific guidelines as to how this should be done, and results reported show that the stress prediction for the same location in the local region may vary as much as 50% depending on the particular global-local scheme used.

Whitcomb and Raju [32] proposed another FE method and solved the problem by superposition. Their method is slightly more efficient than other FE methods proposed because the implementation is based on a modified two dimensional analysis (obtained by imposing that there is no in-plane shear deformation) rather than a three dimensional analysis. This analysis cannot be used to predict σ_{1z} nor can it be used for angle-plied laminates ($+\theta$ and $-\theta$ fiber orientations only).

In summary, many different solution methods were proposed over the years for the determination of interlaminar stresses. Most of them are limited to thin laminates (less than 6-10 plies) due to large computation times required for the solution. They also have problems in satisfying some of the conditions of the problem (e.g. stress-free edge or strain compatibility).

2.3 Experimental results

Over the years, various efforts have been made to experimentally measure interlaminar stresses in order to determine which of the analytical methods were more reliable.

Pipes and Daniel [33] used a moiré method to measure the displacements at the top of a $[(25)_4/(-25)_4]s$ graphite epoxy (G/E) laminate. Their results however, are not accurate since only three data points were obtained in the boundary layer. A similar moiré method was used by Oplinger et al [34] to measure the displacements at the top surface and on the free edge of $[+\theta/-\theta]ns$ and $[+\theta_n/-\theta_n]s$ boron epoxy (B/E) laminates. They too had very few data points (approximately five).

X-rays were used by Lou and Walter [35] to measure interlaminar shear strains for two-ply cord-rubber laminates. Two thin narrow radiopaque rubber strips were embedded in two-ply cord rubber laminates. The change in angle between the two initially aligned strips served as the means to measure interlaminar strains.

A more conventional method was used by Kim and Soni [36]. They used miniature strain gages (.008 in long) to measure at the midplane of $[\pm30_n/90_n]s$, $[(\pm30)_n/90]s$ (n=2,4,6) graphite/epoxy specimens. They report fair agreement with the theory in [27] but the size of the strain gages limits the usefulness of the method to laminates for which σ_{zz} does not

vary appreciably with z at the free edge. Otherwise, if σ_{zz}, and hence ε_{zz}, has steep gradients, the strain gage will not be able to reproduce them.

More qualitative results were reported by Whitney [37]. The effect of interlaminar stresses on narrow and wide tensile coupons is discussed and some differences in the stress field of sandwich beam specimens are presented. The discussion is based on stress shapes that are assumed in such a way that they fit the results of Pipes and Pagano [5]. No experimental results are presented.

Pipes et al [38] tested Boron/Epoxy laminates to failure. On the basis of the experimental stress-strain curves of the two laminates they suggested that large nonlinear strains may occur at ply interfaces possibly leading to delamination.

2.4 Discussion

The problem of the determination of interlaminar stresses is complicated and hard to solve analytically. The mere fact that so many different methods of analysis have been published over the last 15 years [5-27], indicates the level of complexity of the problem.

The different methods do not always agree with one another. For example, the FE method in [9] and the FD method in [5], predict a tensile σ_{zz} stress at the free edge of the

+45/-45 interface of a [±45]s laminate while the eigenfunction expansion method in [23,24] predicts a compressive σ_{zz} stress for the same location. A more detailed comparison of the different FE methods is given in [39].

The major problem that all these methods have (except the global-local analysis in [31]) is that, due to computation problems, they can not realistically deal with laminates of more than 10-15 plies. In practice however, the laminates used may have 100 or 200 plies. The reason for this computation limitation is that the computer storage per ply interface required for sufficient resolution in the boundary layer is so large, that the storage required for a practical laminate (say 50 plies thick), is so large that the solution would take a lot of time and would not be cost effective.

The main problems associated with the different analytical methods can be summarized as follows: a) FE and FD methods involve the solution of large systems of equations [5,7,9]; b) The stress free boundary conditions are not always satisfied (e.g. $\sigma_{2z}(x=0) \neq 0$ [7,9,16]); c) There are no guidelines for substructuring or "lumping" parts of a laminate in a manner that can yield reliable results [10,31]; d) FD methods involve lengthy extrapolations [5,11]; and e) Different methods do not agree with one another for the same type of laminate and loading [5,8,9,24].

Finally, before discussing experimental methods, a brief comment on the importance of the stress singularity is in order. The singularities reported in the literature to date [23,26] are very weak. That is, they are more than an order of magnitude smaller than the usual stress singularity of 0.5 at a crack tip in metals. Simple calculations show that for graphite/epoxy systems, the stress singularities become important over a distance from the free edge which is of the order of a few fiber diameters. However, over such a distance, the assumption of material homogeneity made by all analyses breaks down and the bimaterial nature of the laminate (fiber-resin) must be taken into account. Hence, the singularity appears to be important in a region where the assumptions made for the calculation method break down.

As a result, a solution that does not predict a singularity and a solution that does, are equally valid over the range of interest. Very close to the free edge, (within a few fiber diameters) both theories fail and a theory taking into account the properties of the fiber and the matrix separately should be used. Furthermore, as it will be shown in chapter 7, delamination is not a point phenomenon and the stress values right at the free edge are not as important as the actual stress distributions over a region close to the free edge (which is a few fiber diameters wide). Thus, some averaging of the stresses over that region may be required if

theories that treat each ply as homogeneous throughout are used.

The experimental results reported to date are few compared to the number of analytical predictions available, and inconclusive mainly because the measurement of stresses, strains, or displacements is made very difficult by the fact that the boundary layer is very small. So, most methods are based on few data points at special locations on the laminate, mainly on the top or at the free edge. More data are needed and for all interfaces of a laminate in order to establish which of the available analytical methods are more reliable.

CHAPTER THREE

FORMULATION OF THE PROBLEM

3.1 Governing equations

Consider the laminate and the axis system shown in Figure 2.1. The complete state of stress of a composite laminate under tension is described by the 15 equations of elasticity. For any ply, these can be divided into three basic sets of equations.

The first set consists of the three equilibrium equations (neglecting body forces):

$$\frac{\partial \sigma_{11}}{\partial x_1} + \frac{\partial \sigma_{12}}{\partial x_2} + \frac{\partial \sigma_{1z}}{\partial z} = 0 \qquad (3.1a)$$

$$\frac{\partial \sigma_{12}}{\partial x_1} + \frac{\partial \sigma_{22}}{\partial x_2} + \frac{\partial \sigma_{2z}}{\partial z} = 0 \qquad (3.1b)$$

$$\frac{\partial \sigma_{1z}}{\partial x_1} + \frac{\partial \sigma_{2z}}{\partial x_2} + \frac{\partial \sigma_{zz}}{\partial z} = 0 \qquad (3.1c)$$

where σ_{11}, σ_{22}, σ_{zz}, σ_{2z}, σ_{1z}, σ_{12} are the stresses in that ply as shown in Figure 3.1.
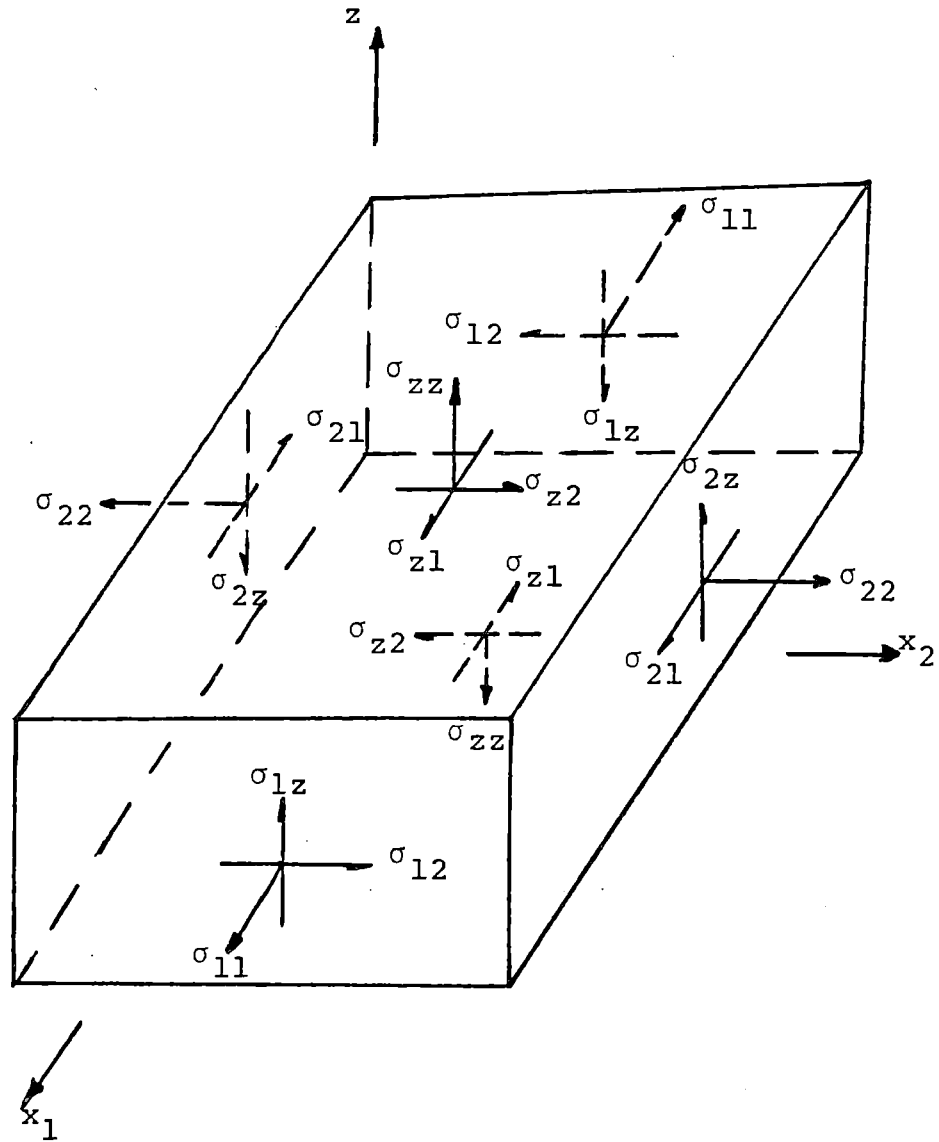
Figure 3.1. Stresses on a section of a ply

The second set consists of the six stress-strain equations:

$$
\begin{Bmatrix} \sigma_{11} \\ \sigma_{22} \\ \sigma_{zz} \\ \sigma_{2z} \\ \sigma_{1z} \\ \sigma_{12} \end{Bmatrix} = \begin{bmatrix} E_{11} & E_{12} & E_{13} & 0 & 0 & E_{16} \\ E_{12} & E_{22} & E_{23} & 0 & 0 & E_{26} \\ E_{13} & E_{23} & E_{33} & 0 & 0 & E_{36} \\ 0 & 0 & 0 & E_{44} & E_{45} & 0 \\ 0 & 0 & 0 & E_{45} & E_{55} & 0 \\ E_{16} & E_{26} & E_{36} & 0 & 0 & E_{66} \end{bmatrix} \begin{Bmatrix} \varepsilon_{11} \\ \varepsilon_{22} \\ \varepsilon_{zz} \\ \gamma_{2z} \\ \gamma_{1z} \\ \gamma_{12} \end{Bmatrix} \tag{3.2a-f}
$$

where E_{ij} are the stiffness coefficients and ε_{11}, ε_{22}, ε_{zz}, ε_{2z}, ε_{1z}, and ε_{12} are the strains in that ply. Note that for convenience, engineering and tensor notations are mixed here. The tensor notation will be used for sresses and strains with the subscript 3 changed into z for emphasis. The engineering notation will be used for elastic stiffnesses and/or compliances.

Finally, the last set is made up of the six strain-displacement relations.

$$
\varepsilon_{11} = \frac{\partial u}{\partial x_1} \qquad\qquad \gamma_{2z} = \frac{\partial v}{\partial z} + \frac{\partial w}{\partial x_2}
$$

$$
\varepsilon_{22} = \frac{\partial v}{\partial x_2} \qquad\qquad \gamma_{1z} = \frac{\partial u}{\partial z} + \frac{\partial w}{\partial x_1} \tag{3.3a-f}
$$

$$
\varepsilon_{zz} = \frac{\partial w}{\partial z} \qquad\qquad \gamma_{12} = \frac{\partial u}{\partial x_2} + \frac{\partial v}{\partial x_1}
$$

where u, v, w are the displacements in that ply.

3.2 Boundary conditions and stress continuity

The above equations are to be solved subject to the following boundary conditions:

a) $\sigma_{zz} = \sigma_{2z} = \sigma_{1z} = 0$ at the top and bottom of the laminate since there is no load applied on those surfaces.

b) $\sigma_{22} = \sigma_{2z} = \sigma_{12} = 0$ at the free edges (corresponding to the two stress-free faces that are perpendicular to the x_2 direction in Figure 2.1).

In addition, at every interface, σ_{zz}, σ_{2z}, σ_{1z} must be continuous.

3.3 Assumptions

The following assumptions are made:

1. Each ply can be modelled as macroscopically homogeneous. That is, the individual properties of fiber and matrix are "smeared out".

2. All six stresses exist. This means that the laminate is not in a state of plane stress as it is in the case with the CLPT where the three interlaminar stresses σ_{zz}, σ_{2z}, and σ_{1z} are taken to be zero.

3. Far from the free edge, i.e. outside the BL, the CLPT solution is recovered. This means that, outside the BL, the interlaminar stresses σ_{zz}, σ_{2z}, and σ_{1z} decay rapidly to zero.

4. Stresses do not depend on x_1. This is a version of the St. Venant principle saying that the details of load introduction are only important very close to the edge at which the load is applied.

5. The laminate is symmetric. This simplifies the analysis somewhat, in that bending-stretching coupling is avoided.

CHAPTER FOUR

THE FORCE-BALANCE METHOD AND SOME OF ITS IMPLICATIONS

4.1 Basic setup

Any physical body at rest, or any part of it, must be under force and moment equilibrium. For the particular problem at hand, the force-balance method requires that every section of a laminate, sufficiently large so that the assumption of homogeneity is still valid, is under overall force and moment equilibrium.

Consider the laminate section shown in Figure 4.1. The laminate is assumed wide enough so that the 2^- face (distance b from the free edge) is far from the free edge and the CLPT solution is recovered so that the interlaminar stresses are zero there.

The dimensions a and b are taken to be the laminate half-length and half-width (see Figure 2.1), but they can have any value as long as the section can still be treated as homogeneous and the 2^- face is far from the free edge.

For convenience, the following coordinate transformation is introduced:

$$x = b - x_2 \qquad (4.1)$$
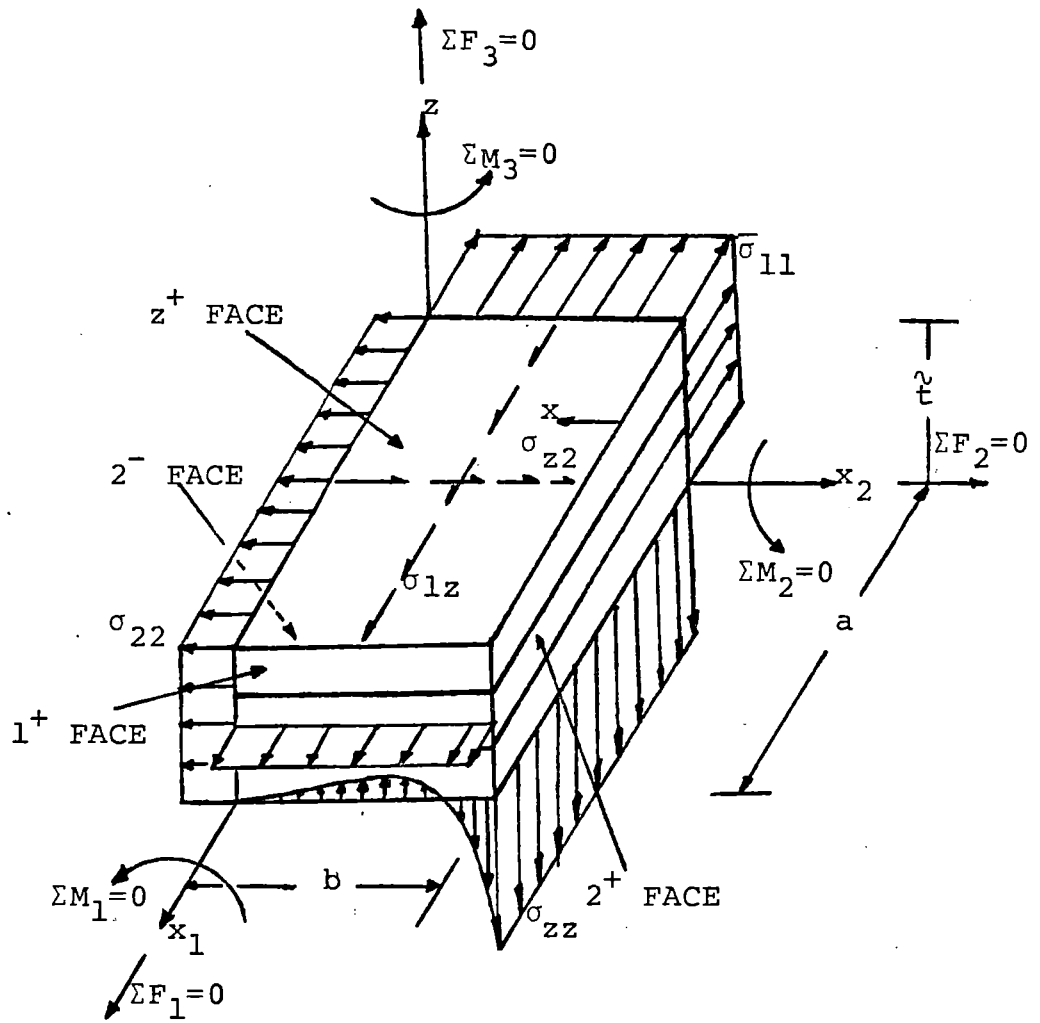
Figure 4.1. Integral equilibrium of a laminate section

so that x is zero at the free edge and equal to b at the center of the laminate.

Taking overall summation of forces in the three directions and setting the result equal to zero, the three force equilibrium equations read (integrals on x are from b to 0)

$\Sigma F_1 = 0$:

$$-\int_{1^+}\sigma_{11}dxdz+\int_{1^-}\sigma_{11}dxdz-\int_{z^+}\sigma_{1z}dx_1dx+\int_{z^-}\sigma_{1z}dx_1dx-\int_{2^-}\sigma_{12}dx_1dz=0 \qquad (4.2)$$

$\Sigma F_2 = 0$:

$$-\int_{2^-}\sigma_{22}dx_1dz-\int_{1^+}\sigma_{12}dxdz+\int_{1^-}\sigma_{12}dxdz-\int_{z^+}\sigma_{2z}dx_1dx+\int_{z^-}\sigma_{2z}dx_1dx=0 \qquad (4.3)$$

$\Sigma F_3 = 0$:

$$-\int_{z^+}\sigma_{zz}dx_1dx+\int_{z^-}\sigma_{zz}dx_1dx+\int_{1^+}\sigma_{1z}dx_2dz-\int_{1^-}\sigma_{1z}dx_2dz=0 \qquad (4.4)$$

The moment equilibrium equations have the form:

$\Sigma M_1 = 0$:

$$-\int_{1^+}\sigma_{1z}(b-x)dxdz+\int_{1^-}\sigma_{1z}(b-x)dxdz+\int_{1^+}\sigma_{12}zdxdz-\int_{1^-}\sigma_{12}zdxdz$$

$$+\int_{2^-}\sigma_{22}zdx_1dz+\int_{z^+}\sigma_{2z}\tilde{t}dxdx_1-\int_{z^+}\sigma_{zz}(b-x)dxdx_1+\int_{z^-}\sigma_{zz}(b-x)dxdx_1=0 \qquad (4.5)$$

$\Sigma M_2 = 0$:

$$-\int_{1^+}\sigma_{11}zdxdz+\int_{1^-}\sigma_{11}zdxdz+\int_{1^-}\sigma_{1z}adxdz-\int_{2^-}\sigma_{12}zdx_1dz+\int_{z^+}\sigma_{zz}x_1dx_1dx$$

$$-\int_{z^-}\sigma_{zz}x_1dx_1dx-\int_{z^+}\sigma_{1z}\tilde{t}dx_1dx=0 \qquad (4.6)$$

44

$$\Sigma M_3 = 0:$$

$$\int_{1^+}\sigma_{11}(b-x)dxdz - \int_{1^-}\sigma_{11}(b-x)dxdz - \int_{1^+}\sigma_{12}a\,dxdz - \int_{2^-}\sigma_{22}x_1dx_1d_z$$

$$-\int_{z^+}\sigma_{2z}x_1dx_1dx + \int_{z^-}\sigma_{2z}x_1dx_1dx + \int_{z^+}\sigma_{1z}(b-x)dxdx_1 - \int_{z^-}\sigma_{1z}(b-x)dxdx_1 = 0 \quad (4.7)$$

Equations 4.2-4.7 are the general force and moment equilibrium equations for a laminate section with the 2^- face outside the boundary layer. The fact that the 2^- face is not inside the boundary layer, simplifies the equations because terms involving interlaminar stresses integrated over that face are zero because the interlaminar stresses are zero there.

Use of the assumption that stresses do not depend on x_1 (i.e. $\partial/\partial x_1 = 0$) yields,

$$\Sigma F_1 = 0:$$

$$-\int_{z^+}\sigma_{1z}dx + \int_{z^-}\sigma_{1z}dx - \int_{2^-}\sigma_{12}dz = 0 \quad (4.8)$$

$$\Sigma F_2 = 0:$$

$$-\int_{z^+}\sigma_{2z}dx + \int_{z^-}\sigma_{2z}dx - \int_{2^-}\sigma_{22}dz = 0 \quad (4.9)$$

$$\Sigma F_3 = 0:$$

$$-\int_{z^+}\sigma_{zz}dx + \int_{z^-}\sigma_{zz}dx = 0 \quad (4.10)$$

$$\Sigma M_1 = 0:$$

$$\int_{z^+}\sigma_{2z}\tilde{t}dx - \int_{z^+}\sigma_{zz}(b-x)dx + \int_{z^-}\sigma_{zz}(b-x)dx + \int_{2^-}\sigma_{22}z\,dz = 0 \quad (4.11)$$

$\Sigma M_2 = 0:$

$$\int_{1^+}\sigma_{1z}dxdz - \int_{2^-}\sigma_{12}zdz + \frac{a}{2}\int_{z^+}\sigma_{zz}dx - \frac{a}{2}\int_{z^-}\sigma_{zz}dx - \frac{t}{t}\int_{z^+}\sigma_{1z}dx = 0 \qquad (4.12)$$

$\Sigma M_3 = 0:$

$$-\int_{1^+}\sigma_{12}dxdz - \frac{a}{2}\int_{2^-}\sigma_{22}dz - \frac{a}{2}\int_{z^+}\sigma_{2z}dx + \frac{a}{2}\int_{z^-}\sigma_{2z}dx + \int_{z^+}\sigma_{1z}(b-x)dx$$

$$-\int_{z^-}\sigma_{1z}(b-x)dx = 0 \qquad (4.13)$$

Equations 4.9 and 4.10 can be placed in the last three equations and the following simplified forms of the moment equilibrium equations are obtained:

$\Sigma M_1 = 0:$

$$\frac{t}{t}\int_{z^+}\sigma_{2z}dx + \int_{z^+}\sigma_{zz}xdx - \int_{z^-}\sigma_{zz}xdx + \int_{2^-}\sigma_{22}zdz = 0 \qquad (4.11a)$$

$\Sigma M_2 = 0:$

$$\int_{1^+}\sigma_{1z}dxdz - \int_{2^-}\sigma_{12}zdz - \frac{t}{t}\int_{z^+}\sigma_{1z}dx = 0 \qquad (4.12a)$$

$\Sigma M_3 = 0:$

$$-\int_{1^+}\sigma_{12}dxdz + \int_{z^+}\sigma_{1z}(b-x)dx - \int_{z^-}\sigma_{1z}(b-x)dx = 0 \qquad (4.13a)$$

As it will be shown in the next chapter, the assumption that stresses do not depend on x_1, the boundary condition that requires that the 2^+ face is stress-free (sections 3.2 and 3.3), and the additional assumption that the x_2 and z dependence can be separated for each of the stresses (this assumption is introduced in the next chapter), result in the force

and moment equilibrium equations 4.8-4.10 4.11a, 4.12a, and 4.13a being identically satisfied.

4.2 Some implications

Consider now equation 4.10. The z^+ face can be made to coincide with the top surface of the laminate, and equation 4.10 will still be valid. On the z^+ face however, σ_{zz} is now zero. Then, equation 4.10 reduces to,

$$\int_{z^-} \sigma_{zz} dx = 0 \tag{4.14}$$

which is valid for any z^- location and hence for any ply interface. Equation 4.14 implies that σ_{zz} plotted as a function of distance x from the free edge, must cross the x axis at least once. Two possible plots for σ_{zz} versus x are shown in figure 4.2. Note that far from the free edge, (x large) σ_{zz} is zero so that the CLPT solution predicting zero σ_{zz} at the far field is recovered.

Another conclusion can be drawn for angle-plied laminates (only $+\theta$ or $-\theta$ fiber orientations), from equation 4.9.

The stress field must recover the CLPT solution far from the free edge. The CLPT predicts that for angle ply laminates

$$\sigma_{22}^L, [\theta i] = 0 \tag{4.15}$$
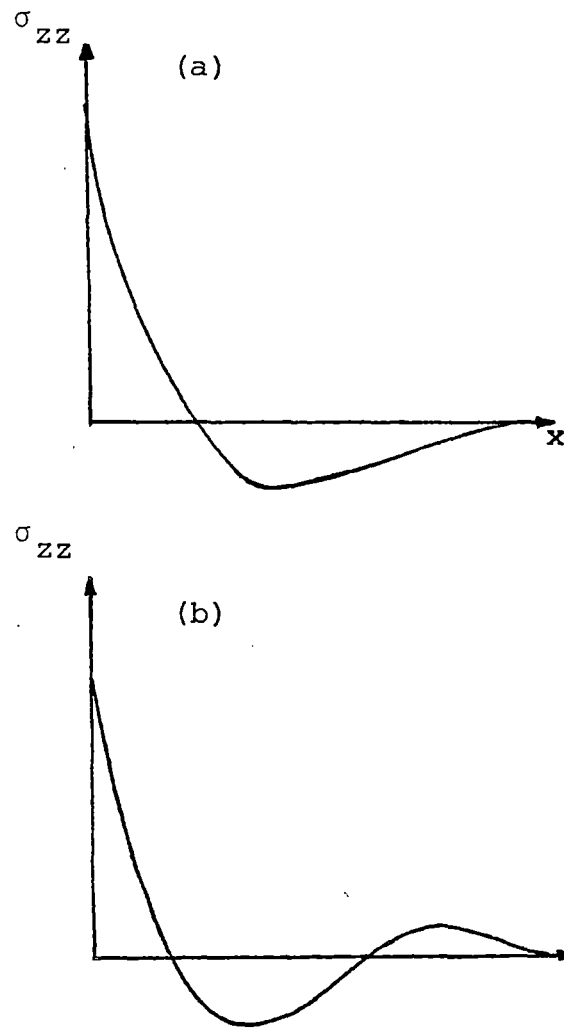
Figure 4.2. Possible shapes ("lowest modes") for σ_{zz}:
(a) one crossing; and (b) two crossings.

in each ply. This means that the force equilibrium equation 4.9 becomes,

$$-\int_{z^+} \sigma_{2z} dx + \int_{z^-} \sigma_{2z} dx = 0 \qquad (4.16)$$

for an angle-plied laminate. Again, by letting the z^+ face coincide with the top surface of the laminate, where σ_{2z} is zero, one obtains:

$$\int_{z^-} \sigma_{2z} dx = 0 \qquad (4.17)$$

for any ply interface. This means that σ_{2z} is either identically zero in each ply, or it crosses the x axis at least once in angle-ply laminates. Possible shapes for σ_{2z} are shown in figure 4.3. It should be noted that σ_{2z} is zero both at the free edge and far from it, in agreement with the stress-free boundary condition in section 3.2 and assumption 3 in section 3.3 (which requires that σ_{2z} is zero far from the free edge so that the CLPT result $\sigma_{2z}=0$ is recovered).

The above result for angle-plied laminates shows that results reported for [±45]s laminates in [5,24], where it appears that σ_{2z} does not cross the x axis, do not satisfy integral force equilibrium in the x_2 direction (see Figure 4.1).

σ_{2z}

(a)

x

σ_{2z}

(b)

x
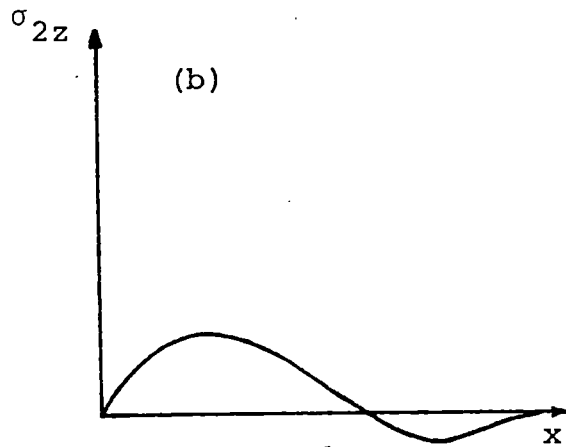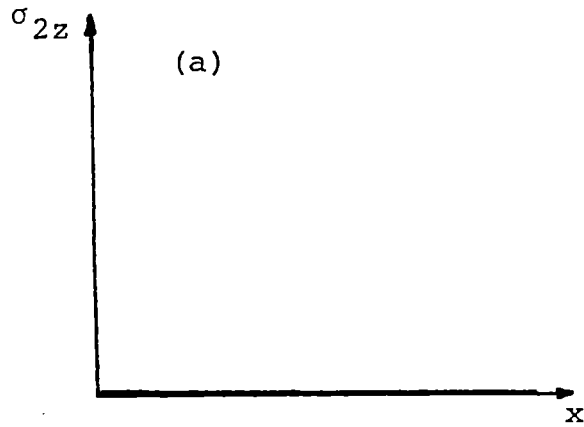
Figure 4.3. Possible shapes ("lowest modes") for σ_{2z}
for an angle-plied laminate: (a) σ_{2z}
identically equal to zero; and (b) σ_{2z}
one crossing

A very similar result as equation 4.17 can be found for cross-plied laminates (only 0° or 90° fiber orientations). using the force equilibrium in the x_1 direction equation 4.8 and based on the fact that σ_{12} is zero for cross-plied laminates:

$$\int_z {}^-\sigma_{1z} dx = 0 \qquad\qquad (4.18)$$

which implies that σ_{1z} is either identically zero in every ply of a cross-plied laminate, or crosses the x axis at least once. Note that there is a slight difference from the σ_{2z} case, in that σ_{1z} does not have to go to zero at the free edge.

It will be shown in chapter 5 that, under the assumption that stresses do not depend on x_1, σ_{1z} is identically zero for a cross-plied laminate.

CHAPTER FIVE

SOLUTION PROCEDURE

5.1 Equilibrium equations and general shape functions for the stresses

The solution to the problem is based on the principle of minimum complementary potential energy. According to this principle [40], out of all admissible stress states, those which also satisfy the requirements of geometric compatibility give stationary values to the complementary energy. Here, the word "admissible" means that the stress state satisfies the equations of equilibrium (3.1), the boundary conditions and the conditions for stress continuity. As an additional requirement, which will turn out to be very useful, satisfaction of integral equilibrium (force and moment balance) will be imposed.

The solution procedure can then be broken up into the following steps:

1. Choose a stress state.

2. Satisfy integral and differential equilibrium.

3. Satisfy boundary conditions and stress continuity.

4. Determine the remaining unknown parameters in the stress expressions by minimizing the complementary energy in the laminate.

Each ply is considered separately (see Figure 5.1) and, by symmetry, a quarter of a ply is sufficient to describe the stress field.

Under the assumption that the stresses do not depend on x_1, the differential equilibrium equations 3.1a-3.1c become,

$$\frac{\partial \sigma_{12}}{\partial x_2} + \frac{\partial \sigma_{1z}}{\partial z} = 0 \tag{5.1}$$

$$\frac{\partial \sigma_{22}}{\partial x_2} + \frac{\partial \sigma_{2z}}{\partial z} = 0 \tag{5.2}$$

$$\frac{\partial \sigma_{2z}}{\partial x_2} + \frac{\partial \sigma_{zz}}{\partial z} = 0 \tag{5.3}$$

and using the fact that $\frac{\partial}{\partial x_2} = -\frac{\partial}{\partial x}$ (see the coordinate transformation of equation 4.1):

$$\frac{\partial \sigma_{12}}{\partial x} = \frac{\partial \sigma_{1z}}{\partial z} \tag{5.4}$$

$$\frac{\partial \sigma_{22}}{\partial x} = \frac{\partial \sigma_{2z}}{\partial z} \tag{5.5}$$

$$\frac{\partial \sigma_{2z}}{\partial x} = \frac{\partial \sigma_{zz}}{\partial z} \tag{5.6}$$
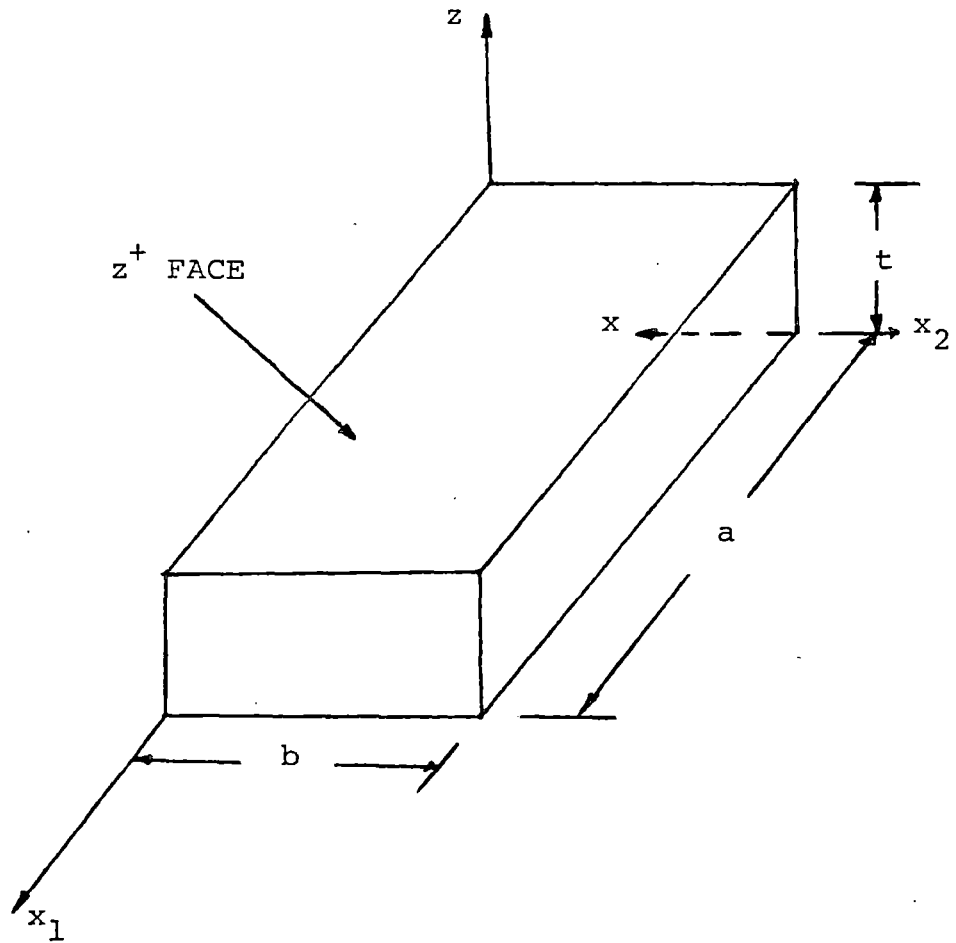
Figure 5.1. Quarter of a single ply of thickness t

At this point, another assumption is introduced. It will be assumed that the x and z dependence for each of the stresses (except σ_{11}) can be separated. Each of these stresses can then be viewed as being represented by a product of two functions (one in x and one in z) together forming an eigenfunction corresponding to a certain stress state.

Under this assumption, the stresses can be written as:

$$\sigma_{11} = f(x,z) \tag{5.7}$$

$$\sigma_{22} = f_{22}(x)\, g_{22}(z) \tag{5.8}$$

$$\sigma_{zz} = f_{33}(x)\, g_{33}(z) \tag{5.9}$$

$$\sigma_{2z} = f_{23}(x)\, g_{23}(z) \tag{5.10}$$

$$\sigma_{1z} = f_{13}(x)\, g_{13}(z) \tag{5.11}$$

$$\sigma_{12} = f_{12}(x)\, g_{12}(z) \tag{5.12}$$

where $f_{ij}(x)$, $g_{ij}(z)$ are functions to be determined. Introducing equations 5.8-5.12 into equations 5.4-5.6 yields the following set of ordinary differential equations:

$$\frac{df_{12}}{dx} = f_{13} \quad \text{(a)} \qquad\qquad g_{12} = \frac{dg_{13}}{dz} \quad \text{(d)}$$

$$\frac{df_{22}}{dx} = f_{23} \quad \text{(b)} \qquad\qquad g_{22} = \frac{dg_{23}}{dz} \quad \text{(e)} \qquad \text{(5.13a-f)}$$

$$\frac{df_{23}}{dx} = f_{33} \quad \text{(c)} \qquad\qquad g_{23} = \frac{dg_{33}}{dz} \quad \text{(f)}$$

It can be seen that equation 5.13a decouples from equations 5.13b and 5.13c. Similarly, equation 5.13d decouples from equations 5.13e and 5.13f. Then, the functions $f_{ij}(x)$ and $g_{ij}(z)$ can be grouped as shown in Table 5.1.

Then, if any one of the functions in a group is known, the other functions in the same group can be determined using the corresponding equations. This means that the minimum number of shape functions that must be assumed is 4, two f_{ij} and two g_{ij} functions. The remaining 6 functions can be determined with the use of the equilibrium equations 5.13a-f.

5.2 Assumed functional forms

Consider now the z dependence of the stresses (g_{ij} functions). The CLPT predicts that far from the free edge σ_{22} and σ_{12} are constant. This implies that g_{22} and g_{12} must be constant because, if they depended on z, σ_{22} and σ_{12} would be functions of z far from the free edge.

Therefore,

$$g_{12} = B_1 \tag{5.14a}$$

$$g_{22} = B_3 \tag{5.14b}$$

And use of the ordinary differential equations 5.13d-5.13f gives:

TABLE 5.1

GROUPS OF FUNCTIONS f_{ij} and g_{ij}

Group	Functions	Corresponding Equations
1	f_{12}, f_{13}	5.13a
2	f_{22}, f_{23}, f_{33}	5.13b, 5.13c
3	g_{12}, g_{13}	5.13d
4	g_{22}, g_{23}, g_{33}	5.13e, 5.13f

$$g_{13} = B_1 z + B_2 \qquad\qquad (5.14c)$$

$$g_{23} = B_3 z + B_4 \qquad\qquad (5.14d)$$

$$g_{33} = B_3 \frac{z^2}{2} + B_4 z + B_5 \qquad\qquad (5.14e)$$

where B_1-B_5 are constants to be determined.

For the x dependence, (f_{ij} functions) one must resort to the conclusions drawn in the previous chapter with the force-balance method. Consider the force equilibrium in the z direction equation 4.14 and Figure 4.2. It appears that σ_{zz} shapes with 2 crossings (Figure 4.2b) or more, correspond to a "higher mode" i.e. a state of stress where the energy stored in the ply and, as a result, in the whole laminate is higher than what it would be if the σ_{zz} versus x plot crossed the x axis once. Some evidence that this is true is given in Appendix 1 where the radius of curvature at an interface of a cross-plied laminate is calculated.

As a result, since a minimum energy state is always sought, if a stress shape similar to that of Figure 4.1a is found to satisfy the governing equations, this will be the minimum energy state and will thus be the required stress shape. For a rapid decay of σ_{zz}, so that far from the free edge σ_{zz} tends to zero, exponential functions must be used.

From table 5.1 it is seen that any of the three functions f_{22}, f_{23}, f_{33} can be assumed and the other two will then be

determined from equations 5.13b, 5.13c. It turns out that the calculations are somewhat simpler if the shape of f_{22} is assumed.

Hence,

$$f_{22} = A_1 e^{-\phi X} + A_2 e^{-\lambda \phi X} + A_3 \qquad (5.15a)$$

The two exponentials guarantee that, for a proper choice of the unknown constants A_1 and A_2, σ_{zz} will cross the x axis once in agreement with equation 4.14 and Figure 4.2a. The unknown constant A_3 is introduced so that, far from the free edge, σ_{22} will approach the usually nonzero CLPT constant value for σ_{22}.

The exponents ϕ and $\lambda \phi$ are also unknown at this point. Note that ϕ has the dimensions of 1/length and λ is dimensionless. The reason for writing the exponents in that form is that the resulting equations for λ and ϕ are simpler to solve than what they would be if the exponents were λ and ϕ instead of ϕ and $\lambda \phi$. This will be clearer later when the equations for λ and ϕ are obtained by minimizing the comple-mentary energy of the laminate.

For f_{12} (or f_{13}) the available information is not as con-clusive. Since σ_{12} must be zero at the free edge, three possi-ble shapes for f_{12} are shown in Figure 5.2 (for positive far-field value of σ_{12}). Again, the argument is made that the
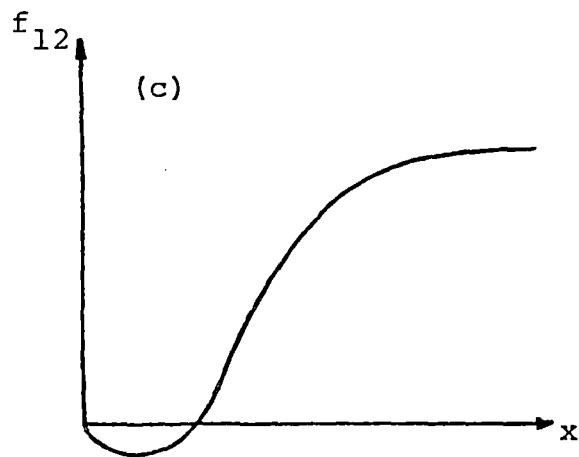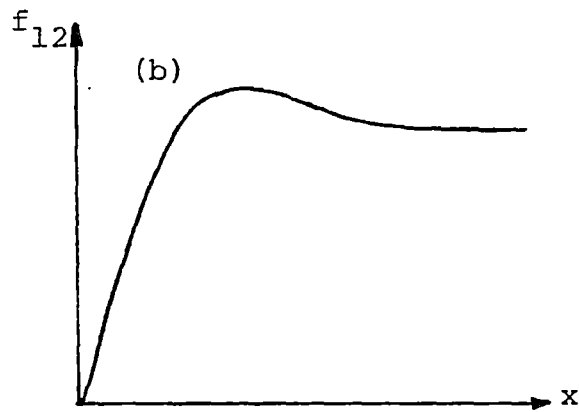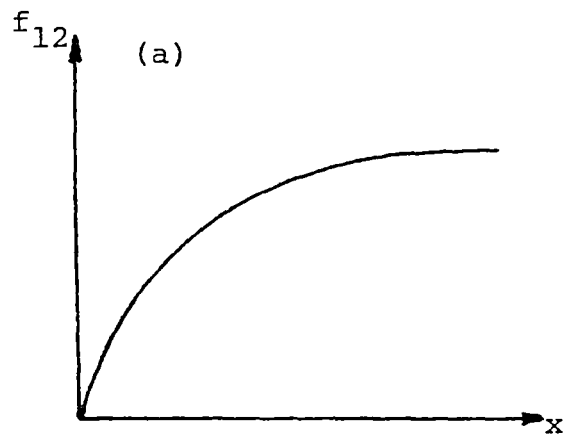
Figure 5.2. Possible shapes ("lowest modes") for f_{12}:
(a) no stationary point; (b) one stationary
point; and (c) one stationary point with
sign reversal

cases corresponding to figures 5.2b and 5.2c result in higher laminate energy and hence, for minimum laminate energy, a shape similar to that in Figure 5.2a should be used.

Then, the following functional form for f_{12} is assumed:

$$f_{12} = A_4 + A_5 e^{-\phi X} \qquad (5.15b)$$

The exponential is used so that σ_{12} approaches "rapidly" its far field CLPT value. The same exponent ϕ is used as for f_{22} in equation 5.15a mainly because a different exponent would result in an inconsistency in the character of the equilibrium equations as is shown in Appendix 2.

Using the differential equations 513a-5.13c and the assumed shapes for f_{22} and f_{12} (equations 5.15a and 5.15b), the remaining f_{ij} functions can be obtained:

$$f_{23} = -A_1 \phi e^{-\phi X} - \lambda \phi A_2 e^{-\lambda \phi X} \qquad (5.15c)$$

$$f_{33} = A_1 \phi^2 e^{-\phi X} + \lambda^2 \phi^2 A_2 e^{-\lambda \phi X} \qquad (5.15d)$$

$$f_{13} = -\phi A_5 e^{-\phi X} \qquad (5.15e)$$

where A_5 is an unknown constant. Table 5.2 summarizes the stress shapes so far.

TABLE 5.2

STRESS SHAPES

Function	Shape
f_{22}	$A_1 e^{-\phi x} + A_2 e^{-\lambda \phi x} + A_3$
f_{33}	$A_1 \phi^2 e^{-\phi x} + \lambda^2 \phi^2 A_2 e^{-\lambda \phi x}$
f_{23}	$-A_1 \phi e^{-\phi x} - \lambda \phi A_2 e^{-\lambda \phi x}$
f_{13}	$-\phi A_5 e^{-\phi x}$
f_{12}	$A_4 + A_5 e^{-\phi x}$
g_{22}	B_3
g_{33}	$B_3 \frac{z^2}{2} + B_4 z + B_5$
g_{23}	$B_3 z + B_4$
g_{13}	$B_1 z + B_2$
g_{12}	B_1

Using the shape functions in table 5.2 and substituting into equations 5.8-5.12 gives the expressions for all the stresses except σ_{11}, in a ply:

$$\sigma_{22} = (A_1 e^{-\phi X} + A_2 e^{-\lambda \phi X} + A_3) B_3 \qquad (5.16)$$

$$\sigma_{zz} = (A_1 \phi^2 e^{-\phi X} + \lambda^2 \phi^2 A_2 e^{-\lambda \phi X})(B_3 \frac{z^2}{2} + B_4 z + B_5) \qquad (5.17)$$

$$\sigma_{2z} = (-A_1 \phi e^{-\phi X} - \lambda \phi A_2 e^{-\lambda \phi X})(B_3 z + B_4) \qquad (5.18)$$

$$\sigma_{1z} = -\phi A_5 e^{-\phi X}(B_1 z + B_2) \qquad (5.19)$$

$$\sigma_{12} = (A_4 + A_5 e^{-\phi X}) B_1 \qquad (5.20)$$

It should be noted that λ and ϕ must be larger than zero so that the exponentials decay rather than grow.

5.3 Determination of σ_{11}

Due to the assumption that the stresses do not depend on x_1, σ_{11} drops out of the equilibrium equations. Two approaches were used for its determination. The first was to assume that in each ply σ_{11} was constant and equal to the CLPT value. The second was to actually determine σ_{11} with the use of the stress-strain and strain-displacement equations.

The second approach, being somewhat involved will be described briefly below. The inverted stress-strain equations 3.2a-3.2c have the form:

$$\epsilon_{11} = S_{11}\sigma_{11} + S_{12}\sigma_{22} + S_{13}\sigma_{zz} + S_{16}\sigma_{12} \tag{5.21}$$

$$\epsilon_{22} = S_{12}\sigma_{11} + S_{22}\sigma_{22} + S_{23}\sigma_{zz} + S_{26}\sigma_{12} \tag{5.22}$$

$$\epsilon_{zz} = S_{13}\sigma_{11} + S_{23}\sigma_{22} + S_{33}\sigma_{zz} + S_{66}\sigma_{12} \tag{5.23}$$

where S_{ij} are compliances for the particular ply in which the strains are evaluated.

Integrating the above equations with respect to x_1, x_2, and z and using the strain-displacement equations 3.3a-3.3c gives:

$$u = (S_{11}\sigma_{11} + S_{12}\sigma_{22} + S_{13}\sigma_{zz} + S_{16}\sigma_{12})x_1 + F(x_2,z) \tag{5.24}$$

$$v = S_{11}\int\sigma_{11}dx_2 + S_{22}\int\sigma_{22}dx_2 + S_{23}\int\sigma_{zz}dx_2 + S_{26}\int\sigma_{12}dx_2 + G(x_1,z) \tag{5.25}$$

$$w = S_{13}\int\sigma_{11}dz + S_{23}\int\sigma_{22}dz + S_{33}\int\sigma_{zz}dz + S_{36}\int\sigma_{12}dz + H(x_1,x_2) \tag{5.26}$$

where F, G, and H are unknown functions.

Then, using these expressions in the strain-displacement equations 3.3e and 3.3f, the following expressions are obtained:

$$x_1 \frac{\partial}{\partial x_2}(S_{11}\sigma_{11} + S_{12}\sigma_{22} + S_{13}\sigma_{zz} + S_{16}\sigma_{12}) + \frac{\partial F}{\partial x_2} + \frac{\partial G}{\partial x_1} =$$

$$= S_{16}\sigma_{11} + S_{26}\sigma_{22} + S_{36}\sigma_{zz} + S_{66}\sigma_{12} \tag{5.27}$$

and

$$x_1 \frac{\partial}{\partial z}(S_{11}\sigma_{11}+S_{12}\sigma_{22}+S_{13}\sigma_{zz}+S_{16}\sigma_{12}) + \frac{\partial F}{\partial z} + \frac{\partial H}{\partial x_1} =$$

$$= S_{45}\sigma_{2z}+S_{55}\sigma_{1z} \qquad (5.28)$$

The right hand sides of equations 5.27 and 5.28 are independent of x_1 because the stresses are assumed to be independent of x_1. This implies that the quantities $x_1\frac{\partial}{\partial x_2}(S_{11}\sigma_{11}+S_{12}\sigma_{22}+S_{13}\sigma_{zz}+S_{16}\sigma_{12})+\frac{\partial G}{\partial x_1}$ and $x_1\frac{\partial}{\partial z}(S_{11}\sigma_{11}+S_{12}\sigma_{22}+S_{13}\sigma_{zz}+S_{16}\sigma_{12})+\frac{\partial H}{\partial x_1}$ must be independent of x_1.

It can be seen that in the first of the two quantities above, $\frac{\partial G}{\partial x_1}$ is not a function of x_2 because G is only a function of x_1 and z (see equation 5.25). The rest of the first quantity however is a function of x_2 and therefore, the two parts separately must be independent of x_1. The fact that $x_1\frac{\partial}{\partial x_2}(S_{11}\sigma_{11}+S_{12}\sigma_{22}+S_{13}\sigma_{zz}+S_{16}\sigma_{12})$ is independent of x_1 implies that:

$$\frac{\partial}{\partial x_2}(S_{11}\sigma_{11}+S_{12}\sigma_{22}+S_{13}\sigma_{zz}+S_{16}\sigma_{12})=0 \qquad (5.29)$$

Similarly, it can be shown that the fact that $x_1\frac{\partial}{\partial z}(S_{11}\sigma_{11}+S_{12}\sigma_{22}+S_{33}\sigma_{zz}+S_{16}\sigma_{12})$ is not a function of x_1 gives:

$$\frac{\partial}{\partial z}(S_{11}\sigma_{11}+S_{12}\sigma_{22}+S_{13}\sigma_{zz}+S_{16}\sigma_{12})=0 \qquad (5.30)$$

Equation 5.29 implies that

$$S_{11}\sigma_{11}+S_{12}\sigma_{22}+S_{13}\sigma_{zz}+S_{16}\sigma_{12}=R(z) \qquad (5.31)$$

and equation 5.30 implies that

$$S_{11}\sigma_{11}+S_{12}\sigma_{22}+S_{13}\sigma_{zz}+S_{16}\sigma_{12}=Q(x_2) \tag{5.32}$$

where R and Q are unknown functions.

Equations 5.31 and 5.32 are compatible with one another only if R and Q are independent of z and x_2 respectively and are equal to the same constant:

$$R(z) = Q(x_2) = C_1 \tag{5.33}$$

Then, from either equation 5.31 or 5.32, the following expression is obtained for σ_{11}:

$$\sigma_{11} = \frac{C_1}{S_{11}} - \frac{S_{12}}{S_{11}}\sigma_{22} - \frac{S_{13}}{S_{11}}\sigma_{zz} - \frac{S_{16}}{S_{11}}\sigma_{12} \tag{5.34}$$

The uknown constant C_1 is determined by requiring that, far from the free edge, σ_{11} is equal to the CLPT value. Letting $\sigma^L_{ij[\theta i]}$ denote CLPT values one obtains:

$$\lim_{x\to\infty} \sigma_{11} = \frac{C_1}{S_{11}} - \frac{S_{12}}{S_{11}}\lim_{x\to\infty}\sigma_{22} - \frac{S_{13}}{S_{11}}\lim_{x\to\infty}\sigma_{zz} - \frac{S_{16}}{S_{11}}\lim_{x\to\infty}\sigma_{12} \tag{5.35}$$

or

$$\sigma^L_{11[\theta i]} = \frac{C_1}{S_{11}} - \frac{S_{12}}{S_{11}}\sigma^L_{22[\theta i]} - \frac{S_{16}}{S_{11}}\sigma^L_{12[\theta i]} \tag{5.36}$$

since the interlaminar stresses are zero far from the free edge (x approaching ∞). From this, C_1 is obtained as,

$$C_1 = S_{11}\sigma^L_{11_{[\theta i]}} + S_{12}\sigma^L_{22_{[\theta i]}} + S_{16}\sigma^L_{12_{[\theta i]}}$$

(5.37)

Finally substituting for C_1 in equation 5.34, the final expression for σ_{11} is:

$$\sigma_{11} = \frac{S_{11}\sigma^L_{11_{[\theta i]}} + S_{12}\sigma^L_{22_{[\theta i]}} + S_{16}\sigma^L_{12_{[\theta i]}}}{S_{11}} - \frac{S_{12}}{S_{11}}\sigma_{22} -$$

$$- \frac{S_{13}}{S_{11}}\sigma_{zz} - \frac{S_{16}}{S_{11}}\sigma_{12}$$

(5.38)

where σ_{22}, σ_{zz}, σ_{12} are given by equations 5.16, 5.17, and 5.20.

Equations 5.38 and 5.16-5.20 give the stresses in each ply. The strains in each ply can be determined with the use of the stress-strain equations 3.2a-f. The displacements in each ply cannot be determined exactly because the strain compatibility condition is satisfied only on the average by minimizing the laminate complementary energy.

5.4 Satisfaction of integral equilibrium equations

It will be shown now that the assumption that, for each stress shape, the x and z dependence can be separated along

with the boundary condition that the 2^+ face (see Figure 4.1) is stress-free, guarantees that the requirements of the force-balance method (equations 4.8-4.10, 4.11a-4.13a) are satisfied.

Consider the quarter-ply shown in Figure 5.1. Using the general expression for σ_{1z} in equation 5.11 and integrating with respect to x, one obtains:

$$\int_{z^+} \sigma_{1z} dx = g_{13}(t) \int_0^b f_{13}(x) dx \qquad (5.39)$$

Equation 5.13a is used to substitute for $f_{13}(x)$. An integration by parts gives,

$$\int_{z^+} \sigma_{1z} dx = g_{13}(t) \int_0^b \frac{df_{12}}{dx} dx = g_{13}(t)(f_{12}(b) - f_{12}(0)) \qquad (5.40)$$

Similarly, if σ_{1z} were integrated over the z^- face,

$$\int_{z^-} \sigma_{1z} dx = g_{13}(o)(f_{12}(b) - f_{12}(o)) \qquad (5.41)$$

Then, subtracting equation 5.41 from equation 5.40,

$$-\int_{z^+} \sigma_{1z} dx + \int_{z^-} \sigma_{1z} dx = (g_{13}(o) - g_{13}(t))(f_{12}(b) - f_{12}(o)) \qquad (5.42)$$

Now using the general expression for σ_{12} in equation 5.12 and integrating yields

$$\int_{2^-} \sigma_{12} dz = f_{12}(b) \int_0^t g_{12}(z) dz \qquad (5.43)$$

Using the equation for g_{12} (equation 5.13d) to substitute in equation 5.43 one gets,

$$\int_{2^-} \sigma_{12} dz = f_{12}(b) \, (g_{13}(t) - g_{13}(o)) \qquad (5.44)$$

Now the boundary condition,

$$\sigma_{12}(x = 0) = 0 \qquad (5.45)$$

implies (see the general expression for σ_{12} equation 5.12) that,

$$f_{12}(0) = 0 \qquad (5.46)$$

Placing 5.46 into 5.42 and then subtracting equation 5.44 from the resulting equation gives:

$$- \int_{z^+} \sigma_{1z} dx + \int_{z^-} \sigma_{1z} dx - \int_{2^-} \sigma_{12} dx = 0 \qquad (5.47)$$

which is identical to equation 4.8, the first of the six integral equilibrium equations. Therefore, it is seen that the assumptions made along with the boundary condition that σ_{12} is zero at the free edge, are equivalent to the equation of force equilibrium in the x_1 direction (equation 4.8).

In a similar manner, using the boundary conditions that σ_{22} and σ_{2z} are zero at the free edge, it can be shown that the other two Force-Balance equations (4.9 and 4.10) are equivalent to the assumptions made on the stress shapes.

The proof that the three moment equations(4.11a-4.13a) are also equivalent to the boundary conditions on σ_{22}, σ_{2z}, σ_{12} and the particular set of assumptions used is very analogous to that used for the force equilibrium equations but, being somewhat more involved, is omitted here. A full proof is given in Appendix 3.

It should be noted that the proof given was for a single ply of thickness t. The proof for any section of a laminate with thickness $\tilde{t}$ (see Figure 4.1) is essentially the same.

This result, that the requirements of the Force-Balance method (equations 4.8-4.13) are automatically satisfied by the set of assumptions and boundary conditions used in the current analysis, does not limit the importance of the Force-Balance method. The conclusions drawn in chapter 4 for general laminates and for angle-plied laminates are very important and cannot be deduced without the use of the force-balance method. Furthermore, if, for a more refined analysis, the assumption that the x and z dependence can be separated were relaxed, equations 4.8-4.13 would be very useful in furnishing important information on the functional form of the stresses to be used.

5.5 Boundary conditions and stress continuity

Before satisfying the boundary conditions, the far field condition that the stresses approach their CLPT value far from the free edge must be satisfied. For σ_{11} this condition is satisfied by construction (see equations 5.35-5.37). For the interlaminar stresses σ_{zz}, σ_{2z}, σ_{1z} the condition is satisfied by the use of decaying exponentials.

It remains to satisfy the far-field condition for σ_{22} and σ_{12}. From equation 5.16,

$$\sigma_{22} = A_1 e^{-\phi X} + A_2 e^{-\lambda \phi X} + A_3 \tag{5.48}$$

The constant B_3 can be taken to be equal to 1 with no loss of generality. This simply scales the constants Ai in the x dependence of the stress shapes (see table 5.2) by $1/B_3$.

Then, the far-field condition

$$\lim_{x \to \infty} \sigma_{22} = \sigma_{22[\theta i]}^{L} \tag{5.49}$$

implies:

$$A_3 = \sigma_{22[\theta i]}^{L} \tag{5.50}$$

Similarly for σ_{12} the far field condition,

$$\lim_{x \to \infty} \sigma_{12} = \sigma_{12[\theta i]}^{L} \tag{5.51}$$

implies

$$A_4 = \sigma_{12[\theta i]}^{L} \tag{5.52}$$

Now consider the boundary conditions at the free edge. The condition that σ_{2z} is zero at the free edge implies,

$$A_1 + \lambda A_2 = 0 \tag{5.53}$$

Similarly, the condition that σ_{22} is zero at the free edge implies that,

$$A_1 + A_2 + A_3 = 0 \tag{5.54}$$

From equations 5.50, 5.53, 5.54 one obtains:

$$A_1 = -\frac{\lambda \, \sigma^L_{22_{[\theta i]}}}{\lambda - 1} \tag{5.55}$$

$$A_2 = \frac{\sigma^L_{22_{[\theta i]}}}{\lambda - 1} \tag{5.56}$$

Finally, the condition that σ_{12} is zero at the free edge gives,

$$A_4 + A_5 = 0 \tag{5.57}$$

and using equation 5.52,

$$A_5 = -\sigma^L_{12_{[\theta i]}} \tag{5.58}$$

So far, all Ai have been determined. For convenience they are summarized in Table 5.3.

Setting $B_1 = 1$ (for the same reason as for B_3) and substituting for Ai, the following expressions are obtained for the stresses in a ply:

TABLE 5.3

CONSTANTS IN THE f_{ij} EXPRESSIONS

A_i	Value
A_1	$-\dfrac{\lambda \; \sigma^L_{22[\theta i]}}{\lambda - 1}$
A_2	$\dfrac{\sigma^L_{22[\theta i]}}{\lambda - 1}$
A_3	$\sigma^L_{22[\theta i]}$
A_4	$\sigma^L_{12[\theta i]}$
A_5	$-\sigma^L_{12[\theta i]}$

$$\sigma_{22} = \sigma^L_{22_{[\theta i]}} \left[1 - \frac{\lambda}{\lambda-1} \left(e^{-\phi X} - \frac{1}{\lambda} e^{-\lambda\phi X} \right) \right] \tag{5.59}$$

$$\sigma_{zz} = \phi^2 \frac{\lambda}{\lambda-1} \left(\lambda e^{-\lambda\phi X} - e^{-\phi X} \right) \left(\sigma^L_{22_{[\theta i]}} \frac{z^2}{2} + \tilde{B}_4 z + \tilde{B}_5 \right) \tag{5.60}$$

$$\sigma_{2z} = \phi \frac{\lambda}{\lambda-1} \left(e^{-\phi X} - e^{-\lambda\phi X} \right) \left(\sigma^L_{22_{[\theta i]}} z + \tilde{B}_4 \right) \tag{5.61}$$

$$\sigma_{1z} = \phi e^{-\phi X} \left(\sigma^L_{12_{[\theta i]}} z + \tilde{B}_2 \right) \tag{5.62}$$

$$\sigma_{12} = \sigma^L_{12_{[\theta i]}} (1 - e^{-\phi X}) \tag{5.63}$$

where

$$\tilde{B}_4 = \sigma^L_{22_{[\theta i]}} B_4 \tag{5.64a}$$

$$\tilde{B}_5 = \sigma^L_{22_{[\theta i]}} B_5 \tag{5.64b}$$

$$\tilde{B}_2 = \sigma^L_{12_{[\theta i]}} B_2 \tag{5.64c}$$

To determine the B_i (or $\tilde{B}_i$), the remaining boundary conditions and the condition of stress continuity at ply interfaces are used.

The numbering scheme shown in Figure 5.3 is introduced, where plies are numbered from top to bottom. The total number of plies in the laminate is n. Also, for each ply, the coordinate system shown in Figure 5.1 is used and is repeated in
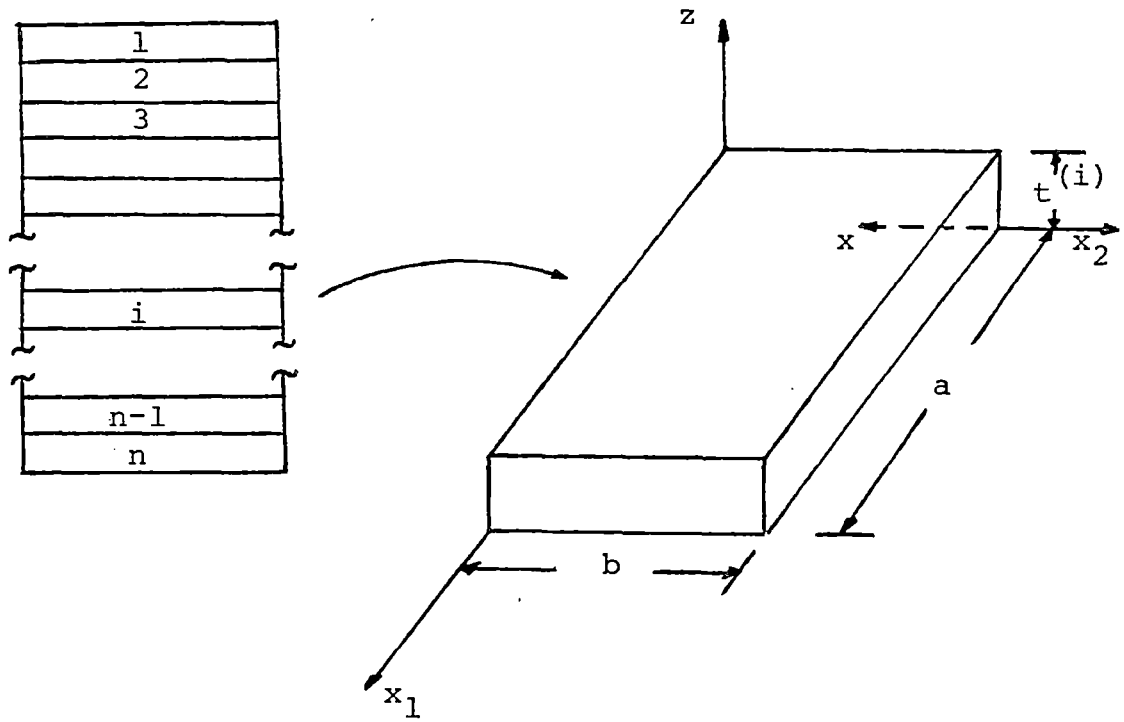
Figure 5.3. Ply numbering scheme and coordinate system

Figure 5.3 for convenience. To differentiate between plies, superscripts denoting the corresponding ply are used.

Since σ_{2z} must be zero at the bottom surface,

$$\sigma_{2z}^{(n)} \ (z=0) = 0 \tag{5.65}$$

which implies that

$$B_4^{(n)} = 0 \tag{5.66}$$

For the next interface up, continuity of σ_{2z} gives:

$$\sigma_{2z}^{(n)} \ (z=t^{(n)}) = \sigma_{2z}^{(n-1)} \ (z=0) \tag{5.67}$$

or using the expression for σ_{2z} (equation 5.61) at any x location

$$\tilde{B}_4^{(n-1)} = \sigma_{22_{[\theta_n]}}^{L} \ t^{(n)} \tag{5.68}$$

The procedure can be repeated for the other interfaces. The general expression for $\tilde{B}_4^{(i)}$ (ith ply) is,

$$\tilde{B}_4^{(i)} = \sum_{j=n}^{i+1} \sigma_{22_{[\theta_j]}}^{L} \ t^{(j)} \tag{5.69}$$

Knowing $\tilde{B}_4^{(i)}$ and using the condition that σ_{zz} is zero at the bottom surface and continuous at the other ply interfaces, the same procedure as for σ_{2z} gives:

$$\tilde{B}_5^{(i)} = \sum_{j=n}^{i+1} \ [\sigma_{22_{[\theta_j]}}^{L} \ \frac{t^{(j)^2}}{2} + \sigma_{22_{[\theta_j]}}^{L} \ t^{(j)} \sum_{k=j-1}^{k=i+1} t^{(k)}] \tag{5.70}$$

with

$$\tilde{B}_5^{(n)} = 0 \tag{5.71}$$

and

$$\tilde{B}_5^{(n-1)} = \sigma_{22_{[\theta_n]}}^L \frac{t^{(n)^2}}{2} \tag{5.72}$$

In exactly the same way as for $\tilde{B}_4^{(i)}$ and using the conditions on σ_{1z}, and equation 5.62 one obtains:

$$\tilde{B}_2^{(i)} = \sum_{j=n}^{i+1} \sigma_{12_{[\theta_j]}}^L t^{(j)} \tag{5.73}$$

with

$$B_2^{(n)} = 0 \tag{5.74}$$

It should be noted that in deriving the above expressions for $B_2^{(i)}$, $B_4^{(i)}$, $B_5^{(i)}$, it was assumed that each ply has a different thickness from its adjacent plies. For the special case where all the plies have the same thickness t, equations 5.69, 5.70, and 5.73 simplify to:

$$\tilde{B}_4^{(i)} = t \sum_{j=n}^{i+1} \sigma_{22_{[\theta_j]}}^L \tag{5.69a}$$

$$\tilde{B}_5^{(i)} = t^2 \sum_{j=n}^{i+1} [\frac{1}{2} \sigma_{22_{[\theta_j]}}^L + (j-i-1) \sigma_{22_{[\theta_j]}}^L] \tag{5.70a}$$

$$\tilde{B}_2^{(i)} = t \sum_{j=n}^{i+1} \sigma_{12_{[\theta_j]}}^L \tag{5.73a}$$

It is important to note that all the stacking sequence effects are "hidden" in the B_i terms. If the stacking sequence

in a laminate is changed, these terms change and, as a result, the exponents λ and ϕ will change.

It can be seen that, with this procedure of determining $\tilde{B}_2$, $\tilde{B}_4$, and $\tilde{B}_5$, all the unknnown $\tilde{B}_i$ will have been determined right after the conditions of stress continuity are applied at the first interface (the one between the first and second ply). The B_i values are summarized in Table 5.4.

All unknowns (except for λ and ϕ) have been determined at this point. The condition that the top of the laminate is stress-free (i.e. $\sigma_{zz}^{(1)}(z{=}t^{(1)}){=}\sigma_{2z}^{(1)}(z{=}t^{(1)}){=}\sigma_{1z}^{(1)}(z{=}t^{(1)}){=}0$) has not been satisfied yet, and it cannot be used to determine λ or ϕ because both λ and ϕ cancel out from the corresponding equations. This condition then, should be identically satisfied and can serve to check if there are any inconsistencies in the stress shapes.

Since the variable ply thickness case is algebraically complicated, only the case with constant ply thickness will be demonstrated, i.e. it will be shown that for a symmetric laminate where all the plies have the same thickness, the stress shapes determined so far guarantee that the top surface of the laminate is stress-free. However, this is still valid for laminates with plies of variable thickness.

At the top of the laminate, the condition that σ_{zz} is zero takes the form (see equations 5.60, 5.69a, and 5.70a),

TABLE 5.4

CONSTANTS IN THE g_{ij} EXPRESSIONS

$B_j^{(i)}$	Value
$B_1^{(i)}$	1
$B_2^{(i)}$	$\displaystyle\sum_{j=n}^{i+1} \sigma^L_{12[\theta j]} \, t^{(j)}$
$B_3^{(i)}$	1
$B_4^{(i)}$	$\displaystyle\sum_{j=n}^{i+1} \sigma^L_{22[\theta j]} \, t^{(j)}$
$B_5^{(i)}$	$\displaystyle\sum_{j=n}^{i+1} \left[\sigma^L_{22[\theta j]} \frac{t^{(j)2}}{2} + \sigma^L_{22[\theta j]} \, t^{(j)} \sum_{k=j-1}^{k=i+1} t^k \right]$

$$\sigma^L_{22[\theta_1]} \frac{t^2}{2} + [\sigma^L_{22[\theta_n]} + \ldots + \sigma^L_{22[\theta_2]}] \, t^2 +$$

$$\frac{t^2}{2} [\sigma^L_{22[\theta_n]} + \ldots + \sigma^L_{22[\theta_2]}] + t^2 [(n-2) \, \sigma^L_{22[\theta_n]} +$$

$$+ (n-3) \, \sigma^L_{22[\theta_{n-1}]} + \ldots + \sigma^L_{22[\theta_3]}] = 0 \qquad (5.75)$$

or rearranging and cancelling out the thickness terms,

$$\frac{1}{2} [\sigma^L_{22[\theta_n]} + \ldots + \sigma^L_{22[\theta_1]}] + (n-1) \, \sigma^L_{22[\theta_n]} +$$

$$(n-2) \, \sigma^L_{22[\theta_{n-1}]} + \ldots + 2\sigma^L_{22[\theta_3]} + \sigma^L_{22[\theta_2]} = 0 \qquad (5.76)$$

This equation must be satisfied identically.

The first quantity in parentheses, however, is zero for a symmetric laminate loaded only in the x_1 direction due to the fact that the forces in the x_2 direction must add up to zero by force equilibrium i.e.

$$t(\sigma^L_{22[\theta_n]} + \sigma^L_{22[\theta_{n-1}]} + \ldots + \sigma^L_{22[\theta_1]}) = 0 \qquad (5.77)$$

Using the fact that for a symmetric laminate,

$$\sigma^L_{22[\theta_i]} = \sigma^L_{22[\theta_{n-j+1}]} \qquad (5.78)$$

the remaining part of the left hand side of equation 5.76 can be rewritten as:

$$(n-1) \, \sigma^L_{22[\theta_n]} + (n-2) \, \sigma^L_{22[\theta_{n-1}]} + \ldots + 2\sigma^L_{22[\theta_3]} +$$

$$+ \sigma^L_{22[\theta_2]} = \frac{n-1}{2} (\sigma^L_{22[\theta_n]} + \ldots + \sigma^L_{22[\theta_1]}) \qquad (5.79)$$

which is valid for n>2. For n=2 the requirement that the laminate be symmetric implies that both plies have the same fiber orientation and hence there are no interlaminar stresses. Now the right hand side of 5.79 is equal to zero (see equation 5.77) and, therefore, equation 5.76 is satisfied.

In a similar manner it can be shown that the conditions that σ_{2z} and σ_{1z} are zero at the top surface of the laminate are also satisfied. Hence the analysis so far has no inconsistencies.

5.6 Energy minimization and the determination of λ and ϕ

Up to now, the equilibrium equations, both in integral and differential form have been used and the boundary conditions and stress continuity requirements are satisfied. The stress expressions derived match asymptotically the CLPT solution. Also, most of the stress-strain and strain-displacement equations were used for the determination of σ_{11} in each ply. Note that there is no need to satisfy any of the strain-displacement equations since the minimization of the complementary energy is equivalent to satisfying these equations on the average. It was convenient to use some of the strain-displacement equations however, in order to determine σ_{11}.

All the stress expressions are summarized in Table 5.5. where $\tilde{B}_2^{(i)}$, $\tilde{B}_4^{(i)}$ and $\tilde{B}_5^{(i)}$ are given by equations 5.73a, 5..69a, and 5.70a and the superscript i refers to the ith ply (see Figure 5.3).

It should be noted that different λ and ϕ values could have been assumed for each ply. However, stress continuity requires that σ_{zz}, σ_{2z} and σ_{1z} are continuous at a ply interface. Then, if different λ and ϕ values were used, the continuity conditions would result in equations where the left hand sides would be expressed in terms of different exponentials than those in the right hand sides. This would imply that the coefficients multiplying these exponentials should be zero and, as a result the interlaminar stresses would be zero in each ply, which is impossible. Therefore, λ and ϕ must be constant throughout the laminate.

The only remaining unknowns now are λ and ϕ. These are determined by minimizing the complementary energy of the whole laminate which is equivalent to satisfying the compatibility requirement in an average (variational) sense.

The total complementary energy in the laminate is

$$\Pi_c = \sum_{i=1}^{n} \Pi_c^{(i)} \tag{5.80}$$

where $\Pi_c^{(i)}$ is the complementary energy in the ith ply and,

$$\Pi_c^{(i)} = \iiint_V \frac{1}{2} (\underset{\sim}{\sigma}^T \underset{\sim\sim}{S} \underset{\sim}{\sigma}) \, dV - \iint_{A\sigma} \underset{\sim}{T}^T \underset{\sim}{\bar{u}} \, dA \tag{5.81}$$

TABLE 5.5

STRESS EXPRESSIONS FOR EACH PLY

Stress	Expression
σ_{11}	$\dfrac{S_{11}\sigma^L_{11_{[\theta i]}}+S_{12}\sigma^L_{22_{[\theta i]}}+S_{16}\sigma^L_{12_{[\theta i]}}}{S_{11}} - \dfrac{S_{12}}{S_{11}}\sigma_{22}$ $- \dfrac{S_{13}}{S_{11}}\sigma_{zz} - \dfrac{S_{16}}{S_{11}}\sigma_{12}$
σ_{22}	$\sigma^L_{22_{[\theta i]}}[1 - \dfrac{\lambda}{\lambda-1}(e^{-\phi X} - \dfrac{1}{\lambda}e^{-\lambda\phi X})]$
σ_{zz}	$\phi^2 \dfrac{\lambda}{\lambda-1}(\lambda e^{-\lambda\phi X} - e^{-\phi X})(\sigma^L_{22_{[\theta i]}}\dfrac{z^2}{2} + \hat{B}_4 z + \hat{B}_5)$
σ_{2z}	$\dfrac{\lambda}{\lambda-1}(e^{-\phi X} - e^{-\lambda\phi X})(\sigma^L_{22_{[\theta i]}}z + \hat{B}_4)$
σ_{1z}	$\phi e^{-\phi X}(\sigma^L_{12_{[\theta i]}}z + \hat{B}_2)$
σ_{12}	$\sigma^L_{12_{[\theta i]}}(1 - e^{-\phi X})$

where V is the volume of the ith ply,

A_σ is the area of the surface over which displacements $\bar{u}$ are prescribed, $;\underset{\sim}{T}$ is a vector with the tractions corresponding to $\bar{u}$, $;\underset{\sim}{\sigma}$ is the stress vector, and $;\underset{\sim}{S}$ is the compliance tensor for the ith ply given by:

$$
\underset{\sim}{S} = \begin{bmatrix}
S_{11} & S_{12} & S_{13} & 0 & 0 & S_{16} \\
S_{12} & S_{22} & S_{23} & 0 & 0 & S_{26} \\
S_{13} & S_{23} & S_{33} & 0 & 0 & S_{36} \\
0 & 0 & 0 & S_{44} & S_{45} & 0 \\
0 & 0 & 0 & S_{45} & S_{55} & 0 \\
S_{16} & S_{26} & S_{36} & 0 & 0 & S_{66}
\end{bmatrix}
\tag{5.82}
$$

If the Sij values for a 0° ply are known, the entries in $\underset{\sim}{S}$ can be computed for any ply with the use of the usual tensor transformation relations.

For a 0° ply,

$$
S_{11} = \frac{1}{E_{11}}
\tag{5.83}
$$

$$
S_{22} = \frac{1}{E_{22}}
\tag{5.84}
$$

$$
S_{33} = \frac{1}{E_{33}}
\tag{5.85}
$$

$$
S_{44} = \frac{1}{G_{23}}
\tag{5.86}
$$

$$
S_{55} = \frac{1}{G_{13}}
\tag{5.87}
$$

$$S_{66} = \frac{1}{G_{12}} \qquad (5.88)$$

$$S_{12} = - \frac{\nu_{12}}{E_{11}} \qquad (5.89)$$

$$S_{13} = - \frac{\nu_{13}}{E_{11}} \qquad (5.90)$$

$$S_{23} = - \frac{\nu_{23}}{E_{22}} \qquad (5.91)$$

where $E_{11}, E_{22}, E_{33}, G_{12}, G_{13}, G_{23}, \nu_{12}, \nu_{13}, \nu_{23}$ are unidirectional ply constants and can be determined from the experimentally measured values of E_L, E_T, ν_{LT}, G_{LT}, E_{Lz}, ν_{Lz}, G_{Lz} [4].

It can be seen that,

$$\Pi_C = \Pi_C(\lambda, \phi) \qquad (5.92)$$

Then, for Π_C to be stationary,

$$\delta\Pi_C = 0 \qquad (5.93)$$

which implies that the equations

$$\frac{\partial \Pi C}{\partial \lambda} = 0 \qquad (5.94)$$

$$\frac{\partial \Pi C}{\partial \phi} = 0 \qquad (5.95)$$

must be satisfied. Terms in the expression of Π_c that do not depend on λ or ϕ will not appear in equations 5.94 or 5.95 and hence can be neglected in the Π_c expression.

Consider now the second term in equation 5.81. In general, far from the points where the load is introduced, the displacement u is not constant with x. However, at the points where the load is introduced, (say at the loading grips of a tensile specimen), the displacement u throughout the laminate is constant. This is the prescribed displacement in the laminate. (Prescribed in the sense that at the edges of the laminate where the loading is introduced, the entire surface is forced to have the same displacement).

This displacement will be the same as the displacement of a center point M at the two ends of the laminate as illustrated in Figure 5.4 which can be determined easily

$$u_m = \int \frac{\partial u_m}{\partial x_1} \, dx_1 \Bigg|_{x_1 = a} \tag{5.96}$$

where the origin is taken at the center of the laminate (see Figure 5.4).

But the strain at point M will be the same as the strain ε_{11} at the center of the laminate. So,

$$\frac{\partial u_m}{\partial x_1} = \varepsilon_{11} \tag{5.97}$$
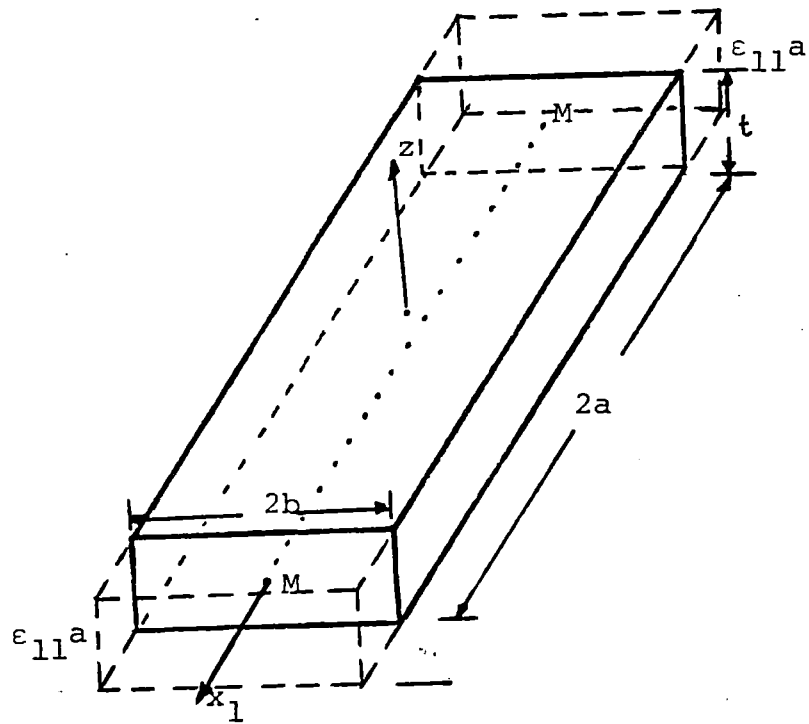
Figure 5.4. Single ply under tension

and that ε_{11} is constant. The expression for ε_{11} in terms of the stresses is given in equation 5.21. If the expression developed for σ_{11}, equation 5.38, is used to substitute for σ_{11} in equation 5.21 the following expression for ε_{11} is obtained:

$$\varepsilon_{11} = S_{11}^{(i)} \sigma_{11[\theta i]}^{L} + S_{12}^{(i)} \sigma_{22[\theta i]}^{L} + S_{16}^{(i)} \sigma_{12[\theta i]}^{L} \qquad (5.98)$$

where i corresponds to any ply since the above expression is constant for all plies and since the interlaminar stresses are zero in the laminate center.

Therefore, using equation 5.96,

$$u = (S_{11}^{(i)} \sigma_{11[\theta i]}^{L} + S_{12}^{(i)} \sigma_{22[\theta i]}^{L} + S_{16}^{(i)} \sigma_{12[\theta i]}^{L}) x_1 + C_2 \qquad (5.99)$$

By symmetry, at $x_1 = 0$ u must be zero and therefore C_2 is zero. Hence,

$$u_m = (S_{11}^{(i)} \sigma_{11[\theta i]}^{L} + S_{12}^{(i)} \sigma_{22[\theta i]}^{L} + S_{16}^{(i)} \sigma_{12[\theta i]}^{L}) a \qquad (5.100)$$

Since the stresses are independent of x_1, the x_1 integration in the first term of equation 5.81 will simply yield a factor 2a (the specimen length) multiplying the remaining portion of that term.

Then, $\Pi_c^{(i)}$ can be evaluated per unit of longitudinal length. Also, by symmetry, only one quarter of the ply needs to be considered.

As a result, substituting for $\underset{\sim}{S}$, u_M, and σ_{11} (from equations 5.82, 5.100, and 5.38 respectively) and using the fact that σ_{zz} integrates to zero when integrated with respect to x (equation 4.14):

$$
\pi_c^{(i)} = \int_0^b \int_0^t \{\frac{1}{2} (S_{22} - \frac{S_{12}^2}{S_{11}}) \sigma_{22}^2 + \frac{1}{2} (S_{33} - \frac{S_{13}^2}{S_{11}}) \sigma_{zz}^2 +
$$

$$
\frac{S_{44}}{2} \sigma_{2z}^2 + \frac{S_{55}}{2} \sigma_{1z}^2 + \frac{1}{2} (S_{66} - \frac{S_{16}^2}{S_{11}}) \sigma_{12}^2 + k_1 S_{12}\sigma_{22} +
$$

$$
k_1 S_{16}\sigma_{12} + (S_{23} - \frac{S_{12}S_{13}}{S_{11}}) \sigma_{22} \sigma_{zz} + (S_{26} - \frac{S_{12}S_{16}}{S_{11}}) \sigma_{12}\sigma_{22} +
$$

$$
(S_{36} - \frac{S_{13}S_{16}}{S_{11}}) \sigma_{zz}\sigma_{12} + S_{45}\sigma_{2z}\sigma_{1z}\} \, dxdz \tag{5.101}
$$

where

$$
k_1^{(i)} = \frac{S_{11}^{(i)}\sigma_{11[\theta i]}^L + S_{12}^{(i)}\sigma_{22[\theta i]}^L + S_{16}^{(i)}\sigma_{12[\theta i]}^L}{S_{11}^{(i)}} \tag{5.102}
$$

and t, σ_{ij}, Sij, k_1 are quantities corresponding to the ith ply, and the coordinate system shown in Figure 5.1 is used.

If the expressions 5.59-5.63 are used, the integrals in equation 5.101 can be evaluated. For simplicity the following assumption is introduced:

$$
e^{-\phi b}, e^{-\lambda \phi b} = 0 \tag{5.103}
$$

This implies that the laminate is wide enough so that ϕb or $\lambda \phi b$ is very large. A simple order of magnitude analysis is needed to determine how large b should be, for equation 5.103 to be valid. Recall that $1/\phi$ has the dimensions of length. The length scales of the problem are $t^{(i)}$, h, b. Since equation 5.103 requires that b is essentially infinite, ϕ cannot scale with b. It cannot scale with $t^{(i)}$ either because ϕ is constant throughout the laminate and the thickness of a single (arbitrary) ply cannot determine its magnitude. The only possibility that remains is that ϕ scales with the laminate thickness h. So,

$$\phi h = O(1) \tag{5.104}$$

and

$$\phi b = \frac{b}{h} \tag{5.105}$$

Arbitrarily, one can consider equation 5.103 to be satisfied if $b/h > 10$. Then, $e^{-\phi b} \approx 4.5 \times 10^{-5}$. Using equation 5.105, the condition on b can be written,

$$b > 10h \tag{5.106}$$

Thus, if equation 5.106 is satisfied, equation 5.103 will be valid.

Each of the integrals in equation 5.101 can be evaluated with the substitution of the expressions for the stresses from equations 5.59-5.63.

$$\int_0^b \int_0^t \left(S_{22} - \frac{S_{12}^2}{S_{11}}\right) \sigma_{22}^2 \, dxdz = \frac{-3\lambda^4 + \lambda^3 + 4\lambda^2 + \lambda - 3}{\phi\lambda(\lambda-1)^2(\lambda+1)} \, d_1$$

$$\int_0^b \int_0^t \left(S_{33} - \frac{S_{13}^2}{S_{11}}\right) \sigma_{zz}^2 \, dxdz = \frac{\lambda^2\phi^3}{\lambda+1} \, d2$$

$$\int_0^b \int_0^t \frac{S_{44}}{2} \sigma_{2z}^2 \, dxdz = \frac{\lambda\phi}{\lambda+1} \, d3$$

$$\int_0^b \int_0^t \frac{S_{55}}{2} \sigma_{1z}^2 \, dxdz = \phi d4$$

$$\int_0^b \int_0^t \left(S_{66} - \frac{S_{16}^2}{S_{11}}\right) \sigma_{12}^2 \, dxdz = -\frac{d5}{\phi}$$

(5.107a-k)

$$\int_0^b \int_0^t k_1 S_{12} \sigma_{22} \, dxdz = -\frac{\lambda+1}{\lambda\phi} \, d6$$

$$\int_0^b \int_0^t k_1 S_{16} \sigma_{12} \, dxdz = -\frac{d7}{\phi}$$

$$\int_0^b \int_0^t \left(S_{23} - \frac{S_{12}S_{13}}{S_{11}}\right) \sigma_{22} \sigma_{zz} \, dxdz = -\frac{\lambda\phi}{\lambda+1} \, d8$$

$$\int_0^b \int_0^t \left(S_{26} - \frac{S_{12}S_{16}}{S_{11}}\right) \sigma_{12} \sigma_{22} \, dxdz = \frac{-3\lambda^3 - \lambda^2 + 2\lambda + 2}{\lambda\phi(\lambda^2-1)} \, d9$$

$$\int_0^b \int_0^t \left(S_{36} - \frac{S_{13}S_{16}}{S_{11}}\right) \sigma_{zz} \sigma_{12} \, dxdz = -\frac{\lambda\phi}{\lambda+1} \, d10$$

$$\int_0^b \int_0^t S_{45} \sigma_{2z} \sigma_{1z} \, dxdz = \frac{\lambda\phi}{\lambda+1} \, d11$$

where terms independent of λ, ϕ have been omitted, and,

$$d_1 = \frac{(\sigma^L_{22_{[\theta i]}})^2 \, t}{2} \; (S_{22} - \frac{S_{12}^2}{S_{11}})$$

$$d_2 = \frac{t}{120} \, [\; 3 \, (\sigma^L_{22_{[\theta i]}})^2 \, t^4 + 15 \, \sigma^L_{22_{[\theta i]}} \, \hat{B}_4 \, t^3 +$$

$$20 \, \sigma^L_{22_{[\theta i]}} \, \hat{B}_5 \, t^2 + 20(\hat{B}_4)^2 \, t^2 + 60 \, \hat{B}_4 \, \hat{B}_5 \, t +$$

$$60(\hat{B}_5)^2] \, (S_{33} - \frac{S_{13}^2}{S_{11}})$$

$$d_3 = \frac{t}{6} \, [(\sigma^L_{22_{[\theta i]}})^2 \, t^2 + 3 \, \sigma^L_{22_{[\theta i]}} \, \hat{B}_4 \, t + 3(\hat{B}_4)^2) \, S_{44}$$

$$d_4 = \frac{t}{6} \, ((\sigma^L_{12_{[\theta i]}})^2 \, t^2 + 3 \, \sigma^L_{12_{[\theta i]}} \, \hat{B}_2 \, t + 3(\hat{B}_2)^2) \, S_{55}$$

$$d_5 = \frac{3}{2} \, (\sigma^L_{12_{[\theta i]}})^2 \, t \, (S_{66} - \frac{S_{16}^2}{S_{11}})$$

$$d_6 = \sigma^L_{22_{[\theta i]}} t \, k_1 \, S_{12} \qquad\qquad (5.108a\text{-}k)$$

$$d_7 = \sigma^L_{12_{[\theta i]}} t \, k_1 \, S_{16}$$

$$d_8 = \sigma^L_{22_{[\theta i]}} \frac{t}{12} [\sigma^L_{22_{[\theta i]}} t^2 + 3 \, \mathring{B}_4 \, t + 6 \, \mathring{B}_5](S_{23} - \frac{S_{12}S_{13}}{S_{11}})$$

$$d_9 = \frac{\sigma^L_{12_{[\theta i]}} \; \sigma^L_{22_{[\theta i]}} \, t}{2} \; (S_{26} - \frac{S_{12}S_{16}}{S_{11}})$$

$$d_{10} = \sigma^L_{12_{[\theta i]}} \frac{t}{12} [\sigma^L_{22_{[\theta i]}} t^2 + 3 \, \mathring{B}_4 \, t + 6 \, \mathring{B}_5](S_{36} - \frac{S_{13}S_{16}}{S_{11}})$$

$$d_{11} = \frac{t}{12} [2 \, \sigma^L_{12_{[\theta i]}} \, \sigma^L_{22_{[\theta i]}} t^2 + 3 \, \sigma^L_{22_{[\theta i]}} \, \mathring{B}_2 \, t +$$

$$3 \, \sigma^L_{12_{[\theta i]}} \, \mathring{B}_4 \, t + 6 \, \mathring{B}_4 \, \mathring{B}_2] \, S_{45}$$

In the above, t, $\sigma^L_{ij[\theta i]}$, $\underset{\sim}{B}{}^{(i)}_j$ are quantities for the ith ply.

It should be noted that in the case where instead of using equation 5.38, σ_{11} is taken to be equal to $\sigma^L_{11[\theta i]}$ the second term in 5.81 is independent of λ and ϕ and the expressions for d_i simplify. The d_i values for this case are given in Appendix 4. Equations 5.107a-k are still valid but with the d_i values as given in Appendix 4.

Substituting these results into equation 5.101 and using equation 5.80 to obtain the laminate energy Π_c,

$$\Pi_c = -(f_6 + \frac{f_1}{2})\frac{1}{\lambda\phi} - (f_6 + f_7 + \frac{f_5}{2})\frac{1}{\phi} + (f_{11} - f_{10} - f_8 +$$

$$+ \frac{f_3}{2})\frac{\lambda\phi}{\lambda+1} + \frac{f_2}{2}\frac{\lambda^2\phi^3}{\lambda+1} + \frac{f_4}{2}\,\phi - (\frac{f_1}{2} + f_9)\frac{3\lambda^2 + 4\lambda + 2}{\lambda(\lambda+1)\,\phi} \qquad (5.109)$$

where

$$f_i = \sum_{j=1}^{n} d_i \qquad (5.110)$$

Note that for the actual implementation of the method only half the laminate (in the z direction) is considered since it is symmetric.

Making Π_c stationary (equations 5.94 and 5.95), results in the following simultaneous equations for λ and ϕ:

$$\frac{\partial \Pi c}{\partial \lambda} = \lambda^4\phi^4 f_2 + 2\lambda^3\phi^4 f_2 + \lambda^2(2f_6 + 2f_{11}\phi^2 + f_3\phi^2 - 2f_{10}\phi^2 -$$

$$- 2f_8\,\phi^2 + 2f_9 + 2f_1) + \lambda(4f_6 + 8f_9 + 6f_1) + 2f_6 + 4f_9 +$$

$$+ 3f_1 = 0 \qquad (5.111)$$

$$\frac{\partial \pi c}{\partial \phi} = 3f_2\lambda^3\phi^4 + \phi^2(f_4\lambda^2 + 2f_{11}\lambda^2 + f_3\lambda^2 - 2f_{10}\lambda^2 - 2f_8\lambda^2 +$$

$$+ f_4\lambda) + \lambda^2(2f_7 + 2f_6 + f_5 + 6f_9 + 3f_1) + \lambda(2f_7 +$$

$$+ 4f_6 + f_5 + 8f_9 + 5f_1) + 4f_9 + 3f_1 + 2f_6 = 0 \qquad (5.112)$$

5.7 Solution of the equations for λ and ϕ

Both equations 5.111 and 5.112 are biquadratic in ϕ. This results from the fact that ϕ is included in both exponents in equation 5.15a. The fact that the two equations are biquadratic in ϕ simplifies their solution greatly since, for a particular λ value, ϕ can readily be obtained. This was the reason alluded to in section 5.2 for making the two exponents in equation 5.15a λ and $\lambda\phi$ rather than λ and ϕ.

Equation 5.112 is cubic in λ. This means that, for a particular ϕ value, the system of equations 5.111 and 5.112 has at least one real λ value as a solution. Furthermore, since 5.111 is quartic in λ and at least one real λ value exists, there must also be another real λ value which satisfies both equations. Otherwise, if there were only one real λ value as a solution, 5.111 would have three complex solutions for λ which is not possible.

In general, the above system of equations has sixteen pairs of λ and ϕ as solutions. All sixteen must be found and the one that minimizes the complementary energy (equation 5.101) must be chosen as the only acceptable solution.

The two equations are solved by using the following iteration scheme:

1. A starting ϕ value is assumed (see below).

2. That value of ϕ is substituted in equation 5.111 which is solved for λ iteratively.

3. Out of the 4 λ's that are solutions of 5.111 the ones that are negative or complex are discarded. Negative solutions are discarded because the exponentials in the stress expressions would increase rather than decay. Complex solutions are discarded because, in general, they result in complex laminate energy. From the remaining λ's the one which, along with the assumed value of ϕ, minimizes Π_c is chosen. If there is only one positive λ value, that one is the one used in the next step.

4. The value of λ found is substituted in 5.112 which is solved for ϕ^2 (exactly) from which ϕ is determined. If there is more than one positive ϕ value, the one which, along with the λ value found in step 3, minimizes Π_c is used.

5. This ϕ value found is used as the corrected ϕ value in step 2.

The procedure is repeated until some predetermined level of accuracy on ϕ is acheived (in this case the requirement was

that two successive ϕ values differ by at most one part in a million).

The above procedure guarantees that no λ, ϕ pair of the possible 16 pairs is "missed".

5.8 <u>Computer implementation</u>

The solution procedure was implemented on a computer program (in FORTRAN) on a PDP-11/34 computer.

The input to the computer program consists of:

1. Laminate information: a) number of plies; b) material type, ply thicknesses, and fiber orientation for each ply; and c) the 8 elastic constants for a 0° ply of each material type.

2. The CLPT solution which was obtained from another program already available.

The output of the program consists of:

1. Compliances Sij for each ply.

2. λ and ϕ.

3. Half-laminate energy.

4. Boundary layer length (the definition of the boundary layer is given in chapter 8).

5. The coefficients multiplying the x dependence in the σ_{zz}, σ_{2z}, σ_{1z} stress expressions for all ply interfaces.

For the initial ϕ value, equation 5.104 can be used. Actually, for reasons to be explained in chapter 8, the initial value used is,

$$\phi_{init} = \frac{4.4}{h} \qquad\qquad (5.113)$$

The iterative solution for the polynomial in λ at step 2 of the solution procedure is accomplished by the Newton-Raphson method. The iteration is considered to have converged when two successive λ values differ by less than .00001.

The complete listing of the program code can be found in Appendix 5.

CHAPTER SIX

SPECIAL CASES

There are two special cases where the analysis simplifies greatly: (1) Angle-plied laminates and (2) Cross-plied laminates. The solutions for these two cases are presented below.

6.1 Angle-plied laminates

Angle-plied laminates are the laminates in which there are only $+\theta$ or $-\theta$ plies and for each $+\theta$ ply there is one $-\theta$ ply.

For these laminates, the CLPT theory predicts that the σ_{22} ply stresses in laminate axes are zero everywhere:

$$\sigma^L_{22_{[\theta i]}} = 0 \qquad (6.1)$$

Then, equations 5.38 and 5.59-5.63 for the ply stresses are greatly simplified to:

$$\sigma^{(i)}_{11} = \frac{S^{(i)}_{11}\sigma^L_{11_{[\theta i]}} + S^{(i)}_{16}\sigma^L_{12_{[\theta i]}}}{S^{(i)}_{11}} - \frac{S^{(i)}_{16}}{S^{(i)}_{11}}\sigma^{(i)}_{12} \qquad (6.2)$$

$$\sigma^{(i)}_{22} = 0 \qquad (6.3)$$

$$\sigma^{(i)}_{zz} = 0 \qquad (6.4)$$

$$\sigma^{(i)}_{2z} = 0 \qquad (6.5)$$

$$\sigma^{(i)}_{1z} = \phi e^{-\phi x}(\sigma^L_{12_{[\theta i]}} z + B^{(i)}_2) \qquad (6.6)$$

$$\sigma_{12}^{(i)} = \sigma_{12_{[\theta i]}}^{L} (1 - e^{-\phi X}) \tag{6.7}$$

The result that $\sigma_{2z}^{(i)} = 0$ everywhere is in agreement with the conclusions of chapter 4 (See Figure 4.3a). Also, as a check that the analysis is consistent, it can be shown that, if equation 6.5 is true, then equations 6.3 and 6.4 follow from the equations of differential equilibrium.

Assume that equation 6.5 is true. Then the differential equilibrium equation 5.2 gives:

$$\frac{\partial \sigma_{22}}{\partial x_2} = 0 \tag{6.8}$$

Then, σ_{22} can only be some function of z:

$$\sigma_{22}^{(i)} = M_1^{(i)}(z) \tag{6.9}$$

where $M_1^{(i)}(z)$ is that unknown function of z. However, the fact that at the free edge $\sigma_{22}^{(i)} = 0$ implies that

$$M_1^{(i)}(z) = 0 \tag{6.10}$$

and, as a result, σ_{22} is zero throughout the ith ply. Thus, equation 6.3 is valid.

Using equation 6.5 to substitute in the differential equilibrium in the z direction equation (equation 5.3) one obtains,

$$\frac{\partial \sigma_{zz}}{\partial z} = 0 \tag{6.11}$$

which means that σ_{zz} is only a function of x_2:

$$\sigma_{zz}^{(i)} = N_1^{(i)}(x_2) \tag{6.12}$$

However, the top surface of a laminate is stress-free and thus $\sigma_{zz}^{(1)}(t)=0$ which implies that

$$N_1^{(1)}(x_2) = 0 \tag{6.13}$$

and σ_{zz} is therefore zero throughout the first ply. Then, applying equation 5.12 at the first ply interface, where it was shown that, due to stress continuity $\sigma_{zz}^{(2)}(z=t)=\sigma_{zz}^{(1)}(z=0)=0$, it follows that

$$N_1^{(2)}(x_2) = 0 \tag{6.14}$$

which implies that σ_{zz} is zero throughout the second ply. This procedure can be repeated for all plies to show that σ_{zz} will be zero throughout the laminate. Hence, equation 6.4 is also valid.

It is important to note that in equations 6.3-6.7, only ϕ is unknown as λ does not appear in the formulation. Substituting the stress expressions 6.3-6.7 in the expression for Π_c and minimizing, one obtains the following equation for ϕ:

$$2f_7 + f_4\phi^2 + f_5 = 0 \tag{6.15}$$

which can be solved exactly to give

$$\phi = \left[-\frac{f_5 + 2f_7}{f_4} \right]^{1/2} \tag{6.16}$$

where f_5, f_7, and f_4 are given by equation 5.110 with the use of equations 5.108d, 5.108e, 5.108g. In the case that the quantity in brackets in equation 6.16 is negative, ϕ is complex and the method fails. (No such case was encountered when sample cases were solved). Thus, for angle-ply laminates the solution can be obtained exactly and no iteration is involved.

6.2 Cross-plied laminates

Cross-plied laminates are the laminates which have only 0° and 90° plies and for each 0° ply there is a 90° ply.

For these laminates the CLPT solution shows that throughout the laminate:

$$\sigma^L_{12_{[\theta i]}} = 0 \tag{6.17}$$

Substituting this result in the stress expressions 5.59-5.63 yields

$$\sigma^{(i)}_{22} = \sigma^L_{22_{[\theta i]}} [1 - \frac{\lambda}{\lambda - 1} (e^{-\phi X} - \frac{1}{\lambda} e^{-\lambda \phi X})] \tag{6.18}$$

$$\sigma^{(i)}_{zz} = \phi^2 \frac{\lambda}{\lambda - 1} (\lambda e^{-\lambda \phi X} - e^{-\phi X})(\sigma^L_{22_{[\theta i]}} \frac{z^2}{2} + \tilde{B}^{(i)}_4 z + \tilde{B}^{(i)}_5) \tag{6.19}$$

$$\sigma^{(i)}_{2z} = \phi \frac{\lambda}{\lambda - 1} (e^{-\phi X} - e^{-\lambda \phi X})(\sigma^L_{22_{[\theta i]}} z + \tilde{B}^{(i)}_4) \tag{6.20}$$

$$\sigma^{(i)}_{1z} = 0 \tag{6.21}$$

$$\sigma^{(i)}_{12} = 0 \tag{6.22}$$

Equation 6.22 is in agreement with the well-known fact that the in-plane shear stress σ_{12} is zero for 0° and 90° plies. Then, equation 6.21 can be shown to follow from the equations of differential equilibrium.

From equation 5.1 (differential equilibrium in the x_1 direction),

$$\frac{\partial \sigma_{1z}^{(i)}}{\partial z} = 0 \tag{6.23}$$

which means that σ_{1z} is a only a function of x_2. This can be expressed as

$$\sigma_{1z}^{(i)} = N_2^{(i)}(x_2) \tag{6.24}$$

Again, the requirement that the top surface is stress-free gives $N_2^{(1)}(x_2)=0$ from which σ_{1z} is found to be zero in the first ply. Repeating the procedure at each interface as was done for σ_{zz} in the previous section, it can be shown that σ_{1z} is zero throughout the entire laminate.

Introducing 6.18-6.22 in the expression for Π_c and differentiating with respect to λ and ϕ, the following two equations are obtained:

$$\lambda^4 \phi^4 f_2 + 2\lambda^3 \phi^4 f_2 + \lambda^2 (2f_6 + f_3\phi^2 - 2f_8\phi^2 + 2f_1) +$$

$$\lambda(4f_6 + 6f_1) + 2f_6 + 3f_1 = 0 \tag{6.25}$$

and

$$2f_6\lambda^2 + 4f_6\lambda + 2f_6 + 3f_2\lambda^3\phi^4 + f_3\lambda^2\phi^2 - 2f_8\lambda^2\phi^2 + 3f_1\lambda^2 +$$

$$+ 5f_1\lambda + 3f_1 = 0 \tag{6.26}$$

Note that equations 6.25 and 6.26 could also be obtained directly by performing the integrations in the Π_c expression (see equations 5.101, 5.107) and setting $\sigma_{12}=0$ (equation 6.22).

With some manipulation, equation 6.26 can be rewritten as

$$2f_2\lambda^3\phi^4 + \lambda^2(2f_6 + f_3\phi^2 - 2f_8\phi^2 + 2f_1) + \lambda(4f_6 +$$

$$+ 6f_1) + 2f_6 + 3f_1 + f_2\lambda^3\phi^4 + f_1\lambda^2 - f_1\lambda = 0 \qquad (6.26a)$$

and subtracting equation 6.25 from equation 6.26a one gets:

$$- \lambda^4\phi^4 f_2 + f_2\lambda^3\phi^4 + f_1\lambda^2 - f_1\lambda = 0 \qquad (6.26b)$$

or rearranging,

$$\lambda(\lambda-1)(f_1 - \lambda^2\phi^4 f_2) = 0 \qquad (6.26c)$$

There are three possible conditions under which this equation will be satisfied. Consider first the case where

$$f_1 - \lambda^2\phi^4 f_2 = 0 \qquad (6.27)$$

Then, solving for ϕ

$$\phi = [\frac{1}{\lambda} (\frac{f_1}{f_2})^{1/2}]^{1/2} \qquad (6.28)$$

which can be substituted in equation 6.25 to obtain an equation for λ:

$$\lambda^2(2f_6 + 3f_1) + \lambda(4f_6 + 8f_1 + \sqrt{\frac{f_1}{f_2}} (f_3 - 2f_8)) + 2f_6 + 3f_1 = 0 \qquad (6.29)$$

or rearranging

$$\lambda^2 + \lambda \, \frac{\sqrt{\frac{f_1}{f_2}} \, (f_3 - 2f_8) + 4f_6 + 8f_1}{2f_6 + 3f_1} + 1 = 0 \qquad (6.30)$$

It can be shown that for some cases ($[0_n/90_n]$s AS1/3501-6 laminates for example) the above equation has complex roots (See Appendix 6). For such cases, equations 6.30 and 6.28 cannot be used to determine λ and ϕ because these would turn out to be complex. For such cases, the remaining two possibilities are from equation 6.26c:

either $\lambda=0$

or $\lambda-1=0$

For the case where $\lambda=0$, equations 5.59-5.63 reduce to the CLPT solution which is not valid close to the free edge. The only case that remains is

$$\lambda = 1 \qquad (6.31)$$

Going back to equation 5.15a it can be seen that the two eigenfunctions $e^{-\phi x}, e^{-\lambda \phi x}$, which are used to approximate the stress shapes, coincide for $\lambda=1$. However, for σ_{zz} to cross the x axis at least once, at least two eigenfunctions of this type are needed. In a manner analogous to the theory of differential equations where, if the two solutions of a second order differental equation coincide, one of them must be multiplied by x, one can assume that the two modes in the present case are $e^{-\phi x}$ and $xe^{-\phi x}$.

So the equation corresponding to equation 5.15a for the cross-plied case is

$$\sigma_{22} = e^{-\phi x} (A_1 + A_2 x) + A_3 \tag{6.32}$$

Following the procedure described in section 5.1 the non-zero stresses in a cross-plied laminate are found to be:

$$\sigma_{22}^{(i)} = \sigma_{22_{[\theta i]}}^{L} [1 - (1 + \phi x)e^{-\phi x}] \tag{6.33}$$

$$\sigma_{2z}^{(i)} = \phi^2 x \, e^{-\phi x} [\tilde{B}_4^{(i)} + \sigma_{22_{[\theta i]}}^{L} z] \tag{6.34}$$

$$\sigma_{zz}^{(i)} = \phi^2 e^{-\phi x} (1 - \phi x)(\tilde{B}_4^{(i)} z + B_5^{(i)} + \sigma_{22_{[\theta i]}}^{L} \frac{z^2}{2}) \tag{6.35}$$

where $\tilde{B}_4$, $\tilde{B}_5$ are the same as before (equations 5.69, 5.70). Also, σ_{11} is again given by equation 5.38.

Substituting these into the expression for Π_c:

$$\frac{\partial \Pi c}{\partial \phi} = \frac{11}{4} \frac{f_1}{\phi^2} + \frac{3}{4} f_2 \phi^2 + \frac{1}{4} f_3 + \frac{2f_6}{\phi^2} - \frac{f_6}{2} \tag{6.36}$$

where f_i are the same as in equation 5.107.

The ϕ value that makes Π_c stationary is given by,

$$\frac{\partial \Pi_c}{\partial \phi} = 0 \tag{6.36a}$$

This is the only equation since λ is not present in this case. The above equation can be rewritten as

$$3f_2 \phi^4 + (f_3 - 2f_8)\phi^2 + 11f_1 + 8f_6 = 0 \tag{6.37}$$

from which ϕ is found to be:

$$\phi = \left[\frac{-(f_3 - 2f_8) + [(f_3 - 2f_8)^2 - 12f_2 \ (11f_1 + 8f_6)]}{6f_2}\right]^{1/2} \qquad (6.38)$$

Again, if the quantity in the brackets is negative, ϕ is complex and the method fails. No such cases have been encountered so far. If such a case were encountered, one would have to use a different eigenfunction (e.g. $x^2 e^{-\phi x}$) along with $e^{-\phi x}$ in equation 5.15a.

This analysis is used if equation 6.30 has no real solutions. If it does, then equations 6.28 and 6.30 can be used to determine λ and ϕ for cross-plied laminates. A special case where equation 6.30 has real roots is presented in chapter 7. For that particular case, the solution obtained using equations 6.30 and 6.28 is compared with the results obtained if equations 6.33-6.35, and 6.38 are used (also in chapter 7). Note that, no matter which of the two methods is used, the λ and ϕ values can be determined exactly without any iterations.

6.3 Comments on the special cases

It is seen that for angle-plied or cross-plied laminates the solution is greatly simplified. The two unknown parameters λ and ϕ can be determined in closed form and no iterations are

required. The cross-plied case is slightly more involved because in some cases the original eigenfunctions coincide and a slightly different analysis is required.

Both of these special cases, angle-ply or cross-plied laminates, were incoporated in the computer program. For cross-plied laminates the case where both λ and ϕ exist is checked first and, if equation 6.30 has complex roots, the different analysis, where only ϕ is present is used.

CHAPTER SEVEN

DISCUSSION AND RESULTS

Several applications of the theory presented in the previous chapters are discussed in this chapter. The predictions of the present analysis are compared to the predictions of other analytical methods. Some further implications of the stress model are also discussed.

7.1 Typical stress distributions and characteristics

Analyses were performed on a large number of laminates. The presentation of results of the calculation of interlaminar stresses for any particular laminate requires a large number of graphs to show each of the stresses at each of the ply interfaces. Therefore, it is not feasible to show the results of a variety of laminates. Thus, two laminates have been chosen to illustrate the major characteristics of the solution. These laminates are [±15/0]s and [0/±15]s laminates (AS1/3501-6 system) and typical stress plots for these two laminates are shown in this section. The first laminate is known to fail by delamination [41] and results for the second will be presented so that some of the effects of changing the stacking sequence in a laminate can be examined. Plots showing

stresses as functions of x, the distance from the free edge, will be presented only at ply interfaces, since these, being the weakest regions through the thickness of a laminate, are most important for delamination considerations. Solutions for other z locations can be accomplished just as easily. In addition, only results for the top half of the laminate are presented since, at the remaining part, the stresses repeat symmetrically with respect to the midplane (or antisymmetrically in the case of shear stresses).

The CLPT solution for both laminates is shown in Table 7.1. The same uniaxial loading of 889 MPa is used for both. The interlaminar normal stress σ_{zz} at the first three ply interfaces is shown in Figure 7.1 for the [±15/0]s laminate. The corresponding plot for the [0/±15]s laminate is shown in Figure 7.2. The interlaminar shear stresses σ_{2z} and σ_{1z} are shown in Figures 7.3 and 7.5 for the [±15/0]s laminate and in Figures 7.4 and 7.6 for the [0/±15]s laminate respectively.

A number of general comments can be made upon examination of Figures 7.1 through 7.6. One, the normal stress σ_{zz} reaches its maximum magnitude at the free edge and then drops to zero within a few millimeters from the free edge after crossing the x axis once, in agreement with the predictions of chapters 4 and 5. Two, the shear stress σ_{2z} is zero at the free edge, in agreement with the stress-free boundary condition, rises to some maximum value and drops to zero within a

TABLE 7.1

CLPT SOLUTIONS FOR $[\pm 15/0]_s$ AND $[0/\pm 15]_s$ LAMINATES
(APPLIED LOAD $\bar{\sigma}_{11}$ = 889 MPa)

Stresses In [MPa]	$[\pm 15/0]_s$			$[0/\pm 15]_s$		
	Ply 1 (+15°)	Ply 2 (-15°)	Ply 3 (0°)	Ply 1 (0°)	Ply 2 (+15°)	Ply 3 (-15°)
$\sigma^L_{11[\theta i]}$	839	839	990	990	839	839
$\sigma^L_{22[\theta i]}$	16.0	16.0	-31.9	-31.9	16.0	16.0
$\sigma^L_{12[\theta i]}$	193	-193	0	0	193	-193
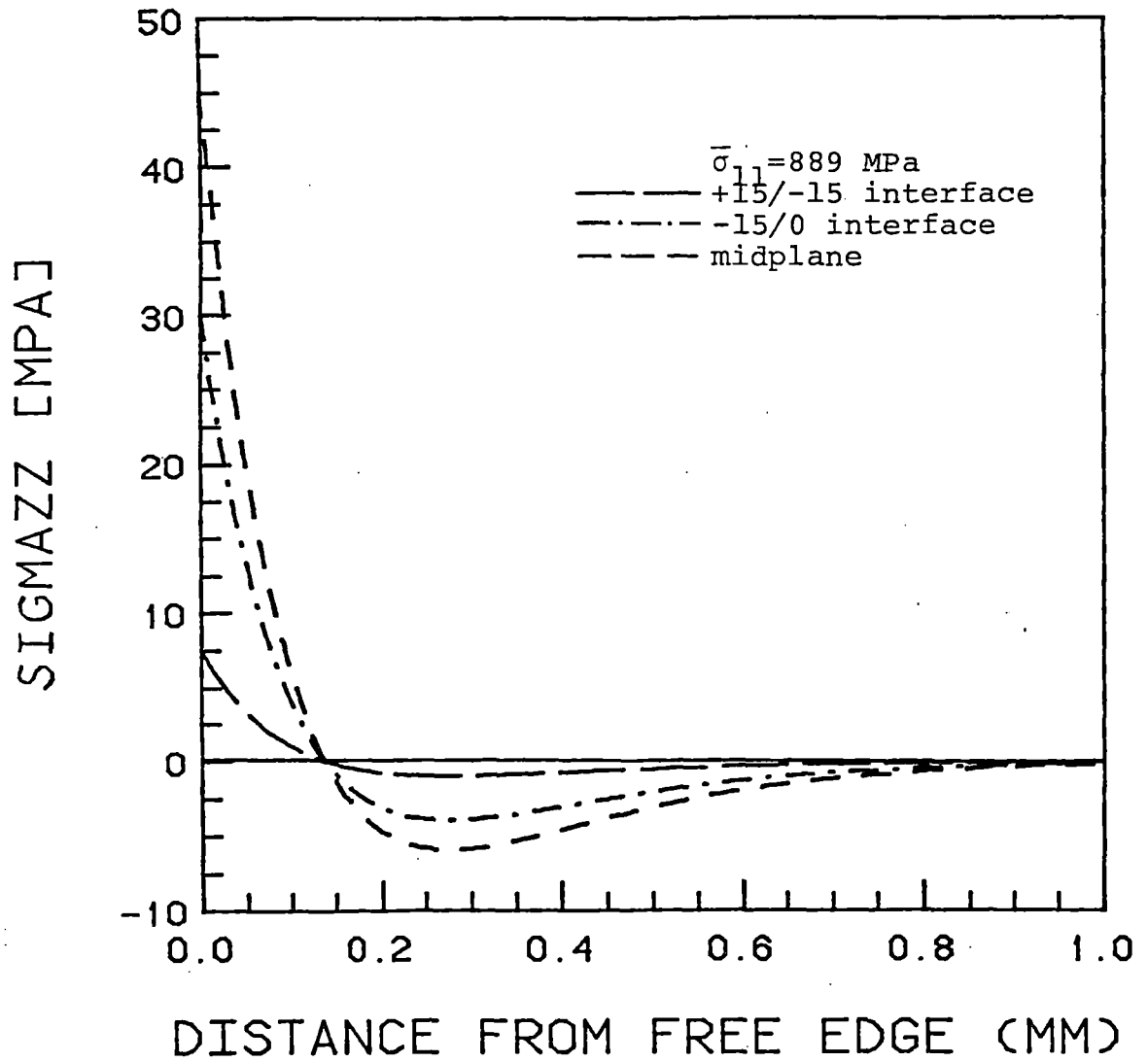
Figure 7.1. Calculated interlaminar normal stress σ_{zz} for $[\pm 15/0]_s$ laminate
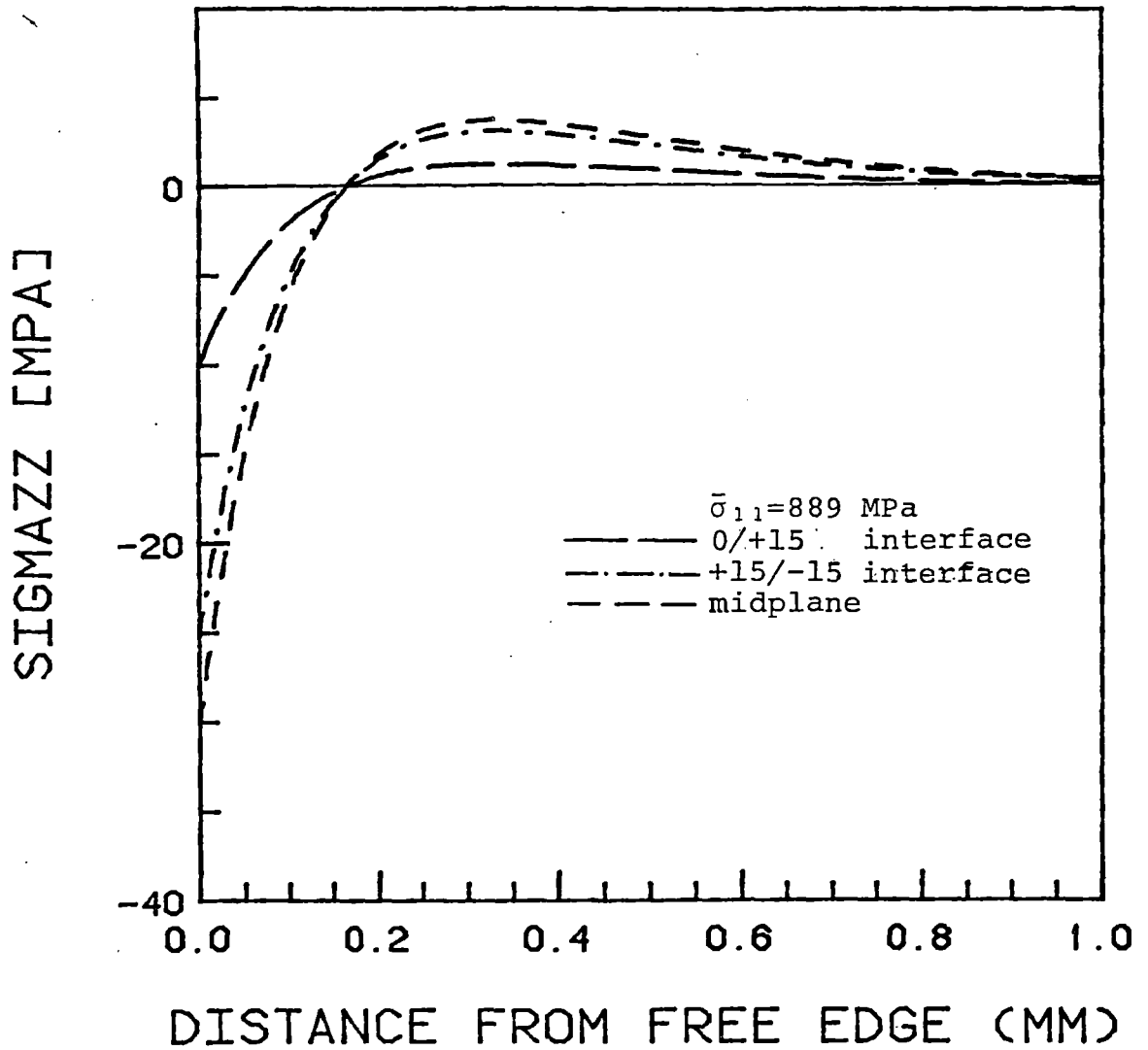
Figure 7.2. Calculated interlaminar normal stress σ_{zz}
for $[0/\pm 15]_s$ laminate
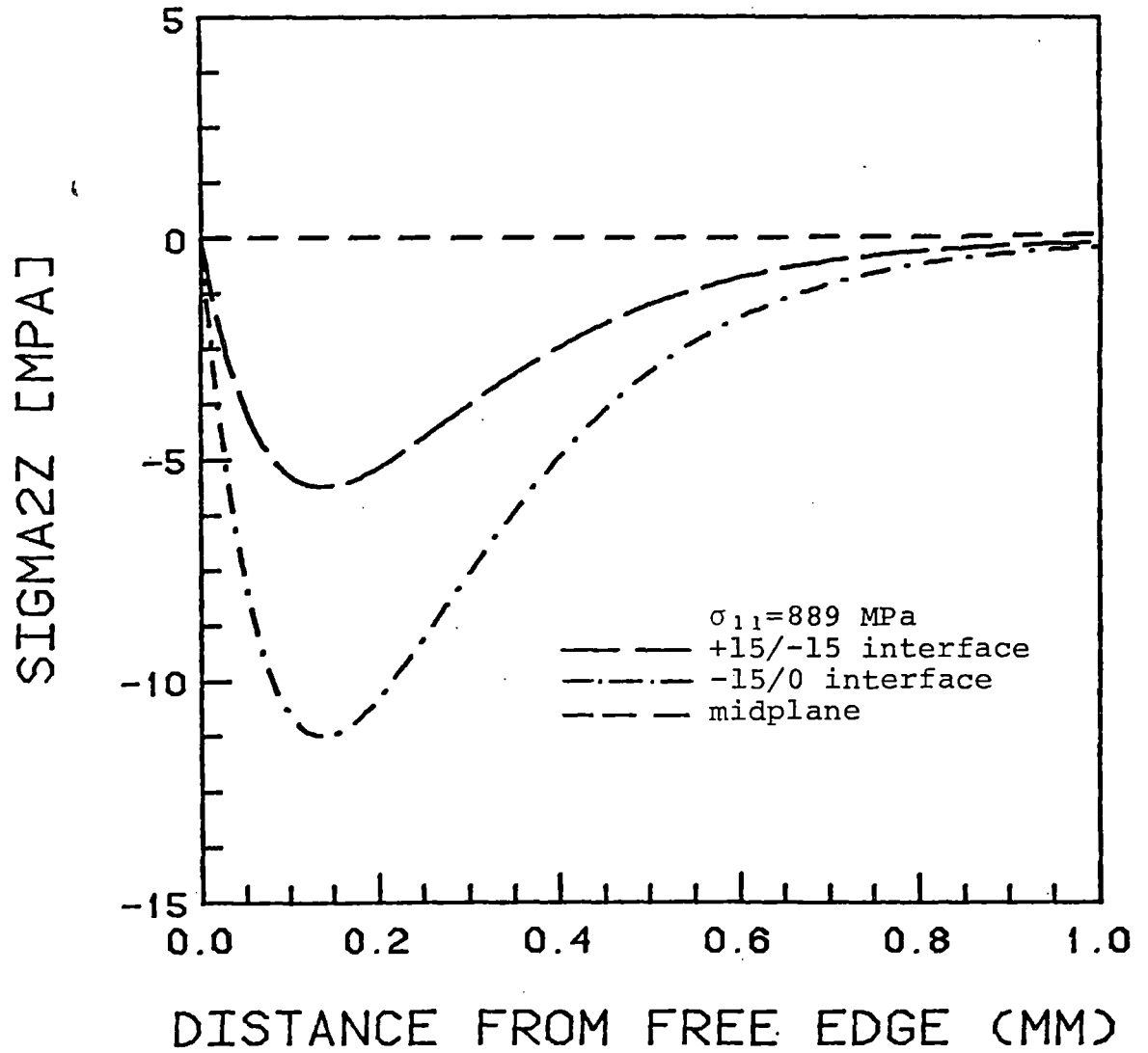
Figure 7.3. Calculated interlaminar shear stress σ_{2z} for $[\pm 15/0]_s$ laminate.
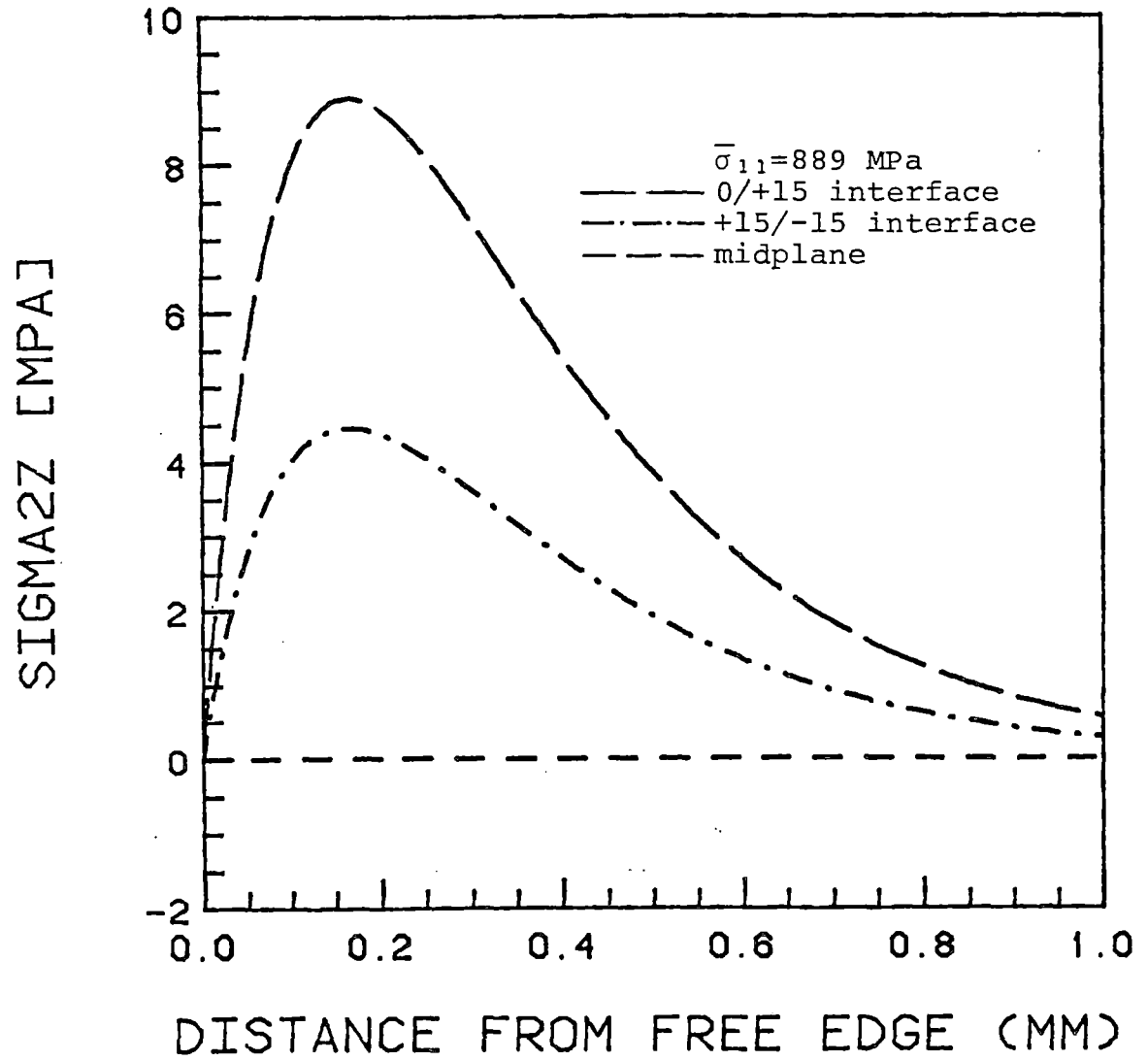
Figure 7.4. Calculated interlaminar shear stress σ_{2z} for $[0/\pm 15]_s$ laminate
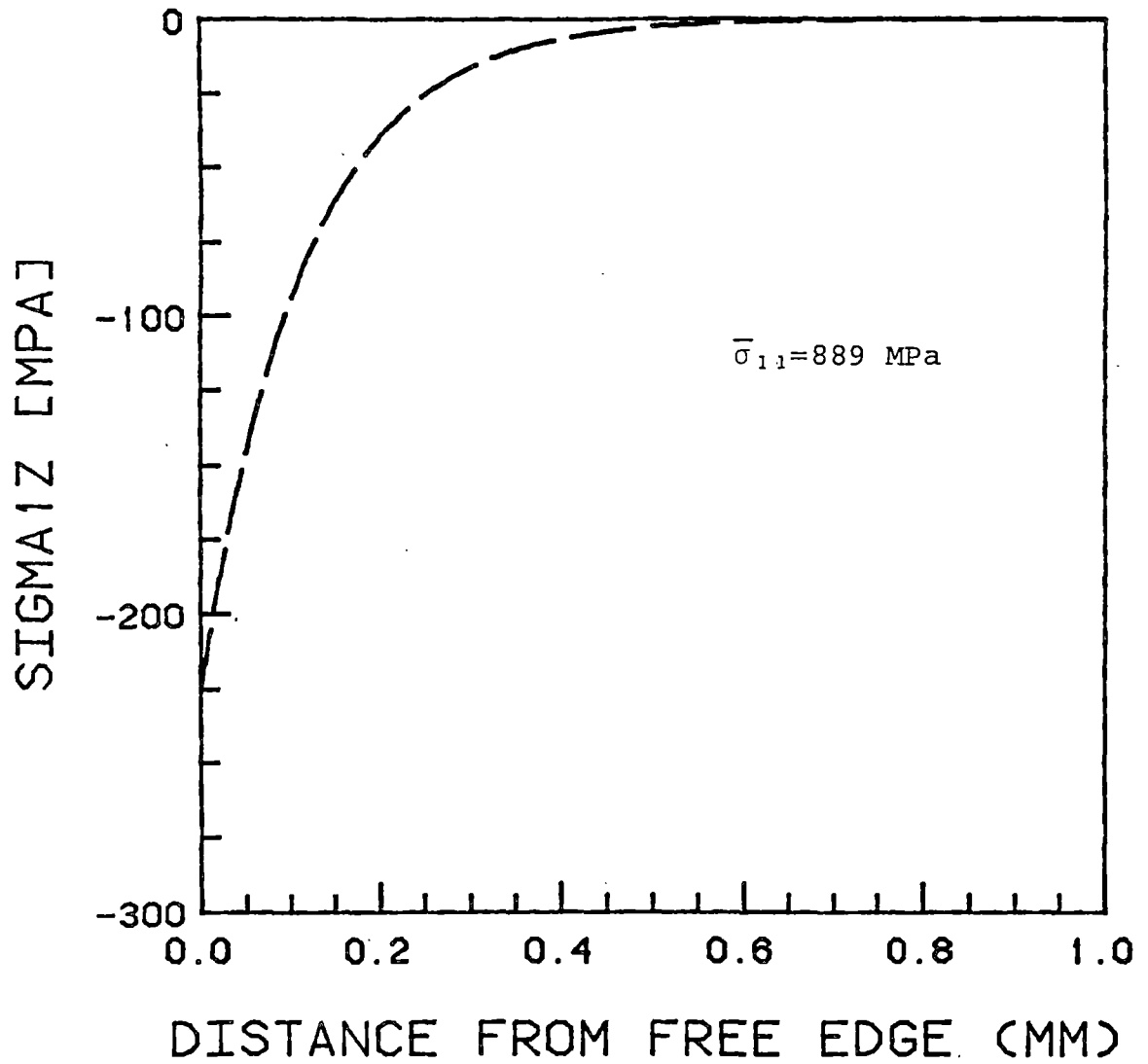
Figure 7.5. Calculated interlaminar shear stress σ_{1z} for $[+15/0]_s$ laminate at $+15/-15$ interface ($\bar{\sigma}_{1z} = 0$ at the other two interfaces)
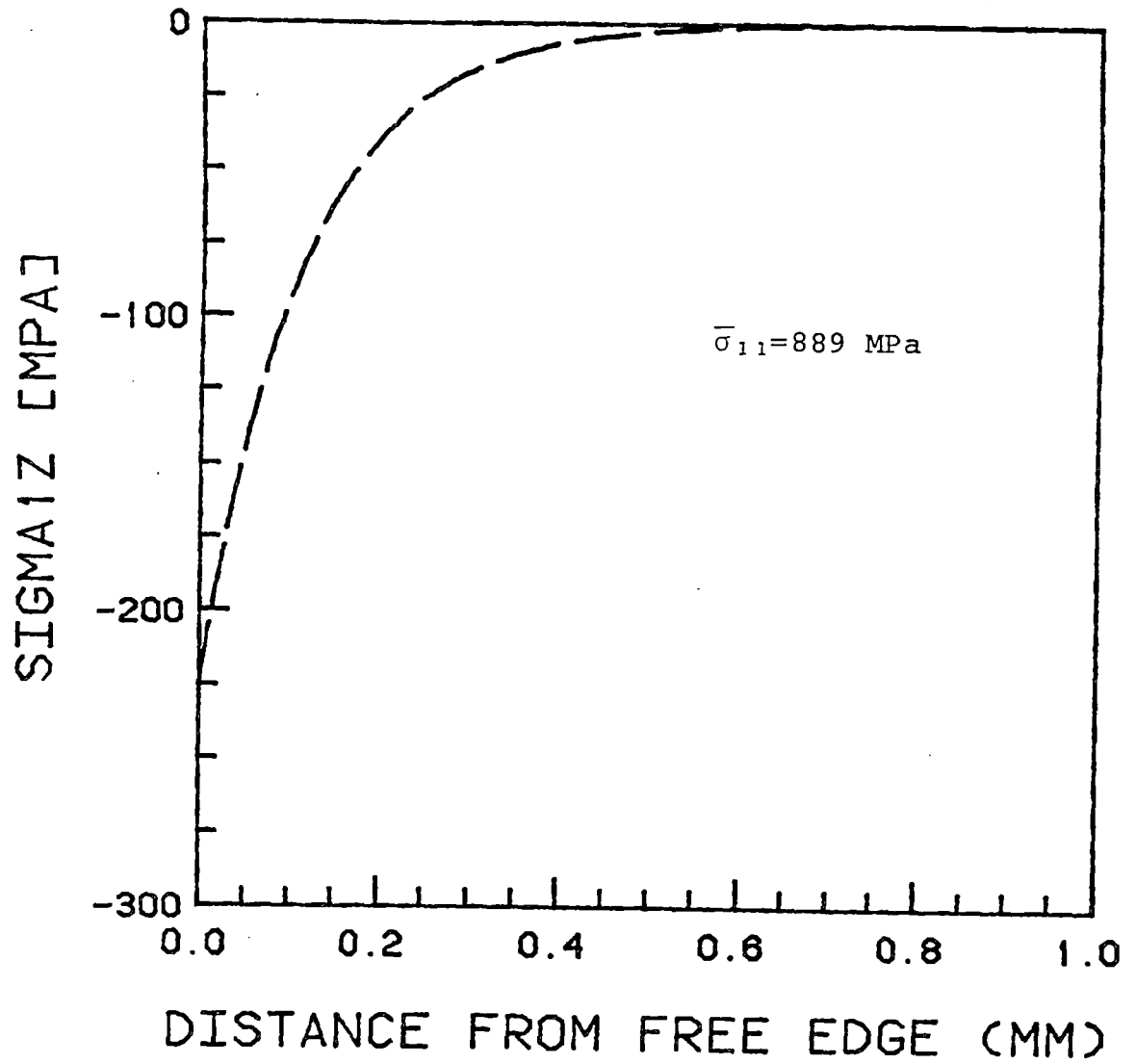
Figure 7.6. Calculated interlaminar shear stress σ_{1z} for $[0/\pm 15]_s$ laminate at $+15/-15$ interface ($\bar{\sigma}_{1z} = 0$ at the other two interfaces)

few millimeters from the free edge without crossing the x axis. Three, the shear stress σ_{1z} reaches its maximum value at the free edge and drops to zero within a few millimeters from the free edge without crossing the x axis. Four, the point at which σ_{zz} crosses the x axis is the same for all interfaces (see Figures 7.1 and 7.2). Similarly, the point at which σ_{2z} reaches its maximum value does not change from interface to interface (see Figures 7.3 and 7.4) This is a result of the fact that the shape of the interlaminar stresses is governed only by the values of λ and ϕ which, being laminate constants, do not change from interface to interface. Five, all interlaminar stresses drop to zero within a small distance (about a millimeter) from the free edge (for a discussion on the boundary layer see section 7.5) thus matching the CLPT prediction of zero interlaminar stresses far from the free edge. Six, changing the stacking sequence, thereby having the 0° ply on the outside rather than at the midplane, changes the sign of the σ_{zz} and σ_{2z} stresses but does not change the sign of σ_{1z}. This is very important in the case of the normal stress σ_{zz} because it turns from tensile (for [±15/0]s) to compressive (for [0/±15]s) at the free edge and therefore will not cause delamination in the [0/±15]s laminate. The maximum stress values (absolute magnitudes) are not the same for the two stacking sequences, that is, moving the 0° ply on the outside of the laminate changes both the

sign of σ_{zz} and σ_{2z} and their shape. On the other hand, σ_{1z} at the +15/-15 interface remains unaffected. Note that at the other two interfaces (Figures 7.5 and 7.6) σ_{1z} is zero.

The through the thickness variation of interlaminar stresses is shown in Figures 7.7, 7.8, and 7.9 for the $[\pm15/0]_s$ laminate. Stresses are plotted as a function of z from the top surface to the midplane of the laminate for x=.05mm. (This value of x is chosen instead of the free edge itself because, at that distance from the free edge, the assumption of homogeneity is still valid). It is important to note that the interlaminar shear stresses σ_{2z} and σ_{1z} (see Figures 7.8 and 7.9) are linear within each ply. They are continuous but their derivatives with respect to z are discontinuous at some ply interfaces (between -15° and 0° and -15° and $+15^{\circ}$ plies in this case). The normal stress σ_{zz} is quadratic within each ply, is continuous, and its derivative with respect to z is also continuous. The discontinuities in the z derivatives of the interlaminar shear stresses result in the "kinks" observed in the stress plots in Figures 7.8 and 7.9 and are due to the fact that the in-plane stresses σ_{22} and σ_{12} are discontinuous at ply interfaces. (The in-plane stress distributions will be presented below). On the other hand, the derivative of σ_{zz} with respect to z is continuous at ply interfaces because (see equilibrium equation 5.6) it is equal to the x derivative of σ_{2z}. The partial derivative of σ_{2z} with
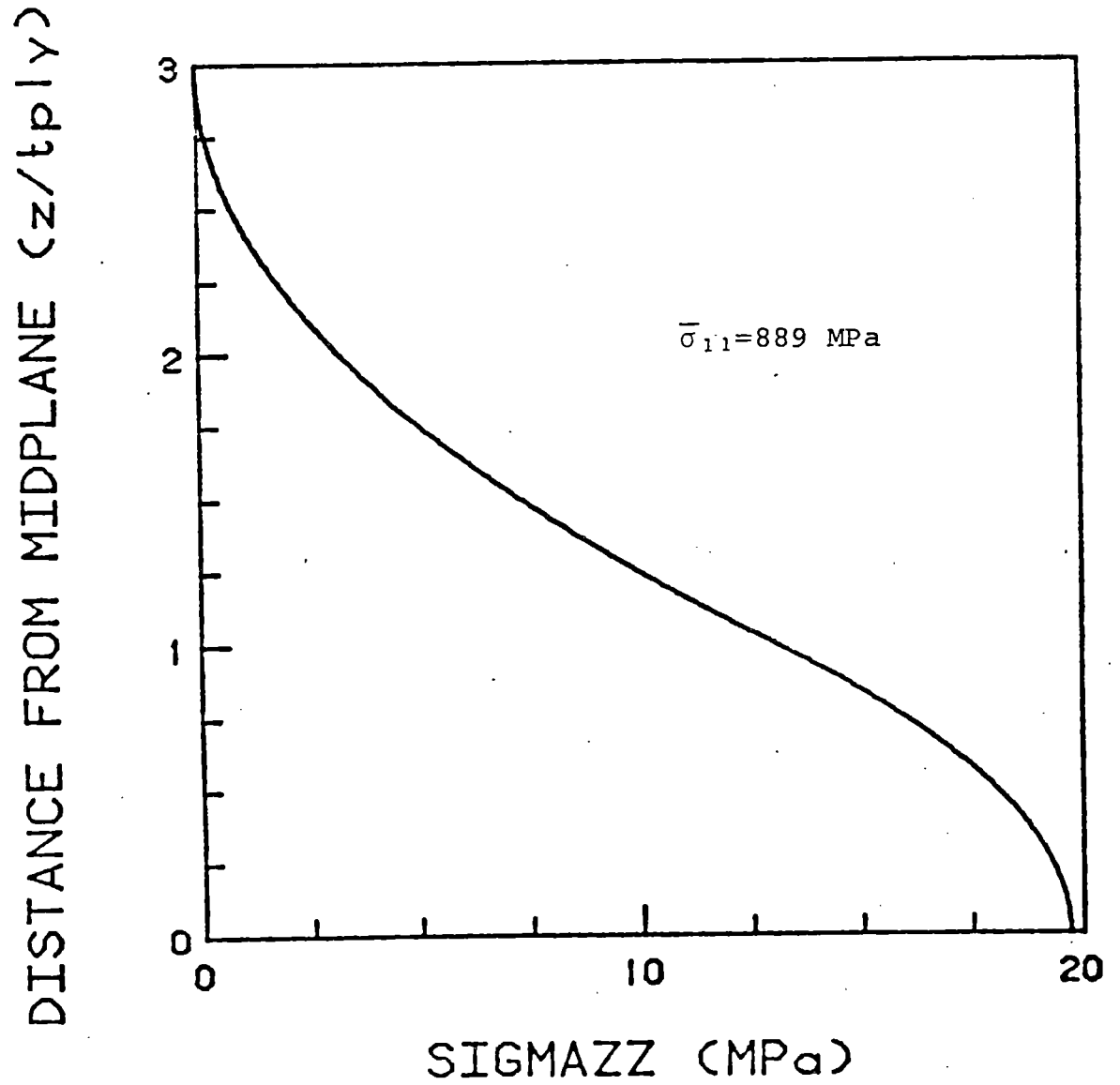
Figure 7.7. Through the thickness variation of σ_{zz}
(from top surface to midplane for
$[\pm15/0]_s$ laminate
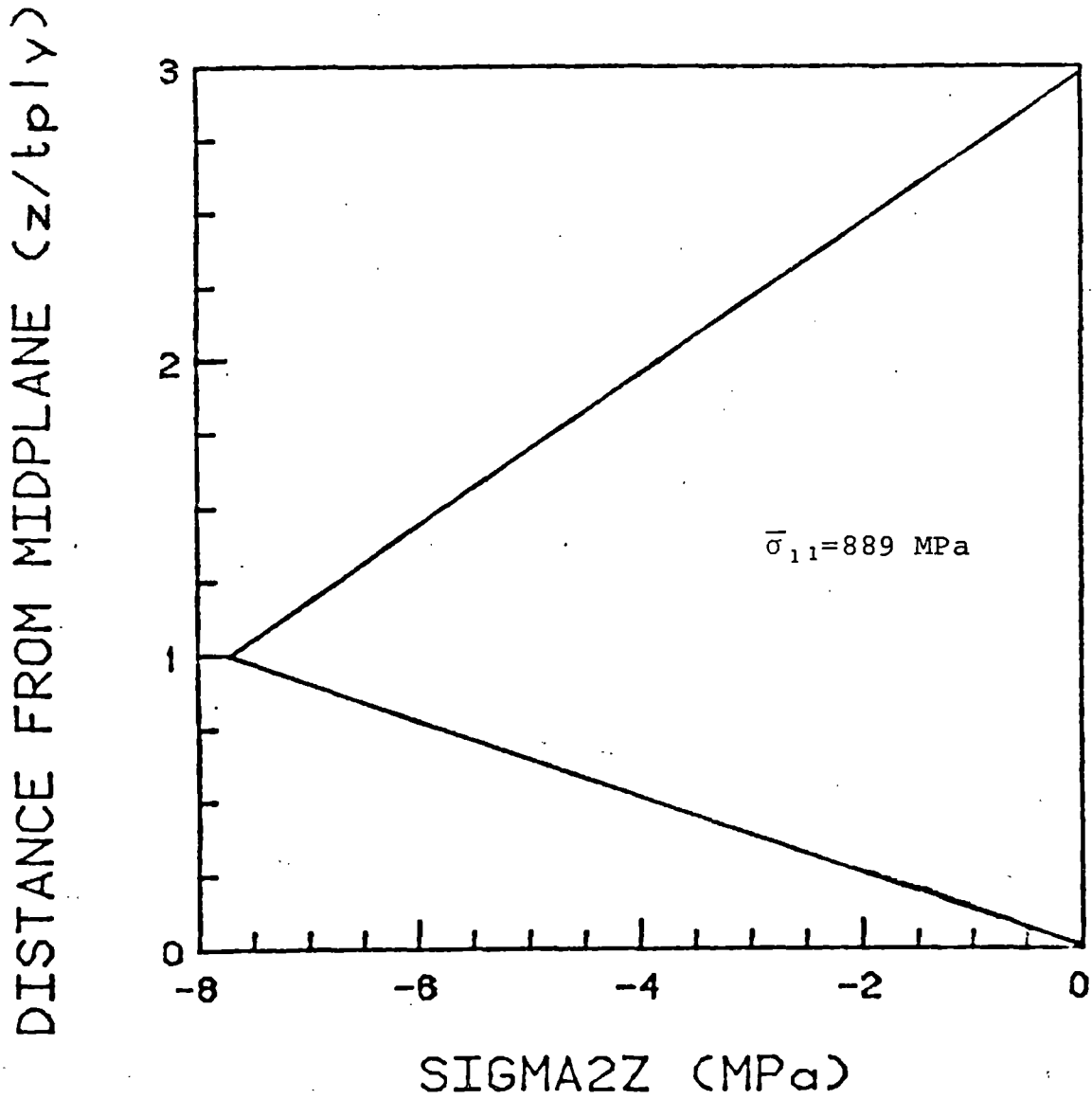
Figure 7.8. Through the thickness variation of σ_{2z} (from top surface to midplane) for $[\pm 15/0]_s$ laminate
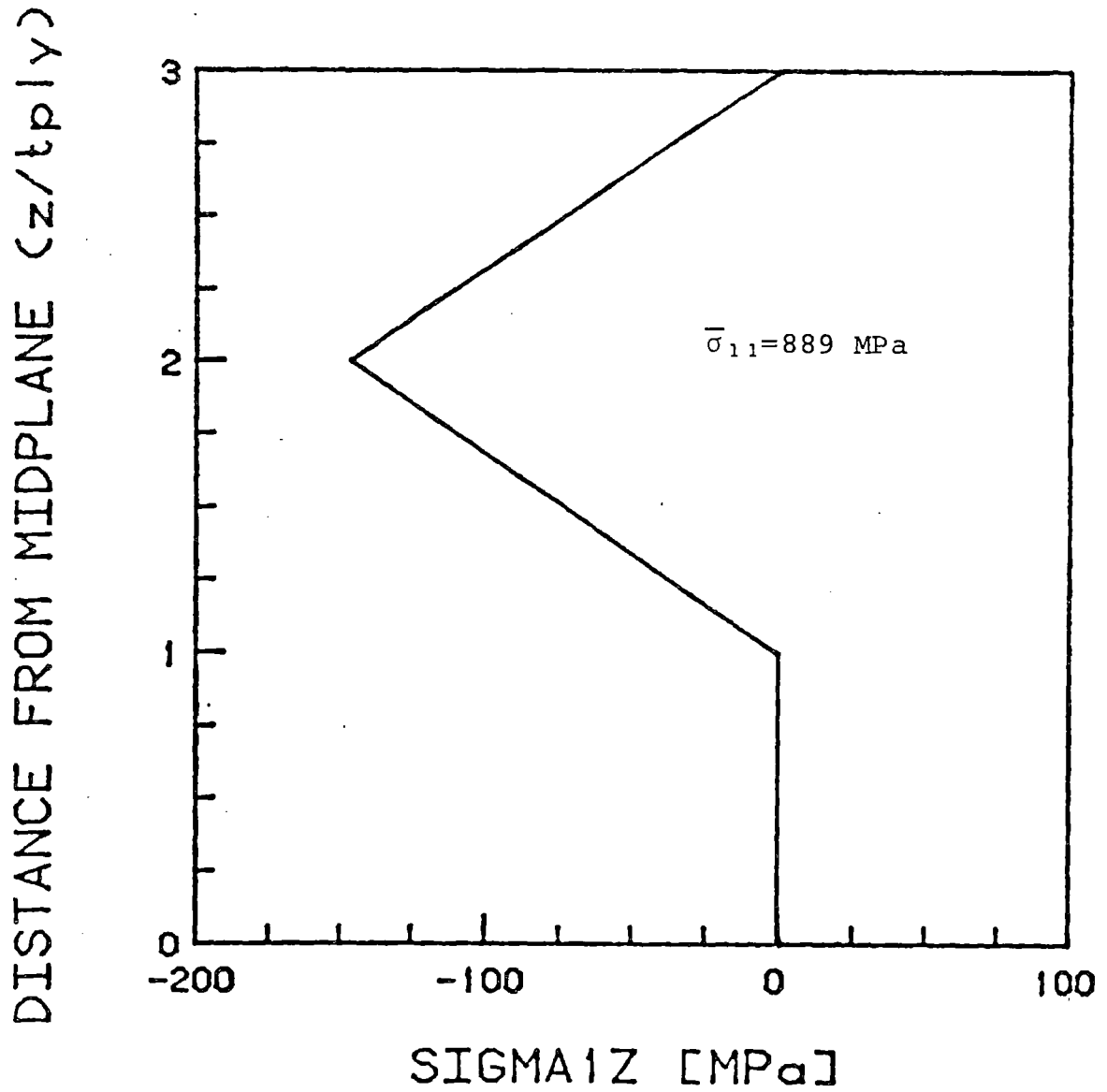
Figure 7.9. Through the thickness variation of σ_{1z} (from top surface to midplane) for $[\pm 15/0]_s$ laminate

respect to x is continuous in z since (see equation 5.10) it is proportional to the function $g_{23}(z)$ which is continuous in z by construction (see section 5.4 on the continuity of σ_{2z}).

All interlaminar stresses are zero at the top surface of the laminate (see Figures 7.7-7.9) in agreement with the boundary condition that the top surface of the laminate is stress-free. The numerical values generated by the computer program for σ_{2z} and σ_{1z} at the midplane are six to seven orders of magnitude smaller than at other interfaces. Thus, the shear stresses σ_{2z} and σ_{1z} are zero at the midplane (see Figures 7.8 and 7.9) in agreement with the argument made in [5] that, due to symmetry, these stresses must be zero there.

The situation for the in-plane stresses σ_{11}, σ_{22}, and σ_{12} is quite different from that for the interlaminar stresses. Consider the expression for σ_{12} (equation 5.63) which is repeated here for convenience:

$$\sigma_{12} = \sigma^L_{12_{[\theta_i]}}(1 - e^{-\phi X}) \tag{5.63}$$

If, at a ply interface, the two adjacent plies do not have the same fiber orientations, $\sigma^L_{12[\theta_i]}$ is different in the two plies and σ_{12} is discontinuous at a ply interface. Even if the fiber orientation is $+\theta$ in one ply and $-\theta$ in the next, $\sigma^L_{12[\theta_i]}$ changes sign at the ply interface and hence σ_{12} is discontinuous. As a result, the z derivative of σ_{1z} will be discontinuous (see equilibrium equation 5.4).

For σ_{22} the expression is (equation 5.59)

$$\sigma_{22} = \sigma^{L}_{22_{[\theta i]}} \left[1 - \frac{\lambda}{\lambda-1} \left(e^{-\phi X} - \frac{1}{\lambda} e^{-\lambda \phi X} \right) \right] \tag{5.59}$$

Again, the only part of the expression that changes from one ply to another is $\sigma^{L}_{22_{[\theta i]}}$. Only if the plies adjacent to the interface of interest have the same fiber orientations $(+\theta/+\theta)$ or fiber orientations of opposite sign $(+\theta/-\theta)$ will $\sigma^{L}_{22_{[\theta i]}}$ remain the same, thus resulting in σ_{22} being continuous at that interface. In all other cases σ_{22} is discontinuous across a ply interface. As a result, the z derivative of σ_{2z} (see equilibrium equation 5.5) will be discontinuous except at $+\theta/+\theta$ or $+\theta/-\theta$ interfaces.

The expression for σ_{11} (equation 5.38) is.

$$\sigma_{11} = \frac{S_{11}\sigma^{L}_{11_{[\theta i]}} + S_{12}\sigma^{L}_{22_{[\theta i]}} + S_{16}\sigma^{L}_{12_{[\theta i]}}}{S_{11}} - \frac{S_{12}}{S_{11}}\sigma_{22} - \frac{S_{13}}{S_{11}}\sigma_{zz} - \frac{S_{16}}{S_{11}}\sigma_{12} \tag{5.38}$$

This expression does not change across an interface only if the adjacent plies have the same fiber orientations $(+\theta/+\theta)$ or fiber orientations of opposite sign $(+\theta/-\theta)$. The reason is that in these cases S_{11}, S_{12}, S_{13}, $\sigma^{L}_{11_{[\theta i]}}$, $\sigma^{L}_{22_{[\theta i]}}$ do not change across an interface and S_{16}, $\sigma^{L}_{12_{[\theta i]}}$ shift sign so that their product $S_{16}\sigma^{L}_{12_{[\theta i]}}$ does not change across an interface. For all other cases, σ_{11} will be discontinuous at a ply interface.

It should be pointed out that these discontinuities in σ_{11}, σ_{22}, and σ_{12} are a result of the requirement that far

from the free edge, the CLPT solution is recovered. The CLPT solution, however, gives σ_{11}, σ_{22}, and σ_{12} stresses that are discontinuous at ply interfaces (see for example the stress values in Table 7.1).

Since the in-plane stresses σ_{11}, σ_{22}, and σ_{12} are generally discontinuous at ply interfaces, the value of these stresses at the interface will depend upon the ply from which the interface is approached in the calculation. This discontinuous nature of the in-plane stresses is their only z dependence. Thus, these stresses are constant through the thickness of an individual ply. Therefore, the variation of the in-plane stresses with distance from the free edge is given for a particular ply in Figures 7.10-7.15.

All in-plane stresses approach their CLPT value far from the free edge. Near the free edge they differ radically from that value and this should be taken into account if these stresses are included in a stress-based failure criterion.

7.2. Variation of ϕ, $\lambda\phi$ with laminate types

The values of ϕ, $\lambda\phi$ for the $[\pm\theta/0]s$ and $[0/\pm\theta]s$ laminate families are shown in Table 7.2 for various values of the lamination angle θ. These values are plotted as a function of θ in Figures 7.16 and 7.17.
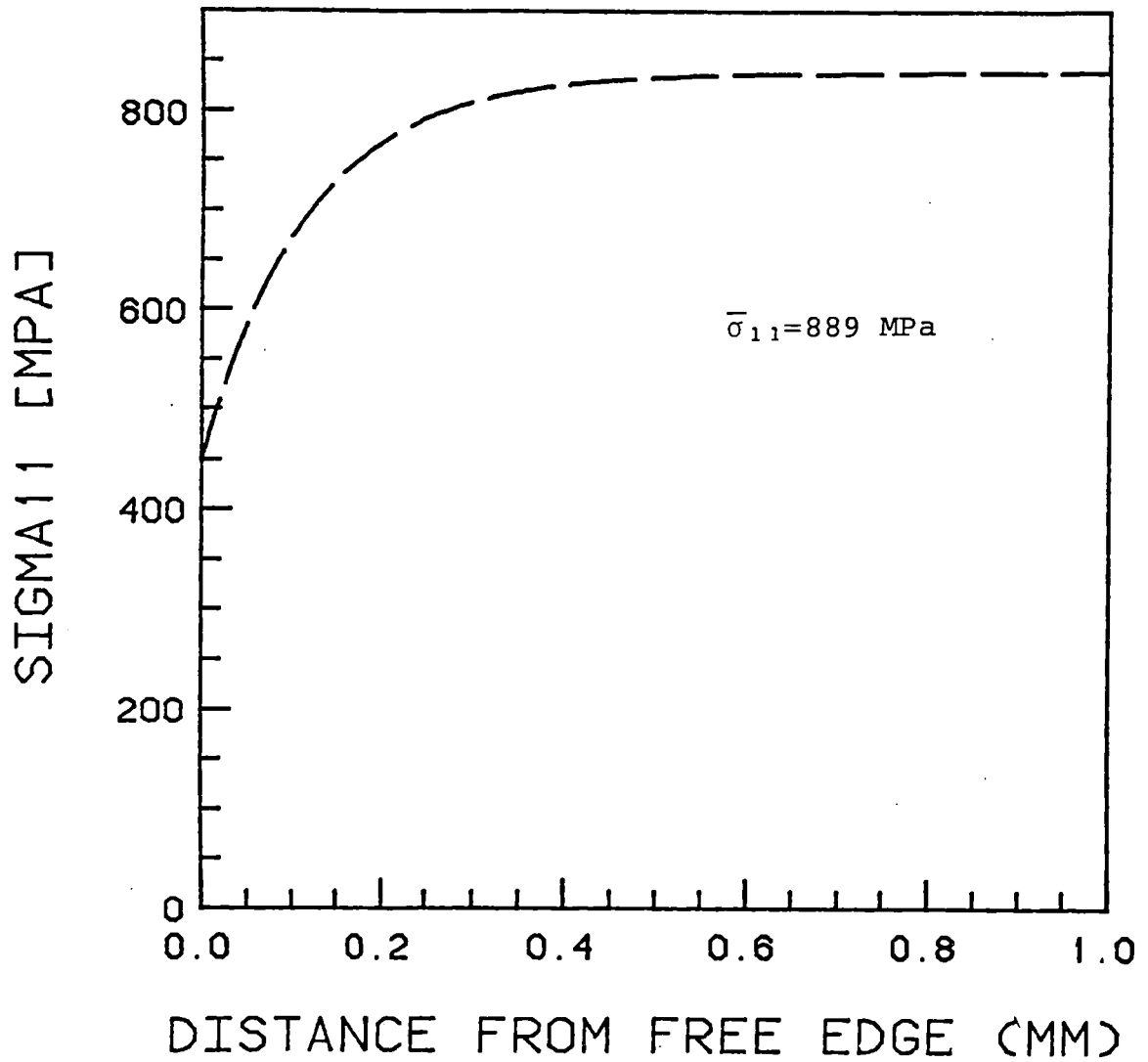
Figure 7.10. Calculated in-plane normal stress σ_{11} in +15° and -15° plies of a $[\pm 15/0]_s$ laminate
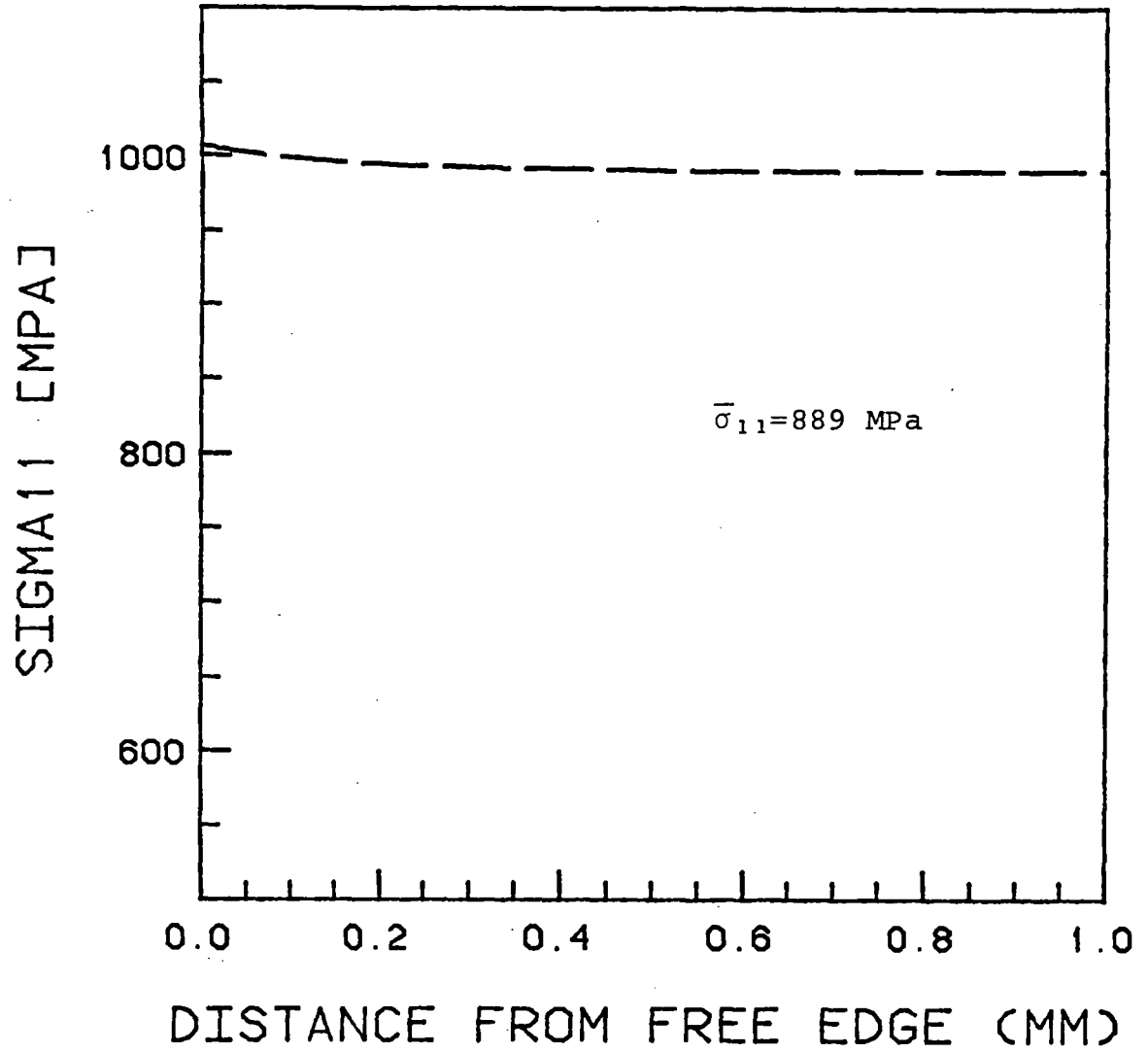
Figure 7.11. Calculated in-plane normal stress σ_{11} in a $0°$ ply of a $[\pm 15/0]_s$
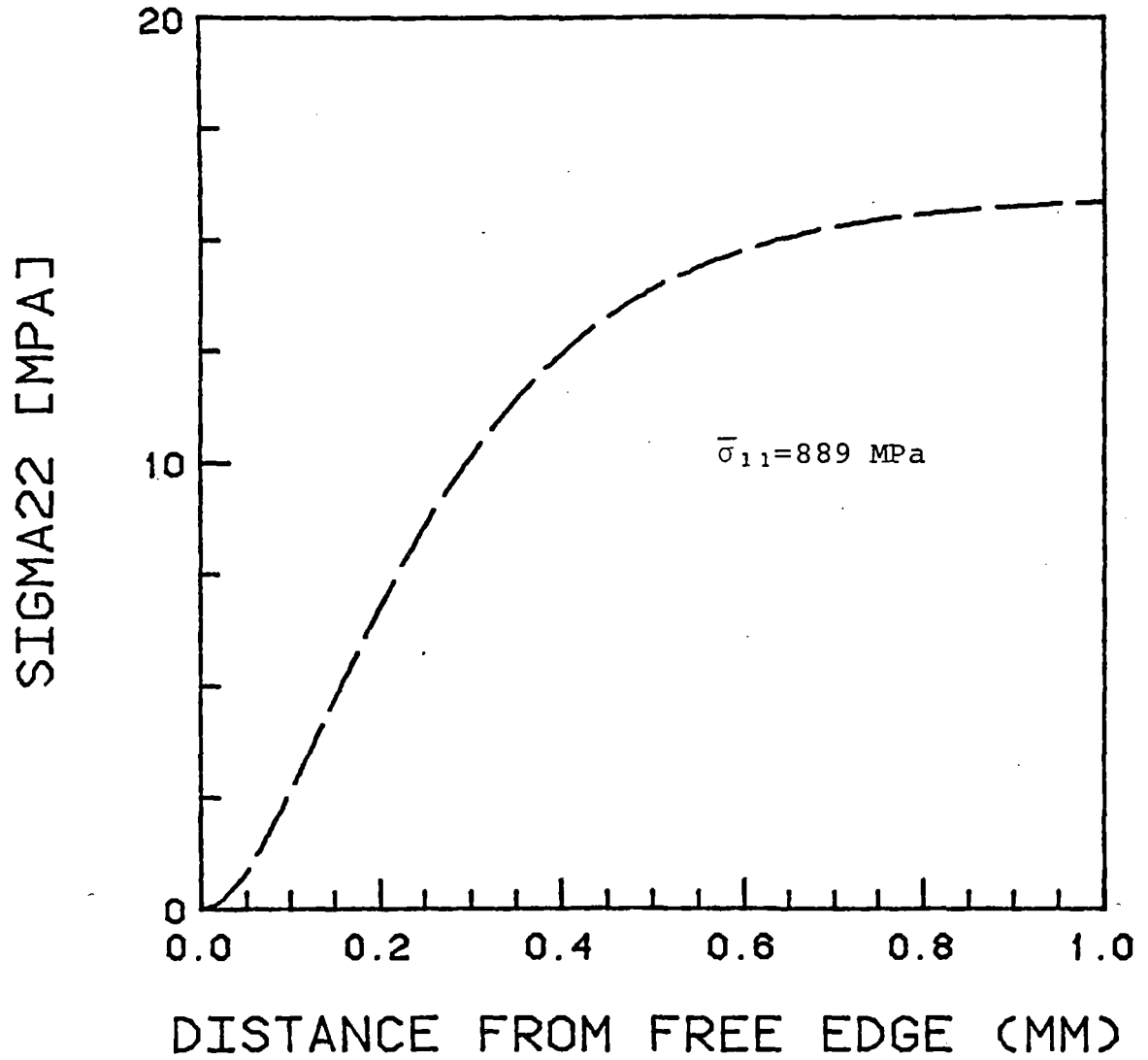
Figure 7.12. Calculated in-plane normal stress σ_{22} in +15° and -15° plies of a $[\pm 15/0]_s$ laminate
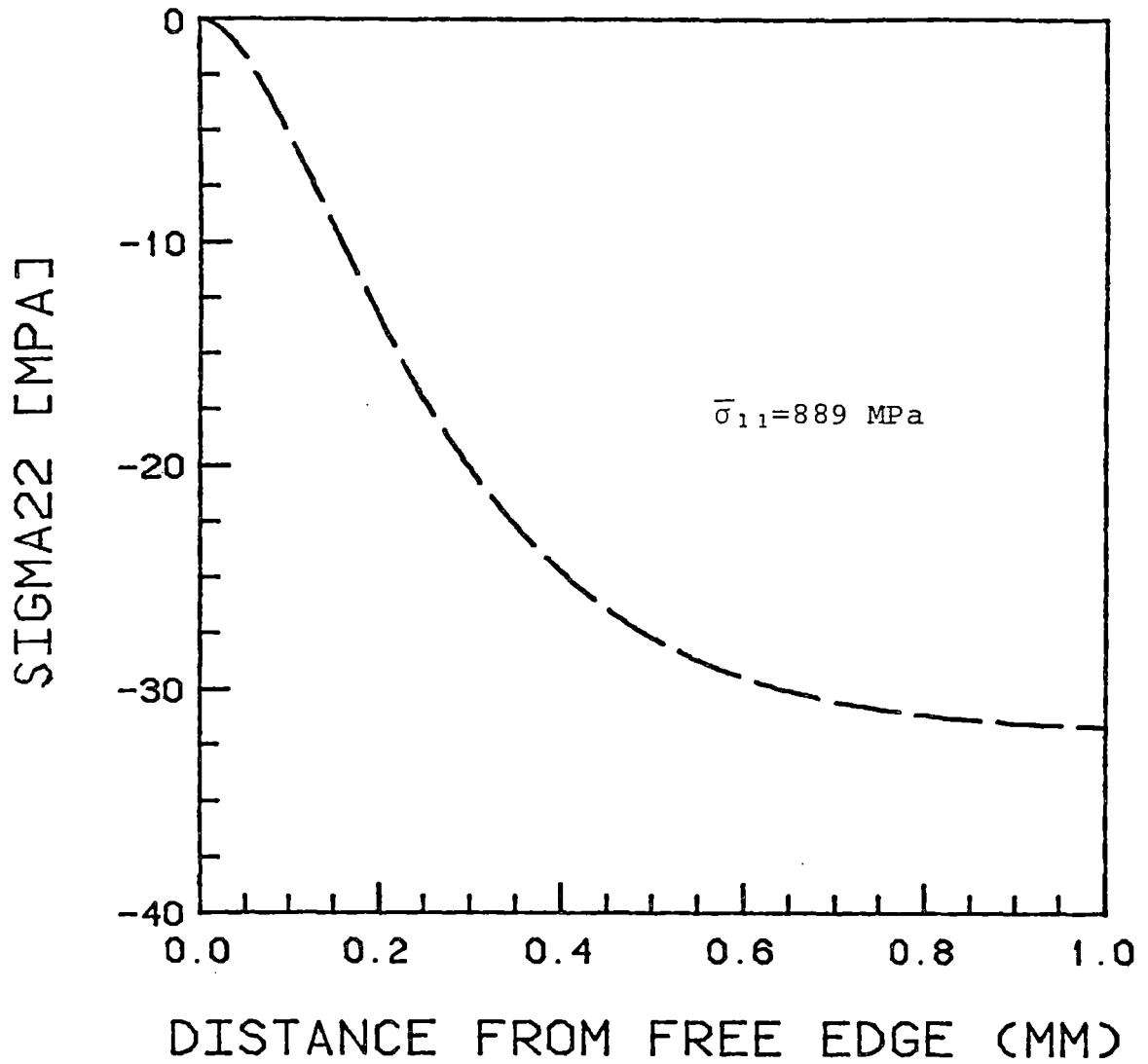
Figure 7.13. Calculated in plane normal stress σ_{22} in a 0° ply of a $[\pm 15/0]_s$ laminate
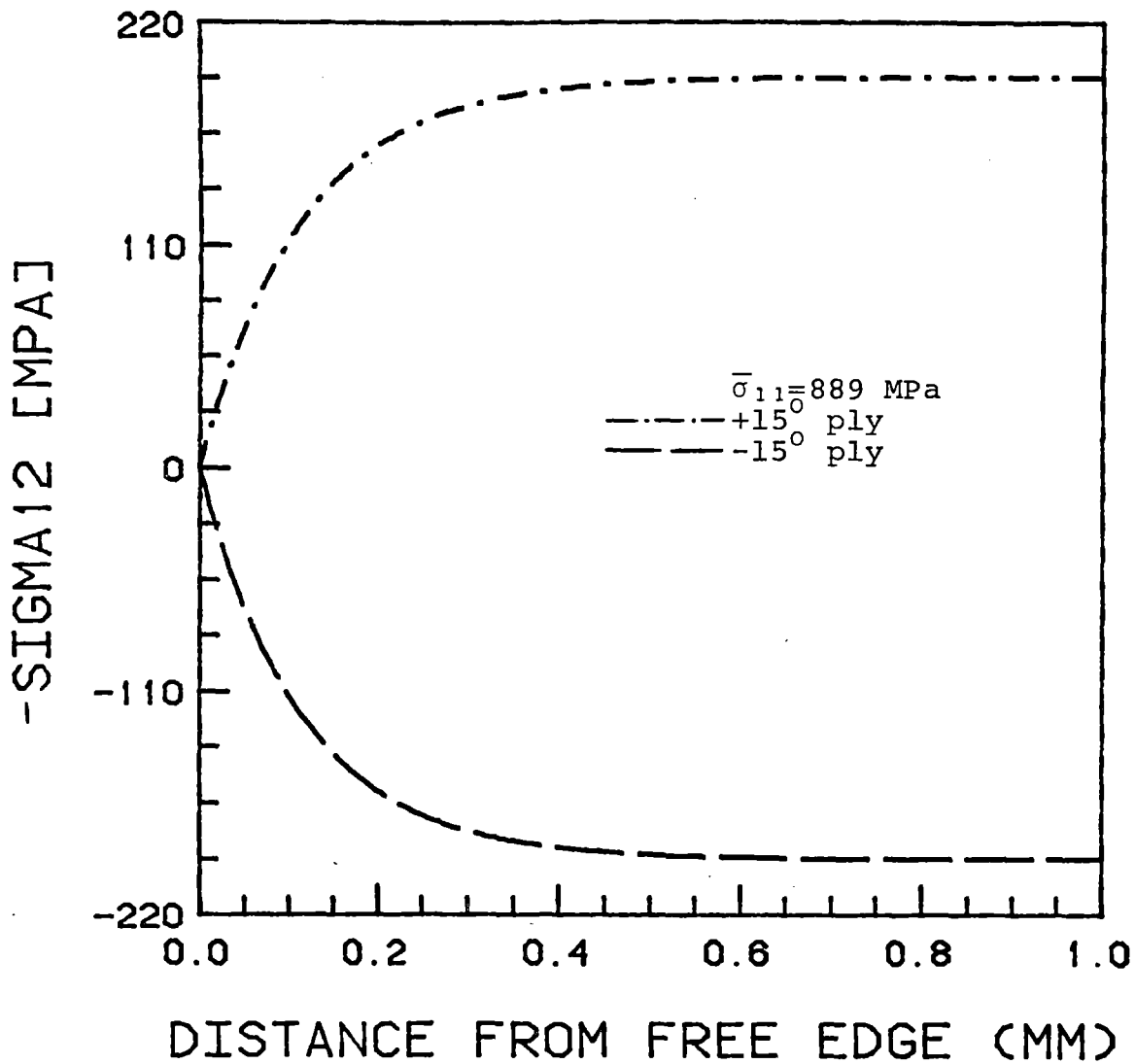
Figure 7.14. In-plane shear stress σ_{12} in $+15°$ and $-15°$
plies of a $[\pm15/0]_s$ laminate
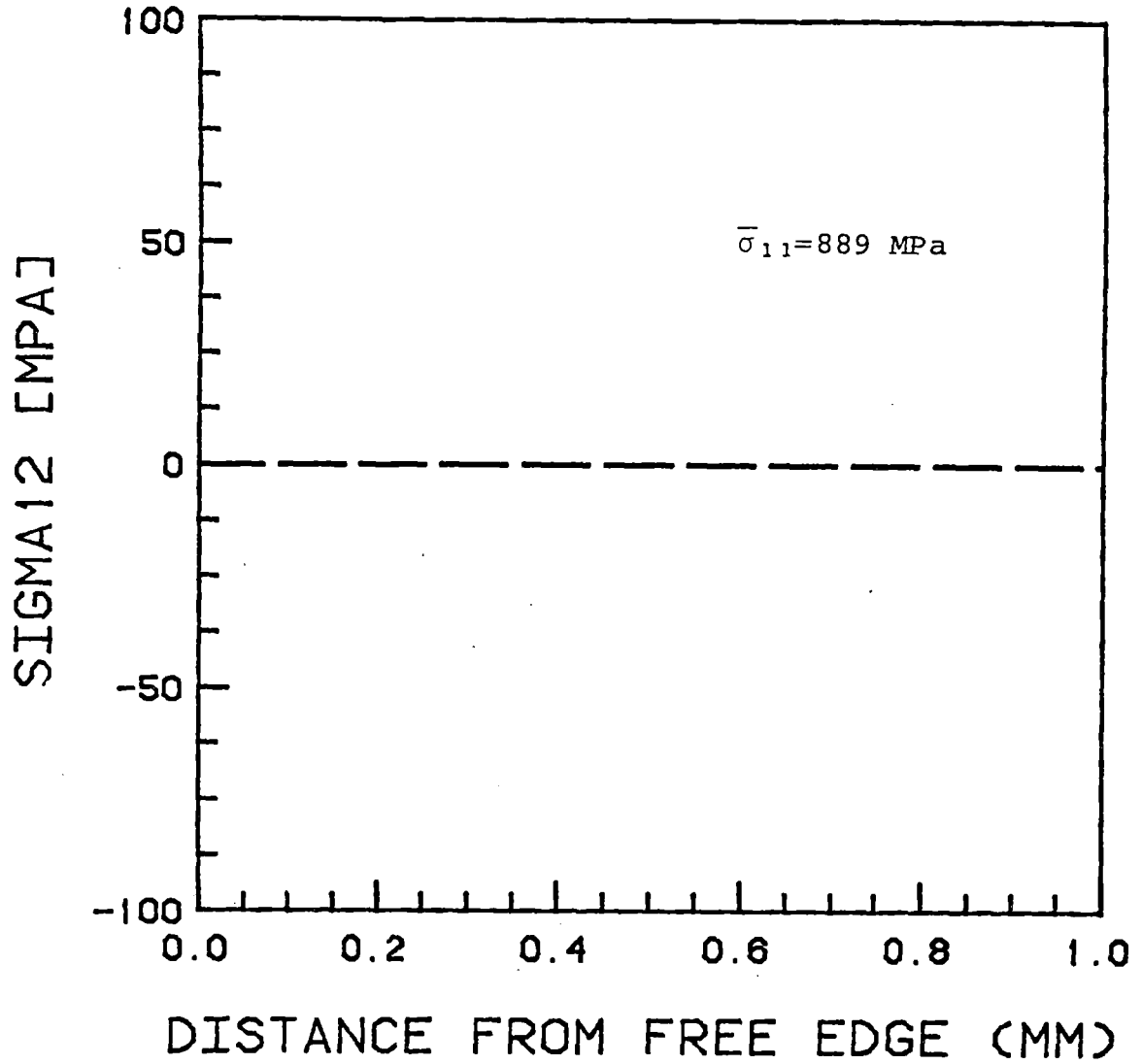
Figure 7.15. In-plane shear stress σ_{12} in a $0°$ ply of a $[\pm 15/0]_s$ laminate

TABLE 7.2

VARIATION OF ϕ, λ AND $\lambda\phi$ WITH LAMINATE TYPE AND LAMINATION ANGLE

	$[\pm\theta/0]_s$			$[0/\pm\theta]_s$		
θ	ϕ	λ	$\lambda\phi$	ϕ	λ	$\lambda\phi$
5	12088	0.42637	5154.1	12089	0.29128	3521.9
10	10358	0.53417	5532.8	10354	0.36249	3753.3
15	8750.9	0.68424	5987.7	8730.6	0.46235	4036.6
20	7602.4	0.84143	6396.9	7549.5	0.57011	4304.0
25	6901.0	0.96886	6684.0	6804.3	0.62242	4507.1
30	6558.1	1.0396	6817.8	6416.3	0.71933	4615.4
35	6487.6	1.0486	6802.9	6309.3	0.73181	4617.2
40	6629.5	1.0046	6659.9	6430.9	0.70177	4513.1
45	6958.3	0.92061	6405.9	6761.6	0.63615	4301.4
50	7493.0	0.80627	6041.4	7322.8	0.54045	3957.6
55	8317.0	0.66431	5525.1	8192.9	0.41107	3367.9
57.5	8888.6	0.57773	5135.3	8792.2	0.32141	5135.3
60	9603.5	0.42558	4087.1	9557.9	0.16948	1619.9
61	9943.3	2.8930	2876.6	9665.0	8.9940	89624
62.5	10463	0.56325	5893.6	10397	1.09738	11409
65	11397	0.44532	5975.1	11231	0.53201	5975.1
70	12190	0.39358	4770.0	12181	0.37053	4513.2
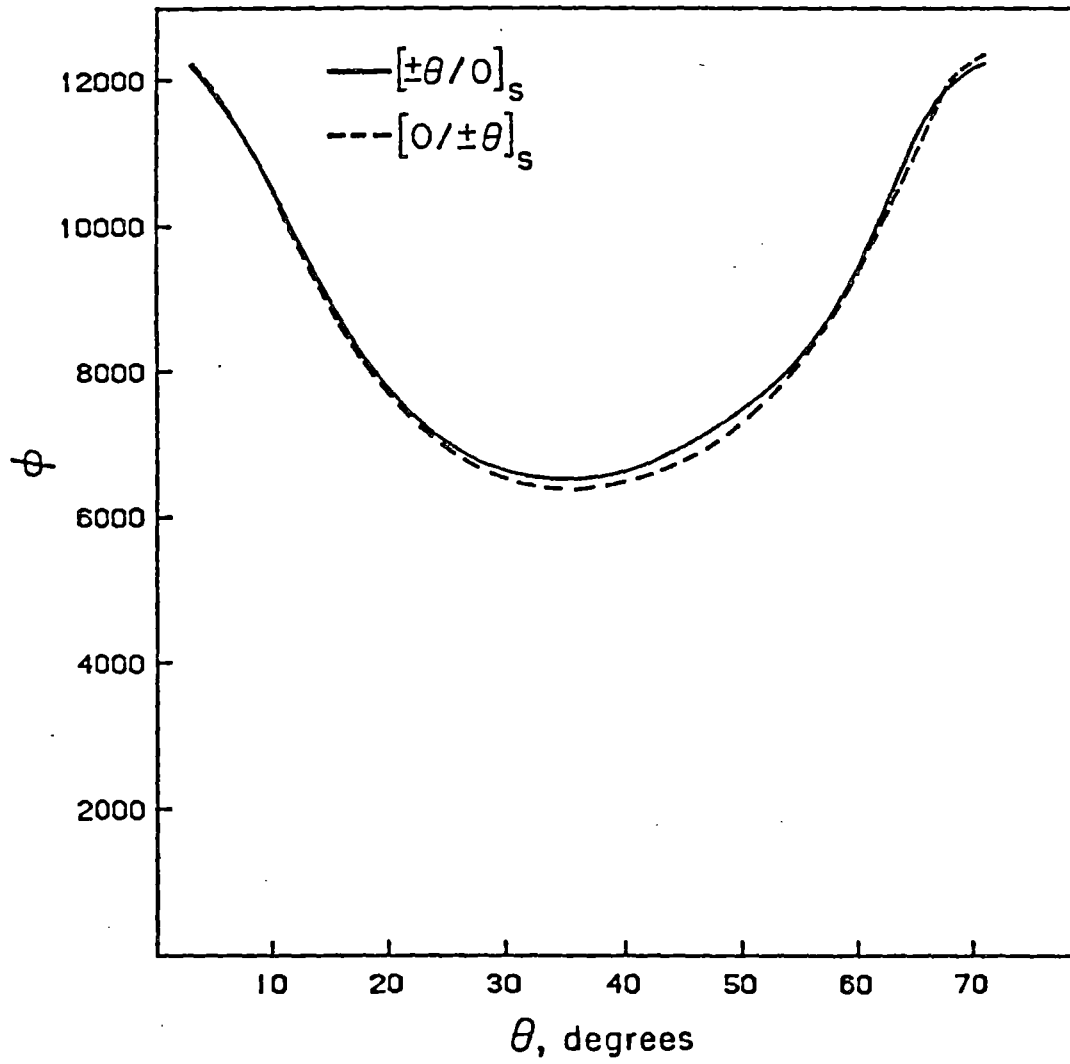
Figure 7.16 Distribution of ϕ as a function of θ for $[\pm\theta/0]_s$ and $[0/\pm\theta]_s$ laminate families

Figure 7.17 Distribution of $\lambda\phi$ as a function of θ
for $[\pm\theta/0]_s$ and $[0/\pm\theta]_s$ laminate families

As it is seen from Table 7.2 and Figure 7.16, for a given angle, ϕ is approximately the same for the two laminate families. As the lamination angle θ increases from 0° to 40°, ϕ decreases. At θ approximately equal to 40°, ϕ reaches a minimum and then increases with increasing lamination angle. The ϕ values for the $[0/\pm\theta]s$ family are always smaller than the ϕ values for the $[\pm\theta/0]s$ family except for lamination angles larger than 65°.

The situation for $\lambda\phi$ is somewhat different as can be seen in Figure 7.17. The values for the $[0/\pm\theta]s$ family are about two thirds of the values for the $[\pm\theta/0]s$ family. For both laminate families $\lambda\phi$ increases with lamination angle up to $\theta \simeq 30^\circ$. It then starts decreasing until θ reaches approximately the value 60°. At this point, (actually at a θ value between 60° and 61°) there is a jump in the curve as shown in Figure 7.17 and the $\lambda\phi$ values become extremely high. For larger lamination angles, $\lambda\phi$ drops rapidly so that for θ larger than 69° the $\lambda\phi$ values are again comparable to the $\lambda\phi$ values that correspond to lamination angles smaller than 60°. This "jump" in the $\lambda\phi$ curve is more pronounced in the $[0/\pm\theta]s$ family. It can be explained easily if one considers the CLPT solution for these laminates. Table 7.3 shows the CLPT solution for the $[\pm60/0]s$ and $[\pm61/0]s$ laminates. The $\sigma_{22[\theta i]}^L$ value is very small. Also, these values have different signs from one laminate to the other in plies that have the same z location in the two

TABLE 7.3

CLPT SOLUTION FOR $[\pm60/0]_S$ AND $[\pm61/0]_S$ LAMINATES

(APPLIED LOAD $\bar{\sigma}_{11}$ = 100 MPa)

Stresses In [MPa]	$[\pm60/0]_S$			$[\pm61/0]_S$		
	Ply 1 (+60°)	Ply 2 (-60°)	Ply 3 (0°)	Ply 1 (+61°)	Ply 2 (-61°)	Ply 3 (0°)
$\sigma^L_{11[\theta i]}$	24.4	24.4	251	24.0	24.0	252
$\sigma^L_{22[\theta i]}$	0.180	0.180	-0.260	-0.012	-0.012	0.024
$\sigma^L_{12[\theta i]}$	5.08	-5.08	0	4.60	-4.60	0

laminates. This means that for some value of the lamination angle between 60° and 61°, $\sigma_{22[\theta i]}^L$ will be identically zero and this then will be the same as the special case presented in section 6.1. As was shown in that section the λ value does not appear in the solution since the stresses whose expressions involve λ are zero identically. Therefore, the eigenfunction $e^{-\phi x}$ (see equations 6.2-6.7) is sufficient to describe the stress shapes. Thus, the solution that involves both λ and ϕ will be consistent with this observation only if the contribution of the eigenfunction $e^{-\lambda \phi x}$ is negligible for lamination angles between 60° and 65°. This means that $\lambda \phi$ must be very large and positive in that region which is exactly the case as illustrated by the $\lambda \phi$ values in Table 7.3 and Figure 7.17. Of course, if θ is equal to that critical value between 60° and 61° for which $\sigma_{22[\theta i]}^L$ is exactly zero, λ will be infinite.

Another way to explain this behavior is to note that in this region of lamination angles $(60^\circ-65^\circ)$ the solution should be similar to the solution obtained for angle-ply laminates in section 6.1. This can be demonstrated by actually determining the ϕ value for laminates with θ values between 60° and 65° using the solution method developed for angle-plied laminates. For example, for a $[0/\pm61]s$ laminate treated as an angle-ply laminate the ϕ value is found to be 9959.507 m^{-1} while the general method using both λ and ϕ gives a ϕ value of 9965.006 m^{-1}. The difference between the two is only .055%.

It should be noted that an analogous situation may occur if the stacking sequence and ply orientations in a laminate are such that the in-plane shear stress $\sigma_{12[\theta i]}^{L}$ is zero in all plies. In that case the solution should be very similar to that obtained for cross-plied laminates in section 6.2.

7.3 Constant versus variable longitudinal stress in each ply

It was indicated in section 5.2 that, instead of determining σ_{11} in each ply with the use of the strain-displacement equations, the CLPT value $\sigma_{11[\theta i]}^{L}$ could be used for σ_{11} throughout each ply. This latter procedure is obviously less rigorous and would be preferred only if it gave similar predictions for the interlaminar stresses since it simplifies the calculations somewhat (see expressions for the constants d_i in equation 5.108 and appendix A4).

This is not the case however. Not only does σ_{11} differ in the boundary layer by as much as 95% as shown in Figure 7.18, but the σ_{zz}, σ_{2z} and σ_{1z} predictions show appreciable differences (from 5% to 20% in regions close to the free edge) between the two approaches as illustrated in Figures 7.19, 7.20, and 7.21. Therefore, the more rigorous approach to determine σ_{11} (equation 5.38) should be used.
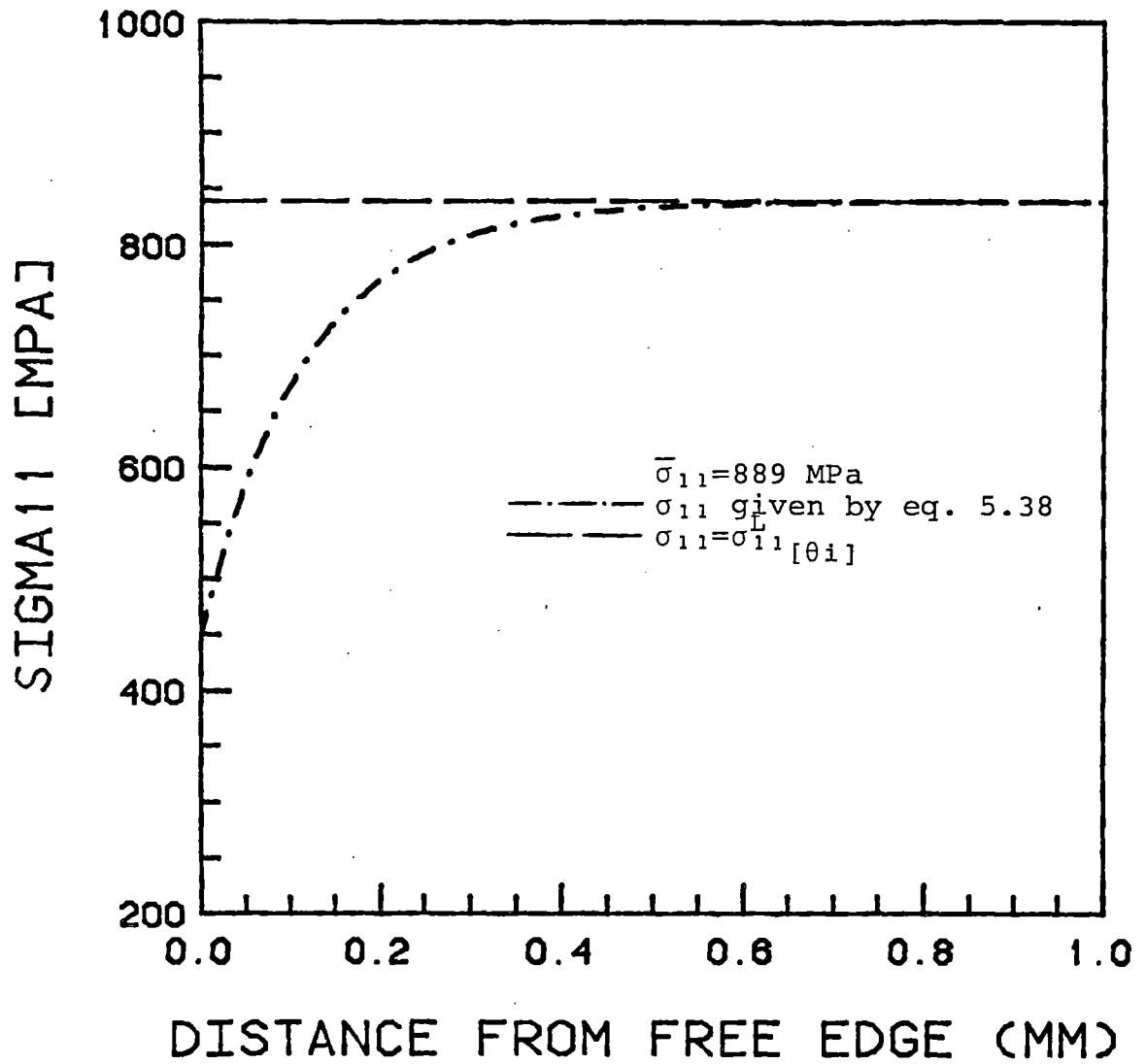
Figure 7.18. Calculated in-plane normal stress σ_{11} at [15/-15 interface for $[\pm 15/0]_s$ laminate for the two methods of determining σ_{11}
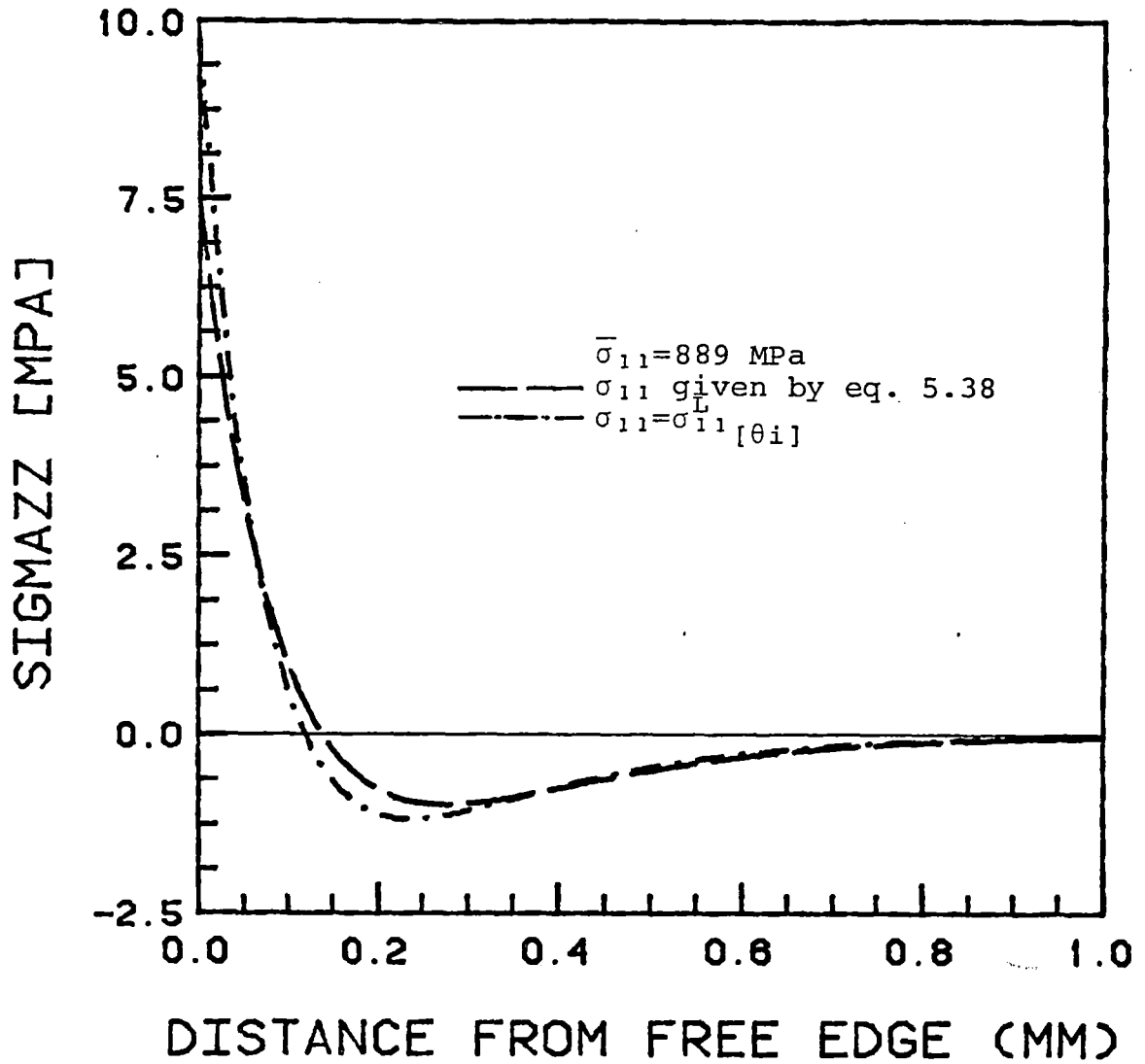
Figure 7.19. Calculated interlaminar normal stress σ_{zz} at +15/-15 interface for $[\pm 15/0]_s$ laminate for the two methods of determining σ_{11}
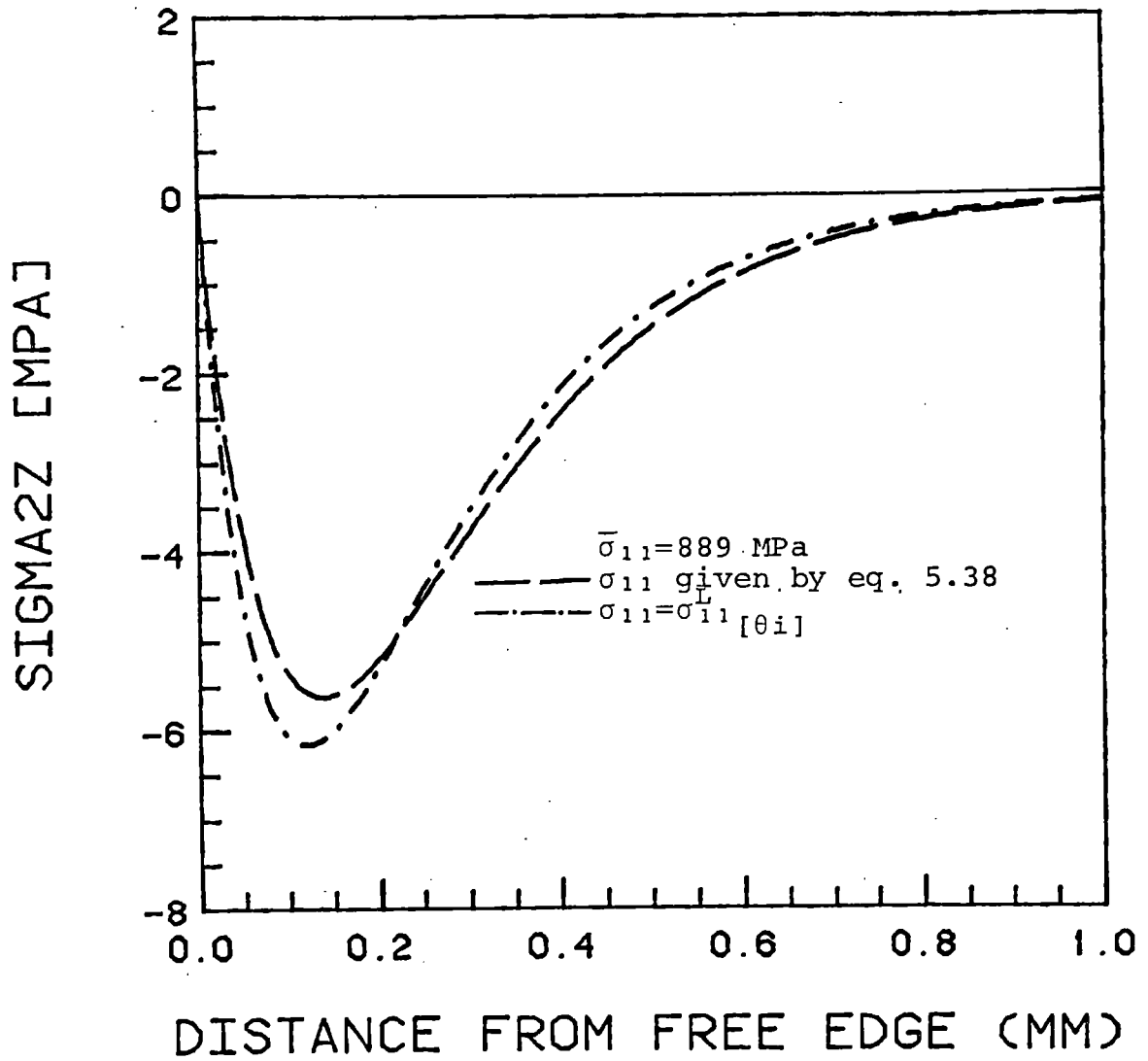
Figure 7.20. Calculated interlaminar shear stress σ_{2z} at +15/-15 interface for $[\pm15/0]_s$ laminate for the two methods of determining σ_{11}
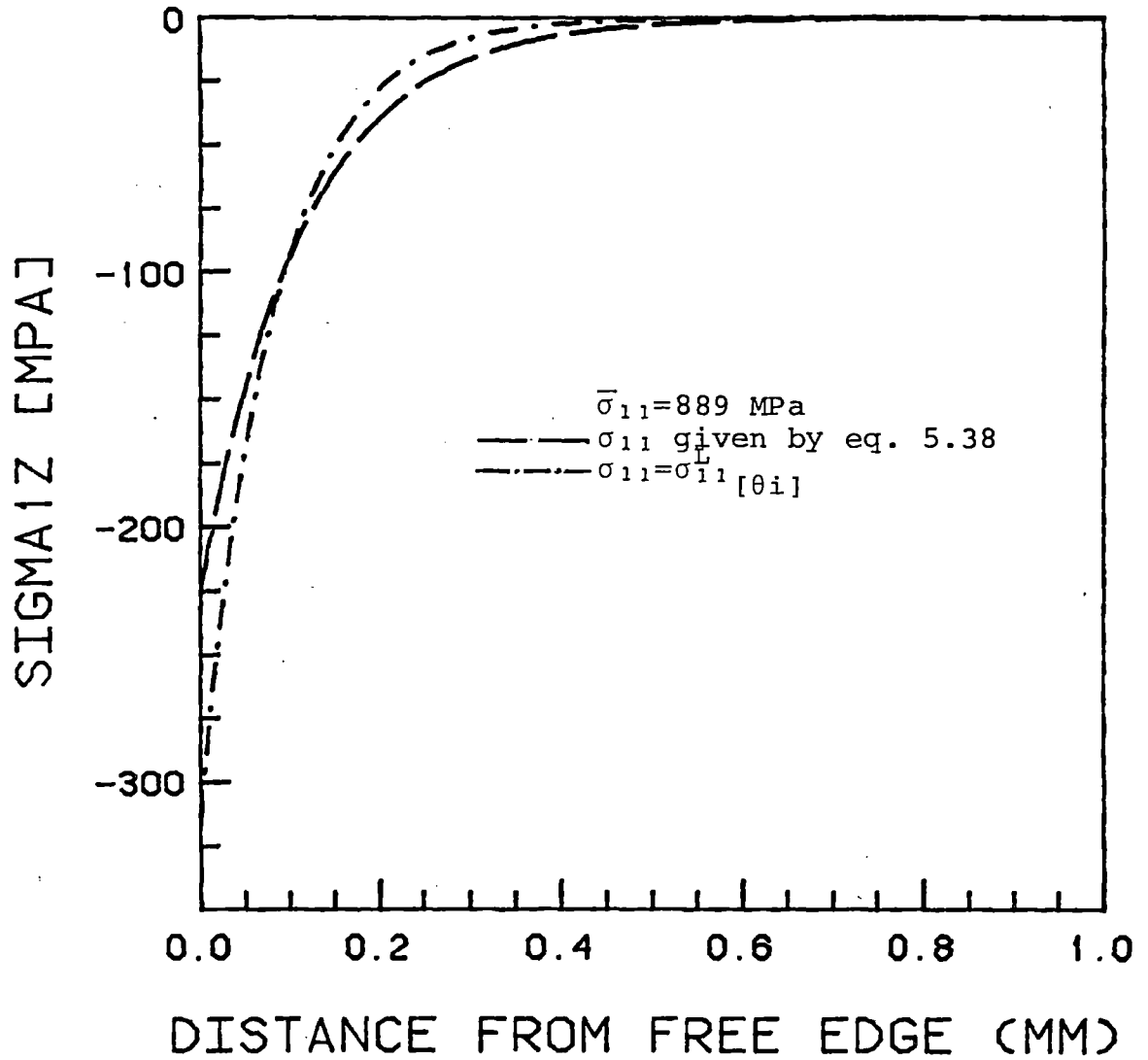
Figure 7.21. Calculated interlaminar shear stress σ_{1z} at +15/-15 interface for $[\pm15/0]_s$ laminate for the two methods of determining σ_{11}

7.4 Sensitivity of the solution to basic ply three dimensional elastic constants

In all the analyses presented in chapter 2, except the one in [31], the values for G_{23} and ν_{23} of the basic unidirectional ply used are taken to be the same as those of G_{13} and ν_{13}. This, however, is not the case. These three-dimensional elastic constants were measured by Knight and Pagano [42] and were found to be quite different from the values usually assumed. Actually, ν_{23} was even found to be larger than 0.5. The elastic constants used in other analyses as well as those used in this analysis (the measured values) are shown in Table 7.4.

The interlaminar stresses σ_{zz}, σ_{2z} and σ_{1z} at the +15/-15 interface of the [±15/0]s laminate obtained using the two different sets of elastic constants, are shown in Figures 7.22, 7.23, and 7.24. The differences are small and one might be tempted to say that it is not very important which set of constants is used. However, for other laminates the differences may be appreciable. For example, for a [±60/0]s laminate the set of elastic constants used by most investigators results in the discriminant of the ϕ polynomial (equation 5.112) being negative irrespective of the starting ϕ value. This means that both λ and ϕ are complex in this case which is not allowed. On

TABLE 7.4

ELASTIC CONSTANTS USED IN THE PRESENT (MEASURED)
AND IN OTHER (ASSUMED) ANALYSES

Constant	Measured	Assumed
E_{11}	130 GPa	138 GPa
E_{22}	10.5 GPa	14.5 GPa
E_{33}	10.5 GPa	14.5 GPa
G_{12}	6 GPa	5.9 GPa
G_{13}	6 GPa	5.9 GPa
G_{23}	4.8 GPa	5.9 GPa
ν_{12}	0.28	0.21
ν_{13}	0.28	0.21
ν_{23}	0.54	0.21
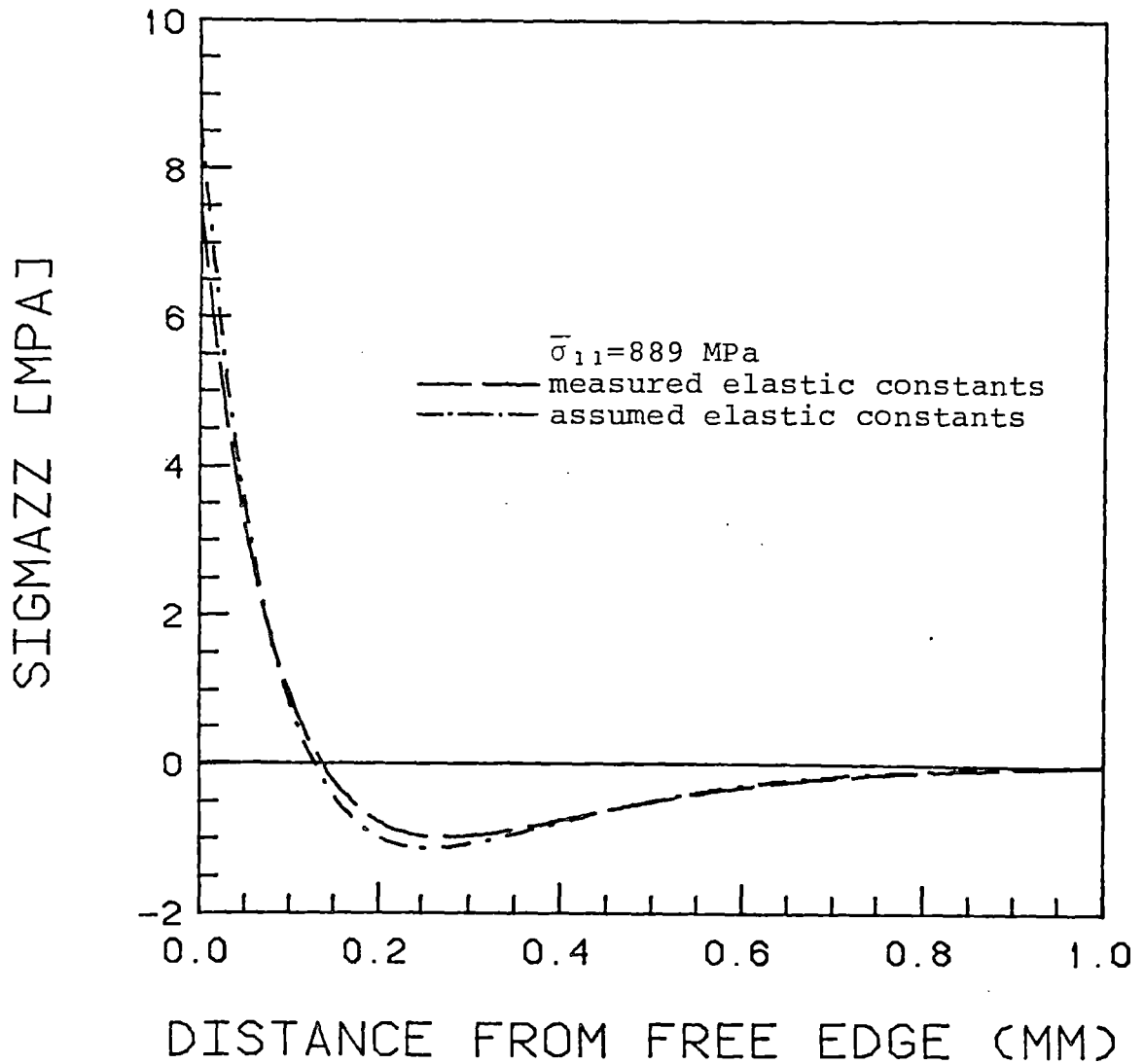
Figure 7.22. Calculated interlaminar normal stress σ_{zz}
for $[\pm 15/0]_s$ laminate at +15/-15 interface
using two different sets of elastic
constants
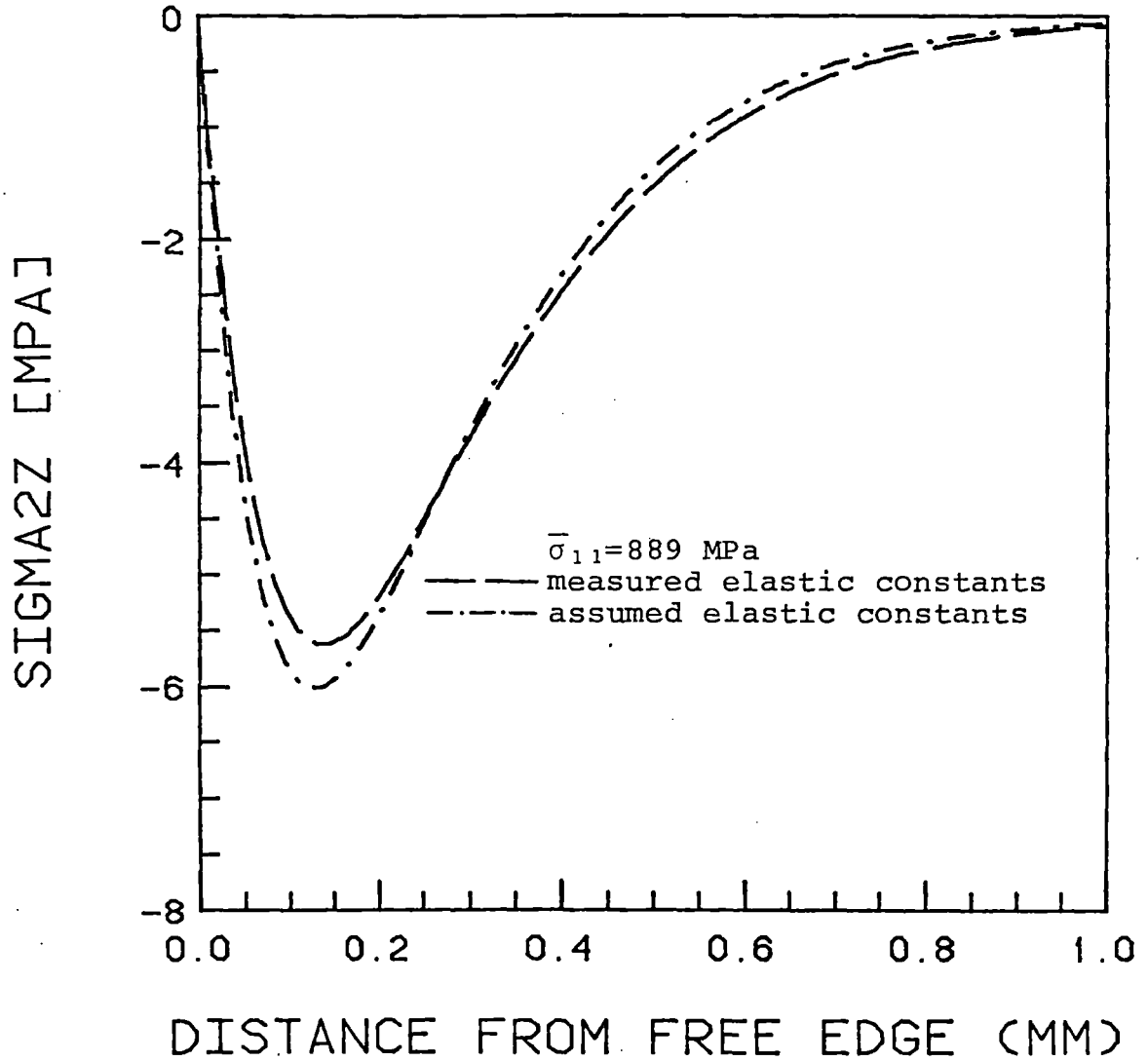
Figure 7.23. Calculated interlaminar shear stress σ_{2z}
for $[+15/0]_s$ laminate at +15/-15
interface using two different sets of
elastic constants
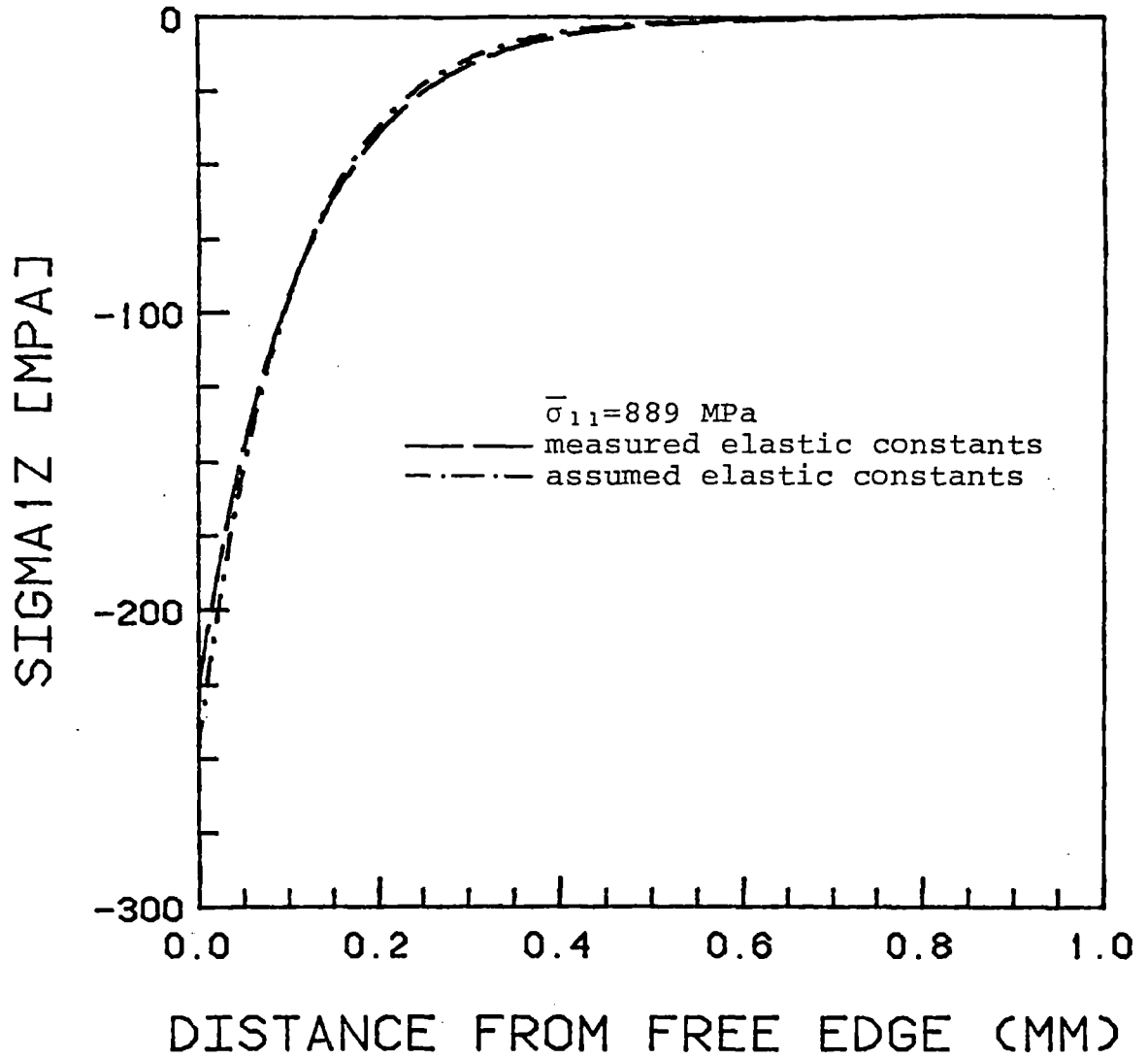
Figure 7.24. Calculated interlaminar shear stress σ_{1z} for $[\pm 15/0]_s$ laminate at +15/-15 interface using two different sets of elastic constants

the other hand, if the proper set of elastic constants is used, the solution can be obtained without any problems.

The conclusion is that if the three-dimensional elastic constants have been measured, they should be used as they do not add to the complexity of the problem and will result in a more accurate answer than the use of the assumed constants. However, if measured three-dimensional elastic constants are not available, the results show that using the assumed G_{23} and ν_{23} for the basic ply results in acceptable answers for most laminates.

7.5 The boundary layer

The boundary layer is the region, close to the free edge, in which the interlaminar stresses are appreciable. The exact definition of the boundary layer size is rather arbitrary and there are several possible ways of defining it [5,24]. In the present investigation two possible definitions are used depending on whether σ_{zz} exists or not. The simpler one will be presented first.

(a) For laminates in which σ_{zz} is everywhere zero (e.g. in the case of angle-plied laminates) the boundary layer is defined as the distance from the free edge at which σ_{1z} drops to 1% of its value at the free edge. This can be expressed in the form

$$e^{-\phi x_{BL}} = 0.01 \tag{7.1}$$

which leads to the expression

$$x_{BL} = \frac{4.4}{\phi} \tag{7.2}$$

Actually with this definition, the stress σ_{1z} at a distance equal to the boundary layer width is exactly equal to 1.2% of the value at the free edge.

(b) For most laminates, σ_{zz} is generally nonzero and can be used to define the boundary layer instead. The boundary layer is thus defined as the distance over which equation 4.14 is "almost" satisfied, i.e. the distance over which 99% of σ_{zz} is counterbalanced. This can be expressed in the form (see Figure 7.25b)

$$0.99 \int_0^{x_0} \sigma_{zz}dx = - \int_{x_0}^{x_{BL}} \sigma_{zz}dx \tag{7.3}$$

For the special case of a cross-plied laminate, equation 6.35 the expression for σ_{zz} placed into equation 7.3 gives:

$$0.99 \int_0^{x_0} (1 - \phi x)e^{-\phi x} = - \int_{x_0}^{x_{BL}} (1 - \phi x) e^{-\phi x}dx \tag{7.4}$$

where x_0 is defined as the point where σ_{zz} crosses the x axis (see Figure 7.25b) and is equal to $1/\phi$ for this special case.

The following equation for x_{BL} can be obtained from equation 7.4:

$$x_{BL} = \frac{1}{\phi} \ell n (100 \, x_{BL}\phi e) \tag{7.5}$$

σ_{1z}

(a)

$0.01\sigma_{1z}(x=0)$

x_{BL} x

σ_{zz}

(b)

$|B|=0.99|A|$

A

B

x_{BL}

x
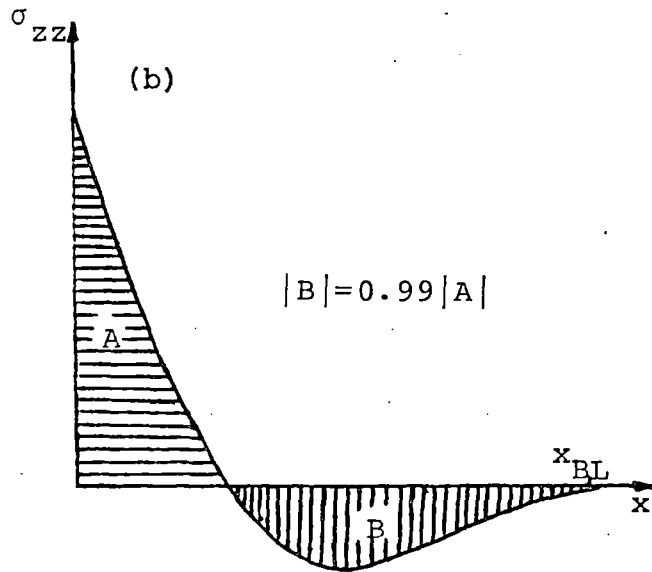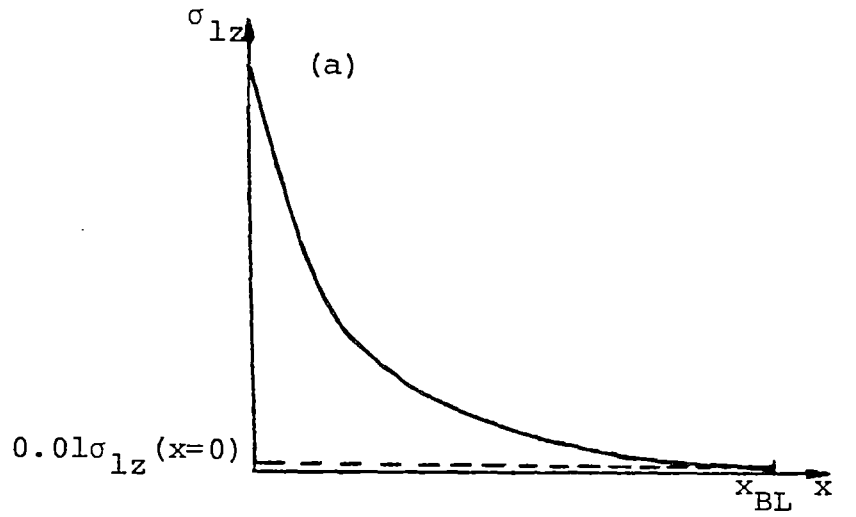
Figure 7.25. Boundary layer definitions for (a) angle-
plied laminates; and (b) all other laminates

and x_{BL} can be solved for by iteration. Convergence (the difference between two successive x_{BL} values being less than .00001) is achieved after few iterations (four to five) if $x = 1/\phi$ is used as the starting value for x_{BL}. If the cross-plied laminate is such that equation 6.30 has real solutions and both λ and ϕ exist, the boundary layer size is determined using the expressions derived below for general laminates.

For a general type laminate, the expression for σ_{zz} (equation 5.60) placed in equation 7.3 gives

$$e^{-\phi x_{BL}} - e^{-\lambda \phi x_{BL}} = 0.01 \ (e^{-\phi x_0} - e^{-\lambda \phi x_0}) \qquad (7.6)$$

after integration and cancellation of like terms. Note that x_0, the point at which σ_{zz} crosses the x axis, is given by

$$x_0 = \frac{\ell n \lambda}{\phi(\lambda - 1)} \qquad (7.7)$$

This can be determined by setting equation 5.60 equal to zero and solving for the distance x.

Using x_0 as the starting value for x_{BL}, equation 7.7 can be solved iteratively. However, one should distinguish between the case where $\lambda < 1$ and the case where $\lambda > 1$. In both cases, since x_0 is the starting value, the corrected value for x_{BL}

after each iteration must be larger than the x_{BL} value for the previous iteration.

If $\lambda < 1$, equation 7.6 can be rewritten as:

$$x_{BL} = \frac{\ln(e^{-\phi x_{BL}} - B)}{\lambda \phi} , \quad \lambda < 1 \tag{7.8}$$

where

$$B = 0.01 \, (e^{-\phi x_0} - e^{-\lambda \phi x_0}) \tag{7.9}$$

Equation 7.8 guarantees that, at each iteration, the corrected value of x_{BL} is larger than the previous x_{BL} value.

If $\lambda > 1$, equation 7.8 cannot be used because each new value of x_{BL} is smaller than the previous value. So, starting with x_0, each corrected x_{BL} value is smaller than x_0 and the scheme will not converge.

Instead, equation 7.6 can be rearranged as follows:

$$x_{BL} = \frac{\ln(e^{-\lambda \phi x_{BL}} + B)}{\phi} , \quad \lambda > 1 \tag{7.10}$$

where B is given by equation 7.9. This equation guarantees that, each corrected value of x_{BL} is larger than the previous one and, if x_0 is used as the starting value, after some iterations the scheme will converge.

Some comments on the boundary layer are in order. One, these three means for determining the boundary layer length

were incorporated into the program. The iteration schemes used are very efficient (four to five iterations are usually enough for accuracy up to the fifth decimal place). The only exception is the [±40/0]s laminate for which there was no convergence on the boundary layer length after 300 iterations. It is suspected that this problem arises from the fact that λ is almost equal to 1 for this laminate (actually $\lambda=1.004$).

Two, it should be again emphasized that the boundary layer size is not a quantity that can be accurately determined or measured. It is just used as an indicator of the size of the region over which the interlaminar stresses are important. If a consistent definition is used, then laminates can be compared on this basis. These definitions of the boundary layer are also independent of the applied load since λ and ϕ are independent of the applied load.

Three, the boundary layer is the same for any ply interface of a particular laminate since it depends only on λ and ϕ which are constant throughout the laminate. Therefore, the boundary layer is a laminate property. Table 7.5 shows the boundary layer sizes for the [±θ/0]s and the [0/±θ]s laminate families.

Four, equation 7.2 can be used to obtain a good starting value for ϕ in order to solve the equations for λ and ϕ (equations 5.111 and 5.112). As it was pointed out in equation

TABLE 7.5

BOUNDARY LAYER WIDTH FOR $[\pm\theta/0]_s$ AND $[0/\pm\theta]_s$ LAMINATES

θ	$[\pm\theta/0]_s$ [mm]	$[0/\pm\theta]_s$ [mm]
5	1.124	1.550
10	1.099	1.501
15	1.091	1.459
20	1.103	1.437
25	1.125	1.434
30	1.143	1.439
35	1.150	1.447
40	*	1.459
45	1.146	1.483
50	1.147	1.541
55	1.170	1.708
57.5	1.209	1.957
60	1.417	3.181
61	0.562	0.501
62.5	1.046	0.703
65	1.151	1.017
70	1.197	1.252

*No convergence on the boundary layer width after 300 iterations

5.104, ϕ is of order $O(1/h)$ where h is the laminate thickness. Comparing equation 7.2 and equation 5.104 one gets:

$$x_{BL} = O(h) \tag{7.11}$$

Then, considering Figure 7.25a, and using the definition of the boundary layer for angle-plied laminates one obtains:

$$h \simeq \frac{4.4}{\phi} \tag{7.12}$$

which solved for ϕ gives an order of magnitude estimate for ϕ and can be used as the starting ϕ value. This coincides with equation 5.113:

$$\phi_{init} = \frac{4.4}{h} \tag{5.113}$$

7.6 Concept of "effective ply thickness"

Built into the analysis are the following two basic facts. One, if, in a symmetric laminate, next to each ply another identical ply (i.e. the same material with the same fiber orientation) is added as illustrated in Figure 7.26a, the boundary layer thickness doubles exactly. Two, if a symmetric laminate is doubled by adding to it, symmetrically, another laminate, as illustrated in Figure 7.26b, the boundary layer thickness remains the same. Also, σ_{zz} at the mid-plane

(a)

(b)
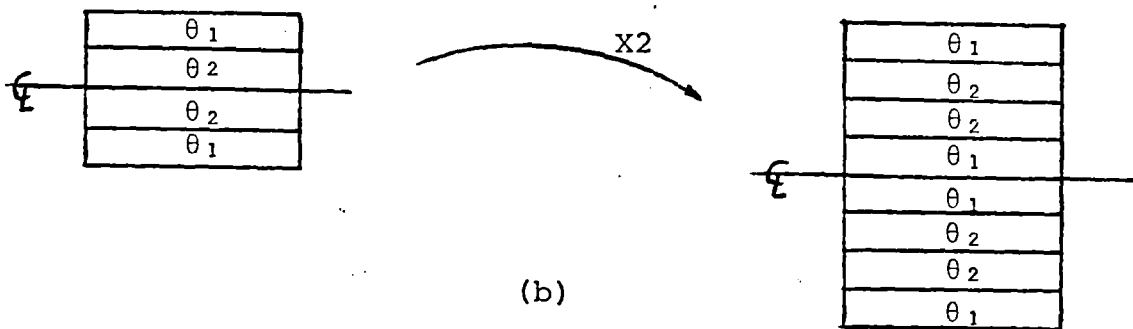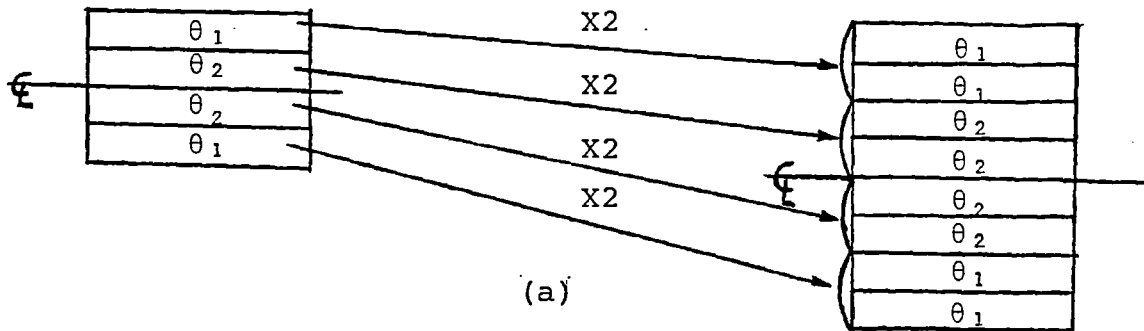
Figure 7.26. Two possible ways to vary the thickness of a laminate: (a) each individual ply is doubled; and (b) laminate as a whole is doubled symmetrically

is zero since each individual sublaminate is self-equilibrating.

The difference in the boundary layer between these two cases is that, in the first case, each pair of identical plies acts as a single ply whose thickness is double the thickness of the plies in the second case. Thus, in the first case, the "effective ply thickness" is twice what it is in the second case. Note that in both cases the laminate thickness is the same. This means that the boundary layer size is determined by the "effective ply thickness" and not just by the laminate thickness. Unfortunately, a way has not yet been found to determine the effective ply thickness of any laminate and only in special cases like the one above can the effective ply thickness be determined. For this reason, for the time being, the boundary layer size is assumed to be a strong function of the laminate thickness, and equation 7.2 is considered to be a good starting point for determining the starting value of ϕ in the iteration scheme.

Table 7.6 shows the boundary layer values for these two cases and the boundary layer length for the "parent" laminate as determined by the computer program for a [±15/0]s laminate.

TABLE 7.6

EFFECT OF EFFECTIVE PLY THICKNESS ON BOUNDARY LAYER SIZE

Laminate	Laminate Thickness [mm]	Effective Ply Thickness [mm]	Boundary Layer [mm]
$[\pm 15/0]_s$	0.804	0.134	1.09054
$[(+15)_2/(-15)_2/0_2]_s$	1.608	0.268	2.18108
$[\pm 15/0]_s 2$	1.608	0.134	1.09054

7.7 Comparison with previous analysis techniques

In this section, the present method will be compared to other methods of analysis. It is important to note that this is done in order to show the predictions of different methods of analysis, and not to validate this analysis since there is no analysis that can be presented as correct due to lack of conclusive experimental data.

In all the cases that are presented below, the laminate is subjected to a uniaxial load corresponding to an extensional strain of 1000 microstrain. The same elastic properties are used as those used by other investigators.

7.7.1 [±45]s laminate

The [±45]s laminate has been used by different investigators as the test case to compare their analysis technique with other analyses. For this reason, predictions obtained for a [±45]s laminate by the present method of analysis will be presented first and compared to the predictions of other investigators. It should be noted that for this laminate, as for any other angle-plied laminate, the CLPT predicts that $\sigma_{22[\theta i]}^{L}$ is zero.

Figures 7.27-7.31 show the stresses (except σ_{22} which is zero for all analyses) as a function of distance from the free edge at the +45/-45 interface of a [±45]s laminate as predicted by the finite difference method of Pipes and Pagano,
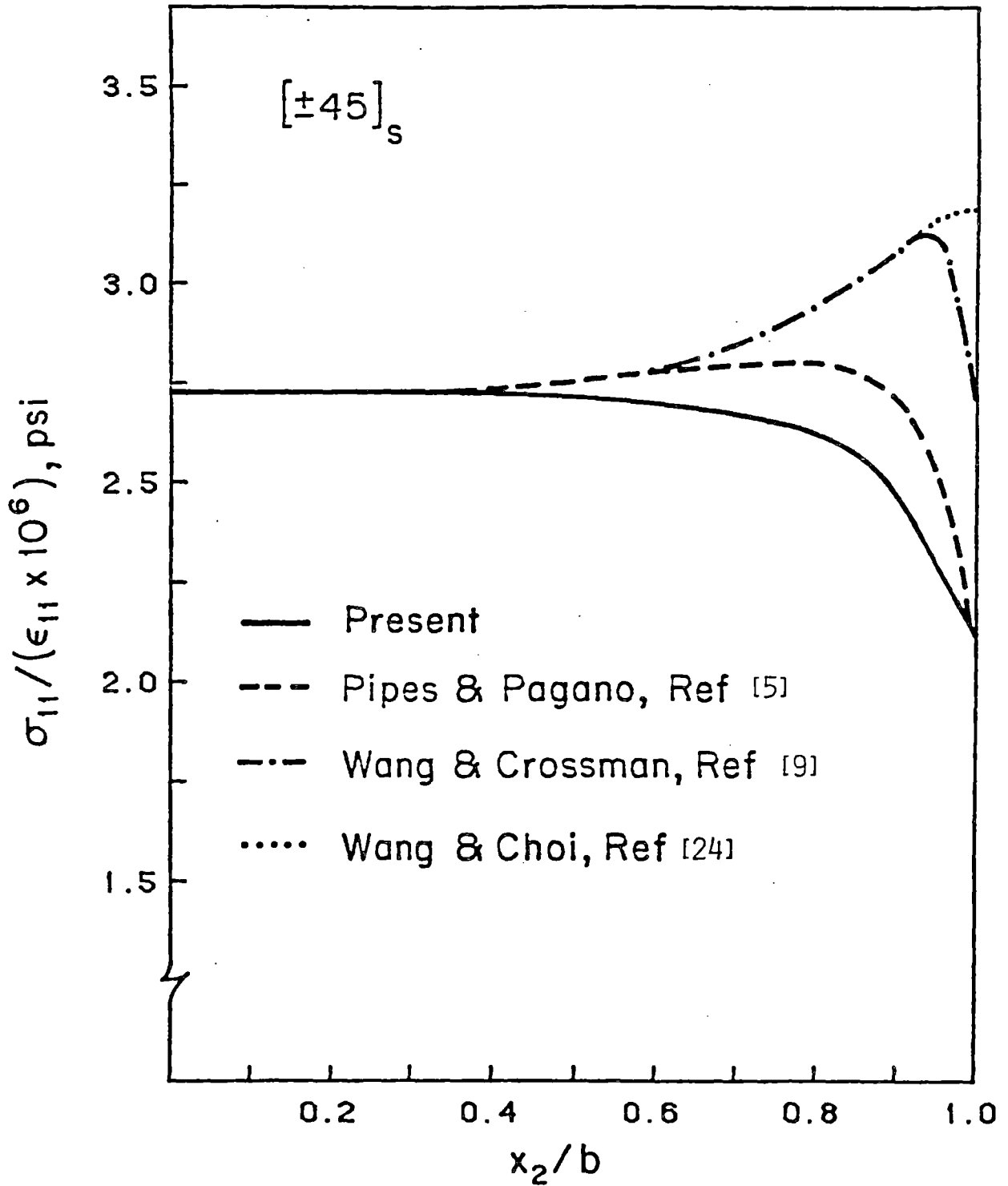
Figure 7.27   In-plane σ_{11} stress at +45/-45 interface for $[\pm45]_s$ laminate calculated by various methods
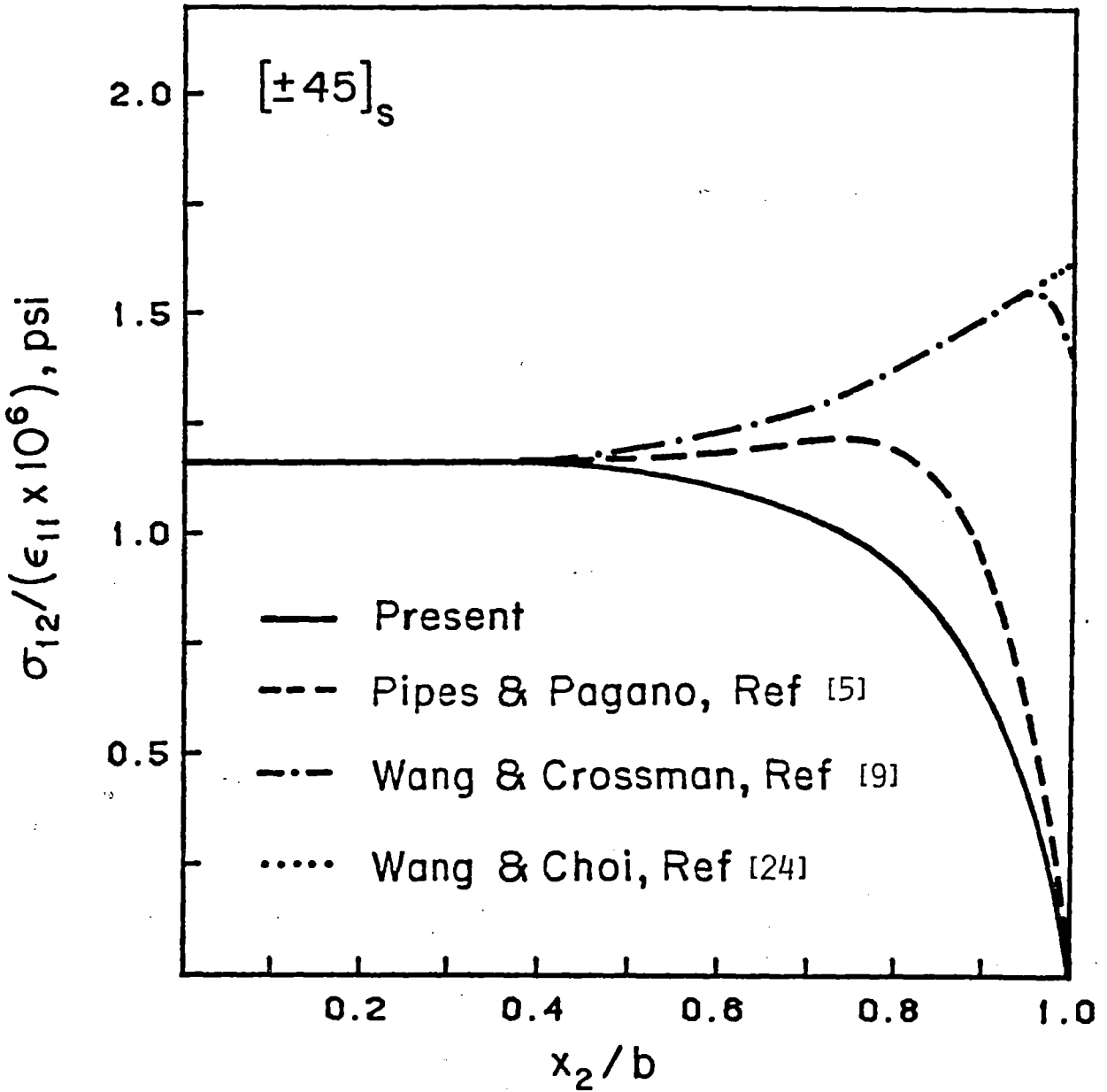
Figure 7.28   In-plane shear stress σ_{12} at +45/-45 inter-
face for $[\pm 45]_s$ laminate calculated by
various methods
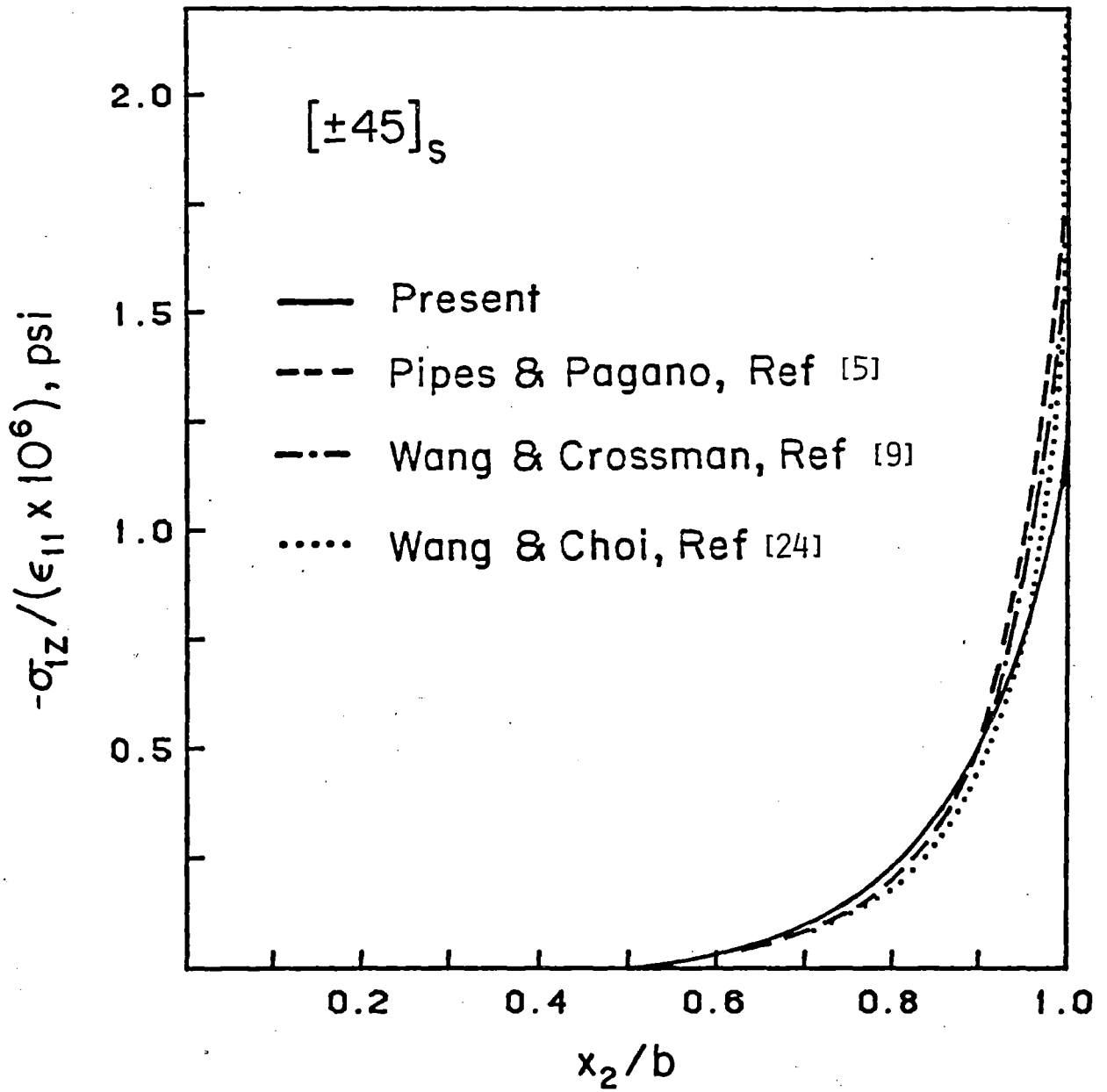
Figure 7.29 Interlaminar shear stress $-\sigma_{1z}$ at +45/-45 interface for [±45]$_s$ laminate calculated by various methods
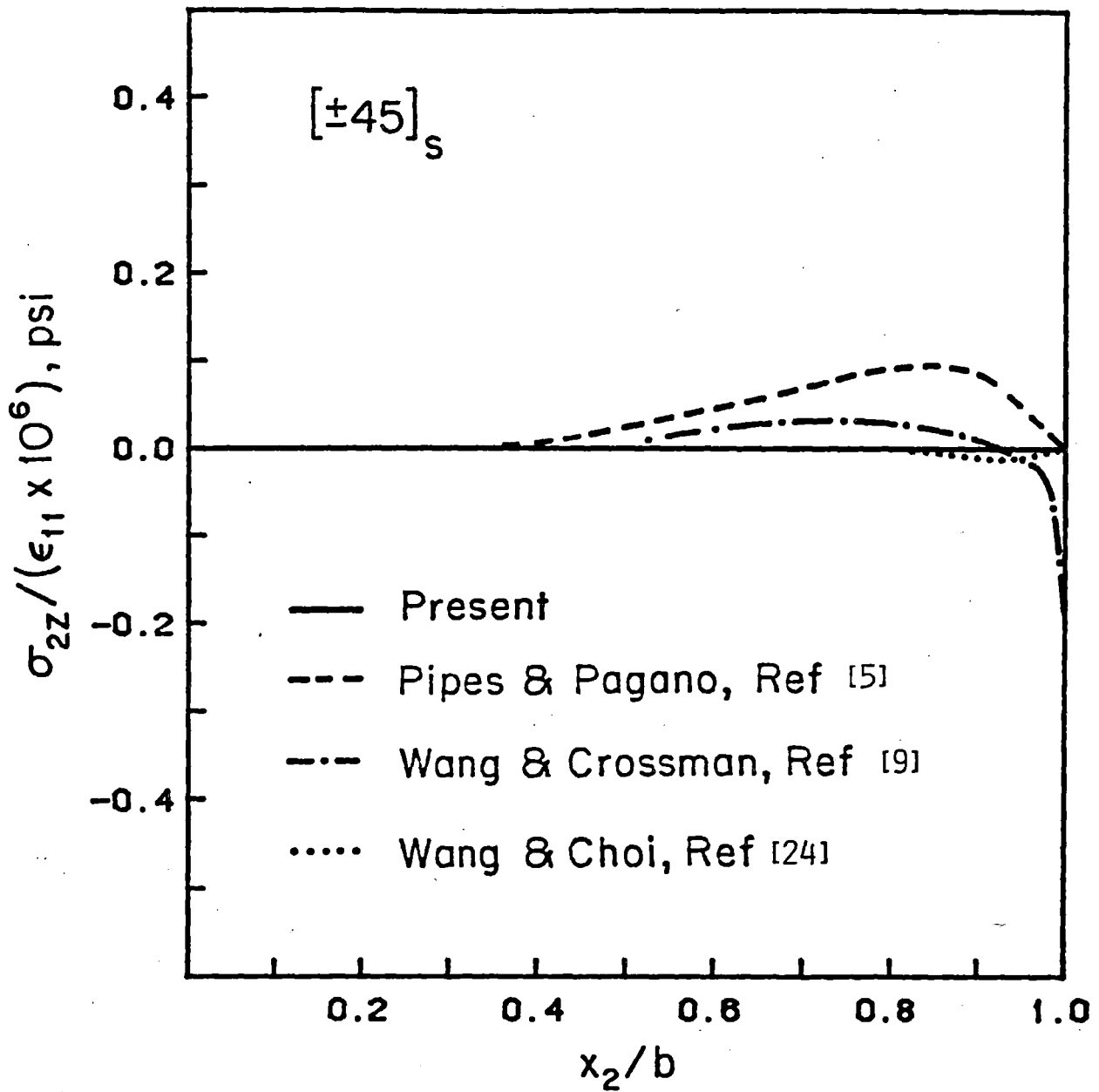
Figure 7.30 Interlaminar shear stress σ_{2z} at +45/-45
interface for $[\pm 45]_s$ laminate calculated by
various methods
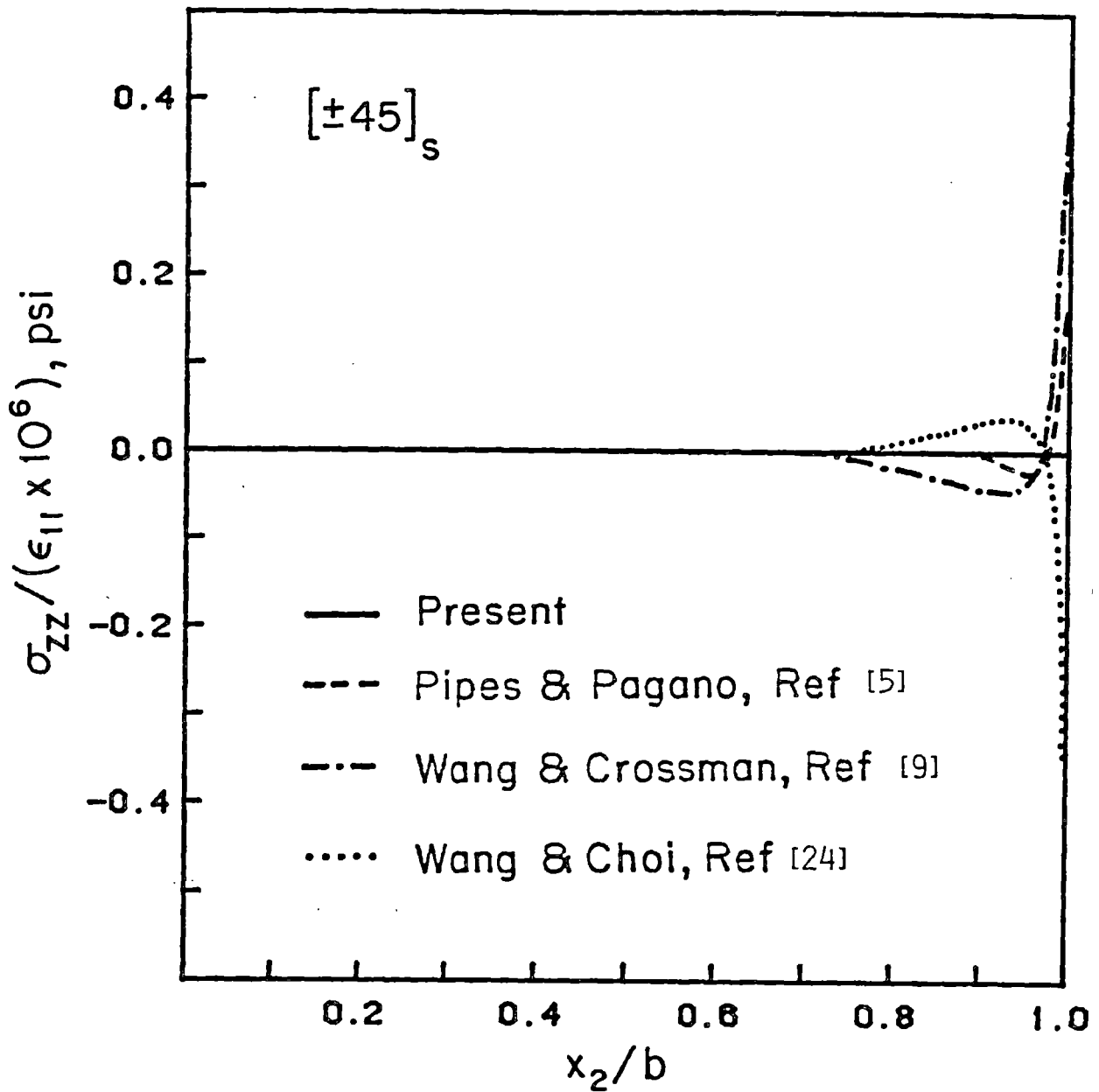
Figure 7.31 Interlaminar normal stress σ_{zz} at +45/-45 interface for $[\pm 45]_s$ laminate calculated by various methods

the finite element analysis of A.S.D. Wang and Crossman [9], the elasticity solution of S.S Wang and Choi [24], and by the present analysis.

The longitudinal stress σ_{11} is shown in Figure 7.27. All analyses approach the CLPT solution far from the free edge but they differ significantly close to the free edge. It should be recalled that very close to the free edge (within a few fiber diameters as discussed in chapter 2) the assumptions on material homogeneity made in all analyses break down and therefore no one method is expected to be more accurate than the others. The present investigation is closer to the FD analysis by Pipes and Pagano [5].

The in-plane shear stress σ_{12} is shown in Figure 7.28. Again, all methods approach the CLPT value at the far field. Near the free edge, the four methods give different predictions. The FE solution by Wang and Crossman [9] does not satisfy the boundary condition that σ_{12} is zero at the free edge while the other three methods do. The present analysis is again closest to the FD analysis by Pipes and Pagano [5].

Figure 7.29 shows the negative of the interlaminar shear stress σ_{1z}. There is excellent agreement among all solution methods. There are some differences very close to the free edge (recall that the analysis in [24] predicts singular σ_{1z} stresses at the free edge but the singularity becomes dominant

only when the assumption that each ply can be treated as homogeneous breaks down).

The interlaminar shear stress σ_{2z} is shown in Figure 7.30. The present analysis predicts that σ_{2z} is identically zero. The other analyses predict nonzero but small (compared to σ_{11}, σ_{12}, and σ_{1z}) stress values and, again, as in the case of the σ_{12} stress, the FE analysis by Wang and Crossman [9] does not satisfy the boundary condition that σ_{2z} is zero at the free edge. All other methods correctly predict that σ_{2z} is zero at the free edge. Far from the free edge, all methods match the CLPT which predicts that σ_{2z} is zero. An important difference among the four methods should be pointed out. As it was shown in section 4.2, σ_{2z} is either identically zero, which is the prediction of the present analysis, or crosses the x axis at least once which is the prediction of the FE analysis in [9]. Therefore, it appears that the analyses in [5] and [24], where σ_{2z} is nonzero and does not cross the x axis, do not satisfy integral force equilibrium in the transverse direction as expressed by equation 4.9.

The interlaminar normal stress σ_{zz} is shown in Figure 7.31. Even though all analyses predict stress values that are small compared to the σ_{11}, σ_{12}, and σ_{1z} stresses, they differ significantly from one another. The present analysis predicts that σ_{zz} is identically zero. The other analyses predict that σ_{zz} is nonzero but the analysis in [9] predicts that σ_{zz} is

tensile at the free edge while the analysis in [24] predicts that σ_{zz} is compressive at the free edge.

7.7.2 [±45/0/90]s laminate

The quasi-isotropic graphite epoxy [±45/0/90]s laminate was studied by Wang and Crossman [9] using the finite element method. Interlaminar stresses for this laminate as predicted by the present analysis and by Wang and Crossman [9] are shown in Figures 7.32-7.37.

The two methods predict very similar σ_{zz} stresses for the three interfaces from the midplane to the second interface (-45/0) as is shown in Figures 7.32-7.34 . The predictions for σ_{zz} at the first interface (Figure 7.35) are quite different. The present analysis has only one crossing of the x axis while the analysis in [9] has two. Furthermore, the present analysis predicts that σ_{zz} is tensile at the free edge while the analysis in [9] predicts that σ_{zz} is compressive there.

Figure 7.36 compares the predictions for σ_{1z} at the first (+45/-45) interface. The two methods differ significantly.

The predictions for σ_{2z} at the third (0/90) interface are shown in Figure 7.37. In this case the two methods are in very good agreement except at the free edge where the analysis in [9] predicts a nonzero value for σ_{2z} and hence does not satisfy the stress-free boundary condition $\sigma_{2z}(x/b=0)=0$.
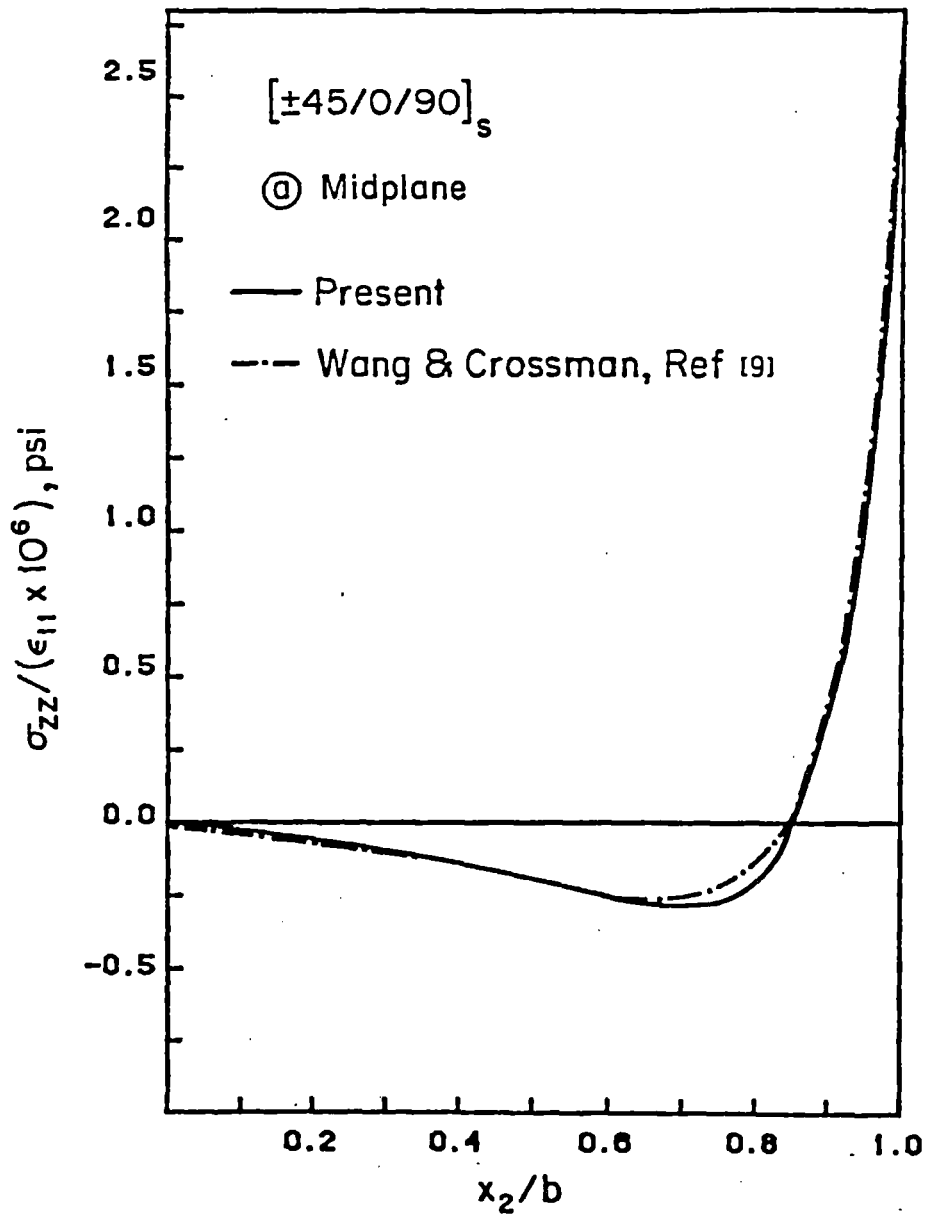
Figure 7.32 Interlaminar normal stress σ_{zz} at midplane of $[\pm 45/0/90]_s$ laminate calculated by present method and Wang and Crossman (ref. 9)
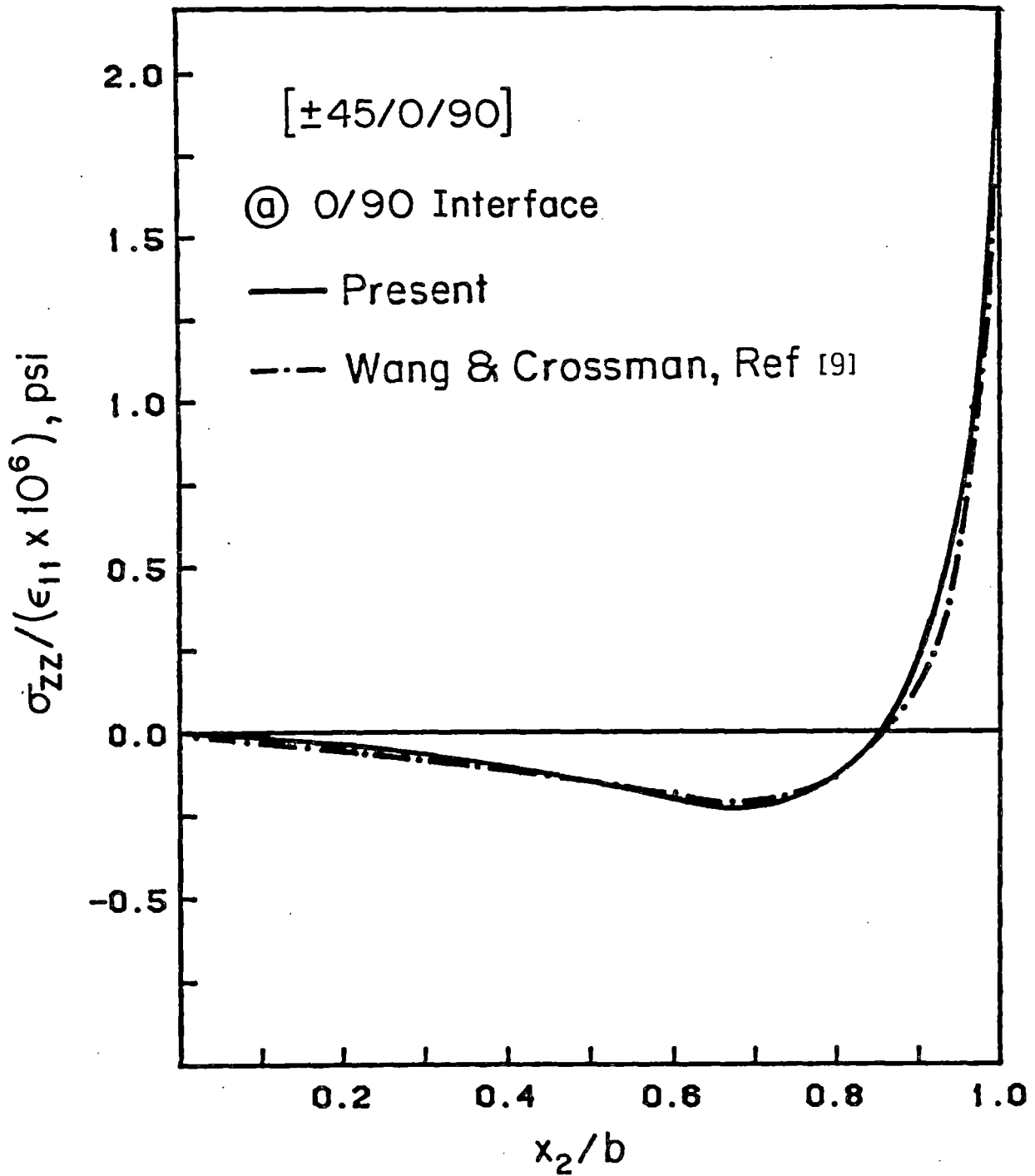
Figure 7.33 Interlaminar normal stress σ_{zz} at 0/90
interface for $[\pm 45/0/90]_s$ laminate
calculated by present method and Wang
and Crossman (Ref. 9)
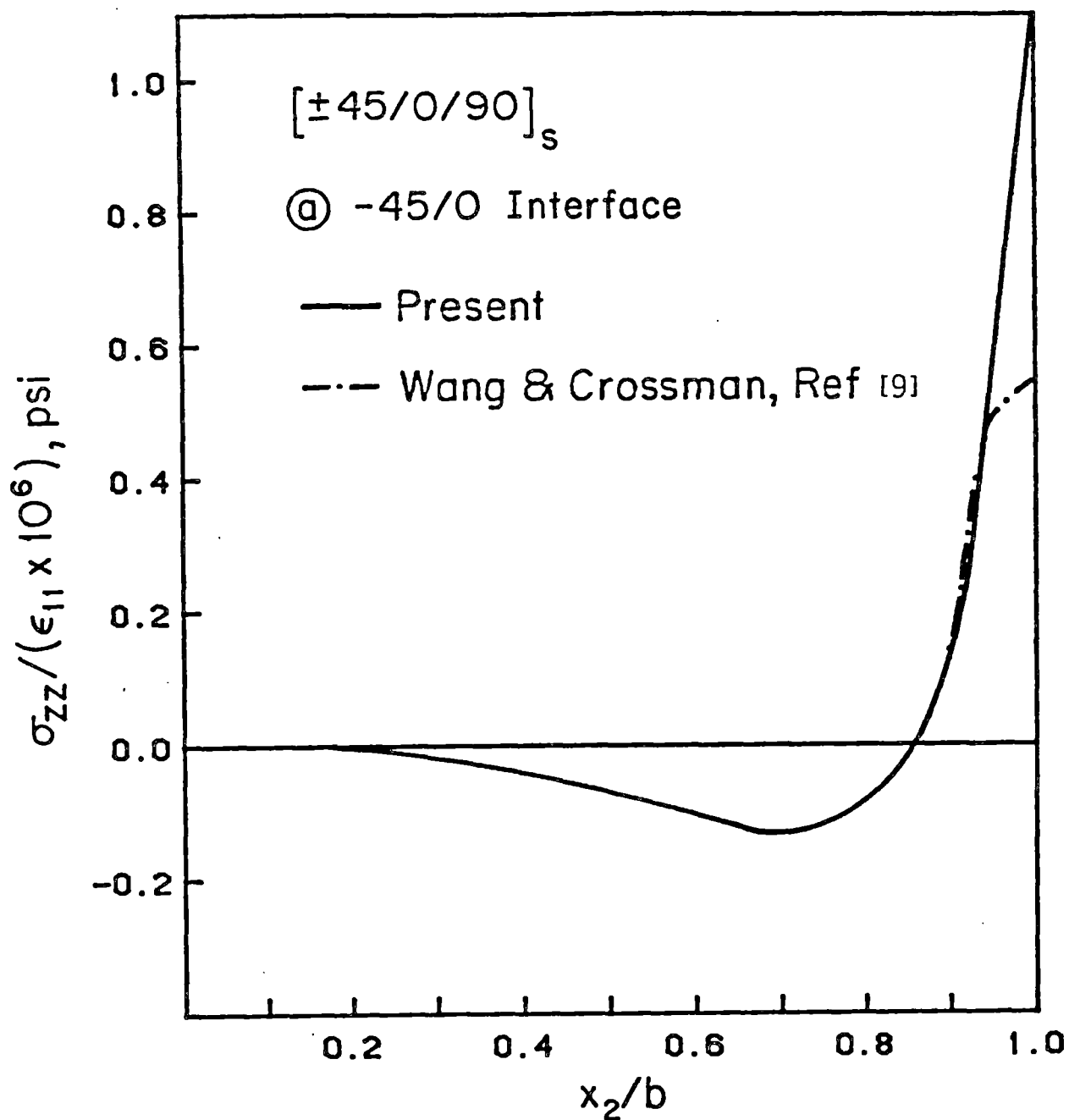
Figure 7.34 Interlaminar normal stress σ_{zz} at -45/0 interface for $[+45/0/90]_s$ laminate calculated by present method and Wang and Crossman (Ref. 9)
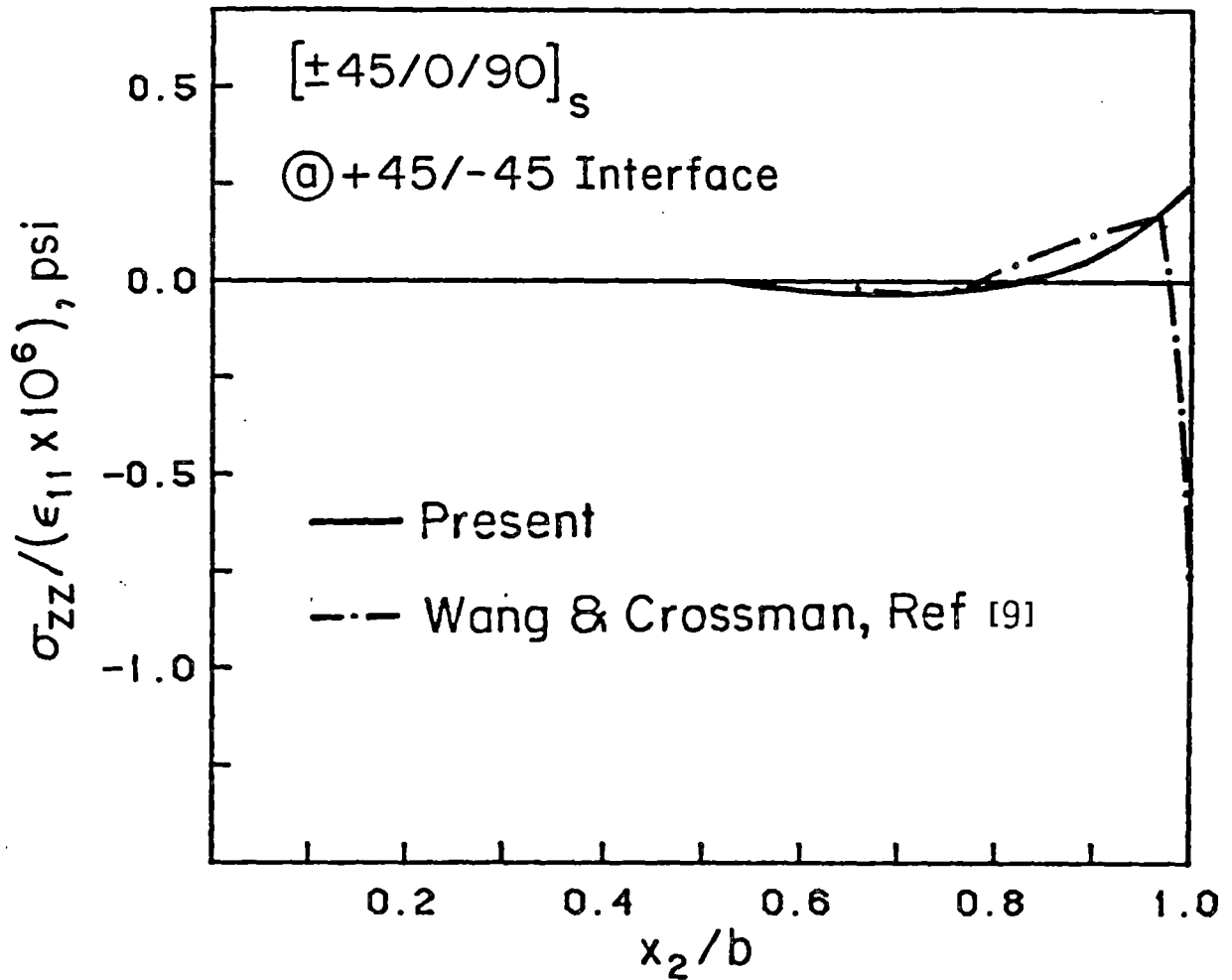
Figure 7.35 Interlaminar normal stress σ_{zz} at +45/-45 interface for $[\pm 45/0/90]_s$ laminate calculated by present method and Wang and Crossman (Ref. 9)
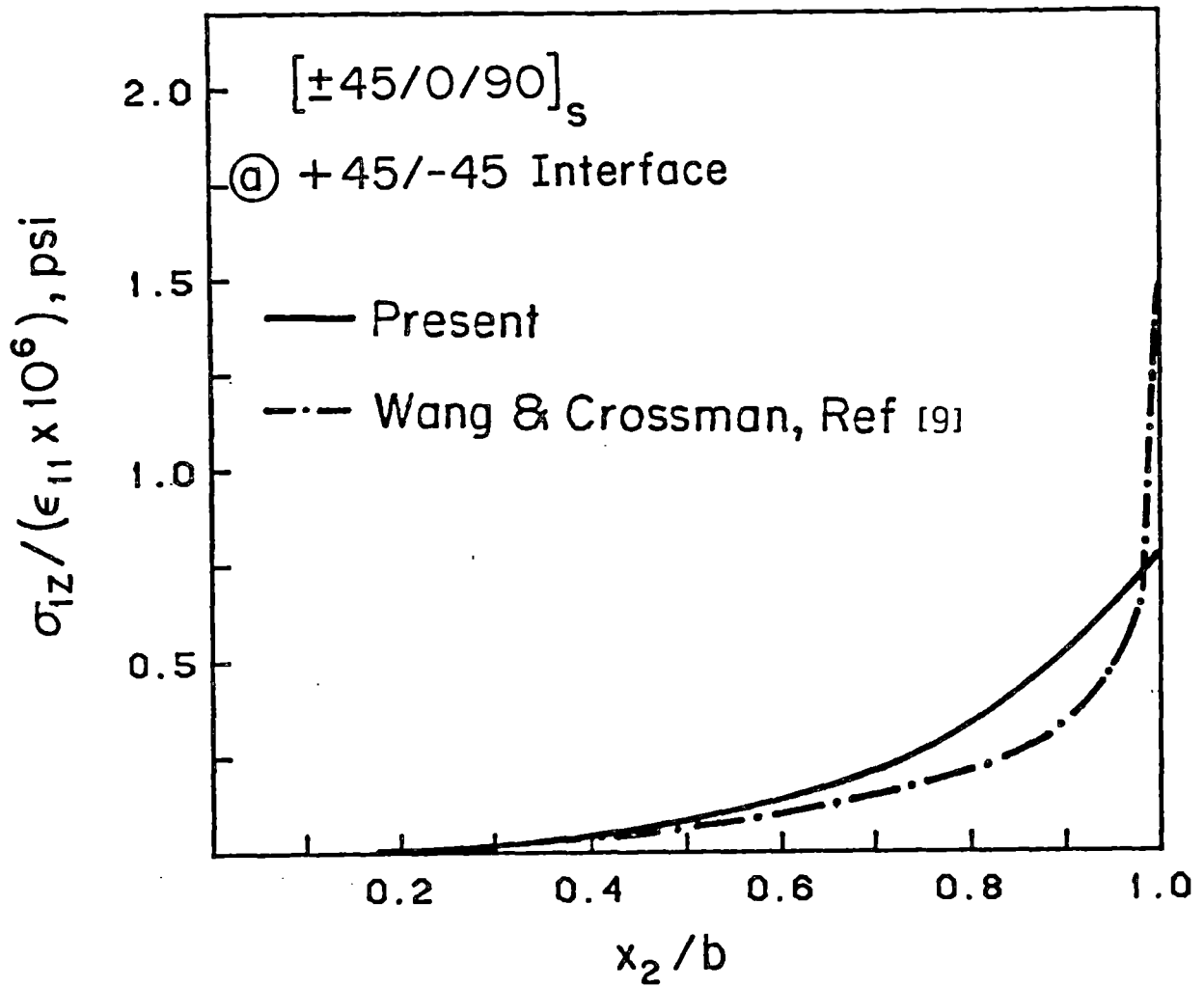
Figure 7.36 Interlaminar shear stress σ_{1z} at +45/-45 interface for $[\pm 45/0/90]_s$ laminate calculated by present method and Wang and Crossman (Ref. 9)
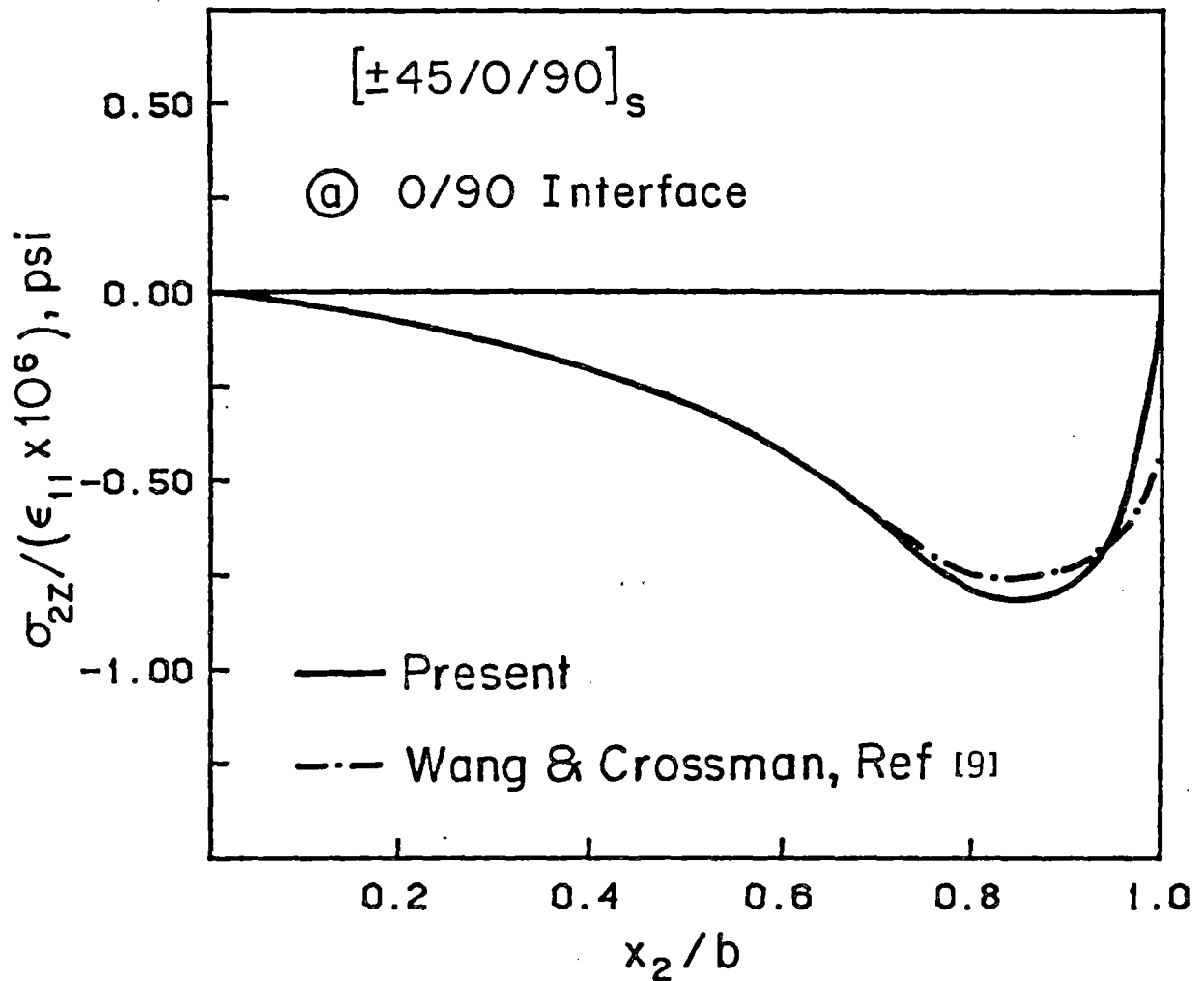
Figure 7.37 Interlaminar shear stress σ_{2z} at 0/90 interface for $[\pm 45/0/90]_s$ laminate calculated by present method and Wang and Crossman (Ref. 9)

7.7.3 [0/90]s laminate.

The prediction for the σ_{zz} stress in the [0/90]s cross-plied laminate is presented in Figure 7.38. Note that for this laminate the CLPT predicts that $\sigma^L_{12[\theta i]}$ is zero throughout the laminate and this, (see section 6.2) results in σ_{12} and σ_{1z} being zero throughout the laminate.

Figure 7.38 shows the σ_{zz} stress at the 0/90 interface of a [0/90]s laminate as predicted by the present analysis and the analyses by Pagano and Pipes in [12]. For the present analysis, the modified version for cross-plied laminates presented in section 6.2 had to be used because the original method (see discussion on equation 6.30 in section 6.2) gave complex values for λ and ϕ. There is good agreement between the three methods except very close to the free edge where the present method predicts stresses which are 35% higher than the prediction of the methods in [12].

7.7.4 Further results and implications for cross-plied laminates

It was pointed out in section 6.2 that there are cross-plied laminates for which both methods of analysis, as presented in section 6.2, are valid. Such a case is illustrated in Figures 7.39 and 7.40. The laminate is a [0/90]s
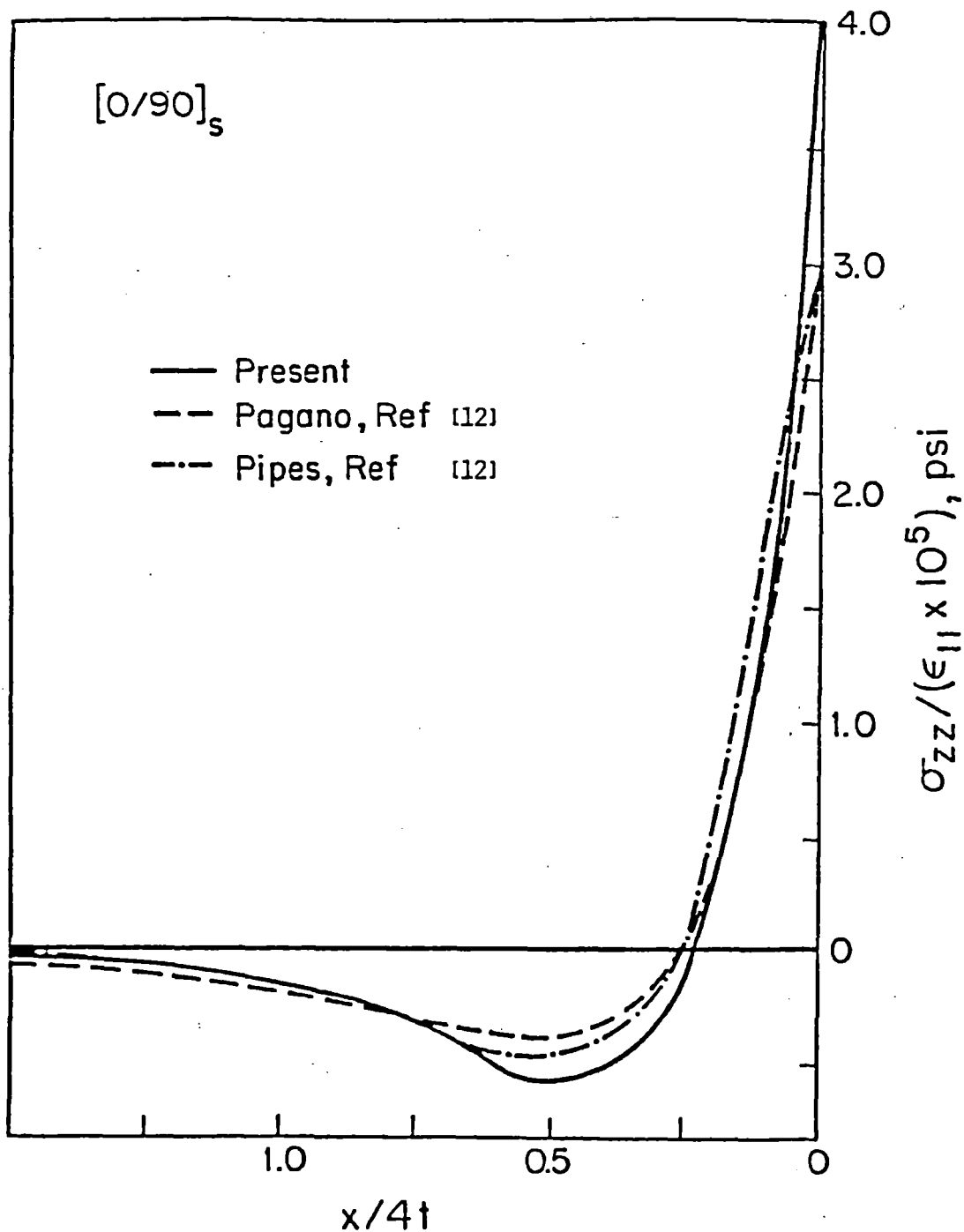
Figure 7.38 Interlaminar normal stress σ_{zz} at 0/90
interface for [0/90]$_s$ laminate calculated
by present method and Pagano and Pipes
(Ref. 12)
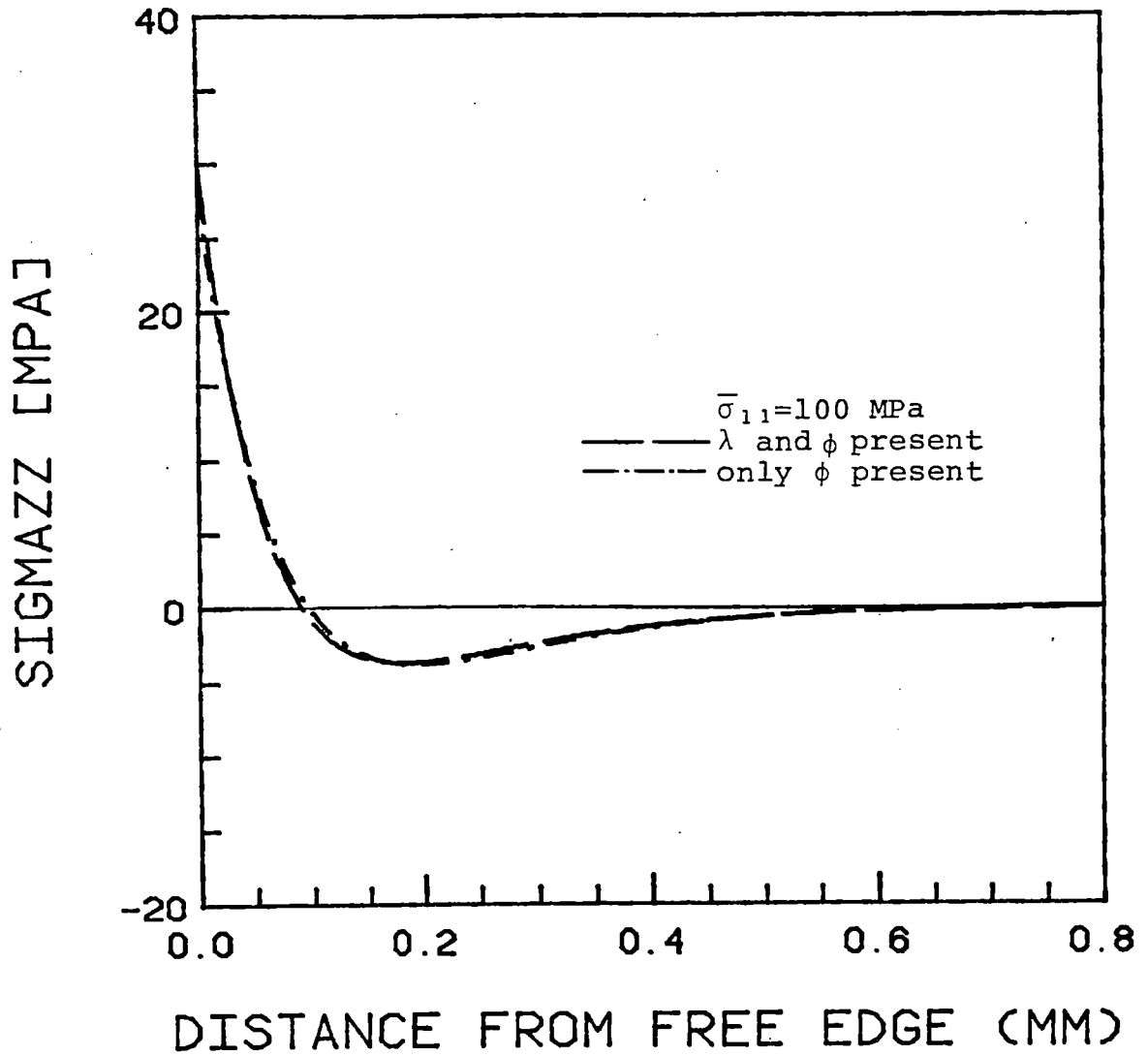
Figure 7.39.Interlaminar normal stress σ_{zz} at the mid-
plane of a $[0(\text{resin only})/90]_s$ laminate
as predicted by the two methods for cross-
plied laminates
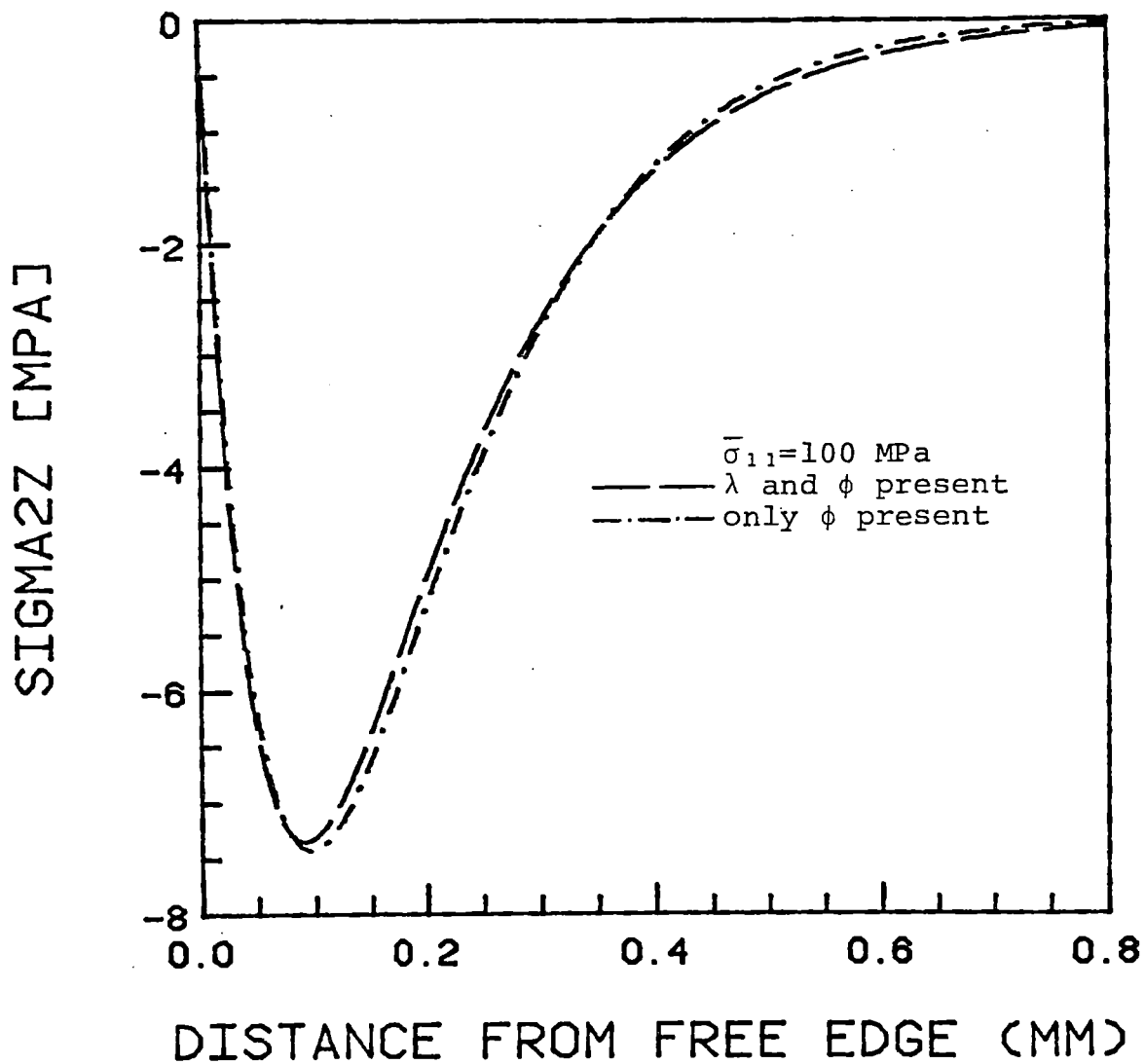
Figure 7.40. Interlaminar shear stress σ_{2z} at the 0/90
interface of a $[0(\text{resin only})/90]_s$
laminate as predicted by the two methods
for cross-plied laminates

laminate where the material for the first ply is only the 3501-6 resin (with Young's modulus of 3.5 GPa and Poisson's ratio 0.3) of thickness 0.134mm (chosen arbitrarily). Note that actually this first ply is isotropic but the laminate can still be treated as a cross-plied laminate. The second ply is a 90° ply of AS1/3501-6 material. The laminate is loaded in tension by a $\bar{\sigma}_{11}$ stress of 100 MPa. It turns out that both solution methods for cross-plied laminates are applicable. Figure 7.39 shows the σ_{zz} stress as a function of distance from the free edge at the midplane of the laminate as predicted by the two methods. There is excellent agreement. Figure 7.40 shows the σ_{2z} stress at the 0/90 interface. Again, the two methods are in very good agreement. This implies that in cases where the first method of analysis (see section 6.2) fails and λ and ϕ cannot be used, the alternative method, where only ϕ is present, is very reliable since for cases where both methods are valid it gives predictions that are very close to those obtained by the more accurate method.

Another important conclusion can be drawn using this laminate which may better clarify the role of the two eigenfunctions $e^{-\phi x}$ and $e^{-\lambda \phi x}$. It was shown by Pagano [12] that the modified plate theory by Whitney and Sun [13] can be used for cross-plied laminates to obtain expressions for σ_{zz} at the midplane which can be expressed in terms of two expo-

nentials. It can be seen that the expression for q, the interlaminar normal stress σ_{zz}, in [12]

$$q = M_0^* \frac{\lambda_1 \lambda_2}{\lambda_1 - \lambda_2} (\lambda_2 e^{-\lambda_2 \xi} - \lambda_1 e^{-\lambda_1 \xi})$$

is identical with the σ_{zz} expression of the present analysis (equation 5.60) provided the first method of analysis for cross-plied laminates (both λ and ϕ present) is valid. This implies that in such special cases, the present analysis matches the predictions of the plate theory developed by Pagano [12] and Whitney and Sun [13].

7.8 Significance of the resin layer between plies

It was mentioned in chapter two that between the plies of a laminate there exists a thin resin layer where no fibers are present [3]. This layer is usually so thin that in all the analyses presented in chapter two, as well as in the present analysis, it is neglected. More specifically, each ply is assumed to be homogeneous in the analysis and half of each interply layer is treated as part of each of two neighboring plies. The present analysis however, is versatile enough to account for that layer and efficient enough so that the increase in the number of plies does not affect the computation time significantly.

Each laminate, therefore, can be considered as composed of anisotropic layers separated by thin isotropic resin layers. These isotropic layers will be considered as additional plies. The underlying assumption here is that these plies are thick enough so that the assumption of material homogeneity is valid.

The laminate used to present results is the [±15/0]s laminate (AS1/3501-6 system). If the resin plies are included (denoted by R) the laminate becomes [+15/R/-15/R/0/$\overline{R}$]s where the resin ply next to the midplane is half as thick as the other resin plies as denoted by the overbar. Using an Olympus SZ-III-Tr microscope (160X magnification) the average thickness of the resin layer was found to be 7.5 microns. This is on the order of one fiber diameter (AS1 fibers). Each resin layer was treated as isotropic with a Young's modulus of 3.5 GPa and a Poisson's ratio of 0.3 (the elastic constants of the 3501-6 epoxy resin). The thickness of the graphite/epoxy plies was kept equal to the nominal thickness of 0.134 mm. The laminate was loaded in tension by a $\overline{\sigma}_{11}$ stress of 889 MPa (the same as for the cases presented in Figures 7.1-7.24). The CLPT solution for the case without the resin layers is given in Table 7.1. The CLPT solution for the case with the resin layers is shown in Table 7.7.

The σ_{zz} stress at the midplane as predicted by the two models is shown in Figure 7.41. The σ_{2z} stress and the σ_{1z}

TABLE 7.7

CLPT SOLUTION FOR $[+15/R/-15/R/0/\bar{R}]_s$ LAMINATE

(APPLIED LOAD $\bar{\sigma}_{11} = 889$ MPa)

Stress [MPa]	PLY 1 +15	PLY 2 R	PLY 3 -15	PLY 4 R	PLY 5 0	PLY 6 $\bar{R}$
$\sigma^L_{11_{[\theta i]}}$	877	24.7	877	24.7	1034	24.7
$\sigma^L_{22_{[\theta i]}}$	17.2	-11.3	17.2	-11.3	-32.9	-11.3
$\sigma^L_{12_{[\theta i]}}$	202	0	-202	0	0	0
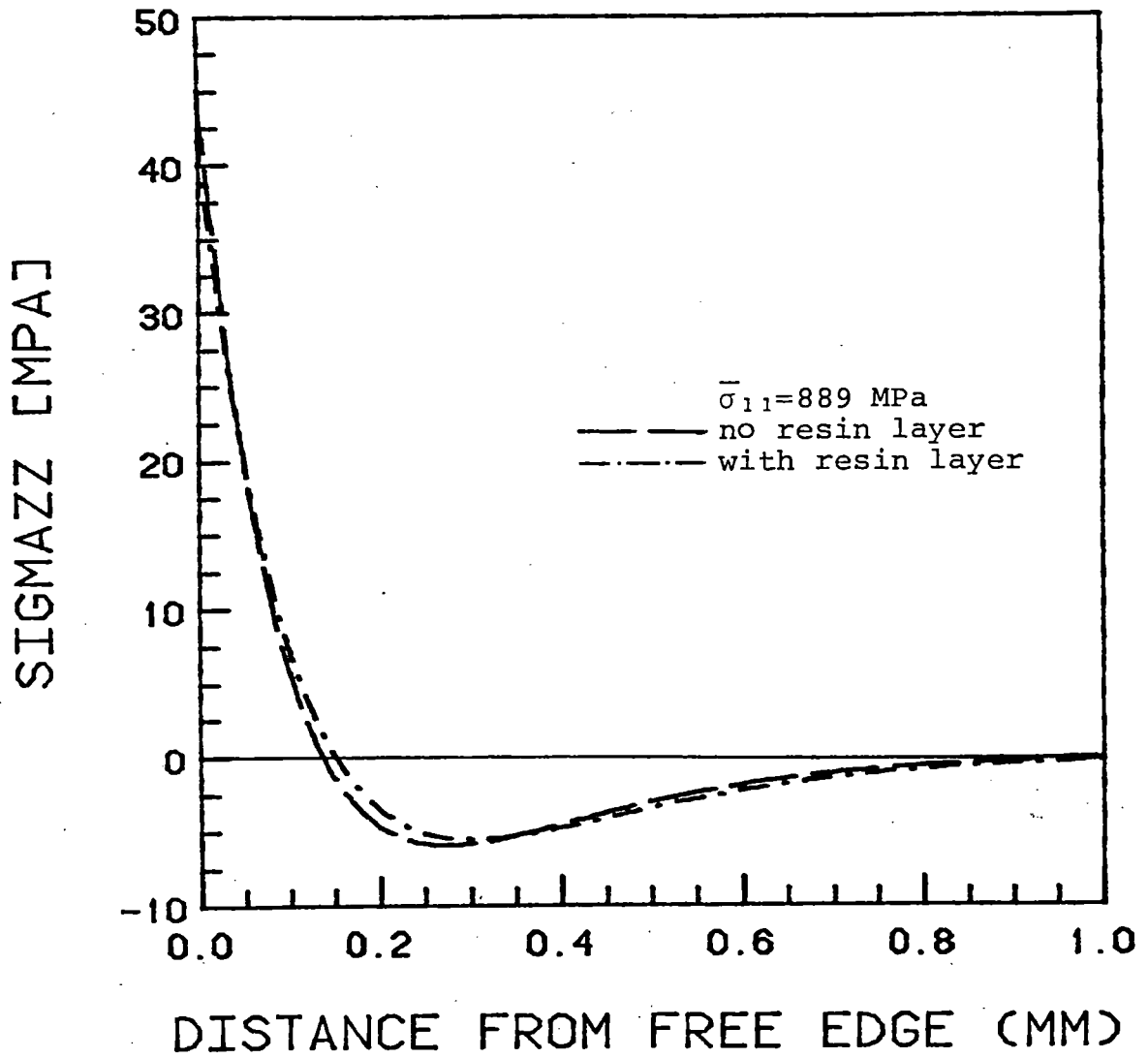
Figure 7.41. Effect of the resin layer between plies on the predictions for the σ_{zz} stress at the mid-plane of a $[\pm 15/0]_s$ laminate

stress at the +15/-15 interface are shown in Figures 7.42 and 7.43. The two models are in excellent agreement. This implies that the assumption that the resin layer can be incorporated into the two neighboring plies is valid.

7.9 Evaluation of the Computer Program

The solution procedure as implemented on the computer is very flexible. Hybrid laminates with plies of different thicknesses and different materials can be analyzed as easily as a typical single-material laminate.

The iteration scheme has excellent convergence characteristics in that no instabilities were encountered in the cases analyzed so far. Furthermore, in most cases convergence was achieved within 10 to 15 iterations. The Newton-Raphson method used to determine the four roots of the λ polynomial has very good convergence characteristics as well.

Thick laminates can also be analyzed with relative ease. So far, up to 100-ply laminates have been analyzed successfully. For the 100-ply laminate there were more than 15 different ply orientations and the layup was such that no simplifications (e.g. treating part of the laminate as a substructure) could be used in the solution and each of the 100 plies had to be considered separately. The computer program was transferred to a VAX-11/782 computer so that actual CPU
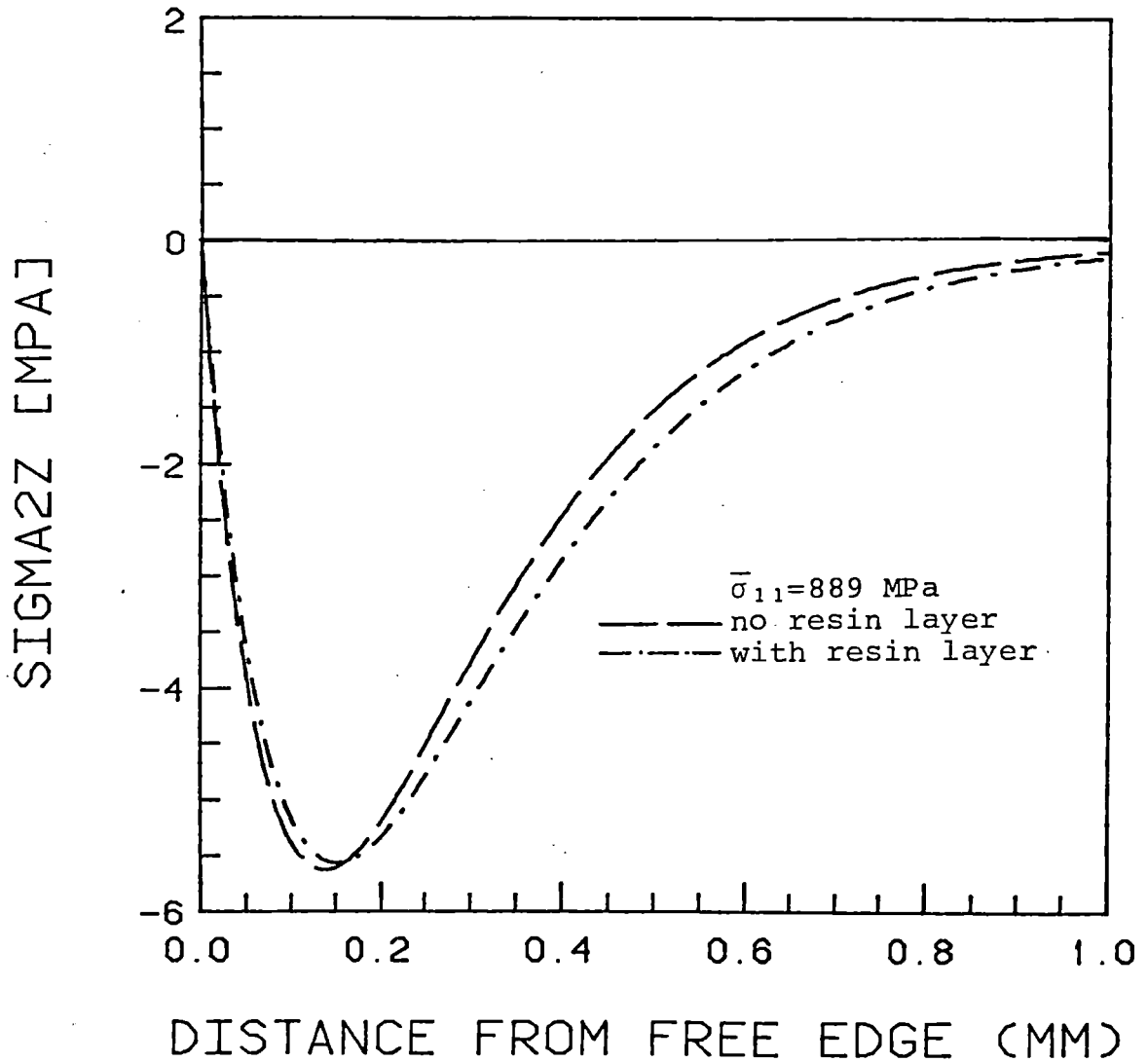
Figure 7.42. Effect of the resin layer between plies on the predictions for the σ_{2z} stress at the +15/-15 interface of a $[\underline{+15}/0]_s$ laminate
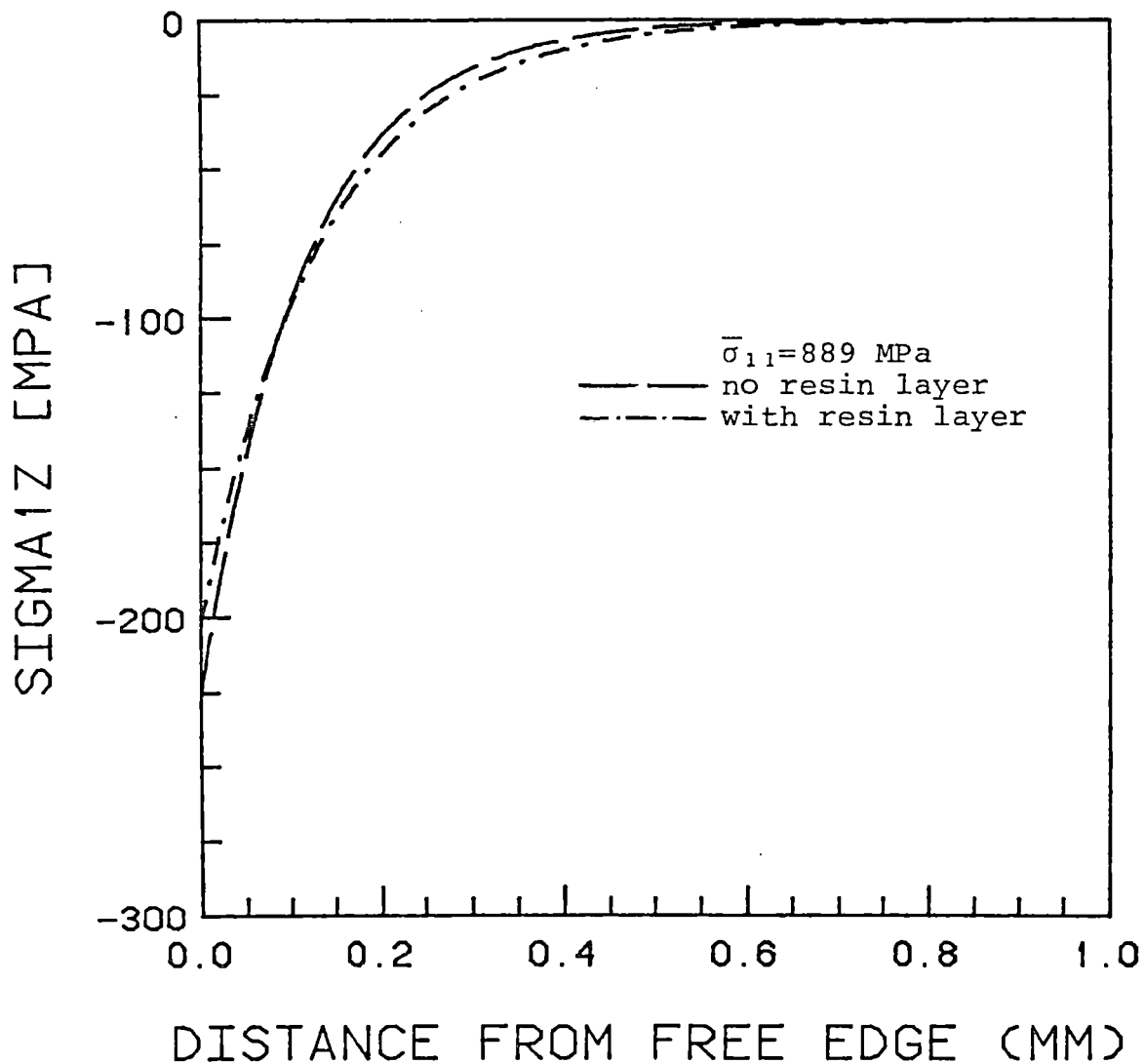
Figure 7.43. Effect of the resin layer between plies on the predictions for σ_{1z} stress at the [15/-15 interface of a $[\pm15/0]_s$ laminate

times could be calculated for different cases. Table 7.8 shows some of the cases run along with the CPU times on the VAX computer and the computation times on the PDP-11/34. The computation times on the PDP-11/34 computer are the real times (determined using a watch) and not CPU times. From Table 7.8, a number of conclusions can be drawn. One, the computation time does not depend strongly on the number of plies. This is shown by the last two entries in the table where doubling the number of plies of a laminate increases the computation time only by 25% (part of which is extra time needed to calculate stress coefficients for the excess plies). The computation time will mainly depend on the relative values of the coefficients in the λ and ϕ polynomials. As a result, laminates with plies well exceeding 100 (possibly up to 500) could be analyzed without increasing the computation times to a great extent. Two, the program can be used easily on home computers. Most home computers of today are more powerful (and faster) than a PDP-11/34. So, the computation times on home computers will be acceptable. Furthermore, the program code is fairly short (about 650 executable statements) and does not take up much of memory space (19K).

Computation times have been reported in the literature for [±45]s laminates [5,9]. These solutions have been accomplished on different computers, and hence a direct comparison cannot be made easily. However, the large (greater than two

TABLE 7.8

COMPUTATION TIMES FOR DIFFERENT LAMINATES

Number of plies	Number of iterations	CPU time (VAX 11/782) [sec]	Actual time (PDP 11/34) [sec]
4	0*	1.00	2
6	8	1.01	15
12	15	2.66	30
50	50	3.29	80
100	69	5.37	120

*Solution is obtained in closed form.

orders of magnitude) difference between these and the present analysis technique indicate the efficiency of the present method. The finite difference scheme developed by Pipes and Pagano [5] required 120 seconds of CPU time on an IBM 360-365. The finite element technique of Wang and Crossman [9] needed 18 seconds of CPU time on a UNIVAC-1108. The present method used only 0.2 seconds of CPU time on the VAX-11/782 to analyze the [±45]s case. Even the analysis of 6-ply laminates as shown in Table 7.8 required less time (at least an order of magnitude) than these previous analysis techniques did for just a simple laminate.

CHAPTER EIGHT

SPECIMEN PREPARATION AND EXPERIMENTAL SETUP

It was already indicated in the discussion in chapter 2 that an experimental technique to measure interlaminar stresses is needed in order to determine which of the analytical methods available are more reliable. Such a technique has not yet been devised. The two basic reasons are the following: (1) the boundary layer width is very small and obtaining enough data within the boundary layer is difficult; and (2) it is hard to take measurements inside the laminate. The only measurements that can be taken with some ease are on the top or the bottom surface of the laminate (inside the boundary layer) and at the face of the free edge itself.

With these limitations in mind the following experimental method was used. First high density moiré grids were glued to the specimen to define points on the top surface of the laminate very close to the free edge (within the boundary layer). Then the distances of these points from a reference point before and after loading were measured thereby determining the u and v displacements of these points.

It should be noted that this method is limited because only quantities on the top surface of the laminate are measured and these are only in-plane quantities. However, since

the in-plane quantities change from their CLPT values in the
boundary layer, the method is expected to give important data
which will be helpful not only in validating analytical meth-
ods but also in furnishing a better understanding for the
mechanisms of delamination.

8.1 The specimens

Three laminates were made, all of the AS1/3501-6
graphite/epoxy system: $[\pm15/0]s$, $[(+15)_5/(-15)_5/0_5]s$, and
$[(+45)_{10}/(-45)_{10}]s$. The first laminate was chosen as a test lam-
inate to check the experimental technique before applying it
to the other laminates which were the actual laminates for the
experiment. The second laminate was chosen because it is
known to fail by delamination [41]. The third laminate was
chosen because it is the one used as the test case by differ-
ent investigators for the calculation of interlaminar stresses
and the data obtained can be compared to the predictions of
different analytical methods. The thickness of these last two
laminates was chosen so as to increase the boundary layer size
without introducing undue complications in the manufacturing
procedure. By increasing the effective ply thickness (see
section 7.5) the boundary layer size increases and it is easi-
er to obtain more data points in the boundary layer than with
thinner laminates. For the $[(+15)_5/(-15)_5/0_5]s$ laminate, the

boundary layer width is predicted to be 5.5 mm by the present analysis (versus 1.09 mm for a [±15/0]s laminate) and for the [(+45)$_{10}$/(-45)$_{10}$]s laminate the boundary layer width is predicted to be 5.27 mm (versus 0.527 mm for a [±45]s laminate).

Standard TELAC manufacturing techniques [43] were used throughout the manufacture except for one detail. A smooth surface was needed for the application of the moiré grid onto the specimen. For this reason, the laminates were cured with one side in direct contact with an aluminum cure plate. The cure plate was sprayed with mold release before curing.

As per standard practice, 300 mm by 350 mm plates as layed up were cured in an autoclave under a 30 inch Hg vacuum, 85 psi pressure and in a two step temperature cycle: one hour at 240°F followed by two hours at 350°F. This cure cycle is shown in Figure 8.1. The laminates were postcured in an oven at 350°F for 8 hours. The resulting laminates had the correct resin content and their thickness was very close to the nominal value. The average measured thicknesses for the three laminates are given in Table 8.1. There are five coupons per laminate and six thickness measurements were taken per coupon. The overall average measured per ply thickness is 0.133 mm compared to the manufacturer's nominal per ply thickness of 0.134 mm. The surface of the laminates that was in contact with the aluminum cure plate came out smooth and did not have

AUTOCLAVE
TEMPERATURE (°F)

350

240

150

70

PLUS 8 HOUR
POSTCURE
AT 350°F

10 35   95 115   235 275 280
                                                        TIME

AUTOCLAVE
PRESSURE (PSI)

85

10 35   95 115   235 275 280
                                            TIME

VACUUM (IN. HG)

28

10 35   95 115   235 275 280
                                            TIME
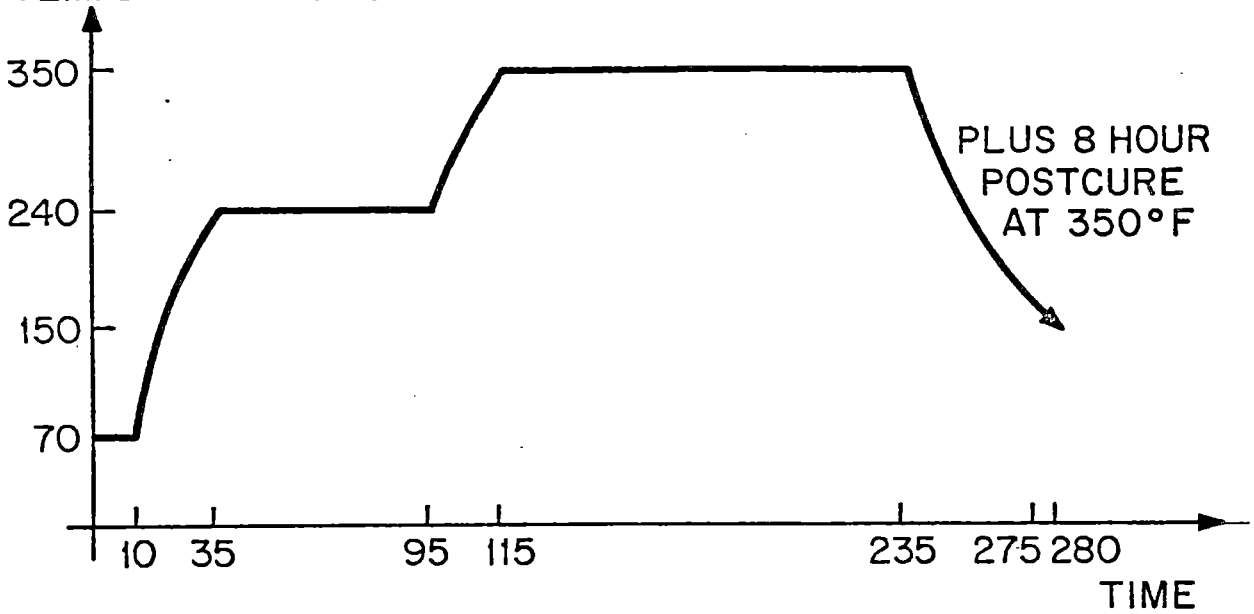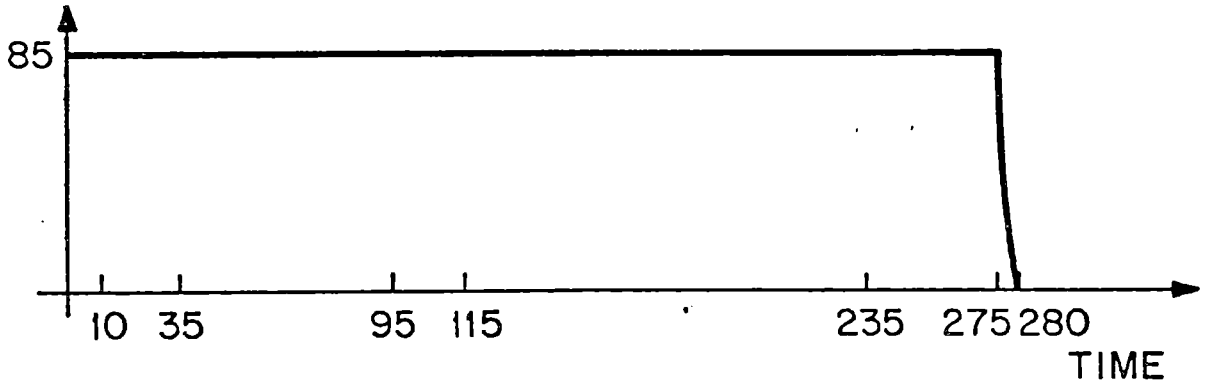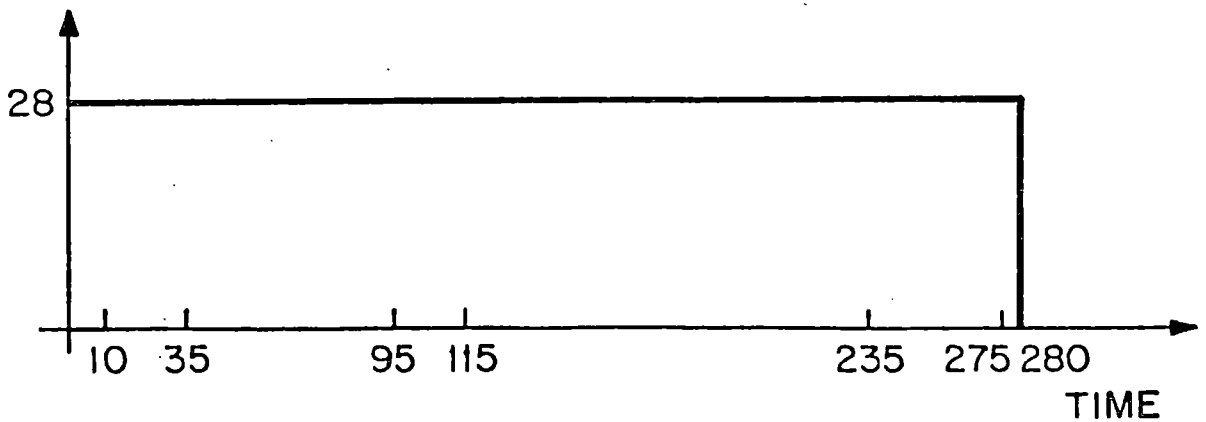
Figure 8.1. Graphite/Epoxy autoclave cure cycle

TABLE 8.1

AVERAGE LAMINATE THICKNESSES

Laminate	Thickness (mm)	Nominal Thickness (mm)
$[\pm 15/0]_s$	0.79	0.802
$[(+15)_5/(-15)_5/0_5]_s$	3.982	4.02
$[(+45)_{10}/(-45)_{10}]_s$	5.69	5.36

the wavy pattern (with dimples) usually present on surfaces cured while covered with peel-ply.

Each cured laminated plate was cut into five coupons using a high speed diamond abrasive rotating disk. Two strain gages were placed on each of the coupons used for the actual experiment, on the side which originally had the peel-ply. One was placed longitudinally in order to measure the longitudinal modulus and one was placed in the transverse direction to measure the Poisson's ratio. These values are measured in order to compare them (as some type of quality control) to the theoretical value obtained from CLPT. The width of the coupons was chosen to be 54 mm instead of 50 mm, which is the standard TELAC coupon width, in order to satisfy the requirement (see section 5.6) that the width to thickness ratio in each specimen be at least 10 for the theory to be valid. The test section in each coupon was 200 mm long. The measured thicknesses and widths of the coupons are summarized in Table 8.2.

The loading tabs were made following the standard TELAC procedure. For the [±15/0]s laminate, 12-ply thick glass tabs were used. For the other two laminates 36-ply thick tabs were used. The laminate configuration for the glass tabs was a symmetric 0/90 repeating layup with the proper number of plies. The loading tabs were bonded to the graphite/epoxy coupons in a secondary bond operation using FM-123-2 film adhesive. This was accomplished at 50 psi and 225°F for two

TABLE 8.2

AVERAGE COUPON THICKNESSES AND WIDTHS

Laminate	Coupon	Measured Thickness [mm]	Coef. of Variation (%)	Measured Width [mm]	Coef. of Variation (%)
$(15_5/-15_5/0_5]_s$	1	3.79	9.96	53.8	4.71
	2	4.01	1.95	53.8	4.71
	3	4.08	2.54	53.8	0.00
	4	3.92	4.24	53.8	0.00
	5	4.11	1.38	53.7	8.16
$[45_{10}/-45_{10}]_s$	1	5.79	11.1	54.01	0.94
	2	5.83	16.1	54.03	6.60
	3	5.47	15.9	54.05	4.11
	4	5.98	6.29	53.78	10.7
	5	5.48	11.8	54.09	6.80

hours. This resulted in the specimen illustrated in Figure 8.2.

8.2 The moiré grid

The moiré grids were obtained from Measurement Group Inc. These were Photolastic Type FTG transferable moiré grids of two different densities: 200 lines/inch (8 lines/mm) and 500 lines/inch (20 lines/mm). The grids are supplied in 4x4 inch (100x100 mm) sheets and can be cut to smaller pieces depending upon the application. Each grid consists of a film of mutually perpendicular black gelatin lines 0.025 mm thick which are deposited on a polyester carrier (0.15 mm thick). This results in the pattern illustrated in the photograph in Figure 8.3. The carrier is removed after the grid is applied to the specimen. Since the displacements of the grid points are measured directly using a microscope, no master grid (or grille) is needed.

To apply the grid, the instructions given by the manufacturer were used. The procedure is briefly as follows:

1. An area of the top surface of the specimen slightly larger than the grid piece to be used is spray-painted with silver paint to give a sharper contrast between the grid lines and the specimen surface beneath the grid.

TOP VIEW   SIDE VIEW
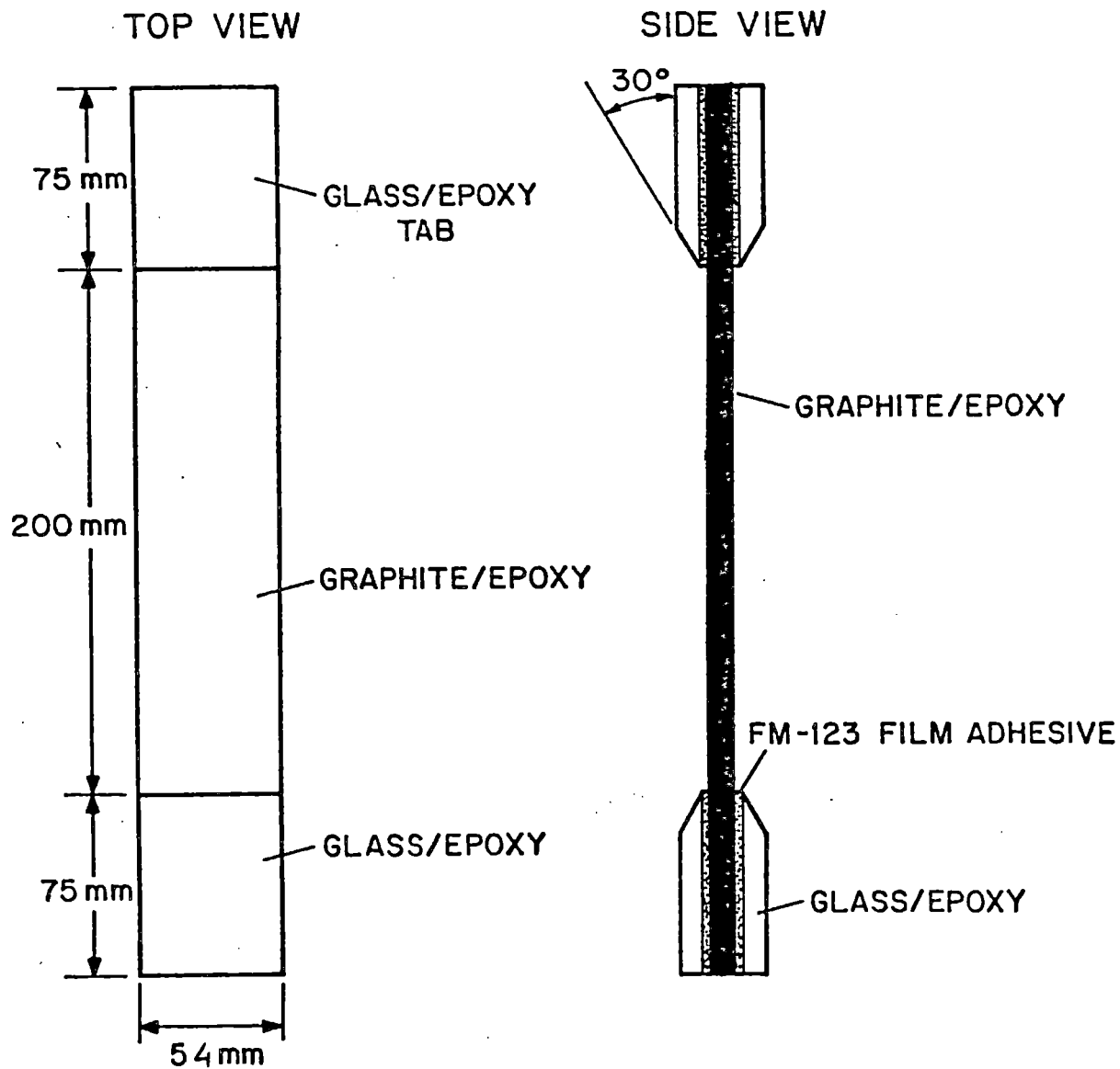
Figure 8.2.Characteristics of the coupon specimen
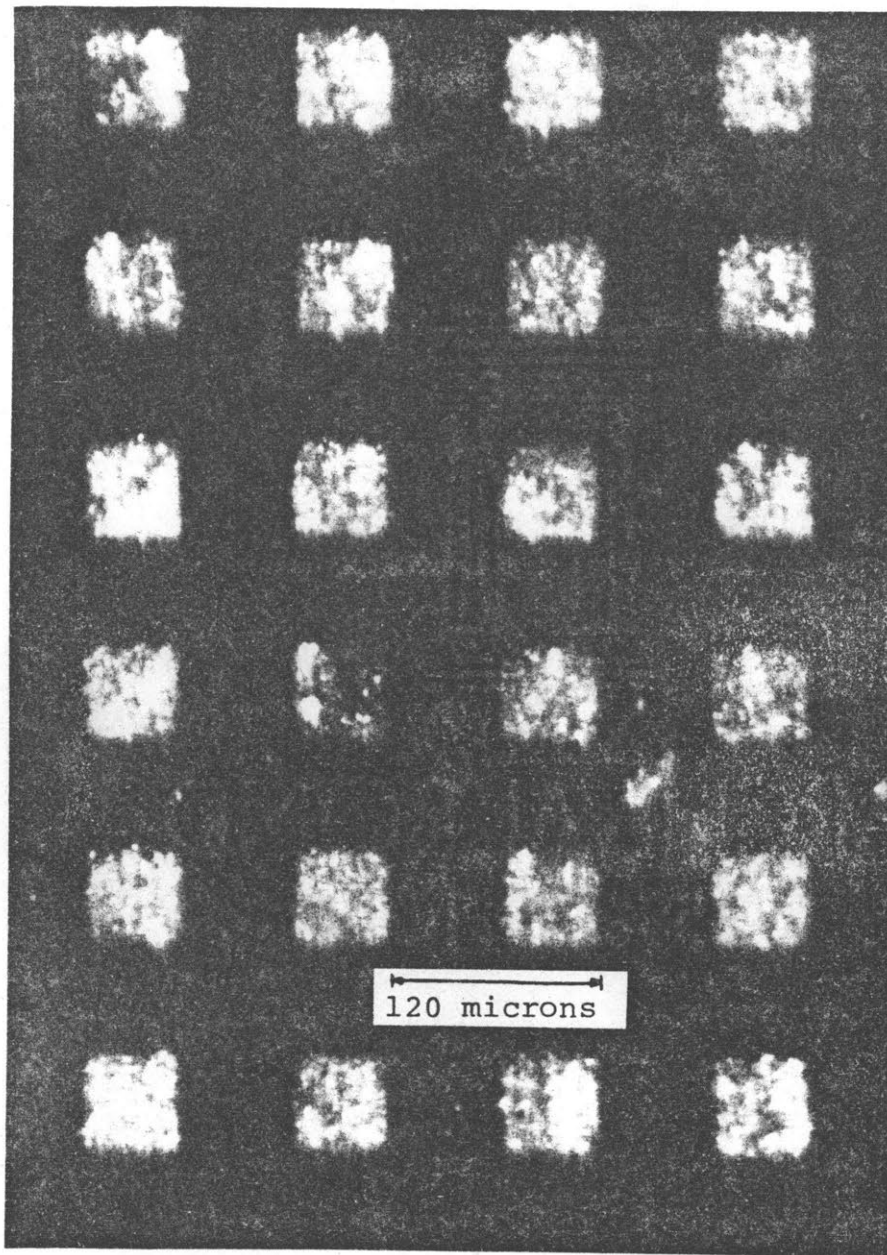
Figure 8.3. Moiré grid pattern (200 lines/inch) under
the microscope (40X magnification)

2. A thin coat of Type VPAC-1 adhesive (also supplied by the manufacturer) is applied on the specimen surface which is preheated to approximately 110°F for about 1 minute. The adhesive is also preheated to approximately 120°F before the resin and hardener are mixed.

3. The grid piece is placed in contact with the adhesive with the grid surface down (carrier surface up).

4. A sheet of silicon rubber approximately 3 mm thick is placed over the grid and a pressure of about 35 kPa (5 psi) is applied.

5. The adhesive is either left to cure at room temperature for 36 hours or is put in the autoclave at 180°F for one hour in order to cure.

6. After curing, the grid carrier is removed to expose the grid surface.

Care must be taken so that one of the edges of the grid piece is aligned with one of the free edges of the specimen. For this, a microscope at 7X magnification is used.

8.3 Test setup

The measurements of surface displacements had to be taken with the specimen under load. Thus, the specimen was placed in an MTS 810 testing machine with hydraulic grips.

An SZ-III-Tr Olympus microscope was used to take the measurements. This stereo microscope is capable of magnifications up to 240X. At that magnification, data can be acquired every 50 microns with the 500 lines/in grid and every 90 microns with the 200 lines/in grid.

A stand was built to hold the microscope close to the specimen during testing so that in situ measurements could be taken. Figure 8.4 shows a schematic drawing of the stand. The stand consists of four basic parts.

First is the base table with four legs whose height can be adjusted by changing their lower section with extensions of variable length. The height of the table used is 122 cm. The top of the table is 84 cm long by 61 cm wide and the stage attachment takes up only a small area (30.5 cm by 33 cm) so that a lot of room is left to be used for placing tools or taking notes during mounting, testing, and dismounting. A shelf was made between the ground and the top surface of the table (distance 67 cm from the top surface of the table) and parallel to the ground where sandbags are placed during testing to absorb any vibrations transmitted to the stand through the ground or by sudden movements of the experimenter.

The second part of the apparatus is a stage attached on a wooden base vertical to the table. This wooden base is firmly attached to the table with a Dexion rack. The stage is capable of horizontal (parallel to the specimen when the specimen is
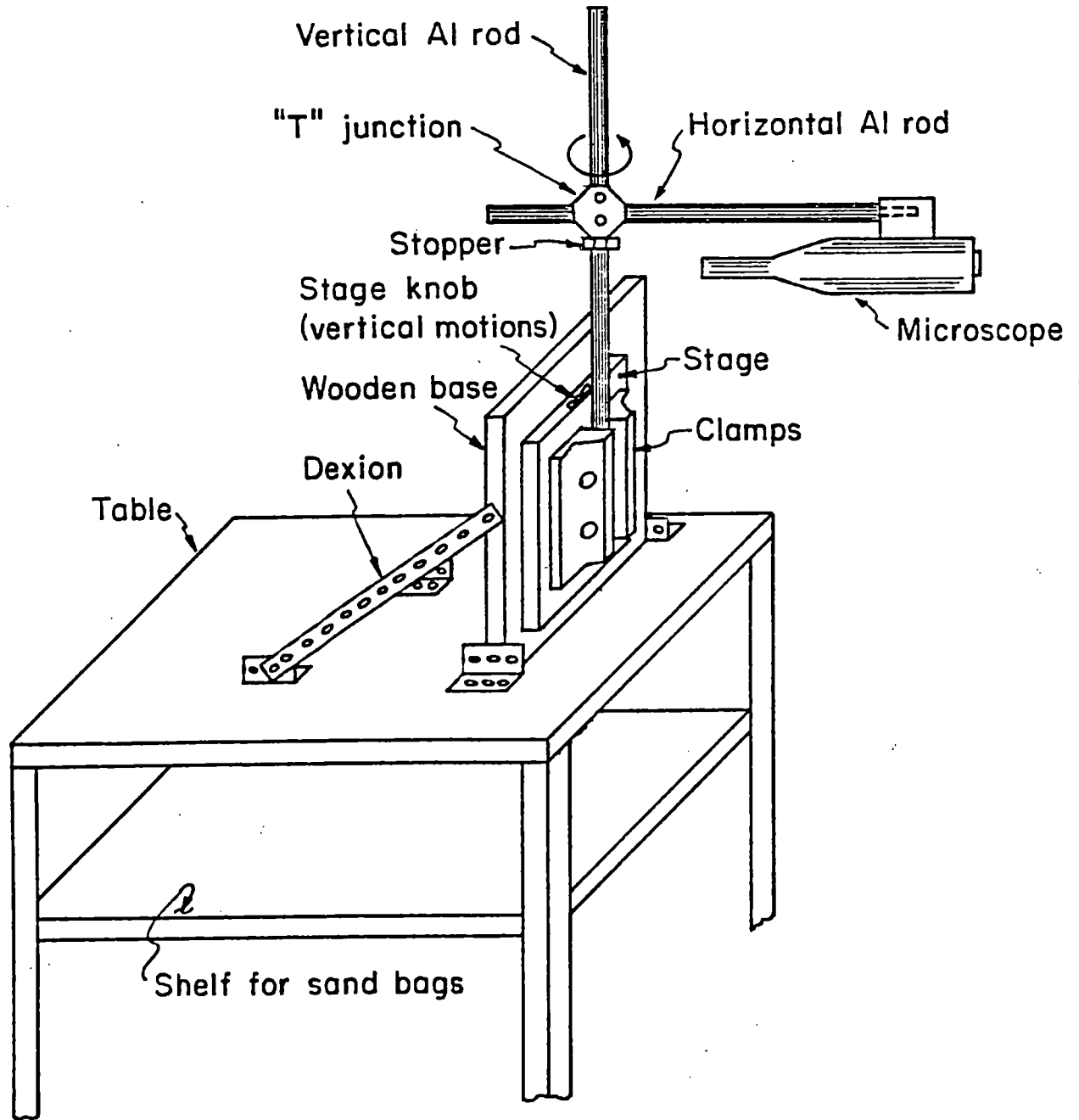
Figure 8.4 Microscope stand (not to scale)

gripped in the testing machine) and vertical displacements accomplished with the use of calibrated knobs. These displacements have a range of about 13 cm. This enabled the microscope which was attached to the stand to scan an area on the specimen surface which was much larger than the grid area.

The third part is an aluminum rod (2.38 cm in diameter and 43 cm long) attached to the stage (perpendicular to the ground) with the use of V-blocks and clamps. Another aluminum rod (also 2.38 cm in diameter but 76 cm long) is attached to the first rod through a "T" shaped junction with two holes at 90 degrees. This second rod was perpendicular to the first i.e. perpendicular to the specimen surface and parallel to the ground. The end of the rod that is close to the specimen surface was milled down to fit exactly a cylindrical slot at the side of the microscope. A set of four screws is used to firmly attach the microscope (via the slot) on this horizontal aluminum rod. -

The fourth part is the "T" shaped junction. This junction is attached to the two rods with the use of four screws (two per rod). It can slide on both rods making it possible to place the microscope within a wide range of distances from the ground or from the testing machine. The junction can also rotate in a plane parallel to the ground making it possible to rotate the second (horizontal) rod. In this way, the specimen in the testing machine may be viewed through the microscope at

a variety of angles if needed. A groove (27 cm long) was drilled along the horizontal rod to serve as a guide for the two screws on the junction corresponding to that rod. An aluminum ring with three screws is placed around the vertical rod right under the "T" junction to serve as a stopper (see Figure 8.4). The entire apparatus with a specimen mounted in the testing machine is pictured in the photograph in Figure 8.5.

Overall, the stand is very versatile. The height of the horizontal rod can be adjusted by moving the "T" junction up or down on the vertical rod. The angle at which the specimen is viewed can be changed by rotating the "T" junction (and hence the horizontal rod). The distance of the microscope from the specimen can be adjusted by moving the horizontal rod closer to or further from the specimen prior to tightening the screws in the "T" junction. More accurate movements of the microscope are possible in all three directions. With respect to an observer looking at the specimen, more accurate motions up or down and to the left or to the right are accomplished through use of the two stage knobs. Motion towards or away from the specimen is accomplished by using the focusing knob of the microscope.

The use of the sandbags decreased the vibrations significantly. However, there were still some vibrations coming mainly from the rods when the stage or the microscope were touched in order to change the microscope location or during
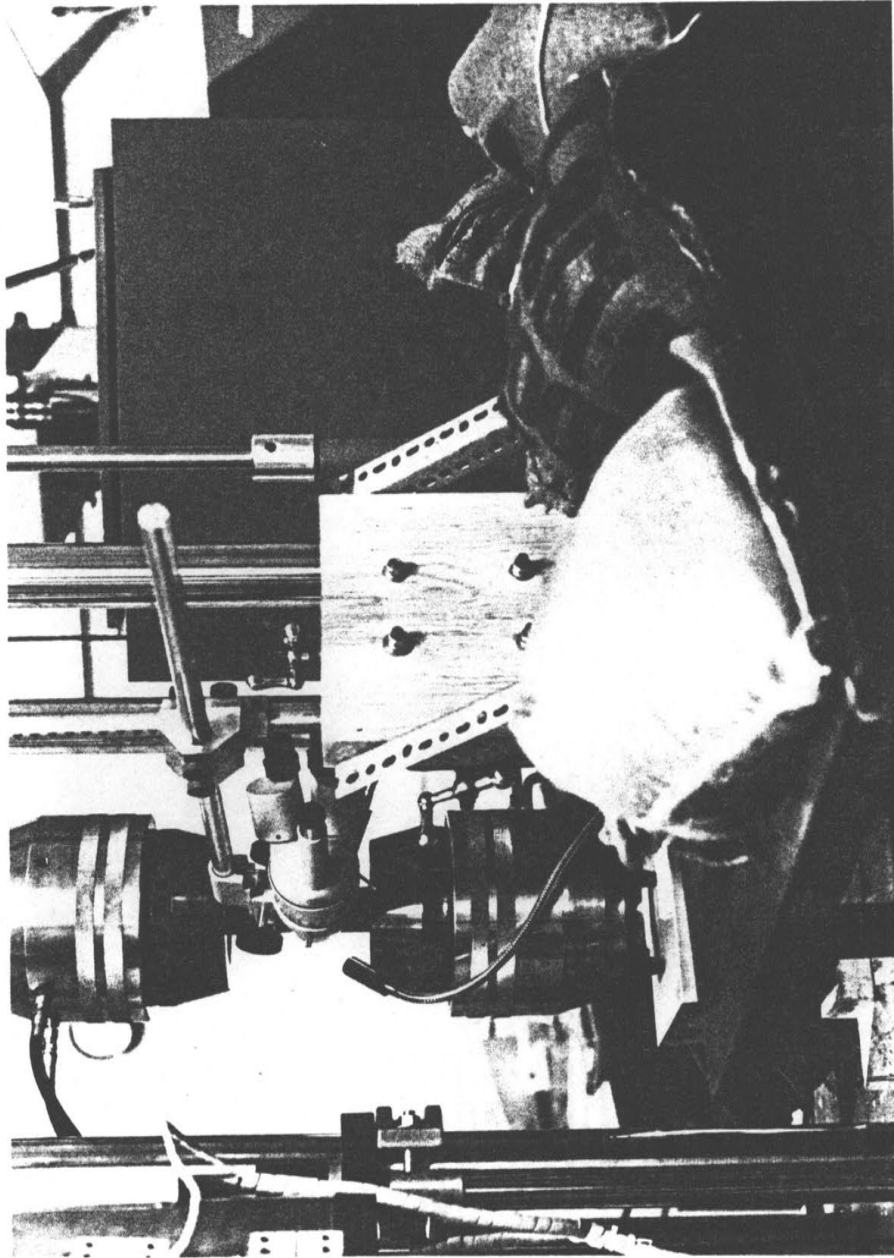
Figure 8.5. Experimental setup

focusing but they subsided quickly each time (within a few seconds) making it possible to take meaningful data.

8.4 Test procedure

After trying both grid types on coupons of the [±15/0]s laminate, it was decided to use the 200 lines/inch grid instead of the 500 lines/inch one mainly because at the particular magnification (240X) and with the particular silver paint used, the square points on the 200 lines/inch grid were much brighter and sharper than the square points on the 500 lines/inch grid making measurements more accurate.

A system of levels was used to verify that the axis of the microscope was perpendicular to the surface of the specimen when it was gripped in the testing machine.

Each coupon was put in the grips of the testing machine and a vertex of one of the grid squares was chosen as an origin as close to the free edge as possible (see Figure 8.6). Then, before loading, the distances of the vertices of the grid squares around the origin (originally a 20 grid points by 20 grid points square was covered) were measured by eye using the scale in one of the eyepieces of the microscope. The procedure was repeated after loading to a desired stress level (keeping the same point as origin). Subtracting the original from the final value for each point in the x_1 and the x_2 (or
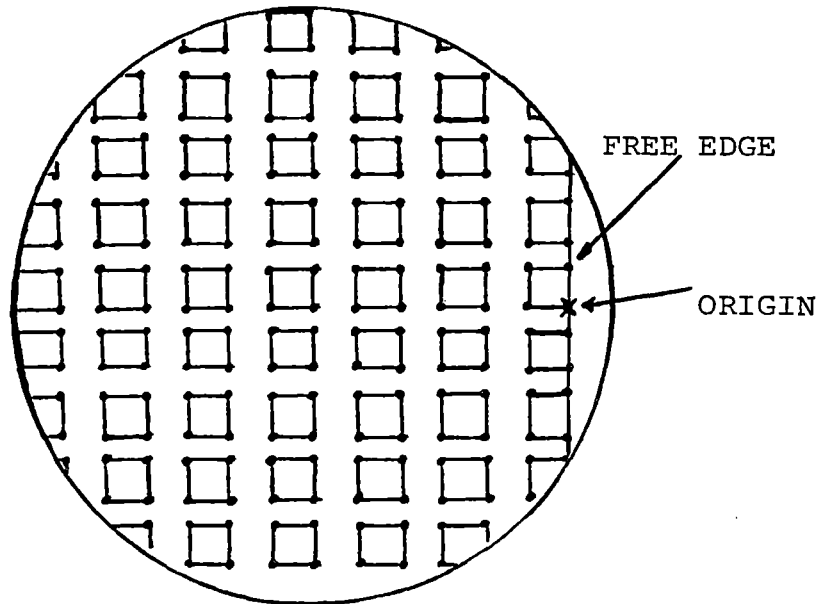
Figure 8.6. Grid pattern under the microscope. Dots
at the vertices of squares denote original
data point locations

x) direction gave the u and v displacements of each point at that particular load level. It is interesting to note that a 20 grid points by 20 grid points square gives a total of 6400 data points per load level per coupon (covering an area of about 4 square mm) and since all these are read off by the experimenter without the use of any data taking device, a single coupon at a single load level takes more than 6 hours to test. For reasons to be discussed below the number of data points per coupon per load level was eventually decreased to 100 data points.

Since it was impossible to mark axes on the grid, measurement of distances from the origin of points that did not lie in the same row or column of grid points that included the origin (see Figure 8.6) was very difficult. Distances of points that were on the same row or column with the origin were easier to measure. This means that u as a function of x_1 and v as a function of x were much easier to measure than u as a function of x and v as a function of x_1.

This difficulty in measuring u as a function of x and v as a function of x_1 reduced the usefulness of covering a whole square of grid points. Eventually, only the displacements of the points lying on the same row and column as the origin were measured for each coupon. In each column 20 points were used and in each row 30-40 points were used to insure that the

points further from the free edge were outside the boundary layer as predicted by the theory for that particular laminate.

The distances of these points from the origin were measured by eye using a micrometer scale attached to one of the eyepieces of the microscope. The error in each measurement (half the width of the smallest division) was ±4.15 microns at 240X magnification. This was the highest magnification possible with the SZ-III-Tr Olympus microscope that was used and no lower magnification could be used since at lower magnifications the resolution was so poor that it was very hard to pick up any difference between the distances of the points from the origin before and after loading. At that magnification however, only five to six grid squares could be seen along a diameter in each field of vision i.e. only the distances of 10 to 12 points from the origin could be measured (see Figure 8.6). To make the ±4.15 microns error in each measurement as small a fraction of the measured distance as possible, each point should be as far from the origin as possible. On the other hand, in order to measure as many distances per field of vision as possible (to avoid changing fields of vision many times which involved shifting the origin each time and introducing a measurement of the order of 2 microns) each point should be as far from the origin as possible. A compromise was found by measuring the distance of every other point from the origin, i.e. one point per square of the grid was used (the

right-most point of each square in a row and the lower point
of each square in a column as is shown in Figure 8.7) instead
of the possible two points per measuring direction (horizontal
or vertical). This gave about five data points per field of
vision per direction which means that for 20 data points in
the vertical direction 4 changes of field of vision were
needed, and for 30 data points in the horizontal direction 6
changes of field of vision were needed. The sampling rate was
approximately 1 data point every 120 microns which means that
a distance of approximately 2400 microns (2.4 mm) was spanned
in the vertical direction (20 data points) and a distance of
3600 microns (3.6 mm) was spanned in the horizontal direction
(30 data points). The error in each measurement was thus $\pm 3\%$
for points closest to the origin, and $\pm 0.6\%$ for points far
from the origin (closest to the other end of the field of
vision). Of course, this pattern repeated every time the field
of vision changed and the origin shifted. Table 8.3 summarizes
all this information.

8.5 Data reduction

The displacements in the x_1 and x directions were deter-
mined as the differences between the unloaded and loaded dis-
tances of each point from the origin.
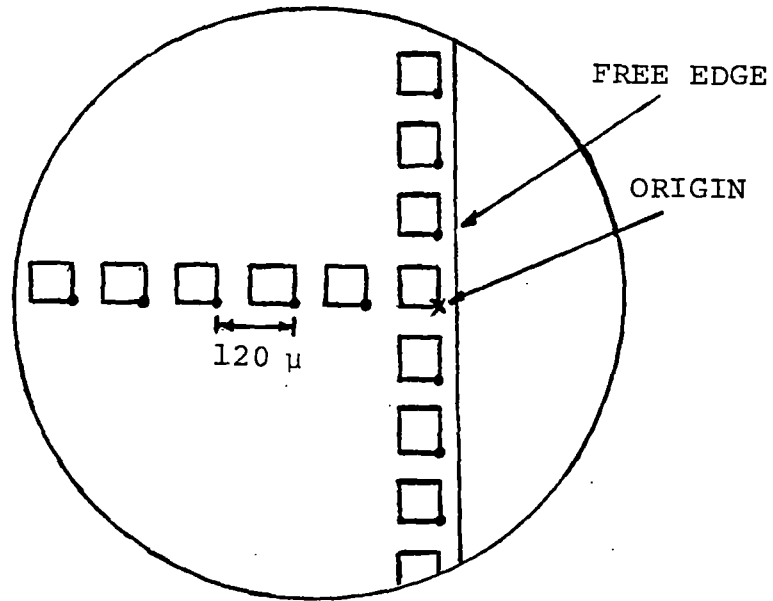
Figure 8.7. Data points (dots at vertices of squares) per field of vision

TABLE 8.3

DATA TAKING INFORMATION

Number of measurements per coupon	100-200
Number of data points in the longitudinal direction	20
Distance spanned in the longitudinal direction	2.4 mm
Number of data points in the transverse direction	30-40
Distance spanned in the longitudinal direction	3.6-5 mm
Sampling rate	1 data pt/ 120 μ
Number of data points per field of vision	5-6
Fields of vision needed in longitudinal direction	4-5
Fields of vision needed in transverse direction	6-7
Average error in each measurement	1.8%
Error induced at each origin shift	2 microns
Average testing time per coupon	2-3 hours

To every u or v displacement value thus measured, the u or v displacement of the origin (which being a point close to the free edge was not stationary during loading) was added. It was very difficult to actually measure this displacement of the origin because, both in the x_1 and the x direction, the origin moved a distance of approximately 1-2 mm and three to six changes of field of vision were required making an accurate measurement difficult. Furthermore, part of this displacement was rigid body motion of the two grips of the testing machine. Thus, even if the distances that the origin moved in the x_1 and the x directions could be measured accurately, these values would not represent the u and v displacements of the origin due to material stretching and contracting. The u displacement of the origin was estimated by multiplying the far-field ε_{11} strain with the x_1 distance between the origin and the lower edge of the loading tab in the top grip of the testing machine which is stationary during loading. The v displacement of the origin was estimated as the product of the far-field ε_{22} strain and the x_2 distance between the origin and the center of the laminate which, by symmetry, is also stationary during loading. It should be noted that there is some uncertainty in this estimation because the origin lies in the boundary layer where the in-plane strains are expected to vary from their far-field values. However the error is small because the boundary layer

is a small fraction of the x_1 and x_2 distances used in the estimations. It can be shown using the theoretical expressions for the u and v displacements that the predicted displacement of the origin (in either of the two directions) differs from the corresponding estimated value by only 1%.

The theoretical predictions for the u and v displacements were obtained by integrating the equations for ε_{11} and ε_{22} (equations 5.21 and 5.22) with respect to x_1 and x respectively. Note that in general, for any x_1, x and z, these equations cannot be integrated because the unknown functions F and G that result (see equations 5.24 and 5.25) cannot be determined in a consistent way. This is due to the approximate nature of the analytical method used which satisfies strain compatibility on the average. If however, x_2 and z are known numbers, as is the case of the u displacement which was measured as a function of x_1 at a fixed x_2 and z location, $F(x_2,z)$ is a constant and can be determined by requiring that u be zero at the edge of the top grip of the testing machine (recall that the top grip does not move during testing). Similarly, for v measured as a function of x_2 (or x) at a fixed x_1 and z location as was the case during the experiment, $G(x_1,z)$ is a constant and can be determined by requiring that v as given by equation 5.25 is zero at the center of the laminate (i.e. at x=b). Then, equations 5.24 and 5.25 give the theoretical predictions

for the u displacement as a function of x_1 and the v displacement as a function of x.

CHAPTER NINE

EXPERIMENTAL RESULTS

The method described in chapter eight was used to obtain experimental plots for u and v for different coupons. Some problems were encountered during testing especially for the thicker laminates. The strain levels reached were low (and hence the displacement values were also low) because at higher loads "clicks" indicating some type of damage were heard which meant that the laminate properties would be different from those of an undamaged laminate and there was no way to measure the exact effect of the damage.

9.1 $[(+15)_5/(-15)_5/0_5]$s laminate

Using coupon number five of this laminate a monotonic test was conducted to find that the first "clicks" were heard at 60% of the failure stress of 624 MPa. This coupon was not used to take displacement data. The remaining coupons were loaded up to approximately 50% of the failure load. Coupon number 4 had a grid failure (the grid did not stick well onto the coupon surface) and was not used to take data.

Using the strain gages on coupons 1, 2, and 3, the Young's modulus and the Poisson's ratios were determined.

These, along with the corresponding values predicted by CLPT, are listed in Table 9.1. A typical stress-strain plot for one of the coupons is shown in Figure 9.1.

The v displacement as a function of x for coupons 1, 2, and 3 is shown in Figures 9.2, 9.4, and 9.6 respectively. The theoretical predictions are also shown. The u displacement as a function of x for coupons 2 and 3 is compared to the theoretical predictions in Figures 9.3 and 9.5.

9.2 [±15/0]s laminate

As it was mentioned in chapter eight, this laminate was used as a test laminate to examine the validity of the experimental technique at the first stages of the experiment. It is interesting to note that with this laminate it was possible to go to a significantly higher strain level (about 5000 microstrain) than with the thicker laminates (about 3500 microstrain) which means that while thicker laminates have the advantage of a large boundary layer, thin laminates may also be useful in obtaining data in the boundary layer because they allow higher strain levels (without any audible "clicks") and hence more accuracy in the measurements. The u and v displacements for coupon 3 of this laminate are compared to the analytical predictions in Figures 9.7 and 9.8 respectively.

TABLE 9.1

COMPARISON OF MEASURED YOUNG'S MODULUS AND POISSON'S RATIO WITH CLPT PREDICTIONS

Coupon	Young's Modulus [GPa]		Poisson's Ratio	
	Measured	CLPT	Measured	CLPT
1	109.9	115.7	0.84	0.67
2	104.8	115.7	0.80	0.67
3	112.8	115.7	0.62	0.67

Figure 9.1. Typical stress-strain plot for $[(+15)_5/(-15)_5/0_5]_s$ laminate (coupon 3)

217
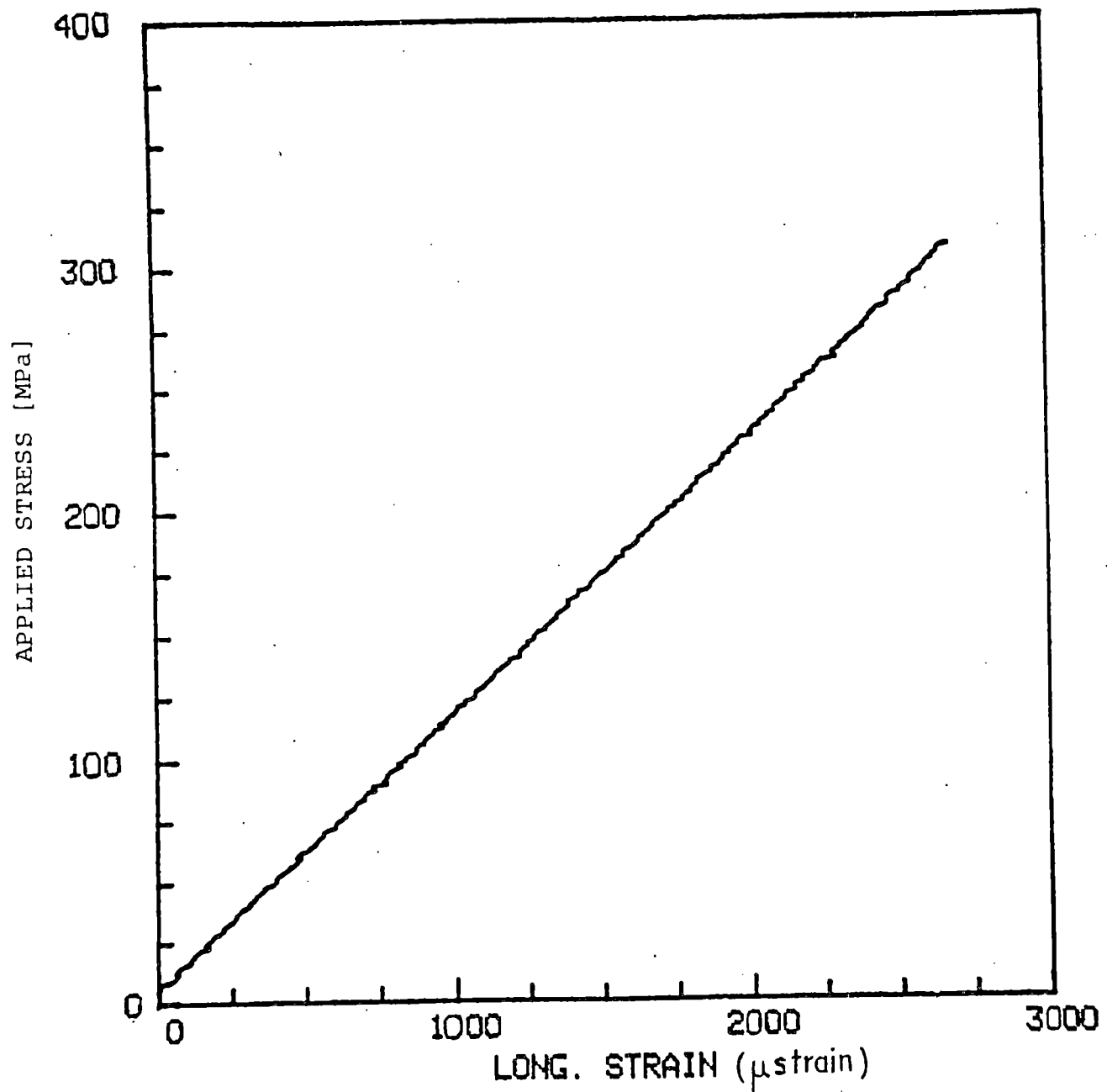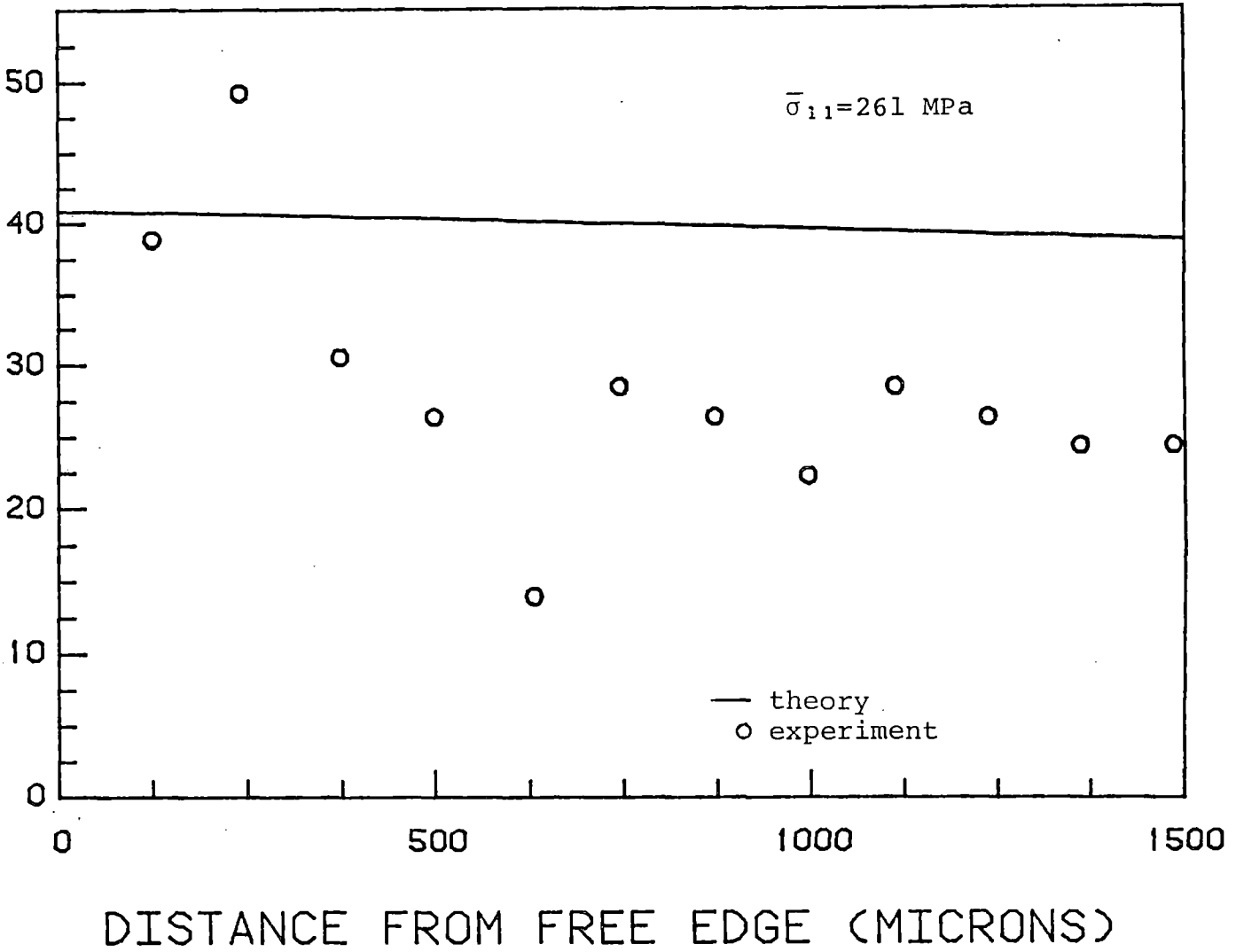
Figure 9.2. Calculated versus measured transverse (v) displacement at the top surface of a $[(+15)_5/(-15)_5/0_5]_s$ laminate (coupon 1)

TRANSV. DISPLACEMENT (MICRONS)

DISTANCE FROM FREE EDGE (MICRONS)

$\bar{\sigma}_{11}=261$ MPa

— theory
O experiment
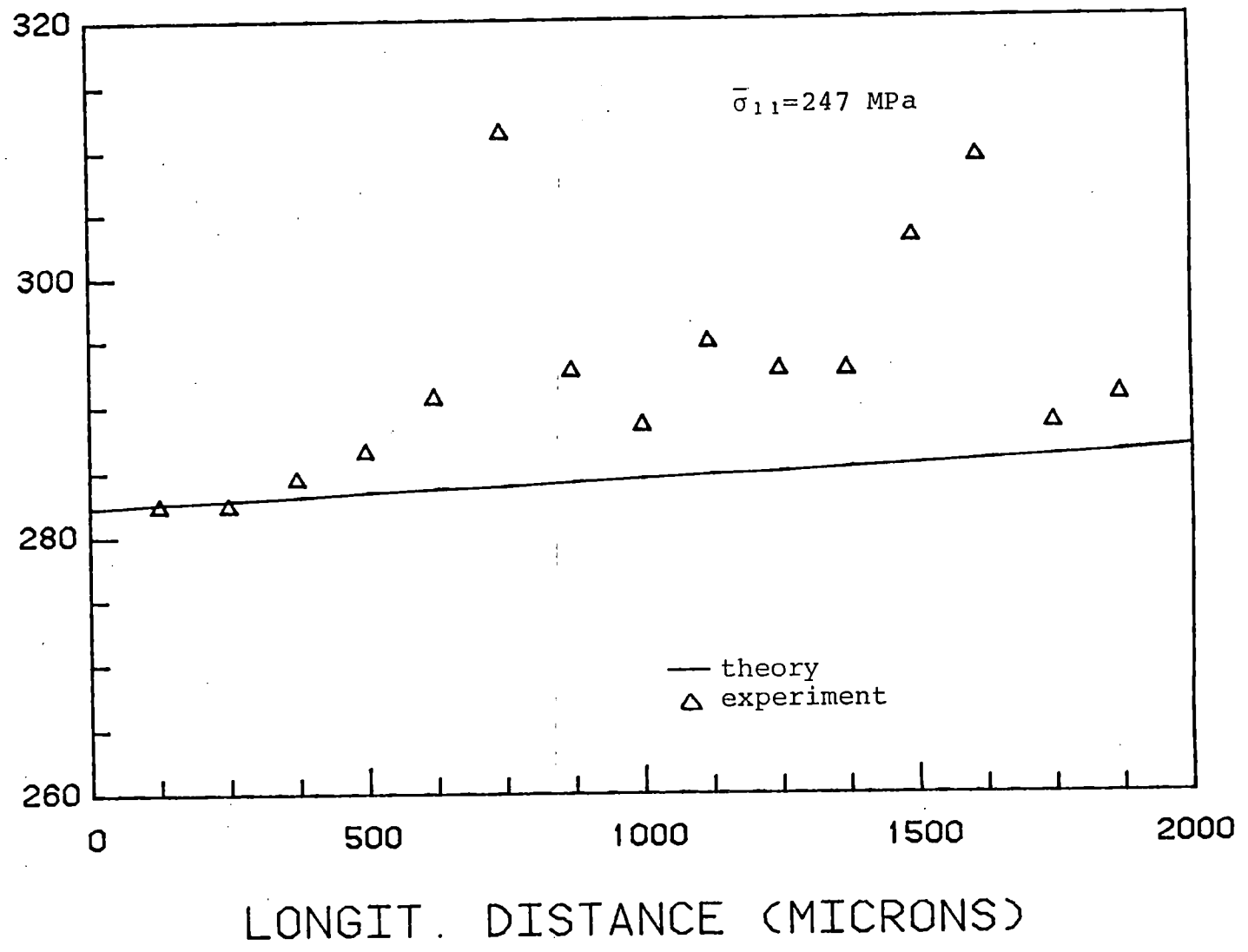
Figure 9.3. Calculated versus measured longitudinal (u) displacement at the top surface of a $[(+15)_5/(-15)_5/0_5]_s$ laminate (coupon 2).
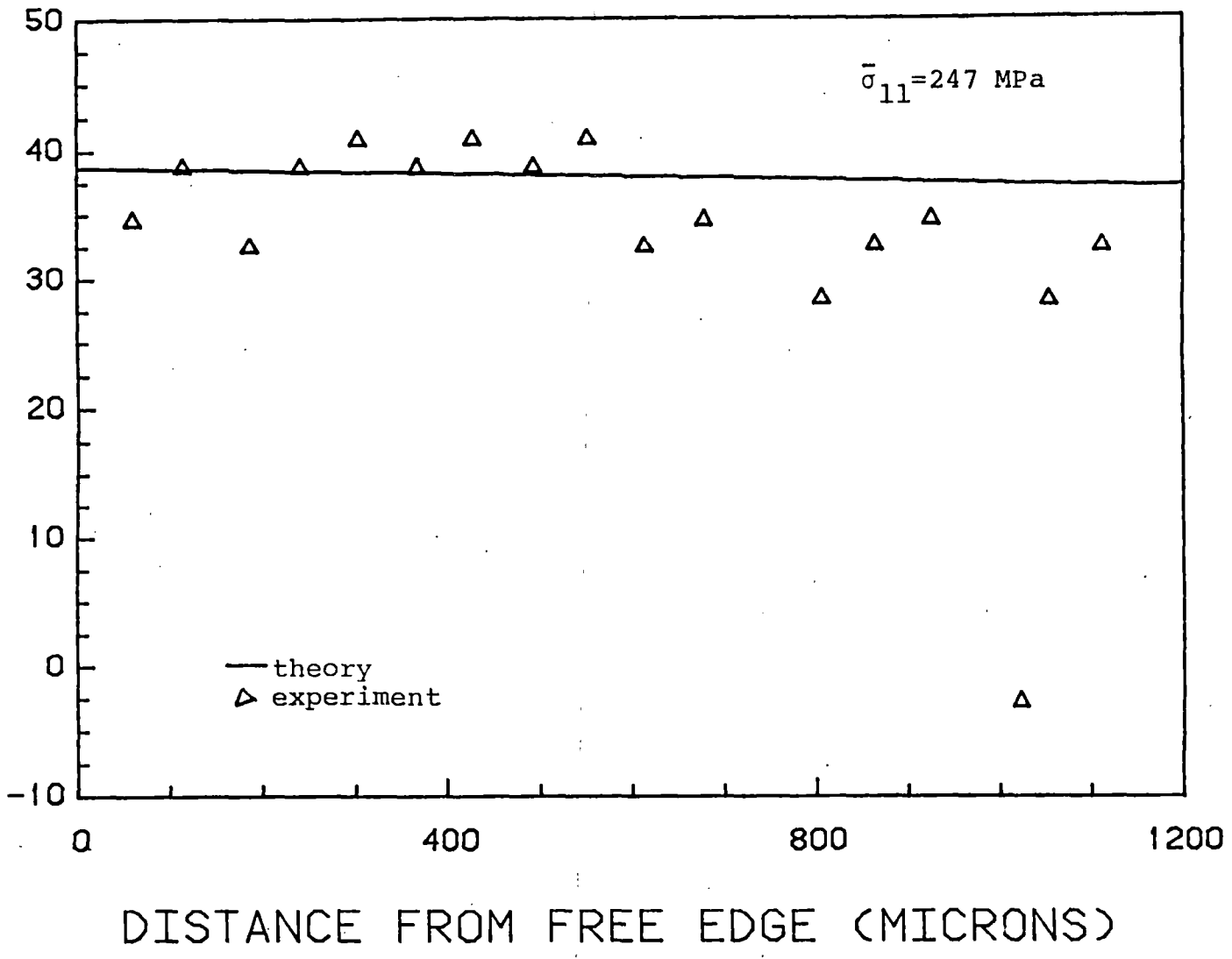
Figure 9.4. Calculated versus measured transverse (v) displacement at the top surface of a $[(+15)_5/(-15)_5/0_5]_s$ laminate (coupon 2)
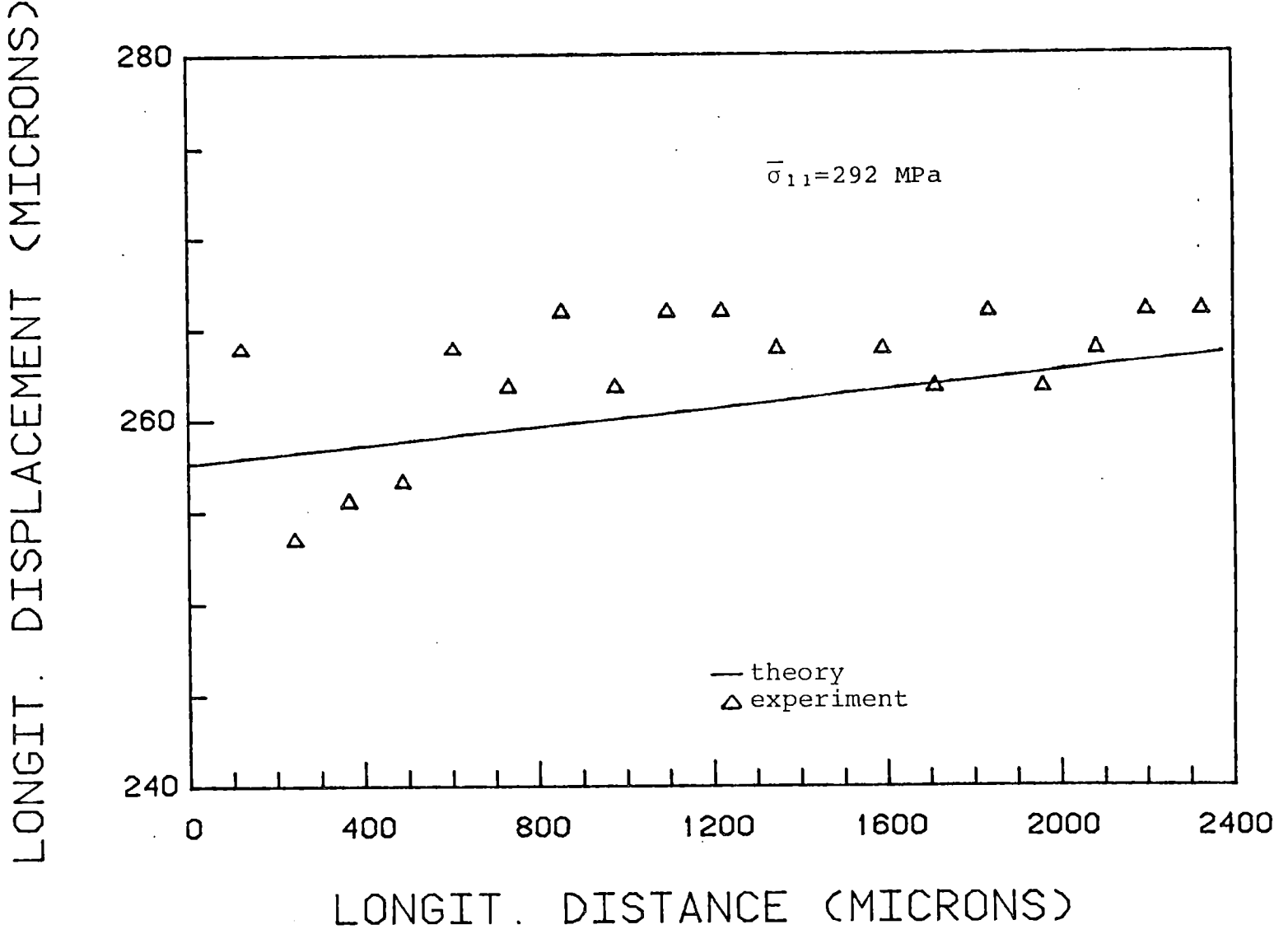
Figure 9.5. Calculated versus measured longitudinal (u) displacement at the top surface of a $[(+15)_5/(-15)_5/0_5]_s$ laminate (coupon 3)

$\bar{\sigma}_{11}=292$ MPa

— theory
△ experiment

LONGIT. DISPLACEMENT (MICRONS)

LONGIT. DISTANCE (MICRONS)

221

Figure 9.6. Calculated versus measured transverse (v) displacement at the top surface of a $[(+15)_5/(-15)_5/0_5]_s$ laminate (coupon 3)

TRANSV. DISPLACEMENT (MICRONS)

DISTANCE FROM FREE EDGE (MICRONS)

$\bar{\sigma}_{11}=121$ MPa

— theory
◇ experiment

LONGIT. DISPLACEMENT (MICRONS)

$\overline{\sigma}_{11}=500$ MPa

—— theory
△ experiment

LONGIT. DISTANCE (MICRONS)
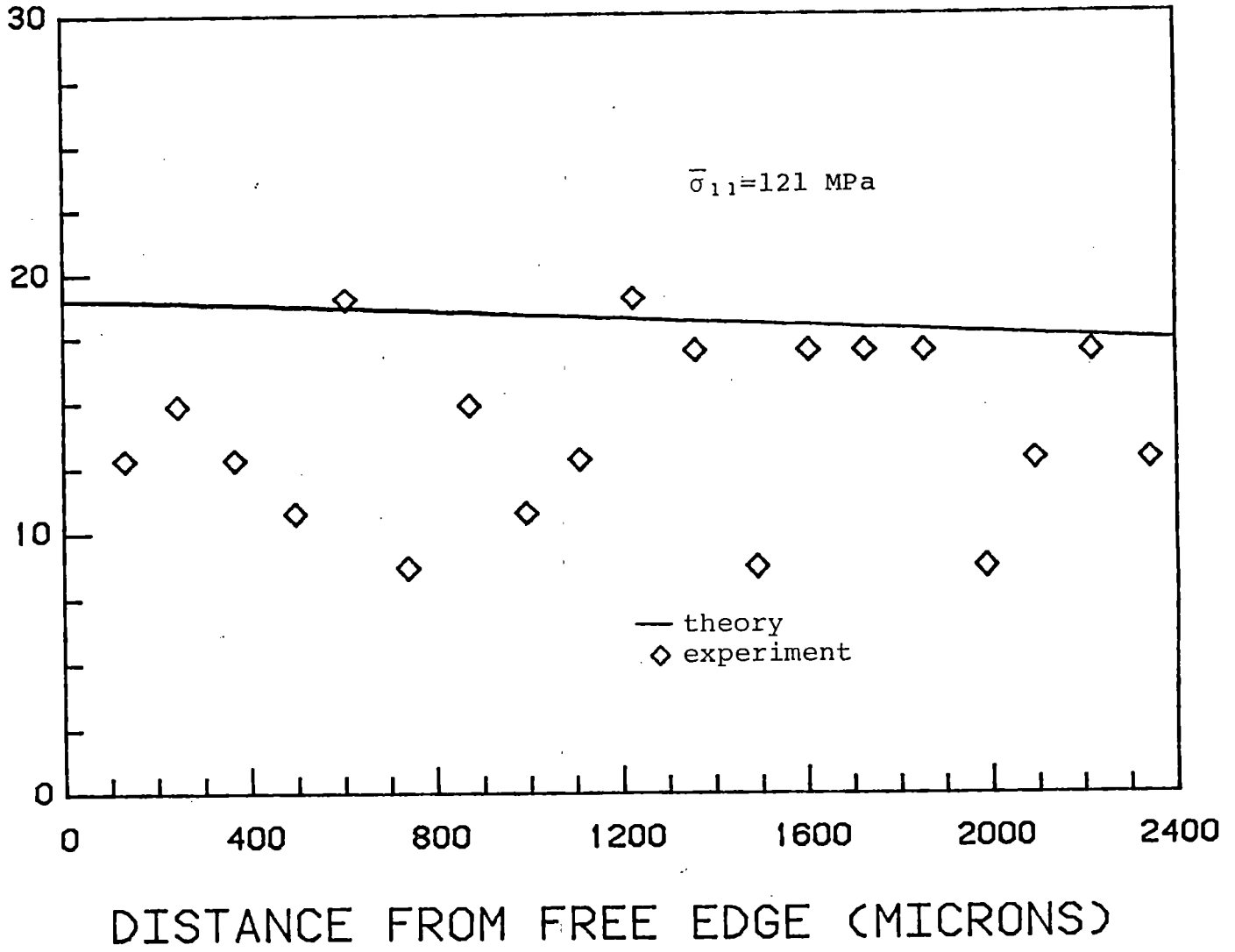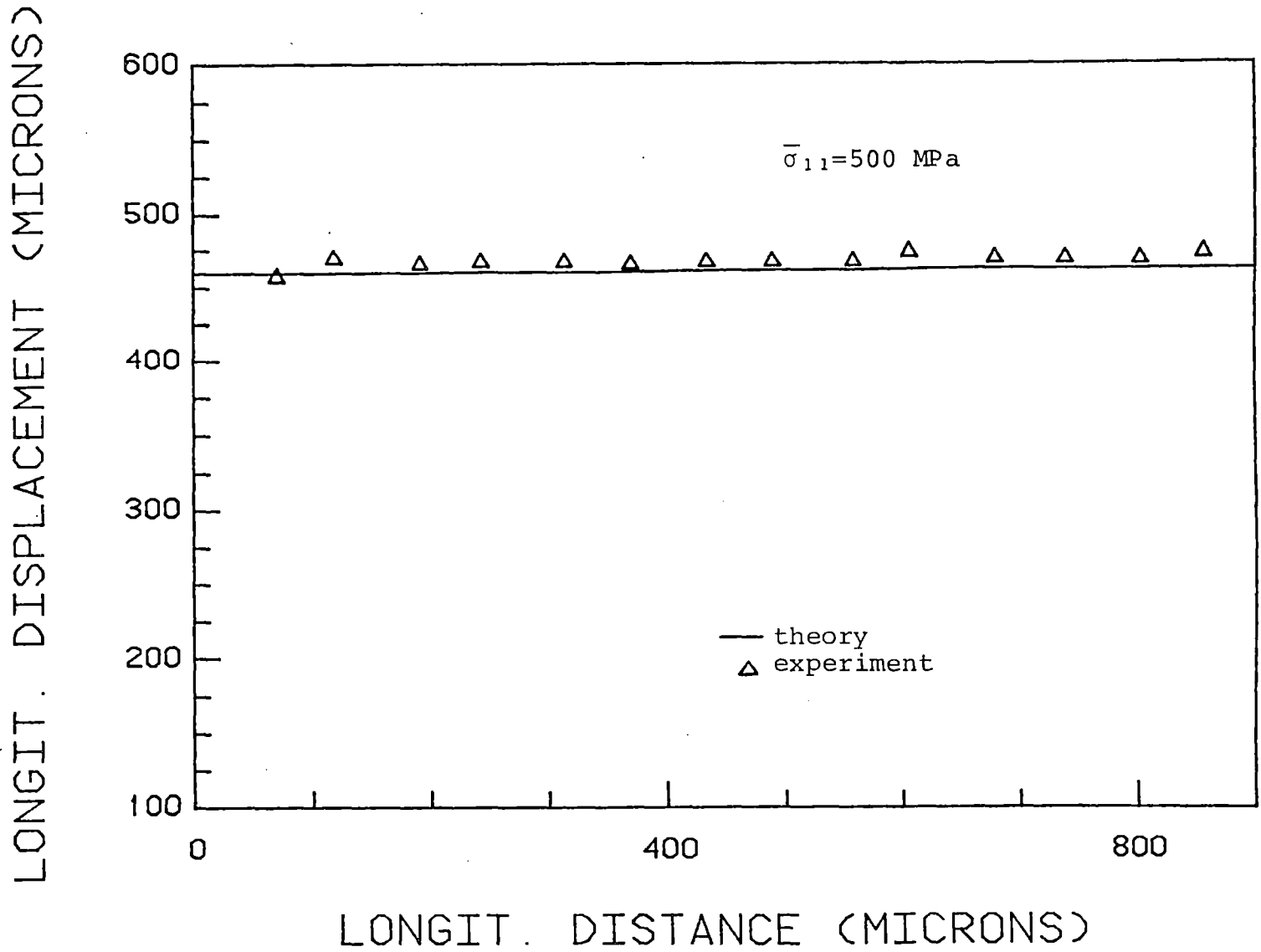
Figure 9.7. Calculated versus measured longitudinal (u) displacement at the top surface of a [±15/0]$_s$ laminate (coupon 3)

TRANSV. DISPLACEMENT (MICRONS)

$\bar{\sigma}_{11}$=553 MPa

— theory
△ experiment

DISTANCE FROM FREE EDGE (MICRONS)
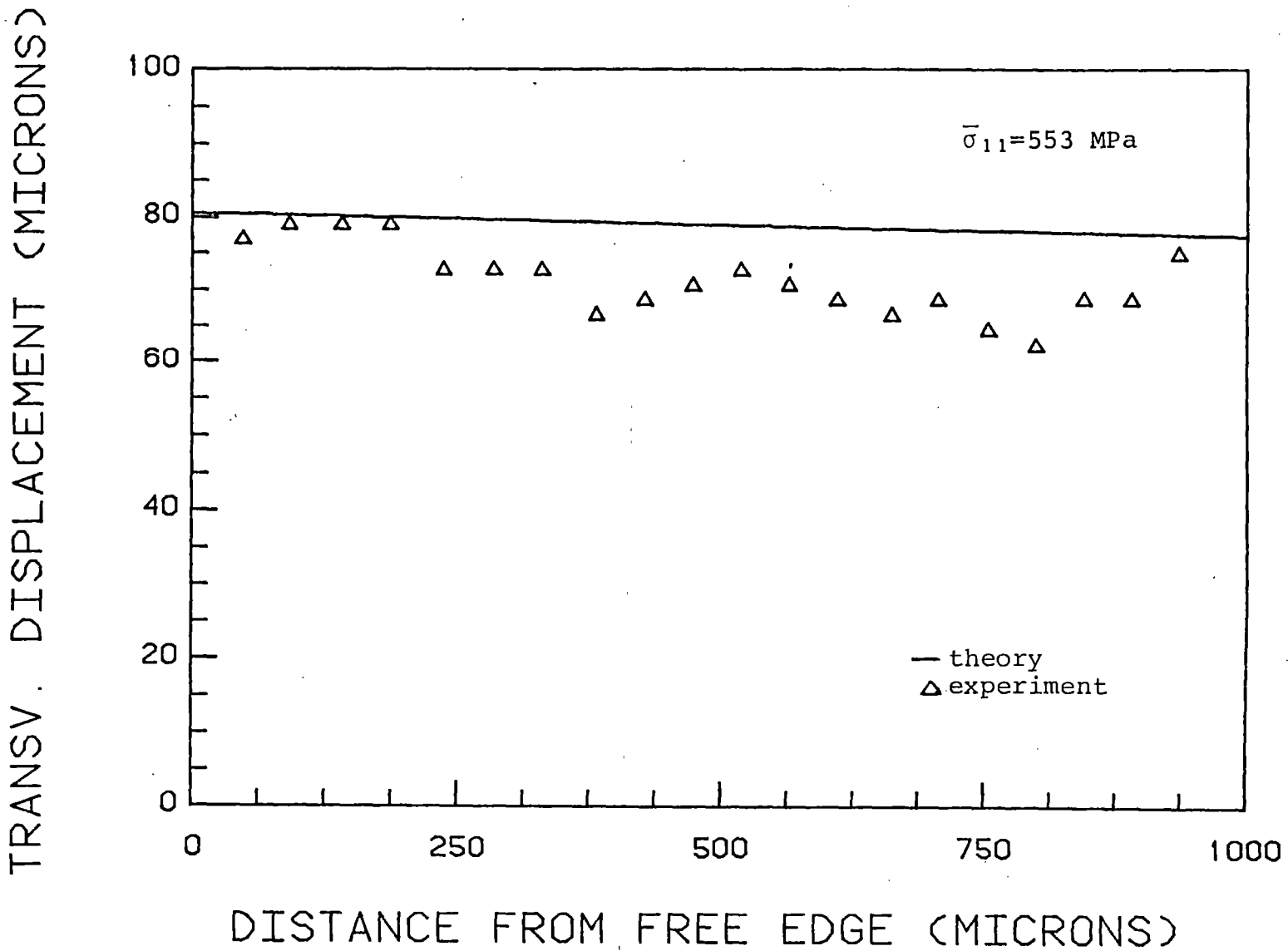
Figure 9.8. Calculated versus measured transverse (v) displacement at the top surface of a $[\pm 15/0]_s$ laminate (coupon 3)

224

9.3 [(+45)$_{10}$/(-45)$_{10}$]s laminate

This laminate exhibits significant nonlinear stress-strain behavior [44]. The linear region of the stress-strain curve is limited to stress levels below 50 MPa. For this reason, the specimens were loaded only up to 30 MPa. However, at such low stress levels the strains were so low that no useful displacement measurements were taken.

9.4 Comments on the experimental results

Even though there is significant experimental scatter, the theoretical predictions have the same trends as the measured data in all cases. In the case of the v displacement for coupon 2 of the [+15$_5$/-15$_5$/0$_5$]s laminate (Figure 9.4), the theory is in very good agreement with the experimental results. Only one data point is far from the theoretical prediction and is obviously wrong since it corresponds to a negative value for the displacement at a location where the displacement should be positive.

The u displacement predictions for coupon 3 of the [+15$_5$/-15$_5$/0$_5$]s laminate (Figure 9.5) and coupon 3 of the [±15/0]s laminate (Figure 9.7) are also in good agreement with the experimental results.

The differences in the remaining plots (Figures 9.2, 9.3, and 9.6) are attributed mainly to the changes of field of vision required during testing. These in some cases induce significant errors and can be seen as patterns in the data points. Any error at each change is added to all data points that follow. Referring to Figures 9.2 and 9.6, this might explain why after the first change of field of vision in the first case (corresponding to the fourth data point in Figure 9.2) and after the third change of field of vision in the second case (corresponding to the fifteenth data point in Figure 9.6) the measured values are consistently lower than the predicted values.

In summary, the theoretical predictions compare well with the experimental results even though there is significant scatter in the data. The plots for the u displacements give an indication that the assumption that stresses do not depend on x_1 is valid. The experimental method is successful in producing many data points within very small distances. Some improvements in the accuracy of the measurements are needed so that more reliable data can be obtained. A more accurate scale on the eyepiece of the microscope would improve the accuracy greatly. It is also suggested that laminates with stacking sequences and material types permitting higher strain levels (in the linear region of the stress-strain curve and at loads lower than the loads at which the first "clicks" are heard) be

used so that the measured displacements are larger and hence the errors are smaller percentages of the measured values.

CHAPTER TEN

CONCLUSIONS AND SUGGESTIONS FOR FURTHER WORK

10.1 Conclusions

A simple approximate method to determine interlaminar stresses at the straight free edges of symmetric and balanced composite laminates was presented. The method is based on the conclusions of the Force-Balance Method and the principle of minimum complementary potential energy. The boundary conditions are exactly satisfied. Far from the free edge the CLPT solution is recovered. Due to the fact that strain compatibility is satisfied in an average (variational) sense, the displacements cannot be determined exactly. This is not much of a drawback however, since for failure analysis considerations only the stresses or the strains are used and both can be determined by the present method in closed form. In particular:

1. The present method predicts in-plane stresses which, in the boundary layer, differ significantly from the CLPT predictions. This must be taken into account if in-plane stress-based failure criteria are used to predict failure of composite laminates.

2. Some effects of changing the stacking sequence were examined. It was found that if the 0° plies of a $[\pm\theta/0]s$ laminate are moved from the midplane to the outside of the laminate (thus forming a $[0/\pm\theta]s$ laminate) the interlaminar normal stress changes from tensile to compressive.

3. In the special cases of angle-plied and cross-plied laminates the solution simplifies and no iterations are needed (which are necessary for general laminates). The solution for these special laminates then can be obtained even faster (in terms of CPU time) than for general laminates.

4. It was shown that for some cross-plied laminates the present method of analysis coincides with a method developed by Pagano [12] which was based on a plate theory presented by Whitney and Sun [13].

5. The concept of the "effective ply thickness" was introduced (chapter seven). It was found that the boundary layer is a strong function of the effective ply thickness. Doubling the effective ply thickness doubles the boundary layer exactly. On the other hand, if the laminate thickness is doubled but the effective ply thickness is kept the same the boundary layer size remains the same.

6. Modelling the resin layer between plies as a separate ply has almost no effect on the stress shapes for AS1/3501-6 graphite/epoxy systems. Thus, the usual approach of incorporating it in the adjacent plies is justified.

7. The results obtained by using the measured out of plane elastic properties were compared to results obtained using the out of plane properties assumed by most investigators. The differences were small and slightly more pronounced in the case of interlaminar shear stress σ_{2z}.

8. Two possible approaches for modelling the in-plane longitudinal stress were examined. One was to assume that it is equal to the CLPT value throughout each ply and the other was to actually determine it using the stress-strain and the strain-displacement equations. The second approach is more accurate and does not require any significant additional effort.

9. The present method was shown to compare well with other methods of analysis. It can deal efficiently with thick laminates (100 plies or more) which the other methods cannot do. It can analyze hybrid or variable ply thickness laminates very effectively. The method is more efficient than other analytical methods proposed in the past.

10. An experimental technique to take in-situ displacement measurements at the top surface of a laminate using moiré grids observed under a microscope was also presented. The results compare well with the theoretical predictions. In all cases the theory shows the same trends as the experiment. Some improvements in the accuracy of taking data are needed so that more conclusive experiments can be performed.

11. The available data on the u displacements inside the boundary layer indicates that the assumption that stresses do not depend on x_1 is valid.

10.2 Recommendations for further work

1. Some modification of the in-plane (CLPT) solution is needed so that discontinuities in the in-plane stresses can be avoided. A possible approach would be to assume that the in-plane stresses (even at the far field) are functions of z.

2. The method can easily be generalized to any type of laminates (unsymmetric and unbalanced) under any type of loading. Also, minor modifications are needed for the analysis to account for thermal loadings.

3. The analysis should be extended to curved free edges (e.g. holes).

4. Some improvements in the accuracy of the experimental technique are needed. A more accurate scale is needed to be attached on the eyepiece of the microscope so that finer resolution can be achieved. It is also suggested that different materials be used with such stacking sequences that the resulting in-plane strains are larger than those measured so far (but still in the linear region of the stress-strain plot) so that the errors in the measurements do not affect the data

as much. Then, the technique can be applied to laminates with holes using polar grids.

5. The possibility of using x-rays to measure strains inside the laminate and not only at its top or bottom surface must be investigated. Very accurate and thin metallic grids can be vapor-deposited on the individual plies of a laminate (cured separately). The resulting plies can then be bonded together using a secondary bond operation.

REFERENCES

1. Tsai, S.W., and Wu, E.M., "A Generalized Theory of Strength for Anisotropic Materials", Journal of Composite Materials , 5, 1971, pp 58-80.

2. Lagace, P.A., "Notch Sensitivity and Stacking Sequence of Laminated Composites", presented at ASTM Seventh Conference: Composite Materials Testing and Design, Pensylvania, April, 1984.

3. Wang, S.S., and Mandell, J.F., "Analysis of Delamination in Unidirectional and Crossplied Fiber Composites Containing Surface Cracks", NASA CR-135248.

4. Tsai, S.W., and Hahn, H.T., Introduction to Composite Materials , Technomic Publishing Co, Westport Conn., 1980, chapter 4.

5. Pipes, R.B., and Pagano, N.J., "Interlaminar Stresses in Composite Materials under Uniform Axial Extension", Journal of Composite Materials , 4, 1970, pp 538-548.

6. Puppo, A.H., and Evensen, H.A., "Interlaminar Shear in Laminated Composites under Generalized Plane Stress", Journal of Composite Materials , 4, 1970, pp 204-220.

7. Rybicki, E.F., "Approximate Three-Dimensional Solutions for Symmetric Laminates under In-Plane Loading", Journal of Composite Materials , 5, 1971, pp 354-360.

8. Stanton, E.L., Crain, L.M., and Neu T.F., "A parametric Cubic Modelling System for General Solids of Composite Material", Int. J. of Numerical Methods in Engineering , 11, 1977, pp 653-670.

9. Wang, A.S.D., and Crossman, F.W., "Some New Results on Edge Effect in Symmetric Composite Laminates", Journal of Composite Materials , 11, 1977, pp 92-106.

10. Wang, A.S.D., and Crossman, F.W., "Calculation of Edge Stresses in Multi-Layer Laminates by Sub-Structuring", Journal of Composite Materials , 12, 1978, pp 76-83.

11. Altus, E., Rotem, A., and Shmueli, M.,"Free Edge Effect in Angle Ply Laminates- A New Three Dimensional Finite Difference Solution", Journal of Composite Materials , 14, 1980, pp 21-30.

12. Pagano, N.J., "On the Calculation of Interlaminar Normal Stress in Composite Laminates", _Journal of Composite Materials,_ 8, 1974, pp 65-82.

13. Whitney J.M., and Sun C.T., "A Higher Order Theory for Extensional Motion of Laminated Composites", _Journal of Sound and Vibration_ , 30, 1973,p 85.

14. Tang, S., "A Boundary Layer Theory- Part I: Laminated Composites in Plane Stress", _Journal of Composite Materials,_ 9, 1975, pp 33-41.

15. Tang, S., and Levy, A., "A Boundary Layer Theory- Part II:Extension of Finite Strip", _Journal of Composite Materials,_ 9, 1975, pp 42-52.

16. Hsu, P.W., and Herakovich, C.T., "Edge Effects in Angle-Ply Composite Laminates", _Journal of Composite Materials,_ 11, 1977, pp 422-428.

17. Pagano, N.J., "Stress Fields in Composite Laminates", _Int. Journal of Solids and Structures_ , 14, 1978, pp 385-400.

18. Pagano, N.J., "Free Edge Fields in Composite Laminates", _Int. Journal of Solids and Structures_ , 14, 1978, pp 401-406.

19. Wang, A.S.D., and Crossman, F.W., "Initiation and Growth of Transverse Cracks and Edge Delamination in Composite Laminates. Part 1. An Energy Method", _Journal of Composite Materials_ , 14, 1980, pp 71-87.

20. Bar-Yoseph, P., and Pian, T.H.H., "Calculation of Interlaminar Stress Concentration in Composite Laminates", _Journal of Composite Materials_ , 15, 1981, pp 225-239.

21. Bogy, D.B., "Edge-Bonded Dissimilar Orthogonal Elastic Wedges under Normal and Shear Loading", _Journal of Applied Mechanics_ , 35, 1968, pp 460-466.

22. Kuo, M.C., and Bogy, D.B., "Plane Solutions for Traction Problems on Orthotropic Unsymmetrical Wedges and Symmetrically Twinned Wedges", _Journal of Applied Mechanics_ , 41, 1974, pp 203-208.

23. Wang, S.S., and Choi, I., "Boundary-Layer Effects in Composite Laminates Part-1. Free Edge Stress Singularities", _Journal of Applied Mechanics_ , 49, 1982, pp 541-548.

24. Wang, S.S., and Choi, I., "Boundary-Layer Effects in Composite Laminates Part-2. Free Edge Stress Solutions and Basic Characteristics", <u>Journal of Applied Mechanics</u>, 49, 1982, pp 549-560.

25. Lekhnitskii, S.G., <u>Theory of Elasticity of an Anisotropic Body</u>, Holden-Day, San Francisco, 1963.

26. Zwiers, R.I., Ting, T.C.T., and Spilker, R.L., "On the Logarithmic Singularity of Free-Edge Stress in Laminated Composites under Uniform Extension", <u>Journal of Applied Mechanics,</u> 49, 1982, pp 561-569.

27. Dempsey, J.R., and Sinclair, G.B., "On the Stress Singularities in the Plane Elasticity of the Composite Wedge", <u>Journal of Elasticity</u>, 9, 1979, pp 373-391.

28. Tong, P. and Pian, T.H.H., "On the Convergence of the Finite Element Methods for Problems with Singularity", <u>Int. Journal of Solids and Structures</u>, 9, 1973, pp 313-321.

29. Wang, S.S., and Yuan, F-G, "A Singular Hybrid Finite Element Analysis of Boundary-Layer Stresses in Composite Laminates" to be published.

30. Swedlow, J.L., "Singularity Computations", <u>Int. Journal of Numerical Methods in Engineering</u>, 12, 1978, pp 1779-1798.

31. Pagano, N.J., and Soni, S.R., "Global-Local Laminate Variational Model", <u>Int. Journal of Solids and Structures</u>, 19, 1983, pp 207-228.

32. Whitcomb, J.D., and Raju, I.S., "Superposition Method for Analysis of Free-Edge Stresses", <u>Journal of Composite Materials</u>, 17, 1983, pp 492-507.

33. Pipes, R.B., and Daniel, I.M., "Moiré Analysis of the Interlaminar Shear Edge Effect in Laminated Composites", <u>Journal of Composite Materials</u>, 5, 1971, pp 255-259.

34. Oplinger, D.W., Parker, B.S., and Chiang, F.P., "Edge-Effect Studies in Fiber-Reinforced Laminates", <u>Experimental Mechanics</u>, 14, 1974, pp 347-354.

35. Lou, A.Y.C., and Walter, J.D., "Interlaminar Shear Strain Measurements in Cord-Rubber Composites", <u>Experimental Mechanics</u>, 18, 1978, pp 457-463.

36. Kim, R.Y., and Soni, S.R., "Initiation of Delamination of Composite Laminates", Proceedings of US-Japan Conference on Experimental Analysis, SESA, Hawaii, 1982, pp 244-251.

37. Whitney,J.M., "Free Edge Effects in the Characterization of Composite Laminates", ASTM STP 521, 1973, pp 167-180.

38. Pipes, R.B., Kaminski, B.E., and Pagano, N.J. "Influence of the Free Edge upon the Strength of Angle Ply Laminates", ASTM STP 521, 1973, pp 218-228.

39. Whitcomb, J.D., Raju, I.S., and Goree, J.G., "Reliability of the Finite Element Method for Calculating Free Edge Stresses in Composite Laminates", Journal of Computers and Structures , 15, 1982, pp. 23-37

40. Crandall, S., Engineering Analysis , Mc Graw-Hill, 1956, chapter 1.

41. Lagace, P.A., "Delamination Fracture under Tensile Loading", in Proceedings of the Sixth Conference on Fibrous Composites in Structure Design, AMMRC MS 83-2, Army Materials and Mechanics Research Center, November, 1983.

42. Knight, M, and Pagano, N.J., "The Determination of Interlaminar Moduli of Graphite/Epoxy Composites", Mechanics of Composites Review, Air Force Wright Aeronautical Laboratory, October, 1981.

43. Lagace, P.A. and Brewer, J.C., TELAC Manufacturing Course Class Notes , Edition 0-2, Technology Laboratory for Advanced Composites Report-81-14, Massachusetts Institute of Technology, September, 1981.

44. Lagace, P.A., "Nonlinear Stress-Strain Behavior of Graphite/Epoxy Laminates", in Proceedings of the 25th Structures, Structural Dynamics and Materials Conference, AIAA/ASME/ASCE/AHS, 1984, pp 63-73.

APPENDIX 1

RADIUS OF CURVATURE FOR A CROSS-PLIED LAMINATE

The analysis in this appendix gives some evidence that σ_{zz} shapes which cross the x axis more than once correspond to higher laminate energies than σ_{zz} shapes which cross the x axis only once.

The displacements in a symmetric laminate under tension are given by Pipes and Pagano [5] as:

$$u = Cx_1 + U(x_2, z) \tag{A1.1}$$

$$v = V(x_2, z) \tag{A1.2}$$

$$w = W(x_2, z) \tag{A1.3}$$

The inverses of the two strain-displacement equations 3.3b and 3.3c can be written as:

$$\varepsilon_{22} = \frac{C_1 S_{12}}{S_{11}} + (S_{22} - \frac{S_{12}^2}{S_{11}}) \sigma_{22} + (S_{23} \frac{S_{13} S_{12}}{S_{11}}) \sigma_{zz} +$$

$$(S_{26} - \frac{S_{12} S_{16}}{S_{11}}) \sigma_{12} \tag{A1.4}$$

$$\gamma_{2z} = S_{44} \sigma_{2z} + S_{45} \sigma_{1z} \tag{A1.5}$$

where equation 5.34 was used to substitute for σ_{11}, C_1 is given by equation 5.37, and all quantities refer to the ith ply.

The strain-displacement equations 3.3b, and 3.3d,

$$\varepsilon_{22} = \frac{\partial v}{\partial x_2} \qquad\qquad \gamma_{2z} = \frac{\partial v}{\partial z} + \frac{\partial w}{\partial x_2}$$

can be used to determine the second derivative of the w displacement with respect to x . Differentiating equation 3.3d with respect to x and using equation A1.5 to substitute for γ_{2z}:

$$\frac{\partial^2 w}{\partial x_2^2} = S_{44} \frac{\partial \sigma_{2z}}{\partial x_2} + S_{45} \frac{\partial \sigma_{1z}}{\partial x_2} - \frac{\partial^2 v}{\partial x_2 \partial z} \qquad (A1.6)$$

Similarly, differentiating equation 3.3b with respect to z and using equation A1.4 to substitute for ε_{22}:

$$\frac{\partial^2 v}{\partial x_2 \partial z} = (S_{22} - \frac{S_{12}^2}{S_{11}}) \frac{\partial \sigma_{22}}{\partial z} + (S_{23} - \frac{S_{13} S_{12}}{S_{11}}) \frac{\partial \sigma_{zz}}{\partial z} + (S_{26} - \frac{S_{12} S_{16}}{S_{11}}) \frac{\partial \sigma_{12}}{\partial z} \quad (A1.7)$$

The last equation can be substituted in equation A1.6 to give:

$$\frac{\partial^2 w}{\partial x_2^2} = S_{44} \frac{\partial \sigma_{22}}{\partial x_2} + S_{45} \frac{\partial \sigma_{1z}}{\partial x_2} - (S_{22} - \frac{S_{12}^2}{S_{11}}) \frac{\partial \sigma_{22}}{\partial z} -$$

$$(S_{23} - \frac{S_{12} S_{13}}{S_{11}}) \frac{\partial \sigma_{zz}}{\partial z} - (S_{26} - \frac{S_{12} S_{16}}{S_{11}}) \frac{\partial \sigma_{12}}{\partial z} \qquad (A1.8)$$

which is valid for any laminate.

Assume now that the laminate is cross-plied, then, as it was shown in equations 6.21 and 6.22, $\sigma_{1z} = \sigma_{12} = 0$. Also, from the fact that σ_{22} is not a function of z, $\frac{\partial \sigma_{22}}{\partial z} = 0$. Thus equation A1.8 simplifies to:

$$\frac{\partial^2 w}{\partial x_2^2} = S_{44} \frac{\partial \sigma_{2z}}{\partial x_2} - (S_{23} - \frac{S_{12} S_{13}}{S_{11}}) \frac{\partial \sigma_{zz}}{\partial z} \qquad (A1.9)$$

which is valid for any ply of a cross-plied laminate.

This equation further simplifies if the equilibrium equation in the z direction (equation 5.3) is used:

$$\frac{\partial^2 w}{\partial x_2^2} = - (S_{44} + S_{23} - \frac{S_{12}S_{13}}{S_{11}}) \frac{\partial \sigma_{zz}}{\partial z}$$

(A1.10)

Considering figures 4.2a and 4.2b, one finds that two possible shapes for $\frac{\partial^2 w}{\partial x_2^2}$ are the ones shown in figure A1.1. However, $\frac{\partial^2 w}{\partial x_2^2}$ is equal to the inverse of one of the principal radii of curvature. Since (see equation A1.3) w is not a function of x_1, $\frac{\partial^2 w}{\partial x_1^2}\frac{\partial^2 w}{\partial x_1 \partial x_2}=0$ and therefore the other two radii of curvature($1/\frac{\partial^2 w}{\partial x_1 \partial x_2}$ and $1/\frac{\partial^2 w}{\partial x_1^2}$) are infinite. Hence, the out of plane shape of any interface will be governed by the shape of $1/\frac{\partial^2 w}{\partial x_2^2}$. Examination of Figure A1.1 yields possible shapes for $1/\frac{\partial^2 w}{\partial x_2^2}$, the radius of curvature, which are shown in Figure A1.2. These plots in turn imply the ply interface shapes that are shown in Figure A1.3.

Clearly, the shape shown in Figure A1.3b is a higher mode shape and corresponds to a higher energy state than that shown in Figure A1.3a. Therefore, for minimum energy the lower mode should be chosen. Thus, if a solution based on a σ_{zz} shape that crosses the x axis once can be found (i.e. if a stress field that satisfies the governing equations and the boundary conditions and has σ_{zz} stresses that cross the x axis once can be found), that shape is the correct solution since it minimizes the laminate complementary energy.
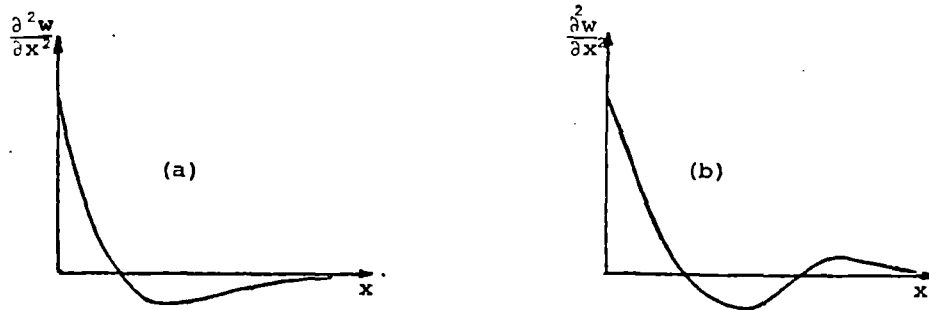
Figure A1.1. Possible shapes for $\dfrac{\partial^2 w}{\partial x_2^2}$ for a cross-plied laminate: (a) σ_{zz} crosses the x axis once; and (b) σ_{zz} crosses the x axis twice
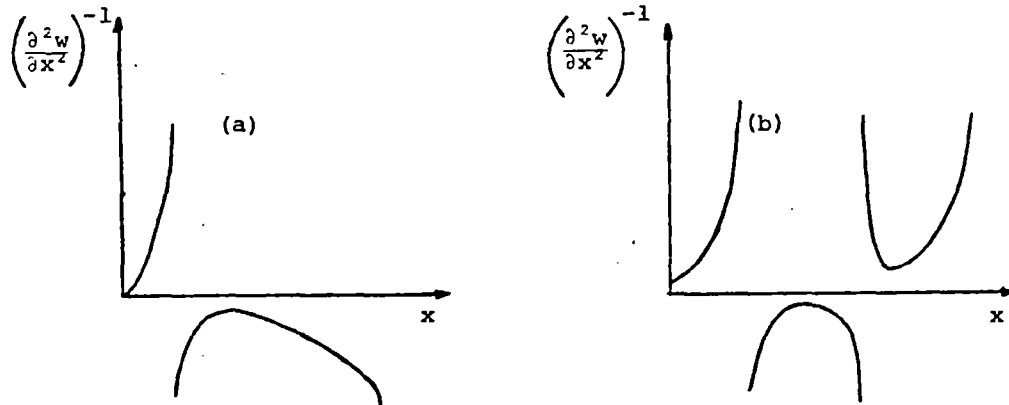
Figure A1.2. Possible shapes of the radius of curvature for a cross-plied laminate: (a) σ_{zz} crosses the x axis once; and (b) σ_{zz} crosses the x axis twice
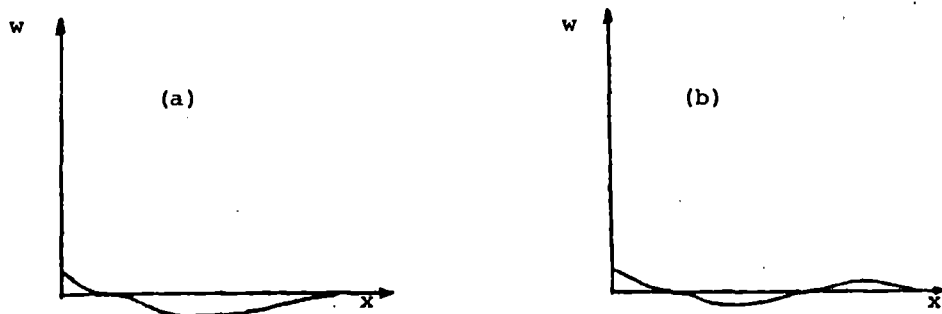
Figure A1.3. Possible out of plane shapes for a ply interface of a cross plied laminate (a) σ_{zz} crosses the x axis once; and (b) σ_{zz} crosses the x axis twice

It should be noted that the above argument is more of an indication than an actual proof. It is valid only for cross-plied laminates and in the case σ_{22} is not a function of z, as is the case in the present analysis. It also assumes that the boundary layer is the same for both modes. Furthermore, it does not account for the differences between the two cases in the stretching part of the energy, treating those differences as small compared to the differences in the bending part of the energy.

APPENDIX 2

CHOICE OF THE EXPONENT IN THE X DEPENDENCE

OF THE IN-PLANE SHEAR STRESS σ_{12}

The reasoning for chosing the exponent ϕ in the expression for $f_{12}(x)$ (equation 5.15b) to be the same as one of the exponents in the expression for $f_{22}(x)$ (equation 5.15a) is explained in this Appendix.

If the assumption that stresses do not depend on x_1 is relaxed, (section 3.3) the equilibrium equations 5.1-5.3 are no longer valid. Instead, the more general form of the equilibrium equations must be used. (Equations 3.1a-c). In that case however, the σ_{12} and σ_{1z} stresses do not decouple from the remaining stresses as was the case in the analysis in chapters 3-5.

Suppose that an effort is made to determine functional forms for the stresses in such a way that equations 3.1a-c are satisfied instead of the special case of equations 5.1-5.3. Also suppose that these stress shapes are in terms of exponential functions in x_2 (or x), and that the assumption that the x_1, x_2 and z dependencies are separable is valid. Consider now the equilibrium equations 3.1a and 3.1c:

$$\frac{\partial \sigma_{11}}{\partial x_1} + \frac{\partial \sigma_{12}}{\partial x_2} + \frac{\partial \sigma_{1z}}{\partial z} = 0 \tag{3.1a}$$

$$\frac{\partial \sigma_{1z}}{\partial x_1} + \frac{\partial \sigma_{2z}}{\partial x_2} + \frac{\partial \sigma_{zz}}{\partial z} = 0 \tag{3.1c}$$

These two equations are coupled because the interlaminar shear stress σ_{1z} appears in both. If the σ_{2z} and σ_{zz} stresses in equation 3.1c have x dependencies that match (i.e. there are no exponents in one term only), then σ_{1z} cannot have an x dependence with an exponent that is different from the exponents in the x dependencies of σ_{2z} and σ_{zz} (i.e. $f_{13}(x)$ must have the same exponents as $f_{23}(x)$ or $f_{33}(x)$) because equation 3.1c could not be satisfied. If this property is to be preserved in the special case where the equilibrium equations 5.1-5.3 are used, σ_{12} must have an x dependence that matches that of σ_{1z} so that equation 5.1 is satisfied. Then, since σ_{1z} must have an x dependence that matches that of σ_{2z} or σ_{zz}, σ_{12} must do the same. Therefore, $f_{12}(x)$ (equation 5.15b) must have either ϕ or $\lambda\phi$ as an exponent. There is no difference in which of the two is chosen. In the analysis in chapter 5 ϕ was used.

APPENDIX 3

MOMENT EQUILIBRIUM EQUATIONS AS A CONSEQUENCE
OF THE BOUNDARY CONDITIONS AND ASSUMPTIONS USED

It will be shown in this appendix, that the moment equilibrium equations (4.11a-4.13a) are a consequence of the assumption that the x and z dependence in each stress shape are separable, and the boundary condition that the side of the laminate is stress-free (boundary condition b in section 3.2).

Consider each of the terms in equation 4.11a (moment about the x_1 axis in Figure 2.1) separately. The first term involves the integral of σ_{2z} with respect to x evaluated on the z^+ face (top face of the laminate section under consideration). This integral can be simplified if σ_{2z} is written in terms of its individual x and z functions, as in equation 5.10 and if the x integration is performed with the use of the equilibrium equation 5.13b. Then,

$$\int_{z^+} \sigma_{2z} dx = g_{23}(\tilde{t}) \int_0^b f_{23} dx = g_{23}(\tilde{t}) [f_{22}(b) - f_{22}(0)] \qquad (A3.1)$$

where b is the width of the laminate section in consideration as shown in Figure 4.1. The fact that σ_{22} is zero at the free edge (stress-free boundary condition) implies that its x function, $f_{22}(x)$, is zero at the free edge. Then, equation A3.1 can be rewritten as:

$$\int_{z^+} \sigma_{2z} dx = g_{23}(\tilde{t}) f_{22}(b) \qquad (A3.2)$$

The integrals in equation 4.11a that involve σ_{zz} can be evaluated in a similar manner. Equation 5.9 is used to express σ_{zz} in terms of its x and z functions, and f_{33} is integrated by parts to give:

$$\int_{z^+} \sigma_{zz} x \, dx = g_{33}(\tilde{t}) \int_0^b f_{33}(x) x \, dx = g_{33}(\tilde{t}) \left[x \int f_{33} dx \Big|_0^b \right.$$

$$\left. - \int_0^b (\int f_{33} dx) dx \right] \tag{A3.3}$$

The integrals on f_{33} can be evaluated as functions of f_{23} if the differential equilibrium equation 5.13c is used. Then:

$$\int_{z^+} \sigma_{zz} x \, dx = g_{33}(\tilde{t}) \left[b f_{23}(b) - \int_0^b f_{23} dx \right] \tag{A3.4}$$

and using the differential equilibrium equation 5.13b to evaluate the integral on f_{23}:

$$\int_{z^+} \sigma_{zz} x \, dx = g_{33}(\tilde{t}) \left[b \, f_{23}(b) - f_{22}(b) + f_{22}(o) \right] \tag{A3.5}$$

Again, using the fact that f_{22} is zero when x is zero, one obtains:

$$\int_{z^+} \sigma_{zz} x \, dx = g_{33}(\tilde{t}) \left[b \, f_{23}(b) - f_{22}(b) \right] \tag{A3.6}$$

Since now σ_{2z} is zero outside the boundary layer (recall that b is outside the boundary layer), $f_{23}(b)$ is zero. Then,

$$\int_{z^+} \sigma_{zz} x \, dx = - g_{33}(\tilde{t}) \, f_{22}(b) \tag{A3.7}$$

In an exactly analogous way one finds

$$\int_{z^-} \sigma_{zz} x \, dx = - g_{33}(o) \, f_{22}(b) \tag{A3.8}$$

Consider now the last integral in equation 4.11a, the one involving σ_{22} . Expressing σ_{22} in terms of its x and z functions as in equation 5.8:

$$\int_{2^-} \sigma_{22} z\,dz = f_{22}(b) \int_0^{\tilde{t}} g_{22}(z)\,z\,dz \tag{A3.9}$$

The integral in the right hand side of equation A3.9 can be evaluated using integration by parts and the differential equilibrium equations 5.13e, 5.13f.

$$\int_{2^-} \sigma_{22} z\,dz = f_{22}(b) \left[z\,g_{23}(z) \Big|_0^{\tilde{t}} - \int_0^{\tilde{t}} g_{23}(z)\,dz \right] =$$

$$= f_{22}(b) \left[\tilde{t}\,g_{23}(\tilde{t}) - g_{33}(\tilde{t}) + g_{33}(0) \right] \tag{A3.10}$$

All the terms in equation 4.11a have been evaluated (equations A3.2, A3.8, A3.9, A3.10) and they can be placed in equation 4.11a to give

$$- \tilde{t} \int_{z^+} \sigma_{2z}\,dx - \int_{z^+} \sigma_{zz} x\,dx + \int_{z^-} \sigma_{zz} x\,dx + \int_{2^-} \sigma_{22} z\,dz =$$

$$= - \tilde{t}\,g_{23}(\tilde{t})\,f_{22}(b) + g_{33}(t)\,f_{22}(b) - g_{33}(o)\,f_{22}(b) +$$

$$+ f_{22}(b)\,\tilde{t}\,g_{23}(\tilde{t}) - f_{22}(b)\,g_{33}(\tilde{t}) + f_{22}(b)\,g_{33}(0) \tag{A3.11}$$

But the right hand side is zero (by cancelling like terms).

Thus, the moment equilibrium equation 4.11a is shown to follow from the boundary conditions and the set of assumptions used in the analysis. In a similar manner, the remaining two moment equilibrium equations (4.12a, 4.13a) can be shown to

follow from the boundary conditions and the set of the assumptions used.

APPENDIX 4

VALUES FOR d_i IF σ_{11} IS ASSUMED TO BE

EQUAL TO ITS CLPT VALUE

If σ_{11} is assumed to be constant throughout each ply and equal to its CLPT value $\sigma_{11[\theta i]}^L$, the d_i expressions (equations 5.108) simplify somewhat and are given by the following:

$$d_1 = (\sigma_{22[\theta i]}^L)^2 \frac{tS_{22}}{2} \tag{A4.1}$$

$$d_2 = \frac{t}{120} S_{33} [3(\sigma_{22[\theta i]}^L)^2 t^4 + 15 \sigma_{22[\theta i]}^L \mathring{B}_4 t^3 +$$

$$20 \sigma_{22[\theta i]}^L \mathring{B}_5 t^2 + 20(\mathring{B}_4)^2 t^2 + 60 \mathring{B}_4 \mathring{B}_5 t +$$

$$60 (\mathring{B}_5)^2] \tag{A4.2}$$

$$d_3 = \frac{t}{6} S_{44} [(\sigma_{22[\theta i]}^L)^2 t^2 + 3 \sigma_{22[\theta i]}^L \mathring{B}_4 t + 3(\mathring{B}_4)^2] \tag{A4.3}$$

$$d_4 = \frac{t}{6} S_{55} [(\sigma_{12[\theta i]}^L)^2 t^2 + 3 \sigma_{12[\theta i]}^L \mathring{B}_2 t + 3(\mathring{B}_2)^2] \tag{A4.4}$$

$$d_5 = \frac{3}{2} (\sigma_{12[\theta i]}^L)^2 t S_{66} \tag{A4.5}$$

$$d_6 = \sigma^L_{22_{[\theta i]}} \; \sigma^L_{11_{[\theta i]}} \; t \; S_{12} \tag{A4.6}$$

$$d_7 = \sigma^L_{12_{[\theta i]}} \; \sigma^L_{11_{[\theta i]}} \; t \; S_{16} \tag{A4.7}$$

$$d_8 = \sigma^L_{22_{[\theta i]}} \; \frac{t S_{23}}{12} \; (\sigma^L_{22_{[\theta i]}} \; t^2 + 3 \; \overset{\scriptstyle\frown}{B}_4 \; t + 6 \; \overset{\scriptstyle\frown}{B}_5) \tag{A4.8}$$

$$d_9 = \frac{\sigma^L_{12_{[\theta i]}} \; \sigma^L_{22_{[\theta i]}} \; t \; S_{26}}{2} \tag{A4.9}$$

$$d_{10} = \sigma^L_{12_{[\theta i]}} \; \frac{t S_{36}}{12} \; (\sigma^L_{22_{[\theta i]}} \; t^2 + 3 \; \overset{\scriptstyle\frown}{B}_4 \; t + 6 \; \overset{\scriptstyle\frown}{B}_5) \tag{A4.10}$$

$$d_{11} = \frac{S_{45}t}{12} \; [2 \; \sigma^L_{12_{[\theta i]}} \; \sigma^L_{22_{[\theta i]}} \; t^2 + 3 \; \sigma^L_{22_{[\theta i]}} \; \overset{\scriptstyle\frown}{B}_2 \; t +$$

$$+ 3 \; \sigma^L_{12_{[\theta i]}} \; \overset{\scriptstyle\frown}{B}_4 \; t + 6 \; \overset{\scriptstyle\frown}{B}_2 \; \overset{\scriptstyle\frown}{B}_5] \tag{A4.11}$$

APPENDIX 5

COMPUTER PROGRAM CODE

The code of the computer program used to implement
the method on a PDP-11/34 computer is listed below.


```
        COMMON/BL1/ST11(50),ST22(50),ST12(50),ANGLE(50),THETA(50),FHI,
       +ALAM,NN,S(50,6,6),XCOF(5),F(11),ROOTR(4),ROOTI(4),COF(5),
       +U(4),FLAM(4),T(50),FT1,FT2,FT3,ALPOLY,PHIPOL,FDISC,PHIS1,PHIS2,
       +FHI1,FHI2,S11(50),S22(50),S33(50),S12(50),S13(50),S23(50),
       +SUM1(50),SUM2(50),SUM3(50),S44(50),S55(50),S66(50),
       +FHIS,FK(50),RROOT(4),PHIP,ALAMP
        COMMON/BL2/M,LT,ITER,IR,ISUBR,ISUBR2
        COMMON/BL3/INDEX
C       DOUBLE PRECISION ST11,ST22,ST12,ANGLE,THETA,PHI,ALAM,S,XCOF,
C      +F,ROOTR,ROOTI,COF,U,FLAM,T,FT1,FT2,FT3,ALPOLY,PHIPOL,FDISC,
C      +PHIS1,PHIS2,PHI1,PHI2,FE11,FE22,FE33,FG12,FG13,FG23,FNU12,
C      +FNU23,FNU13,SUM1,SUM2,SUM3,S44(50),S55(50),S66(50),
C      +INDEX
        DATA F/11*0.0/
        ITER=0
        INDEX=0
        IMULT=1
        ALAM=0.
        ISUBR=0
        ISUBR2=0
        WRITE (5,*) 'INPUT TOTAL NUMBER OF PLIES'
        READ (5,*) NNT2
        NN=NNT2/2
        WRITE(5,*) 'DO ALL PLIES HAVE THE SAME THICKNESS?(YES=1,NO=0)'
        READ(5,*) KK1
        IF(KK1.EQ.1) GOTO 401
        CALL DIFFTH(T,FLTHIK,NN)
        GOTO 402
401     WRITE(5,*) 'INPUT PLY THICKNESS'
        READ(5,*) THICK
        DO 403 I=1,NN
403     T(I)=THICK
        FLTHIK=NNT2*THICK
402     WRITE(5,*) 'INPUT SIGMA11 STRESS VALUES FOR 1ST HALF OF
       +THE LAMINATE'
        READ(5,*) (ST11(J),J=1,NN)
        WRITE(5,*) 'INPUT SIGMA22 STRESS VALUES FOR 1ST HALF OF
       +THE LAMINATE'
        READ(5,*) (ST22(J1),J1=1,NN)
        WRITE(5,*) 'INPUT SIGMA12 STRESS VALUES FOR 1ST HALF OF
```

```
      +THE LAMINATE'
       READ(5,*) (ST12(J2),J2=1,NN)
       WRITE (5,*) 'INPUT ANGLE VALUES FOR 1ST HALF OF THE
      +LAMINATE'
       READ(5,*) (ANGLE(J3),J3=1,NN)
       DO 540 I11=1,NN
 540   THETA(I11)=ANGLE(I11)*3.141592654/180
       WRITE(5,*) 'SIGMA11 STRESSES ARE (FROM TOP TO MIDPLANE)'
       WRITE(5,*) (ST11(J4),J4=1,NN)
       WRITE(5,*) 'THE SIGMA22 STRESSES ARE'
       WRITE(5,*) (ST22(L1),L1=1,NN)
       WRITE(5,*) 'THE SIGMA12 STRESSES ARE'
       WRITE(5,*) (ST12(L2),L2=1,NN)
       WRITE(5,*) 'ANGLE VALUES IN RADIANS'
       WRITE(5,*) (THETA(L3),L3=1,NN)
       WRITE(5,*) 'IS YOUR LAMINATE:OTHER(1),ANGLE-PLY(2),
      +OR CROSS-PLY(3)?'
       READ(5,*)LT
       IF(LT.EQ.1)GOTO 1000
       IF(LT.EQ.2)GOTO 1250
       CALL LAMIN
       FRATIO=F(1)/F(2)
       IF (FRATIO.GT.0.) GOTO 413
       WRITE(5,*) 'RATIO OF F1 TO F2 IS NEGATIVE.METHOD 1 FAILS.
      +PROCEED WITH METHOD 2.'
       GOTO 414
 413   F2=(SQRT(FRATIO)*(F(3)-2*F(8))+2*F(1))/(2*F(6)+3*F(1))
       IF((F2.GT.0.).OR.(F2.LT.-4.))GOTO 415
       WRITE(5,*) 'EQUATION FOR LAMBDA HAS COMPLEX ROOTS. PROCEED
      +WITH METHOD 2.'
       GOTO 414
 415   WRITE(5,*) 'METHOD 1 IS USED'
       BETA=F2+2
       IF(BETA.LT.0.)GOTO 416
       WRITE(5,*) 'LAMBDA IS NEGATIVE. PROCEED WITH METHOD 2.'
       GOTO 414
 416   FDISC=BETA*BETA-4
       ALAM=(-BETA-SQRT(FDISC))/2
       PHI=SQRT(SQRT(FRATIO)/ALAM)
       PHIS=PHI*PHI
       WRITE(5,*) 'PHI IS',PHI
       WRITE(5,*) 'LAMBDA IS',ALAM
       LT=1
       GOTO 1211
 414   GAMA=F(3)-2*F(8)
       FDISC=GAMA*GAMA-12*F(2)*(11*F(1)+8*F(6))
       IF(FDISC.GT.0.)GOTO 541
       WRITE(5,*) 'DISCRIMINANT OF PHI POLYNOMIAL IS NEGATIVE
      +QUIT.'
       GOTO 1010
 541   DELTA=6*F(2)
       ALFA=-GAMA/DELTA
       BETA=SQRT(FDISC)/DELTA
       PHIS1=ALFA+BETA
       PHIS2=ALFA-BETA
       IF(PHIS1.LT.0.)GOTO 542
       PHI=SQRT(PHIS1)
       GOTO 543
 542   PHI=SQRT(PHIS2)
 543   WRITE(5,*) 'PHI EQUALS',PHI
```

```
  -        PHIS=PHI*PHI
           GOTO 1211
 1250      CALL LAMIN
           PHIS=-(F(5)+2*F(7))/F(4)
           IF(PHIS.GT.0.)GOTO 1190
           WRITE(5,*) 'PHI SQUARED IS NEGATIVE. QUIT.'
           GOTO 1010
 1190      PHI=SQRT(PHIS)
           WRITE(5,*) 'THE PHI VALUE IS ',PHI
           GOTO 1211
 1000      CALL LAMIN
           PHI=4.4/FLTHIK
 1001      PHIS=PHI*PHI
           PHIP=PHI
           ALAMP=ALAM
           ITER=ITER+1
           CALL FOCOEL
           CALL ROOT(XCOF,COF,M,ROOTR,ROOTI,IER)
           IF(INDEX.EQ.1)GOTO 1010
           IF(IR.NE.0)GOTO 1018
           WRITE(5,*) 'NO POSITIVE LAMBDA VALUES.QUIT.'
           GOTO 1010
 1018      WRITE(5,*) 'IN MAIN AFTER ROOT IR IS',IR
           IF(IR.EQ.1)GOTO 1020
           CALL ENERGY
           ALAM=RROOT(IR)
           GOTO 1022
 1020      ALAM=RROOT(1)
 1022      WRITE(5,*) 'LAMBDA EQUALS:',ALAM
 1200      CALL FOCOFH
           CALL PHISOL
           IF(INDEX.EQ.1)GOTO 1010
           IF(PHI.LT.PHIP)GOTO 1024
           FRATIO=PHIP/PHI
           GOTO 1026
 1024      FRATIO=PHI/PHIP
 1026      IF(FRATIO.LT..999999)GOTO 1021
           WRITE(5,*) 'CONVERGENCE AT ITERATION #',ITER
           WRITE(5,*) 'PHI IS',PHI,'AND LAMBDA IS',ALAM
           WRITE(5,*) 'PREVIOUS PHI WAS',PHIP,'PREVIOUS LAMBDA
          +WAS',ALAMP
           ISUBR2=0
           CALL CHECK
           GOTO 1211
 1021      IF(ITER.NE.150*IMULT)GOTO 1001
           WRITE(5,*) 'NO CONVERGENCE AFTER',ITER,'ITERATIONS'
           WRITE(5,*) 'VALUES OF PHI, LAMBDA FOR THE LAST
          +TWO ITERATIONS:'
           WRITE(5,*) PHIP,ALAMP
           WRITE(5,*) PHI,ALAM
           ISUBR2=0
           CALL CHECK
           ISUBR2=1
           WRITE(5,*) 'MORE ITERATIONS?(YES=1,NO=0)'
           READ(5,*)KK1
           IF(KK1.EQ.0)GOTO 1029
           WRITE(5,*) 'INPUT PHI VALUE TO CONTINUE ITERATIONS'
           READ(5,*) PHI
           IMULT=IMULT+1
           GOTO 1001
```

```
1029 -CALL PLPREP
      GOTO 1010
1211  CALL PLPREP
1010  STOP
      END
      SUBROUTINE LAMIN
      COMMON/BL1/ST11(50),ST22(50),ST12(50),ANGLE(50),THETA(50),PHI,
     +ALAM,NN,S(50,6,6),XCOF(5),F(11),ROOTR(4),ROOTI(4),COF(5),
     +U(4),FLAM(4),T(50),FT1,FT2,FT3,ALPOLY,PHIPOL,FDISC,PHIS1,PHIS2,
     +PHI1,PHI2,S11(50),S22(50),S33(50),S12(50),S13(50),S23(50),
     +SUM1(50),SUM2(50),SUM3(50),S44(50),S55(50),S66(50),
     +PHIS,FK(50),RROOT(4),PHIP,ALAMP
      COMMON/BL2/M,LT,ITER,IR,ISUBR,ISUBR2
C     DOUBLE PRECISION ST11,ST22,ST12,ANGLE,THETA,PHI,ALAM,S,XCOF,
C    +F,ROOTR,ROOTI,COF,U,FLAM,T,FT1,FT2,FT3,ALPOLY,PHIPOL,FDISC,
C    +PHIS1,PHIS2,PHI1,PHI2,FE11,FE22,FE33,FG12,FG13,FG23,FNU12,
C    +FNU23,FNU13,SUM1,SUM2,SUM3,S44(50),S55(50),S66(50),
C    +S44,S55,S66
      DO 500 I1=1,11
500   F(I1)=0.
      WRITE(5,*) 'ARE ALL PLIES MADE OF THE SAME MATERIAL?
     +(YES=1,NO=0)'
      READ(5,*) KK1
      IF(KK1.EQ.1) GOTO 404
      DO 405 IC=1,NN
      WRITE(5,*) 'FOR PLY NUMBER',IC,'INPUT E11,E22,E33,G12,G13,G23'
      READ(5,*) FE11,FE22,FE33,FG12,FG13,FG23
      WRITE(5,*) 'FOR PLY NUMBER',IC,'INPUT NU12,NU13,NU23'
      READ(5,*) FNU12,FNU13,FNU23
      S11(IC)=1/FE11
      S22(IC)=1/FE22
      S33(IC)=1/FE33
      S12(IC)=-FNU12/FE11
      S13(IC)=-FNU13/FE11
      S23(IC)=-FNU23/FE22
      S44(IC)=1/FG23
      S55(IC)=1/FG13
405   S66(IC)=1/FG12
      GOTO 406
404   WRITE(5,*) 'INPUT E11,E22,E33,G12,G13,G23'
      READ(5,*) FE11,FE22,FE33,FG12,FG13,FG23
      WRITE(5,*) 'INPUT NU12,NU13,NU23'
      READ(5,*) FNU12,FNU13,FNU23
      DO 407 ID=1,NN
      S11(ID)=1/FE11
      S22(ID)=1/FE22
      S33(ID)=1/FE33
      S12(ID)=-FNU12/FE11
      S13(ID)=-FNU13/FE11
      S23(ID)=-FNU23/FE22
      S44(ID)=1/FG23
      S55(ID)=1/FG13
407   S66(ID)=1/FG12
406   DO 510 I2=1,NN
      CALL COMPLI(I2)
      CALL SUM(I2)
      F(1)=F(1)+ST22(I2)**2*T(I2)*(S(I2,2,2)-S(I2,1,2)**2/
     +S(I2,1,1))/2
      F(2)=F(2)+T(I2)/120*(3*ST22(I2)**2*T(I2)**4+15*ST22(I2)*
     +SUM1(I2)*T(I2)**3+20*ST22(I2)*SUM2(I2)*T(I2)**2+20*
```

```
      +SUM1(I2)**2*T(I2)**2+60*SUM1(I2)*SUM2(I2)*T(I2)+60*
      +SUM2(I2)**2)*(S(I2,3,3)-S(I2,1,3)**2/S(I2,1,1))
       F(3)=F(3)+T(I2)/6*(ST22(I2)**2*T(I2)**2+3*ST22(I2)*
      +SUM1(I2)*T(I2)+3*SUM1(I2)**2)*S(I2,4,4)
       F(4)=F(4)+T(I2)/6*(ST12(I2)**2*T(I2)**2+3*ST12(I2)*
      +SUM3(I2)*T(I2)+3*SUM3(I2)**2)*S(I2,5,5)
       F(5)=F(5)+3*(ST12(I2)**2*T(I2))*(S(I2,6,6)-
      +S(I2,1,6)**2/S(I2,1,1))/2
       FK(I2)=(S(I2,1,1)*ST11(I2)+S(I2,1,2)*ST22(I2)+S(I2,1,6)*
      +ST12(I2))/S(I2,1,1)
       F(6)=F(6)+FK(I2)*S(I2,1,2)*ST22(I2)*T(I2)
       F(7)=F(7)+FK(I2)*S(I2,1,6)*ST12(I2)*T(I2)
       F(8)=F(8)+ST22(I2)*T(I2)/12*(ST22(I2)*T(I2)**2+3*SUM1(I2)*
      +T(I2)+6*SUM2(I2))*(S(I2,2,3)-S(I2,1,2)*S(I2,1,3)/S(I2,1,1))
       F(9)=F(9)+ST12(I2)*ST22(I2)*T(I2)*(S(I2,2,6)-
      +S(I2,1,2)*S(I2,1,6)/S(I2,1,1))/2
       F(10)=F(10)+ST12(I2)*T(I2)/12*(ST22(I2)*T(I2)**2+3*SUM1(I2)
      +*T(I2)+6*SUM2(I2))*(S(I2,3,6)-S(I2,1,3)*S(I2,1,6)/S(I2,1,1))
  510  F(11)=F(11)+T(I2)/12*(2*ST12(I2)*ST22(I2)*T(I2)**2+
      +3*ST22(I2)*SUM3(I2)*T(I2)+3*ST12(I2)*SUM1(I2)*T(I2)+
      +6*SUM1(I2)*SUM3(I2))*S(I2,4,5)
       WRITE (5,*) 'F VALUES'
       WRITE (5,*) (F(IS),IS=1,11)
       RETURN
       END
       SUBROUTINE POCOEL
       COMMON/BL1/ST11(50),ST22(50),ST12(50),ANGLE(50),THETA(50),PHI,
      +ALAM,NN,S(50,6,6),XCOF(5),F(11),ROOTR(4),ROOTI(4),COF(5),
      +U(4),FLAM(4),T(50),FT1,FT2,FT3,ALPOLY,PHIPOL,FDISC,PHIS1,PHIS2,
      +PHI1,PHI2,S11(50),S22(50),S33(50),S12(50),S13(50),S23(50),
      +SUM1(50),SUM2(50),SUM3(50),S44(50),S55(50),S66(50),
      +PHIS,FK(50),RROOT(4),PHIP,ALAMP
       COMMON/BL2/M,LT,ITER,IR,ISUBR,ISUBR2
       XCOF(5)=F(2)*PHIS**2
       XCOF(4)=2*XCOF(5)
       XCOF(3)=2*(F(6)+F(9)+F(1))+PHIS*(2*F(11)+F(3)-2*F(10)-
      +2*F(8))
       XCOF(2)=4*F(6)+8*F(9)+6*F(1)
       XCOF(1)=XCOF(2)/2
       M=4
 1240  RETURN
       END
       SUBROUTINE ROOT(XCOF,COF,M,ROOTR,ROOTI,IER)
       COMMON/BL1/ST11(50),ST22(50),ST12(50),ANGLE(50),THETA(50),PHI,
      +ALAM,NN,S(50,6,6),CC1(5),F(11),CC3(4),CC4(4),CC5(5),
      +U(4),FLAM(4),T(50),FT1,FT2,FT3,ALPOLY,PHIPOL,FDISC,PHIS1,PHIS2,
      +PHI1,PHI2,S11(50),S22(50),S33(50),S12(50),S13(50),S23(50),
      +SUM1(50),SUM2(50),SUM3(50),S44(50),S55(50),S66(50),
      +PHIS,FK(50),RROOT(4),PHIP,ALAMP
       COMMON/BL2/LC2,LT,ITER,IR,ISUBR,ISUBR2
       COMMON/BL3/INDEX
       DIMENSION XCOF(5),COF(5),ROOTR(4),ROOTI(4)
C      DOUBLE PRECISION ST11,ST22,ST12,ANGLE,THETA,PHI,ALAM,S,XCOF,
C     +F,ROOTR,ROOTI,COF,U,FLAM,T,FT1,FT2,FT3,ALPOLY,PHIPOL,FDISC,
C     +PHIS1,PHIS2,PHI1,PHI2,FE11,FE22,FE33,FG12,FG13,FG23,FNU12,
C     +FNU23,FNU13,SUM1,SUM2,SUM3,S44(50),S55(50),S66(50),
C     +S44,S55,S66
C      DOUBLE PRECISION XO,YO,X,Y,XPR,YPR,UX,UY,V,YT,XT,UU,XT2,YT2,
C     +SUMSQ,DX,DY,TEMP,ALPHA,ABS
       IFIT=0
```

```
        IR=0
        N=M
        IER=0
        IF(XCOF(N+1))10,25,10
10      IF(N) 15,15,32
15      IER=1
20      IF(IER.EQ.0)GOTO 16
        WRITE(5,*) 'IER IS',IER,'STOP'
        INDEX=1
        GOTO 18
16      DO 18 I4=1,4
        IF(ROOTI(I4).NE.0)GOTO 18
        IR=IR+1
        IF(ROOTR(I4).LT.0)GOTO 19
        RROOT(IR)=ROOTR(I4)
        GOTO 18
19      IR=IR-1
18      CONTINUE
        RETURN
25      IER=4
        GO TO 20
30      IER=2
        GO TO 20
32      IF(N-36) 35,35,30
35      NX=N
        NXX=N+1
        N2=1
        KJ1=N+1
        DO 40 L=1,KJ1
        MMT=KJ1-L+1
40      COF(MMT)=XCOF(L)
45      XO=.00500101
        YO=.01000101
        IN=0
50      X=XO
        XO=-10.0*YO
        YO=-10.0*X
        X=XO
        Y=YO
        IN=IN+1
        GO TO 59
55      IFIT=1
        XPR=X
        YPR=Y
59      ICT=0
60      UX=0.0
        UY=0.0
        V=0.0
        YT=0.0
        XT=1.0
        UU=COF(N+1)
        IF(UU) 65,130,65
65      DO 70 I=1,N
        L=N-I+1
        TEMP=COF(L)
        XT2=X*XT-Y*YT
        YT2=X*YT+Y*XT
        UU=UU+TEMP*XT2
        V=V+TEMP*YT2
        FI=I
```

```
         UX=UX+FI*XT*TEMP
         UY=UY-FI*YT*TEMP
         XT=XT2
70       YT=YT2
         SUMSQ=UX*UX+UY*UY
         IF(SUMSQ) 75,110,75
75       DX=(V*UY-UU*UX)/SUMSQ
         X=X+DX
         DY=-(UU*UY+V*UX)/SUMSQ
         Y=Y+DY
78       IF(ABS(DY)+ABS(DX)-1.0D-05)100,80,80
80       ICT=ICT+1
         IF(ICT-500) 60,85,85
85       IF(IFIT)100,90,100
90       IF(IN-5) 50,95,95
95       IER=3
         GOTO 20
100      DO 105 L=1,NXX
         MMT=KJ1-L+1
         TEMP=XCOF(MMT)
         XCOF(MMT)=COF(L)
105      COF(L)=TEMP
         ITEMP=N
         N=NX
         NX=ITEMP
         IF(IFIT) 120,55,120
110      IF(IFIT) 115,50,115
115      X=XPR
         Y=YPR
120      IFIT=0
122      IF(ABS(Y)-1.0D-4*ABS(X))135,125,125
125      ALPHA=X+X
         SUMSQ=X*X+Y*Y
         N=N-2
         GO TO 140
130      X=0.0
         NX=NX-1
         NXX=NXX-1
135      Y=0.0
         SUMSQ=0.0
         ALPHA=X
         N=N-1
140      COF(2)=COF(2)+ALPHA*COF(1)
145      DO 150 L=2,N
150      COF(L+1)=COF(L+1)+ALPHA*COF(L)-SUMSQ*COF(L-1)
155      ROOTI(N2)=Y
         ROOTR(N2)=X
         N2=N2+1
         IF(SUMSQ) 160,165,160
160      Y=-Y
         SUMSQ=0.0
         GO TO 155
165      IF(N) 20,20,45
         END
         SUBROUTINE ENERGY
         COMMON/BL1/ST11(50),ST22(50),ST12(50),ANGLE(50),THETA(50),PHI,
        +ALAM,NN,S(50,6,6),XCOF(5),F(11),ROOTR(4),ROOTI(4),COF(5),
        +U(4),FLAM(4),T(50),FT1,FT2,FT3,ALPOLY,PHIPOL,FDISC,PHIS1,PHIS2,
        +PHI1,PHI2,S11(50),S22(50),S33(50),S12(50),S13(50),S23(50),
        +SUM1(50),SUM2(50),SUM3(50),S44(50),S55(50),S66(50),
```

```
        -  +PHIS,FK(50),RROOT(4),PHIP,ALAMP
              COMMON/BL2/M,LT,ITER,IR,ISUBR,ISUBR2
        C       DOUBLE PRECISION ST11,ST22,ST12,ANGLE,THETA,PHI,ALAM,S,XCOF,
        C    +F,ROOTR,ROOTI,COF,U,FLAM,T,FT1,FT2,FT3,ALPOLY,PHIPOL,PHIS1,
        C    +PHIS2,PHI1,PHI2,FE11,FE22,FE33,FG12,FG13,FG23,FNU12,FNU13,
        C    +FNU23,SUM1,SUM2,SUM3,FDISC,S44(50),S55(50),S66(50),
        C    +S44,S55,S66
        C       DOUBLE PRECISION SS12,SS16,SS33,SS44,SS55,SS22,SS66,SS45,
        C    +SS36,SS23,SS26
        C       ISUBR=1==>ONE LAMBDA, TWO PHI
              DIMENSION PHIA(4)
              IF(ISUBR.EQ.1)GOTO 517
              KK4=IR
              DO 519 I10=1,KK4
        519   U(I10)=0.
              DO 518 II=1,IR
              PHIA(II)=PHI
        518   FLAM(II)=RROOT(II)
              GOTO 513
        517   KK4=2
              DO 512 I10=1,2
        512   U(I10)=0.
              DO 511 II=1,2
        511   FLAM(II)=ALAM
              PHIA(1)=PHI1
              PHIA(2)=PHI2
        513   DO 520 I5=1,KK4
              FL=FLAM(I5)
              FL2=FL*FL
              FL3=FL2*FL
              FL4=FL3*FL
              FLT=FL+1
              PH=PHIA(I5)
              PH2=PH*PH
              PH3=PH2*PH
        520   U(I5)=-F(6)*(FL+1)/(FL*PH)-F(7)/PH+.5*(F(2)*FL2*
             +PH3/(FL+1)+F(3)*FL*PH/(FL+1)+F(4)*PH+F(1)*(-3*
             +FL4+FL3+4*FL2+FL-3)/((FL-1)**2*FL*(FL+1)*PH)-F(5)/
             +PH)+F(11)*FL*PH/(FL+1)-F(10)*FL*PH/(FL+1)-F(8)*
             +FL*PH/(FL+1)+F(9)*(-3*FL3-FL2+2*FL+2)/(FL*(FL2-1)*PH)
              UF=U(1)
              J=1
              IF(ISUBR.EQ.1)GOTO 509
              DO 516 I=2,IR
              IF(UF.GE.U(I)) GOTO 514
              GOTO 516
        514   UF=U(I)
              J=I
        516   CONTINUE
              IR=J
              GOTO 507
        509   IF(U(1).LT.U(2))GOTO 508
              PHI=PHI2
              GOTO 507
        508   PHI=PHI1
        507   RETURN
              END
              SUBROUTINE FOCOFH
              COMMON/BL1/ST11(50),ST22(50),ST12(50),ANGLE(50),THETA(50),PHI,
             +ALAM,NN,S(50,6,6),XCOF(5),F(11),ROOTR(4),ROOTI(4),COF(5),
```

```
      +U(4),FLAM(4),T(50),FT1,FT2,FT3,ALFOLY,PHIPOL,FDISC,PHIS1,PHIS2,
      +PHI1,PHI2,S11(50),S22(50),S33(50),S12(50),S13(50),S23(50),
      +SUM1(50),SUM2(50),SUM3(50),S44(50),S55(50),S66(50),
      +PHIS,FK(50),RROOT(4),PHIP,ALAMP
      COMMON/BL2/M,LT,ITER,IR,ISUBR,ISUBR2
C     DOUBLE PRECISION ST11,ST22,ST12,ANGLE,THETA,PHI,ALAM,S,XCOF,
C     +F,ROOTR,ROOTI,COF,U,FLAM,T,FT1,FT2,FT3,ALFOLY,PHIPOL,FDISC,
C     +PHIS1,PHIS2,PHI1,PHI2,FE11,FE22,FE33,FG12,FG13,FG23,FNU12,
C     +FNU23,FNU13,SUM1,SUM2,SUM3,S44(50),S55(50),S66(50),
C     +S44,S55,S66
      FT1=3*F(2)*ALAM**3
      FT2=ALAM**2*(F(4)+2*F(11)+F(3)-2*F(10)-2*F(8))+F(4)*ALAM
      FT3=ALAM**2*(F(5)+6*F(9)+3*F(1)+2*(F(7)+F(6)))+
      +ALAM*(F(5)+8*F(9)+5*F(1)+2*(F(7)+2*F(6)))+4*F(9)+3*F(1)+
      +2*F(6)
      RETURN
      END
      SUBROUTINE CHECK
      COMMON/BL1/ST11(50),ST22(50),ST12(50),ANGLE(50),THETA(50),PHI,
      +ALAM,NN,S(50,6,6),XCOF(5),F(11),ROOTR(4),ROOTI(4),COF(5),
      +U(4),FLAM(4),T(50),FT1,FT2,FT3,ALFOLY,PHIPOL,FDISC,PHIS1,PHIS2,
      +PHI1,PHI2,S11(50),S22(50),S33(50),S12(50),S13(50),S23(50),
      +SUM1(50),SUM2(50),SUM3(50),S44(50),S55(50),S66(50),
      +PHIS,FK(50),RROOT(4),PHIP,ALAMP
      COMMON/BL2/M,LT,ITER,IR,ISUBR,ISUBR2
C     DOUBLE PRECISION ST11,ST22,ST12,ANGLE,THETA,PHI,ALAM,S,XCOF,
C     +F,ROOTR,ROOTI,COF,U,FLAM,T,FT1,FT2,FT3,ALFOLY,PHIPOL,FDISC,
C     +PHIS1,PHIS2,PHI1,PHI2,FE11,FE22,FE33,FG12,FG13,FG23,FNU12,
C     +FNU23,FNU13,SUM1,SUM2,SUM3,S44(50),S55(50),S66(50),
C     +S44,S55,S66
      ALFOLY=XCOF(5)*ALAM**4+XCOF(4)*ALAM**3+XCOF(3)*ALAM**2+
      +XCOF(2)*ALAM+XCOF(1)
      PHIPOL=FT1*PHI**4+FT2*PHI**2+FT3
C     ISUBR2=1==>DO NOT PRINT VALUES OF POLYNOMIALS
C     IF(ISUBR2.EQ.1)GOTO 1139
      WRITE(5,*) 'THE VALUES OF LAMBDA AND PHI POLYNOMIALS ARE'
      WRITE(5,*)ALFOLY,PHIPOL
1139  RETURN
      END
      SUBROUTINE PHISOL
      COMMON/BL1/ST11(50),ST22(50),ST12(50),ANGLE(50),THETA(50),PHI,
      +ALAM,NN,S(50,6,6),XCOF(5),F(11),ROOTR(4),ROOTI(4),COF(5),
      +U(4),FLAM(4),T(50),FT1,FT2,FT3,ALFOLY,PHIPOL,FDISC,PHIS1,PHIS2,
      +PHI1,PHI2,S11(50),S22(50),S33(50),S12(50),S13(50),S23(50),
      +SUM1(50),SUM2(50),SUM3(50),S44(50),S55(50),S66(50),
      +PHIS,FK(50),RROOT(4),PHIP,ALAMP
      COMMON/BL2/M,LT,ITER,IR,ISUBR,ISUBR2
      COMMON/BL3/INDEX
C     DOUBLE PRECISION ST11,ST22,ST12,ANGLE,THETA,PHI,ALAM,S,XCOF,
C     +F,ROOTR,ROOTI,COF,U,FLAM,T,FT1,FT2,FT3,ALFOLY,PHIPOL,FDISC,
C     +PHIS1,PHIS2,PHI1,PHI2,FE11,FE22,FE33,FG12,FG13,FG23,FNU12,
C     +FNU23,FNU13,SUM1,SUM2,SUM3,S44(50),S55(50),S66(50),
C     +INDEX
      FDISC=FT2**2-4*FT1*FT3
      IF(FDISC.GT.0)GOTO 1140
      WRITE(5,*) 'AT ITERATION NO',ITER,'THE DISCRIMINANT
      +OF THE PHI POLYNOMIAL IS NEGATIVE.STOP.'
C  IF INDEX=1 QUIT
      INDEX=1
      GOTO 1031
```

```
.1140    PHIS1=(-FT2+SQRT(FDISC))/(2*FT1)
         PHIS2=(-FT2-SQRT(FDISC))/(2*FT1)
         IF((PHIS1*PHIS2).LT.0)GOTO 1141
         IF(PHIS1.LT.0.)GOTO 1144
         PHI1=SQRT(PHIS1)
         PHI2=SQRT(PHIS2)
         ISUBR=1
         GOTO 1031
 1144    WRITE(5,*) 'AT ITERATION NUMBER',ITER,'BOTH PHI
        +VALUES ARE NEGATIVE, QUIT.'
         INDEX=1
         GOTO 1031
 1141    IF(PHIS1.LT.0)GOTO 1142
         PHI=SQRT(PHIS1)
         GOTO 1143
 1142    PHI=SQRT(PHIS2)
 1143    WRITE(5,*) 'THE PHI VALUE IS',PHI
 1031    RETURN
         END
         SUBROUTINE SUM(INN)
         COMMON/BL1/ST11(50),ST22(50),ST12(50),ANGLE(50),THETA(50),PHI,
        +ALAM,NN,S(50,6,6),XCOF(5),F(11),ROOTR(4),ROOTI(4),COF(5),
        +U(4),FLAM(4),T(50),FT1,FT2,FT3,ALPOLY,PHIPOL,FDISC,PHIS1,PHIS2,
        +PHI1,PHI2,S11(50),S22(50),S33(50),S12(50),S13(50),S23(50),
        +SUM1(50),SUM2(50),SUM3(50),S44(50),S55(50),S66(50),
        +PHIS,FK(50),RROOT(4),PHIP,ALAMP
         COMMON/BL2/M,LT,ITER,IR,ISUBR,ISUBR2
C        DOUBLE PRECISION ST11,ST22,ST12,ANGLE,THETA,PHI,ALAM,S,XCOF,
C       +F,ROOTR,ROOTI,COF,U,FLAM,T,FT1,FT2,FT3,ALPOLY,PHIPOL,FDISC,
C       +PHIS1,PHIS2,PHI1,PHI2,FE11,FE22,FE33,FG12,FG13,FG23,FNU12,
C       +FNU23,FNU13,SUM1,SUM2,SUM3,S44(50),S55(50),S66(50),
C       +S44,S55,S66
C        DOUBLE PRECISION SGMA2A,SGMA2B
         SGMA1=0.
         SGMA2A=0.
         SGMA2B=0.
         SGMA3=0.
         IF(INN.EQ.1)GOTO 1050
         DO 550 I8=1,INN-1
         SGMA1=SGMA1+T(I8)*ST22(I8)
         SGMA3=SGMA3+T(I8)*ST12(I8)
         SGMA2A=SGMA2A+T(I8)**2*ST22(I8)/2
 550     CONTINUE
         IF(INN-1.EQ.1)GOTO 1050
         TEMPOR=0.
         DO 560 I9=1,INN-2
         DO 561 J=I9+1,INN-1
 561     TEMPOR=TEMPOR+T(J)
         SGMA2B=SGMA2B+ST22(I9)*T(I9)*TEMPOR
 560     TEMPOR=0.
 1050    SUM1(INN)=SGMA1
         SUM2(INN)=SGMA2A+SGMA2B
         SUM3(INN)=SGMA3
         WRITE(5,*) 'THE SUM VALUES: SUM1,SUM2,SUM3'
         WRITE(5,*)SUM1(INN),SUM2(INN),SUM3(INN)
         RETURN
         END
         SUBROUTINE COMPLI(IND)
         COMMON/BL1/ST11(50),ST22(50),ST12(50),ANGLE(50),THETA(50),PHI,
        +ALAM,NN,S(50,6,6),XCOF(5),F(11),ROOTR(4),ROOTI(4),COF(5),
```

```
      +U(4),FLAM(4),T(50),FT1,FT2,FT3,ALPOLY,PHIPOL,FDISC,PHIS1,PHIS2,
      +PHI1,PHI2,S11(50),S22(50),S33(50),S12(50),S13(50),S23(50),
      +SUM1(50),SUM2(50),SUM3(50),S44(50),S55(50),S66(50),
      +PHIS,FK(50),RROOT(4),PHIF,ALAMP
      COMMON/BL2/M,LT,ITER,IR,ISUBR,ISUBR2
C     DOUBLE PRECISION ST11,ST22,ST12,ANGLE,THETA,PHI,ALAM,S,XCOF,
C     +F,ROOTR,ROOTI,COF,U,FLAM,T,FT1,FT2,FT3,ALPOLY,PHIPOL,FDISC,
C     +PHIS1,PHIS2,PHI1,PHI2,FE11,FE22,FE33,FG12,FG13,FG23,FNU12,
C     +FNU23,FNU13,SUM1,SUM2,SUM3,S44(50),S55(50),S66(50),
C     +S44,S55,S66
C     DOUBLE PRECISION SI,CO
      SI=DSIN(THETA(IND))
      CO=DCOS(THETA(IND))
      S(IND,1,1)=S11(IND)*CO**4+(2*S12(IND)+S66(IND))*SI**2*
      +CO**2+S22(IND)*SI**4
      S(IND,1,2)=(S11(IND)+S22(IND)-S66(IND))*SI**2*CO**2+
      +S12(IND)*(SI**4+CO**4)
      S(IND,1,3)=S13(IND)*CO**2+S23(IND)*SI**2
      S(IND,2,2)=S11(IND)*SI**4+(2*S12(IND)+S66(IND))*SI**2
      +*CO**2+S22(IND)*CO**4
      S(IND,2,3)=S13(IND)*SI**2+S23(IND)*CO**2
      S(IND,3,3)=S33(IND)
      S(IND,1,6)=2*S11(IND)*CO**3*SI-2*S22(IND)*SI**3*CO+
      +(2*S12(IND)+S66(IND))*(SI**3*CO-CO**3*SI)
      S(IND,2,6)=2*S11(IND)*SI**3*CO-2*S22(IND)*CO**3*SI+
      +(2*S12(IND)+S66(IND))*(CO**3*SI-SI**3*CO)
      S(IND,3,6)=2*(S13(IND)-S23(IND))*SI*CO
      S(IND,4,4)=S55(IND)*SI**2+S44(IND)*CO**2
      S(IND,4,5)=(S55(IND)-S44(IND))*SI*CO
      S(IND,5,5)=S55(IND)*CO**2+S44(IND)*SI**2
      S(IND,6,6)=4*(S11(IND)+S22(IND)-2*S12(IND))*SI**2*
      +CO**2+S66(IND)*(CO**4+SI**4-2*SI**2*CO**2)
      WRITE(5,*) 'COMPLIANCES FOR PLY NO.',IND
      WRITE(5,*) 'S11, S12, S13, S22:'
      WRITE(5,*)S(IND,1,1),S(IND,1,2),S(IND,1,3),S(IND,2,2)
      WRITE(5,*) 'S23, S33, S16, S26:'
      WRITE(5,*)S(IND,2,3),S(IND,3,3),S(IND,1,6),S(IND,2,6)
      WRITE(5,*) 'S36, S44, S45, S55:'
      WRITE(5,*)S(IND,3,6),S(IND,4,4),S(IND,4,5),S(IND,5,5)
      WRITE(5,*) 'S66 IS:',S(IND,6,6)
      RETURN
      END
      SUBROUTINE PLPREP
      COMMON/BL1/ST11(50),ST22(50),ST12(50),ANGLE(50),THETA(50),PHI,
      +ALAM,NN,S(50,6,6),XCOF(5),F(11),ROOTR(4),ROOTI(4),COF(5),
      +U(4),FLAM(4),T(50),FT1,FT2,FT3,ALPOLY,PHIPOL,FDISC,PHIS1,PHIS2,
      +PHI1,PHI2,S11(50),S22(50),S33(50),S12(50),S13(50),S23(50),
      +SUM1(50),SUM2(50),SUM3(50),S44(50),S55(50),S66(50),
      +PHIS,FK(50),RROOT(4),PHIF,ALAMP
      COMMON/BL2/M,LT,ITER,IR,ISUBR,ISUBR2
      DIMENSION COEF33(50),COEF32(50),COEF31(50),E1B2(50),E1B3(50),
      +B1D1(50)
      IF(LT.EQ.3)GOTO 569
      IF(ISUBR2.EQ.0)GOTO 567
      WRITE(5,*) 'INPUT PHI,LAMBDA TO PREPARE STRESS COEFFICIENTS'
      READ(5,*) PHI,ALAM
567   VALUE1=PHI*ALAM/(ALAM-1)
569   DO 570 I13=1,NN
      WRITE(5,*) 'PLY NUMBER',I13
      CALL SUM(I13)
```

```
       IF(LT.EQ.3)GOTO 568
       E1B2(I13)=SUM1(I13)*VALUE1
       E1B3(I13)=SUM2(I13)*VALUE1
       B1D1(I13)=SUM3(I13)*PHI
       COEF33(I13)=PHI*VALUE1*ST22(I13)*T(I13)**2/2+PHI*
      +E1B2(I13)*T(I13)+PHI*E1B3(I13)
       COEF32(I13)=VALUE1*T(I13)*ST22(I13)+E1B2(I13)
       COEF31(I13)=PHI*ST12(I13)*T(I13)+B1D1(I13)
       GOTO 570
568    COEF33(I13)=PHIS*(SUM1(I13)*T(I13)+ST22(I13)*T(I13)**2/2+
      +SUM2(I13))
       COEF32(I13)=PHIS*(SUM1(I13)+ST22(I13)*T(I13))
       COEF31(I13)=0.
570    CONTINUE
       WRITE(5,*) 'THE COEFFICIENTS MULTIPLYING THE X DEPENDENCE
      +(FROM LAST INTERFACE TO MIDPLANE)'
       WRITE(5,*) 'FOR SIGMAZZ'
       WRITE(5,*) (COEF33(I14),I14=1,NN)
       WRITE(5,*) 'FOR SIGMA2Z'
       WRITE(5,*) (COEF32(I14),I14=1,NN)
       WRITE(5,*) 'FOR SIGMA1Z'
       WRITE(5,*) (COEF31(I14),I14=1,NN)
       ALAMFI=ALAM*PHI
       WRITE(5,*) 'LAMBDA TIMES PHI EQUALS',ALAMFI
       IF(LT.EQ.1)GOTO 1220
       IF(LT.EQ.2)GOTO 1219
       XZERO=1/PHI
       WRITE(5,*) 'THE VALUE AT WHICH SIGZZ IS ZERO IS',XZERO
       XOLD=XZERO
       BI=100*PHI*2.718281828
       I14=0
1218   XNEW=ALOG(BI*XOLD)/PHI
       IF((XNEW-XOLD).LT.1.0D-8)GOTO 1160
       XOLD=XNEW
       I14=I14+1
       IF(I14.EQ.300)GOTO 1170
       GOTO 1218
1219   BLAYER=4.4/PHI
       WRITE(5,*) 'THE BOUNDARY LAYER WIDTH IS',BLAYER
       GOTO 1180
1220   XZERO=ALOG(ALAM)/(PHI*(ALAM-1))
       BI=.01*(EXP(-PHI*XZERO)-EXP(-ALAMFI*XZERO))
       WRITE(5,*) 'THE VALUE AT WHICH SIGZZ IS ZERO IS',XZERO
       XOLD=XZERO
       I14=0
1280   IF(ALAM.LT.1.0)GOTO 1150
       XNEW=-ALOG(EXP(-ALAMFI*XOLD)+BI)/PHI
       GOTO 1270
1150   XNEW=-ALOG(EXP(-PHI*XOLD)-BI)/ALAMFI
1270   IF((XNEW-XOLD).LT.1.0D-8) GOTO 1160
       XOLD=XNEW
       I14=I14+1
       IF(I14.EQ.300)GOTO 1170
       GOTO 1280
1160   WRITE(5,*) 'THE BOUNDARY LAYER WIDTH IS',XNEW
       GOTO 1180
1170   WRITE(5,*) 'NO CONVERGENCE ON BL AFTER 300 ITERATIONS'
1180   RETURN
       END
       SUBROUTINE DIFFTH(T,FLTHIK,NN)
```

```
        DIMENSION T(50)
        FLTHIK=0.
        DO 303 I=1,NN
        WRITE(5,*) 'INPUT PLY THICKNESS FOR PLY NUMBER',I
        READ(5,*) T(I)
303     FLTHIK=FLTHIK+T(I)*2
        RETURN
        END
```

APPENDIX 6

A CRITERION TO ASSESS THE APPLICABILITY
OF THE TWO METHODS FOR CROSS-PLIED LAMINATES

This appendix gives an example where the original solution method for cross-plied laminates (see section 6.2) fails and the modified analysis presented in the same section must be used.

The unmodified analysis for cross-plied laminates leads to a quadratic equation in λ, expressed in equation 6.30. Let P_1 be the coefficient of λ in equation 6.30, i.e.

$$P_1 = \frac{(\frac{f_1}{f_2})^{1/2} (f_3 - 2f_8) + 4f_6 + 8f_1}{2f_6 + 3f_1} \qquad (A6.1)$$

where the fi are given by equations 5.110 and 5.108. P_1 can be rewritten as:

$$P_1 = \frac{(\frac{f_1}{f_2})^{1/2} (f_3 - 2f_8) + 2f_1}{2f_6 + 3f_1} + 2 \qquad (A6.2)$$

Now the analysis for cross-plied laminates fails if equation 6.30 has no real solutions. This means that the discriminant of equation 6.30 must be negative. Writing

$$P_1 = P_2 + 2 \qquad (A6.3)$$

where

$$P_2 = \frac{\sqrt{\frac{f_1}{f_2}} (f_3 - 2f_8) + 2f_1}{2f_6 + 3f_1} \qquad (A6.4)$$

the condition for the discriminant of equation 6.30 to be negative takes the form:

$$(P_2 + 2)^2 - 4 < 0 \qquad \text{(A6.5)}$$

Rearranging equation A6.5:

$$P_2(P_2 + 4) < 0 \qquad \text{(A6.6)}$$

The above equation is satisfied if

$$-4 < P_2 < 0 \qquad \text{(A6.7)}$$

or, using equation A6.4 to substitute for P_2:

$$-4 < \frac{\sqrt{\frac{f_1}{f_2}}\,(f_3 - 2f_8) + 2f_1}{2f_6 + 3f_1} < 0 \qquad \text{(A6.8)}$$

Equation A6.8 can be used as a criterion to check if the analysis for cross-plied laminates using both λ and ϕ will fail or not. If equation A6.8 is satisfied, the original analysis fails and the modified analysis (see section 6.2) must be used. If equation A6.8 is not satisfied, both analyses are valid but the one which uses both λ and ϕ is expected to be more accurate since the use of two unknown parameters in the formulation, λ and ϕ, can give a better prediction than the use of only one parameter, ϕ.

For $[0n/90n]s$ G/E laminates (AS1/3501-6 system), P_2 has the value -3.857 (if one substitutes for fi in equation A6.4) and hence the method using both λ and ϕ fails. For that case, the modified analysis, where only ϕ is present, must be used.

Equation A6.8 was included in the program code and is used to determine which of the two possible methods for the analysis of cross-plied laminates should be followed.